MECHANISTIC STUDIES ON α-GLYCOSYL TRANSFERASES

by

Renée M. Mosi

B.Sc., University of Victoria, 1992

A THESIS SUBMITTED IN PARTIAL FULFILLMENT OF

THE REQUIREMENTS FOR THE DEGREE OF

DOCTOR OF PHILOSOPHY

in

THE FACULTY OF GRADUATE STUDIES

Department of Chemistry

We accept this thesis as conforming

to the required standard:

THE UNIVERSITY OF BRITISH COLUMBIA

July 1998

In presenting this thesis in partial fulfilment of the requirements for an advanced degree at the University of British Columbia, I agree that the Library shall make it freely available for reference and study. I further agree that permission for extensive copying of this thesis for scholarly purposes may be granted by the head of my department or by his or her representatives. It is understood that copying or publication of this thesis for financial gain shall not be allowed without my written permission.

Department of CHEMISTRY

The University of British Columbia
Vancouver, Canada

Date July 29, 1998

DE-6 (2/88)

ABSTRACT

In order to provide insight into the mechanism of glycogen phosphorylase (phos b) and cyclodextrin glycosyltransferase (CGTase) the modified substrates, 4-deoxy-α-maltotriosyl fluoride (4DαG3F), 4-deoxymaltopentaose (4DG5), and 4-deoxymaltohexaose (4DG6) have been synthesized using chemical and enzymatic means. These types of incompetent substrate analogues can be used to "trick" each enzyme into catalyzing only the first half of its normal reaction in order to trap a glycosyl-enzyme intermediate.

Glycosyl fluorides such as α-maltotriosyl fluoride (αG3F) are good substrates for *Bacillus circulans* 251 CGTase (k_{cat} = 275 s^{-1}, K_m = 2.5 mM) providing a convenient method of measurement. Reaction of the acid/base catalyst mutant of CGTase, Glu257Gln, with 4DαG3F, yielded a stable glycosyl-enzyme intermediate. Using neutral loss mass spectrometry, Asp229 was identified as the catalytic nucleophile. An X-ray structure of the 4-deoxymaltotriosyl moiety bound to Glu257Gln provided the first structural insights into such a covalent intermediate for any α-1,4 glycosyl transferase or α-glycosidase.

The binding of active site mutants of CGTase to the inhibitor acarbose was investigated through measurement of K_i values. Kinetic parameters for αG3F and α-glucosyl fluoride were determined and reasonable correlations were observed in logarithmic plots relating the K_i value for acarbose with each mutant and both k_{cat}/K_m and K_m for the hydrolysis of either substrate by the corresponding mutants. The dependence was greater in the plot of log (k_{cat}/K_m) vs log K_i than in the plot of log K_m indicating that the binding mode of acarbose more closely resembles that of the reaction transition state than of the ground state.

Kinetic results on phos b indicated that 4DG6 was a competitive inhibitor with respect to maltopentaose, but binds noncompetitively with respect to orthophosphate or glucose-1-phosphate. Two trapping experiments in the presence of 4DG6, a radiolabelling study using ^{14}C-glucose-1-phosphate and an electrospray mass spectrometry investigation, provided preliminary evidence for a glycosyl-enzyme intermediate. Analogous experiments were performed with potato phosphorylase using 4DG5 yielding similar results. Positional isotope exchange experiments were attempted with both phosphorylases. Glucose-1-phosphate selectively labelled with ^{18}O at the anomeric position was chemically synthesized for this purpose and ^{31}P NMR was used to follow the extent of isotope exchange.

TABLE OF CONTENTS

LIST OF TABLES

LIST OF FIGURES

LIST OF SCHEMES

ABBREVIATIONS AND SYMBOLS

2Cl2FαGluCl	2-Chloro-2-deoxy-2-fluoro-α-D-glucopyranosyl chloride
2FβGluF	2-Deoxy-2-fluoro-β-D-glucosyl fluoride
2,2FαAraCl	2,2-Difluoro-α-D-*arabino*-hexopyranosyl chloride
5FαGluF	5-Fluoro-α-D-glucosyl fluoride
5FαIdoF	5-Fluoro-α-L-idosyl fluoride
5FαManF	5-Fluoro-α-D-mannosyl fluoride
5FβGluF	5-Fluoro-β-D-glucosyl fluoride
5FβGulF	5-Fluoro-β-L-gulosyl fluoride
5FβIdoF	5-Fluoro-β-L-idosyl fluoride
Abg	*Agrobacterium* β-glucosidase
αCD	α-Cyclodextrin
αGF	α-D-glucosyl fluoride
αG2F	α-Maltosyl fluoride
αG3F	α-Maltotriosyl fluoride
αG6F	α-Maltohexaosyl fluoride
αG9F	α-Maltononaosyl fluoride
AMP	Adenosine-5'-monophosphate
ADP	Adenosine-5'-diphosphate
ATP	Adenosine-5'-triphosphate
βCD	β-Cyclodextrin
Cex	*Cellulomonas fimi* exoglycanase
CGTase	Cyclodextrin glycosyltransferase
cpm	Counts per minute
cps	Counts per second
4DαG2F	4-Deoxy-α-maltosyl fluoride
4DαG3F	4-Deoxy-α-maltotriosyl fluoride
4DG	4-Deoxyglucose
4DG2	4-Deoxymaltose
4DG3	4-Deoxymaltotriose
4DG4	4-Deoxymaltotetraose
4DG5	4-Deoxymaltopentaose
4DG6	4-Deoxymaltohexaose
4DG-[1-^{18}O]-P	4-Deoxy-α-D-glucose-[1-^{18}O]-phosphate
Da	Dalton
DAST	Diethylaminosulphur trifluoride
DCI	Desorption chemical ionization
DMF	Dimethylformamide
DNP2FβC	2,4-Dinitrophenyl-2-deoxy-2-fluoro-β-D-cellobioside
DNP2FβGal	2,4-Dinitrophenyl-2-deoxy-2-fluoro-β-D-galactopyranoside
DNP2FβGlu	2,4-Dinitrophenyl-2-deoxy-2-fluoro-β-D-glucopyranoside
DNP2FβX	2,4-Dinitrophenyl-2-deoxy-2-fluoro-β-D-xylopyranoside
DNP2FβX2	2,4-Dinitrophenyl-2-deoxy-2-fluoro-β-D-xylobioside

DTT	Dithiothreitol
E.C.	Enzyme Commission (classification number) of the International Union of Biochemistry
E. coli	*Escherichia coli*
EDTA	Ethylenediamine tetracetic acid
ES-MS	Electrospray mass spectrometry
γCD	γ-cyclodextrin
G	Glucose
G2	Maltose
G3	Maltotriose
G4	Maltotetraose
G5	Maltopentaose
G6	Maltohexaose
G7	Maltoheptaose
G1P	α-D-glucose-1-phosphate
G-[1-^{18}O]-P	α-D-glucose-[1-^{18}O]-phosphate
G6PDH	Glucose-6-phosphate dehydrogenase
Glyx	Glycogen debranching enzyme
GPD	Glycerophosphate
HF-pyridine	Hydrogen fluoride-pyridine (70 % hydrogen fluoride)
HPLC	High performance liquid chromatography
IMP	Idenosine monophosphate
kDa	kiloDalton
LC/MS	Liquid chromatography/mass spectrometry
MALDI-MS	Matrix assisted laser desorption ion mass spectrometry
MeOH	Methanol
NJT	Nojirimycin tetrazole
NJT-2-O-Pi	Nojirimycin tetrazole-2-O-phosphate
NJT-2-O-CH_2-Pi	Nojirimycin tetrazole-2-O-methyl phosphonate
NMR	Nuclear magnetic resonance
phos b	Rabbit muscle glycogen phosphorylase *b*
Pi	Orthophosphate
PLP	Pyridoxal-5'-phosphate
PIX	Positional isotope exchange
PGM	Phosphoglucomutase
pot phos	Potato phosphorylase
TCA	Trichloroacetic acid
TIC	Total ion chromatogram
TLC	Thin layer chromatography
TNP2,2FαGlu	2,4,6-Trinitrophenyl-2-deoxy-2,2-difluoro-α-D-*arabino*-hexopyranoside
wt	Wild-type

Amino Acid Abbreviations

Ala	(A)	Alanine
Arg	(R)	Arginine
Asn	(N)	Asparagine
Asp	(D)	Aspartate
Cys	(C)	Cysteine
Glu	(E)	Glutamate
Gln	(Q)	Glutamine
Gly	(G)	Glycine
His	(H)	Histidine
Ile	(I)	Isoleucine
Leu	(L)	Leucine
Lys	(K)	Lysine
Met	(M)	Methionine
Phe	(F)	Phenylalanine
Pro	(P)	Proline
Ser	(S)	Serine
Thr	(T)	Threonine
Typ	(W)	Tryptophan
Tyr	(Y)	Tyrosine
Val	(V)	Valine

Kinetic Constants

k_{cat}	Catalytic rate constant
K_i	Dissociation rate constant for the enzyme-inhibitor complex
k_i	First order rate constant of inactivation
K_m	Michaelis-Menten constant
RFK_i	Range finder K_i
V_{max}	Maximal rate of an enzyme-catalyzed reaction

ACKNOWLEDGEMENTS

I wish to express my sincere thanks to my supervisor, Dr. Steve Withers, for all of his advice and encouragement throughout the course of this work. His insight and enthusiasm were a continued source of inspiration for me.

I would like to gratefully acknowledge Dr. Bauke Dijkstra, Dr. Lubbert Dijkhuisen and Mr. Joost Uitdehaag (University of Groningen), for providing all of the CGTase enzymes and for their collaboration on the CGTase crystallography experiments. In addition, special thanks to Mr. Joost Uitdehaag (University of Groningen) for many helpful discussions. I would also like to acknowledge the assistance of Dr. Louise Johnson (University of Oxford) for the crystallographic study of phosphorylase and Dr. Neil Madsen and Mrs. Shirley Sheckosky (University of Alberta) for their kind donation of glycogen debranching enzyme.

I am grateful to all of my co-workers (past and present) for their friendships and assistance. In particular, I would like to acknowledge Dr. Curtis Braun, Dr. Thisbe Lindhorst, Dr. John McCarter, and Mr. David Vocadlo for many valuable suggestions and insights. I am indebted to Mr. Rafael Sala who spent many hours assisting me with the ^{31}P NMR experiments. Special thanks to Mr. Shouming He, Ms. Karen Rupitz, and Ms. Dennise Dombroski for technical assistance.

I would like to thank my family and friends, especially my parents and my brothers, for their love, support and unwavering belief in me. Thank you to my husband Andrew whose love and laughter made it all possible.

For my parents, Ernest and Mary Pollard

and Andrew, with love

CHAPTER 1

GENERAL INTRODUCTION

1.1 GENERAL INTRODUCTION

Carbohydrates are one of the four main classes of biomolecules. From the very basic carbohydrate unit, the monosaccharide, to sugar polymers as in oligo- and polysaccharides, carbohydrates also form important constituents of glycoproteins and glycolipids. Their diversity in structure is reflected in the variety of functions which they perform. Traditionally, carbohydrates are known for their roles in energy storage and as structural components. Thus, starch in plants, and glycogen in animals serve as reservoirs of glucose while cellulose forms the principal component of the cell walls of higher plants, providing them with structural strength. Furthermore, carbohydrate units play a significant role in cell to cell recognition processes. For instance, they have been found to function as blood group determinants and as bacterial surface antigens (*1*).

Carbohydrates are assembled and broken down by two large groups of enzymes; the glycosyl transferases carry out the biosynthesis and the glycosidases (or glycosyl hydrolases) carry out the biodegradation. Hence, these enzymes are of interest for their applications in industry (for example, xylanases in the pulp and paper industry and α-amylases in the brewing industry). As a result, their mechanism of action needs to be well understood. This involves characterizing the intermediates along the reaction pathway as well as identifying the key amino acid residues involved in catalysis. Once the mechanism of catalysis is well defined, it will provide a basis for the engineering of enzymes with improved properties.

1.2 GLYCOSIDASES AND GLYCOSYL TRANSFERASES

The term glycosyl transferase is used to describe any enzyme which catalyzes a transfer of a glycosyl unit to an acceptor, but is generally used to describe a transfer to an acceptor other than water. On the other hand, the term glycosidase is used to describe any enzyme which catalyzes a transfer of a glycosyl unit to water. Within the class of glycosyl transferases, the enzymes can be classified on the basis of the identity of the donor. One group comprises the nucleoside phosphate utilizing transferases. The other group comprises those enzymes which catalyze the transfer of a sugar moiety from an oligosaccharide or polysaccharide to another sugar or to a phosphate moiety. The focus of this thesis will be on two members of the latter group, cyclodextrin glycosyltransferase, which ordinarily catalyzes an intramolecular glycosyl transfer on starch to make cyclic oligosaccharides, and glycogen phosphorylase, which catalyzes the transfer of a glucose moiety between glycogen and a phosphate acceptor.

The glycosyl transferases (and glycosidases) can be further divided into subgroups based on three traditional criteria: glycone specificity, anomeric configuration of the substrate or product, and the stereochemical outcome of the reaction catalyzed. In the case of glycone specificity, glycosyl transferases are categorized based on the sugar, or glycone, to which they are most reactive. For instance, a glucosyl transferase is most reactive towards glucose while a galactosyl transferase is most reactive toward galactose and so on. Nucleotide using glycosyl transferases are also classified as either "α" or "β" based on the configuration of their product. Lastly, glycosyl transferases are also often referred to as being "retaining" or "inverting" depending on the relative stereochemical outcome of the product with respect to the substrate (Figure 1.1). A glycosyl transferase is termed "retaining" if the anomeric

configuration of the substrate and product are identical. On the other hand, the term "inverting" is used to describe a glycosyl transferase-catalyzed reaction that generates a product of opposite anomeric configuration to the substrate. As both of the enzymes studied in this thesis, phosphorylase and cyclodextrin glycosyltransferase (CGTase), are classified as retaining α-glycosyl transferases, the following discussion and examples will focus on this subgroup.

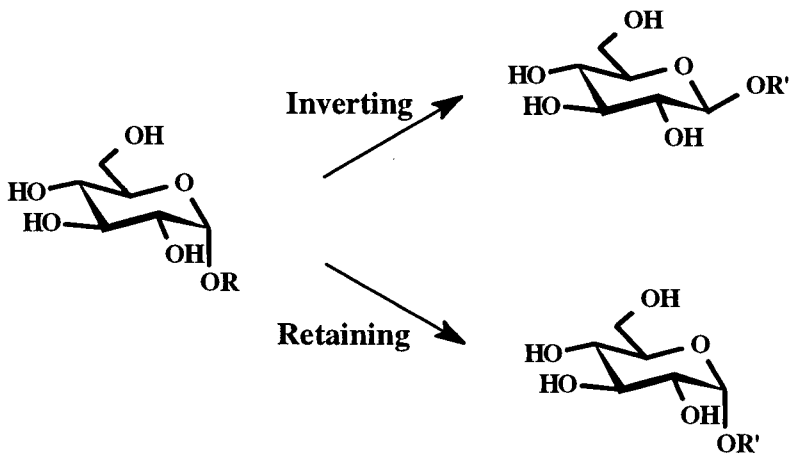

Figure 1.1 The two stereochemical outcomes of a glycosyl transferase-catalyzed reaction illustrated with an α-glucoside

In addition to the general criteria listed above for the classification of glycosidases and glycosyl transferases, it is possible to group enzymes together into families based on sequence similarities (first reported (*2*), recently reviewed (*3*) and expanded to include nucleotide-diphospho-(NDP)-sugar transferases (*4*)). To date, over 1000 glycosidases and non-NDP-dependent transferases/hydrolases have been categorized into a total of 60 unique families while over 553 NDP-sugar utilizing transferases have been classified into 27 families. Members within the same family have the same three dimensional fold. Additionally, since the overall fold is more conserved than their primary sequence it turns out that several families

have similar folds even though this is not evident from the sequence and these families have been assigned to clans on this basis (*5*). This similarity has proven to be useful in helping to identify the residues responsible for specificity and catalysis since once a structural motif is established for one member of the family, comparisons can be made to other enzymes within the group whose structures have not yet been solved. Cyclodextrin glycosyltransferase (E.C. 2.4.1.19) is found in Family 13 along with the α-amylases and α-glucosidases. Glycogen phosphorylase (E.C. 2.4.1.1) has not been classified with other enzymes but it has been found to be structurally similar to a β-glucosyl transferase (E.C. 2.4.1.27) (*6*).

1.3 THE CATALYTIC MECHANISM OF GLYCOSYL TRANSFERASES

The two different stereochemical outcomes of the reactions catalyzed by glycosyl transferases (and glycosidases) are a result of the two distinct mechanisms by which these enzymes operate. The retaining glycosyl transferases operate through a double displacement reaction (Figure 1.2) while the inverting enzymes employ a single displacement mechanism (Figure 1.3).

The key feature of the double displacement mechanism employed by retaining glycosyl transferases (and glycosidases) (Figure 1.2), first proposed by Koshland in 1953, is the formation of a covalent glycosyl-enzyme intermediate (*7*). The first step (glycosylation) involves the attack of the catalytic nucleophile at the anomeric center of the sugar with general acid assistance to aid in the departure of the leaving group. This generates a glycosyl-enzyme intermediate which can then undergo either transglycosylation or hydrolysis in a second step (deglycosylation) with general base assistance facilitating attack of the incoming group. Both steps proceed via transition states with substantial oxocarbenium ion character

(see Section 1.4.3). In addition, non-covalent interactions between enzyme and substrate are believed to be responsible for much of the rate acceleration and provide considerable stabilization of the transition state (see Section 1.4.2).

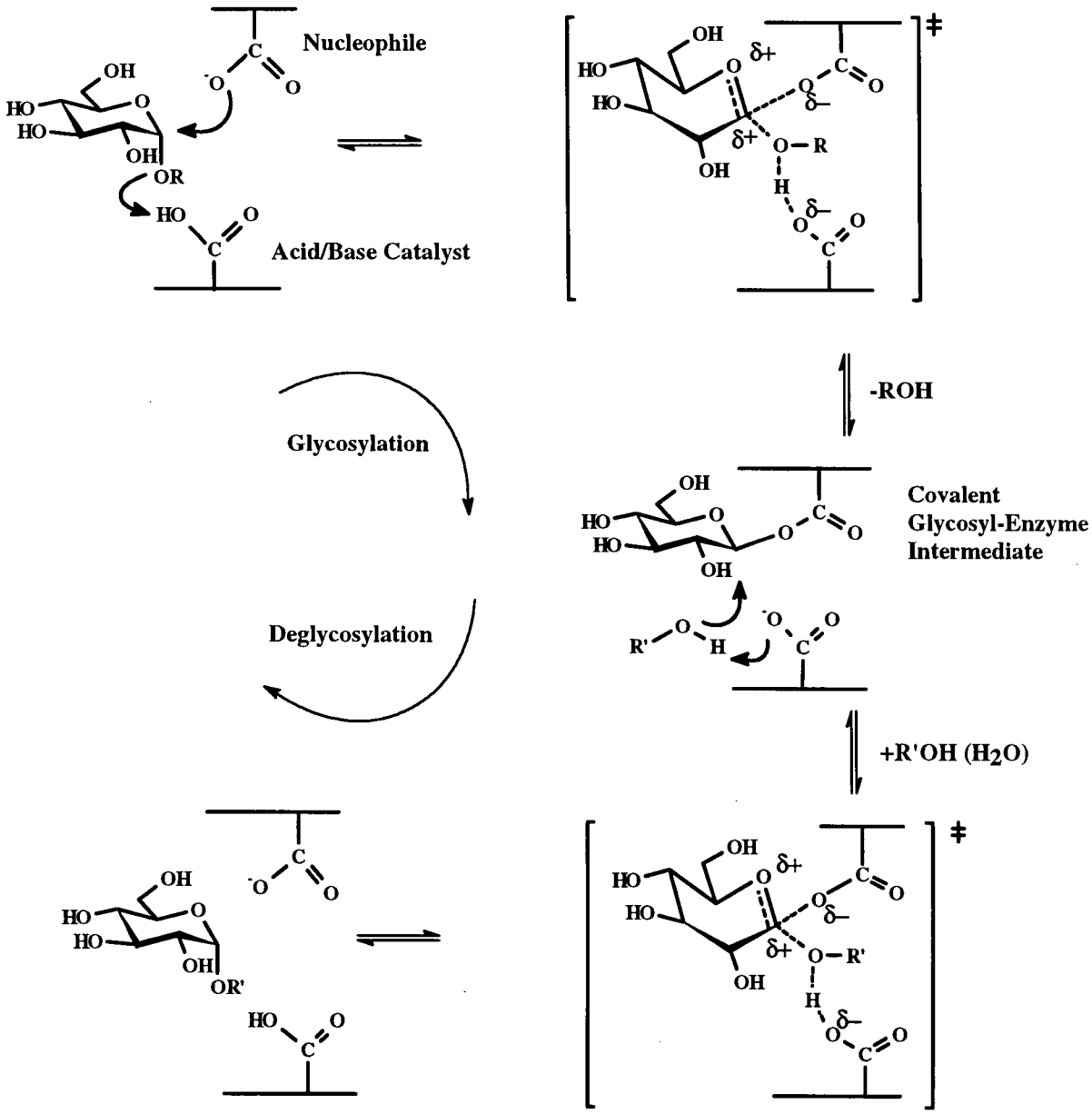

Figure 1.2 The double displacement mechanism for a retaining α-glycosyl transferase

While the single displacement mechanism employed by inverting enzymes differs from the double displacement mechanism, there are several important similarities between the two. Both mechanisms proceed through transition states with substantial oxocarbenium ion-like character and in both cases, a pair of carboxylates function as the catalytic residues. However, some key differences between the two mechanisms are evident. In the inverting mechanism, no covalent intermediate is formed and hence, neither carboxylate functions as a catalytic nucleophile. Instead, one carboxylate functions as a general acid to promote the departure of the leaving group while the other acts as a general base to assist the attack of the incoming acceptor group. By comparison, in the double displacement mechanism, one carboxylate performs the dual role of acid/base catalyst.

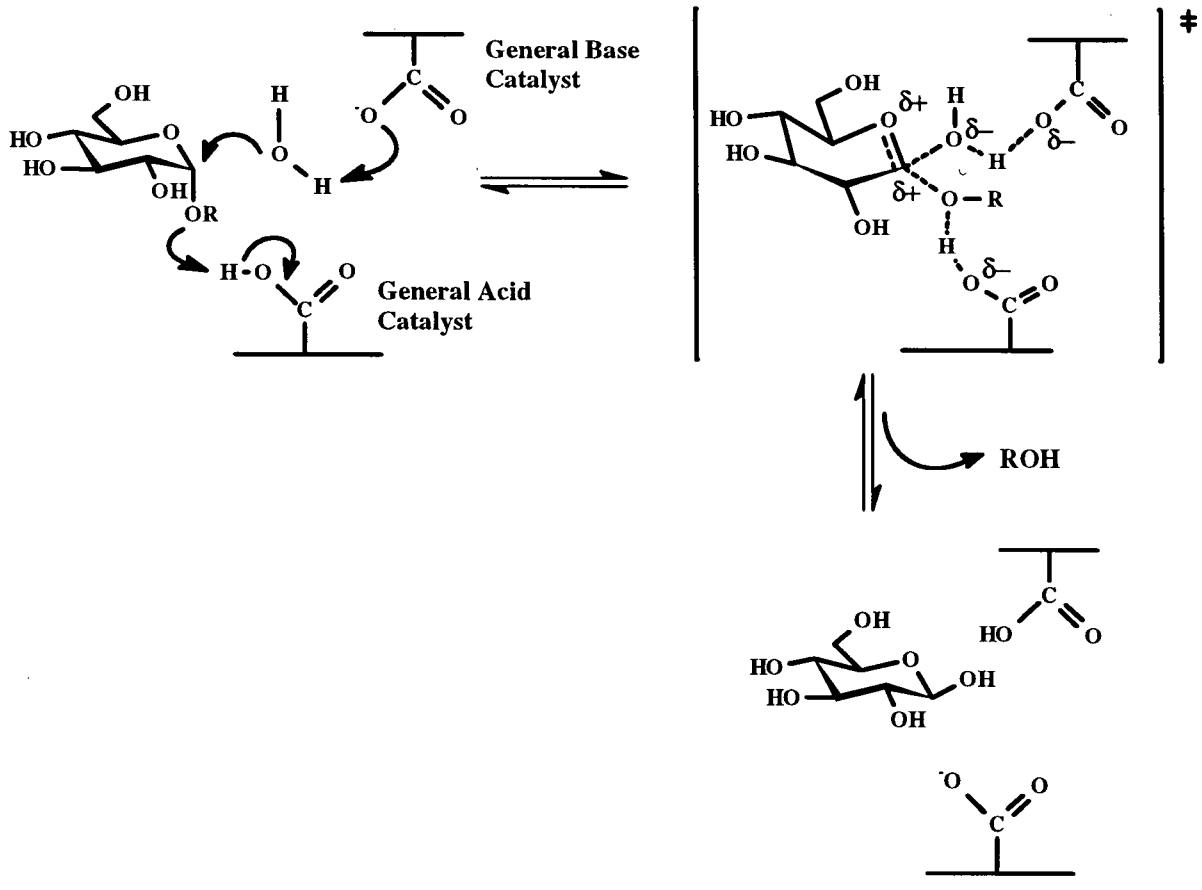

Figure 1.3 The single displacement mechanism for an inverting α-glycosidase

1.4 KEY FEATURES OF THE DOUBLE DISPLACEMENT MECHANISM

1.4.1 Presence of a Nucleophile and Acid/Base Catalyst

Extensive progress has been made in recent years in elucidating the identities and functions of the catalytic carboxylates in many α- and β-glycosidases and glycosyl transferases by means of X-ray crystallography, sequence alignment, site-directed mutagenesis, kinetic analysis of the resulting mutant enzymes, and labelling studies (see (*8-10*) for useful reviews). In all cases, these catalysts have been found to be either glutamic acid or aspartic acid residues (*11*).

1.4.1.1 X-Ray crystallographic insights

Evidence for carboxylates functioning as the acid/base catalyst and the nucleophile comes from extensive structural studies on many enzymes which show the correct positioning of such residues in the active site. In the double displacement mechanism, the attack of the nucleophile at the anomeric center of the sugar is assisted through the donation of a proton from a suitably placed carboxylic acid, the average distance between the two residues is approximately 4.5 - 5.5 Å. In contrast, in inverting enzymes, the two carboxyl groups are separated by a greater distance, approximately 9 - 9.5 Å, presumably to create enough space for the participating water molecule (*12, 13*). The structures of a number of glycosidases have now been determined crystallographically (for a review see (*12*)), however, often this technique is not applicable or available and thus it is necessary to resort to other means of identification. Moreover, it is not always easy to distinguish which carboxylates are important unless the structure determined includes a substrate, substrate analogue or inhibitor bound in the active site (these examples will be discussed more fully in Section 1.4.1.2 and Section

1.4.4). Even with this information, it is possible that carboxylates may be misassigned if the substrate analogue or inhibitor is bound in an unproductive manner.

1.4.1.2 Affinity labels

An alternative approach involves the use of affinity labels to specifically derivatize amino acids in the active site. Affinity labels consist of a reactive functional group, which can react with certain residues on the enzyme and a sugar moiety, which provides affinity for the active site of the glycosidase. However, as the functional group in the molecule often reacts with a number of amino acids on the enzyme, the results of affinity labelling must be interpreted with caution as a specific means of identifying catalytic residues. However, in selected cases, affinity labels have proven to be useful in labelling the acid/base catalyst.

Common affinity labels for β-glycosidases include glycosyl epoxides (**1.1**) (*14, 15*), *N*-bromoacetyl-glycosylamines (**1.2**) (*16-18*) and glycosyl isothiocyanates (**1.3**) (*19*) (Figure 1.4).

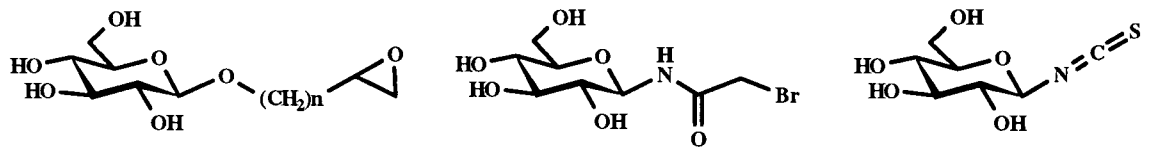

1.1 **1.2** **1.3**

*Figure 1.4 Common affinity labels for β-glycosidases: glycosyl epoxide (**1.1**), N-bromoacetyl-glycosylamine (**1.2**), glycosyl isothiocyanate (**1.3**)*

The main drawback of the O-linked affinity labels is their susceptibility to enzyme catalyzed hydrolysis while the N-linked labels have the advantage of being inert in this respect. Examples where affinity labels have proven successful in determining the identity of the acid/base catalyst of β-glycosidases include the labelling of Glu127 from *Cellulomonas fimi* β-

(1,4)-glucanase with *N*-bromoacetyl-β-D-cellobiosylamine (*20*), and the labelling of Glu198 from Cassava β-glucosidase with *N*-bromoacetyl-β-D-glucosylamine (*18*). The variety of affinity labels available for α-glycosidases is more limited. One example of a successful α-configured affinity label is 1,2-epoxy-3-(α-D-glucopyranosyl)propane (**1.4**) which was shown to be an effective inactivator of two α-glucosyltransferases from *Streptococcus mutans* (*21*). Another example is the bromo-ketone α-C-mannoside (**1.5**) which was used as an affinity label to target the acid/base catalyst of α-glucosidase from *Saccharomyces cerevisiae* (*22*). In this case, it was possible to use the manno configuration of the label as the enzyme has a similar binding affinity for mannosides and glucosides.

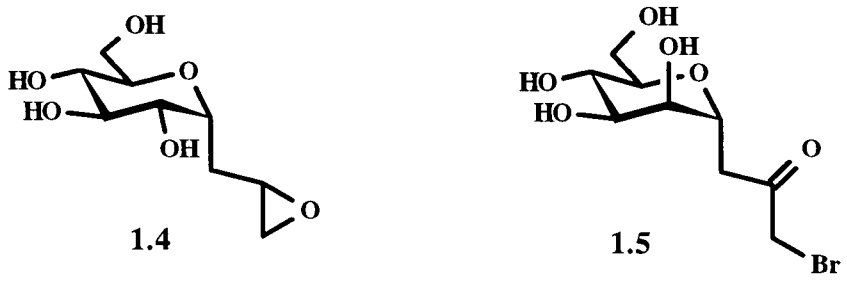

*Figure 1.5 Affinity labels for α-glycosidases: 1,2 epoxy-3-(α-D-glucopyranosyl)propane (**1.4**) and bromo-ketone α-C-mannoside (**1.5**)*

Conclusive evidence for the existence of catalytic carboxylates comes from the X-ray data of retaining glycosidases co-crystallized with either a substrate or inhibitor/affinity label in the active site. The structure of *Bacillus amyloliquefaciens* 1,3-1,4-β-glucanase co-crystallized with an epoxybutyl cellobioside showed a covalent bond between the side chain of Glu105 and the affinity label (*23*). Site-directed mutagenesis of this conserved glutamic acid resulted in an inactive enzyme, thereby confirming the catalytic importance of this carboxylate.

1.4.1.3 Insights from kinetic analysis and site-directed mutagenesis

Although the epoxy glycosides and C-glycosides are sometimes useful in labelling and identifying the catalytic residues, they generally react in a nonspecific manner, resulting in their attachment to many residues throughout the protein. Thus, they are of limited utility for the identification of specific catalytic residues and confirmation of their roles. MacLeod et al. (*24*) have recently developed a strategy for specifically identifying the acid/base catalyst. This method combines sequence alignment with site directed mutagenesis and kinetic analysis. On the basis of sequence alignments, highly conserved carboxylate residues are identified and mutated to either Ala or Gly. These mutants are then subjected to a detailed kinetic analysis using a pair of substrates with different requirements for acid assistance in the presence or absence of additional azide. Such an approach has been used to successfully identify Glu127 and Glu170 as the acid/base catalysts of *Cellulomonas fimi* exoglycanase (*24*) and *Agrobacterium* β-glucosidase (*25*).

A key feature of the double displacement mechanism is the dual role performed by the acid/base catalyst. In the first step, this carboxylate functions as a general acid catalyst while in the second step, it acts as a general base catalyst. Therefore, efficient catalysis requires that the ionization state of this side chain be modulated. Studies of the pH dependence of the kinetic parameters for the reaction of some retaining glycosidases have provided insight into these considerations. Examples include studies with *Agrobacterium sp.* β-glucosidase and *C. fimi* exoglucanase which showed that the pK_a of a key active site residue varies by about 3 pH units during the course of catalysis (*26, 27*). While these experiments provide some information on the ionization state of key active site residues, it may be difficult to assign a specific role or identity to a defined residue. Instead, the use of NMR provides a means of

titrating specific side chains, and thereby determining their individual ionization constants. This approach has been used to determine the pK_a values for the catalytic carboxylates in *B. circulans* xylanase using ^{13}C NMR and selective ^{13}C protein labelling (*28*). In the free enzyme, the pK_a values of 4.6 and 6.7 were measured for the catalytic nucleophile and the acid/base catalyst respectively. The pK_a of the acid catalyst is above the pH optimum for the enzyme (5.5), hence this group is in a protonated state, ready to act as a proton donor. Upon the formation of a covalent glycosyl-enzyme intermediate, the pK_a of the acid/base catalyst decreased to 4.2 (see Section 1.4.4 for a description on the use of mechanism based inactivators to accumulate a glycosyl-enzyme intermediate). This drop in pK_a leaves this group in a deprotonated state and is consistent with its role in the second step of the reaction as a general base catalyst to facilitate deglycosylation.

1.4.2 Non-Covalent Interactions

The concept that the majority of the catalytic power of an enzyme comes from non-covalent interactions between the transition state of the reaction and the active site of the enzyme was first proposed by Pauling in 1946 (*29*). Attempts to quantify the contribution of non-covalent interactions to the rate enhancement of the reactions catalyzed by glycosidases have been carried out using a variety of substrate analogues in which a defined hydroxyl group has been replaced with either a hydrogen or a fluorine atom.

Estimates of the strengths of hydrogen bonds to the individual sugar hydroxyls at the transition state of the reaction were obtained for glycogen phosphorylase using a series of deoxyfluoro- and deoxy-α-D-glucopyranosyl phosphates (*30*). Kinetic analysis of these analogues indicated a 10^2 to 10^5 fold decrease in reactivity over the parent substrate. The

strongest hydrogen bond contributions were found to be from the 3- and 6-positions (approximately 6 kcal/mol each), while interactions at the 2- and 4-positions (3.7 kcal/mol) were less crucial. These results not only confirm the significant role that hydrogen bonding plays in achieving rate acceleration, but also indicate the degree to which phosphorylase has adapted to preferentially bind the transition state over the ground state (see Section 3.1.5). Similar studies have been completed for phosphoglucomutase (*31*), glucoamylase (*32*), *E. coli* β-galactosidase (*33*) and *Agrobacterium* sp. β-glucosidase (*34*).

1.4.3 Oxocarbenium Ion-Like Transition States

Transition state analogues have long provided a valuable tool for probing enzymatic mechanisms. Their design is based on the principle that additional or improved binding interactions develop between the enzyme and substrate in the transition state complex thereby conferring a high degree of reaction specificity and rate acceleration. Thus, analogues which mimic the transition state structure should bind tightly. This transition state analogy, which was first proposed by Pauling in 1946 (*29*) and then further evolved by Lienhard (*35*) and Wolfenden (*36*), has provided the framework for the design of a wide variety of tight-binding reversible enzyme inhibitors. Key characteristics of sugar based transition state analogue inhibitors for glycosidases are a positive charge distributed between C-1 and the ring oxygen, a trigonal anomeric center, and a half-chair like conformation (*37-40*) (Figure 1.6). The strong binding affinity observed for transition state analogues that resemble glycosyl cations supports the idea that an oxocarbenium ion-like transition state exists.

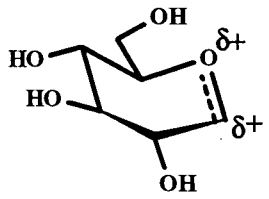

Figure 1.6 Structure of a glycosyl cation

Gluconolactone (**1.6**) and gluconolactam (**1.7**) were two of the first tight binding inhibitors to be identified as a transition state analogues for glycosidases (Figure 1.7). Their half-chair like geometry and resonance charge distribution closely resemble that of the oxocarbenium ion. Typically, these analogues bind some 10^2 to 10^4 times tighter to retaining glycosidases than the corresponding glycoside (*37*). Unfortunately, the instability of the lactone in solution has limited its utility in kinetic analysis.

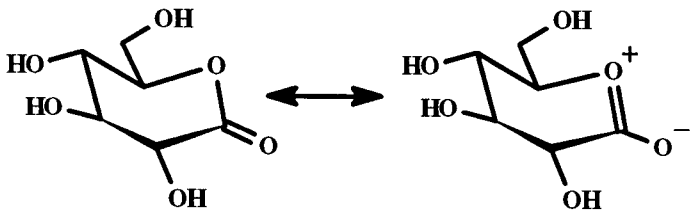

1.6

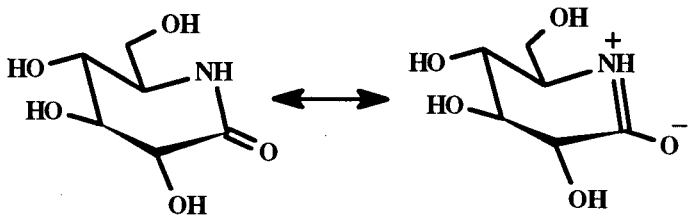

1.7

*Figure 1.7 Resonance structures of the transition state analogues gluconolactone (**1.6**) and gluconolactam (**1.7**)*

Another class of transition state analogues are nojirimycin tetrazole (**1.8**) and manno-nojirimycin tetrazole (**1.9**). Both compounds possess a half-chair conformation and a trigonal anomeric center, thus resembling the oxocarbenium ion-like geometry. These compounds bind some 10^3 to 10^4 fold tighter to glycosidases than the corresponding sugar, glucose or mannose (*39*). The binding efficiencies of **1.8** and **1.9** corresponded to the substrate specificity of the glycosidases tested; the manno- derivatives bound tighter to the mannosidases while the gluco- derivatives bound tighter to the glucosidases.

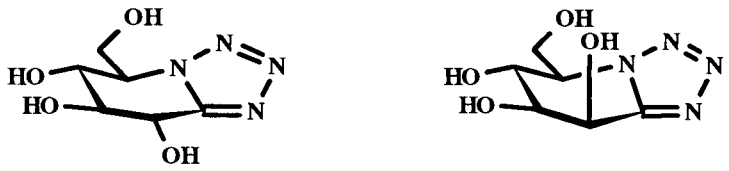

1.8 **1.9**

*Figure 1.8 Structures of the transition state analogues nojirimycin tetrazole (**1.8**) and manno-nojirimycin tetrazole (**1.9**)*

Determination of α-secondary deuterium isotope effects for several retaining glycosidases has provided evidence for the oxocarbenium ion-like character of both the glycosylation and deglycosylation transition states. Studies on *E. coli* β-galactosidase using substrates for which glycosylation was rate limiting yielded values of k_H/k_D = 1.15 - 1.20 and those for which deglycosylation was rate limiting gave values of k_H/k_D = 1.20 - 1.25 (*41*). Kinetic isotope effect values of greater than unity are indicative of a change from sp^3 to sp^2 hybridization at the anomeric center as the reaction proceeds from the ground state to the transition state. The proposed double displacement mechanism requires that both steps have a secondary kinetic isotope effect of greater than one as more sp^2 character is predicted in both of the transition states than either of the preceding ground states. Similar α-secondary

deuterium kinetic isotope effect measurements on *C. fimi* exoglycanase with substrates for which either glycosylation or deglycosylation was rate limiting gave values of k_H/k_D = 1.06 to 1.12 (*27*).

Evidence for the existence of an oxocarbenium ion-like transition state in the reaction of phosphorylase comes from the discovery of linear free energy relationships between the rates of the phosphorylase catalyzed reaction and the non-enzymatic acid-catalyzed hydrolysis of a series of deoxy- and deoxyfluoro-glucopyranosyl phosphates (*30, 42*). The acid-catalyzed hydrolysis of glucose-1-phosphate is known to proceed through an intermediate with positive charge development on the glucosyl ring. Therefore, the observation of a reasonable correlation ($\rho = 0.90$) between the two reactions indicates a similar development of positive charge between the two transition states.

An extension to this approach was developed by Konstantinidis and Sinnott (*43*). By utilizing a pair of substrates differing in the electronic demand placed at the reaction center, it was possible to measure the positive charge present at the transition state. The substrates compared were glycosyl fluorides and 1,1-difluoro glycosides, which differ only in the introduction of a second fluorine at the reaction center. This second fluorine should destabilize the formation of the positively charged transition state, thereby slowing its formation. The rates of glycosidase catalyzed turnover of both groups of substrates were measured and compared and it was predicted that the differences in rates should reflect the size of the developing positive charge to a reasonable approximation. Results were obtained for *A. wentii* β-glucosidase, sweet almond β-glucosidase, and rice α-glucosidase and were consistent with an oxocarbenium ion-like transition state in all cases.

1.4.4 Nature of the Glycosyl-Enzyme Intermediate and Identification of the Catalytic Nucleophile

1.4.4.1 A review of strategies to trap covalent glycosyl-enzyme intermediates

a. Low temperature and rapid denaturation trapping strategies

Both low temperature and rapid-quench methods have been successfully used to provide evidence for a covalent glycosyl-enzyme intermediate in both retaining α-glycosidases and glycosyl transferases. In 1970, Voet and Abeles captured the glucosyl-enzyme intermediate in sucrose phosphorylase and confirmed that the glucosyl moiety was bound to the enzyme through a β-linkage (*44, 45*). This was achieved by incubating the enzyme with radiolabelled sucrose, rapid acid denaturation of the protein and isolation of the radiolabelled peptides. The acid served both as denaturant and, through protonation of the general base catalyst, the low pH slowed the deglycosylation step. An aspartic acid was identified as the nucleophile of *Streptococcus sobrinus* α-glucosyl transferase by rapidly denaturing a reaction mixture of enzyme and radiolabelled sucrose and isolating the labelled peptide (*46, 47*). Low temperature ^{13}C NMR experiments have given evidence for the formation of a β-carboxylacetal ester covalent adduct resulting from the reaction of maltotetraose and porcine α-amylase (*48*). Trapping the intermediate on a glycosidase is a more demanding task than on a glycosyl transferase due to the need to prevent reaction with the omnipresent substrate, water. In order to achieve this on *A. wentii* β-glucosidase, a substrate analogue with a slower deglycosylation step, D-glucal, was employed (*49*). In this case, radiolabelled D-glucal was incubated with the enzyme for a brief period, followed by rapid denaturation, proteolytic digestion and amino acid sequencing to determine the point of attachment as an aspartate residue. The same residue was labelled with conduritol epoxide (*50*) and PNP-2-deoxy-β-D-

glucopyranoside (*51*). Evidence for a covalent glycosyl-enzyme intermediate in the reaction catalyzed by sweet almond β-glucosidase was obtained using low temperatures in combination with a cryogenic solvent (dimethyl sulfoxide) (*52*). At subzero temperatures, a burst of nitrophenol was observed from the reaction of β-glucosidase with PNP-β-D-glucopyranoside, indicating the accumulation of a glycosyl-enzyme intermediate. These approaches have proven extremely valuable, but the need to denature in order to trap raises questions about the true nature of the intermediate in its native state.

b. Inhibitors and mechanism-based inactivators

In place of extreme conditions, such as low temperature and high acidity, inhibitors and mechanism-based inactivators have been valuable in trapping covalent glycosyl-enzyme intermediates. By perturbing the rate at which the enzyme substrate intermediate is accumulated or broken down, it becomes possible to obtain this intermediate in a more native state. In conjunction with NMR and MS methods, these inhibitors have provided strong evidence for the existence of a covalent intermediate and the nucleophilic site of attachment for many glycosidases and glycosyl transferases.

i. Conduritol epoxides

The conduritol epoxides are a class of inhibitors which are believed to label catalytic carboxylates through protonation of the epoxide ring by a proton donating residue, followed by nucleophilic attack to form a covalent adduct, hence enzyme inactivation (Figure 1.9). These inactivators are similar to the epoxy glycosides but are believed to be more specific for active site carboxylates because nucleophile attack occurs at the position analogous to the anomeric center. A number of glycosidases have been inactivated by conduritol epoxides

(*37*). However, these reagents have been shown to occasionally label the acid/base catalyst instead of the nucleophile. For example, reaction of *E. coli* β-galactosidase with [^{3}H]-conduritol C *cis*-epoxide (**1.10**) resulted in the labelling of Glu461 and assignment of this residue as the nucleophile (*53*). It was later shown through the use of 2-deoxy-2-fluoro glycosides, a novel class of mechanism-based inactivators, that Glu537 was the nucleophile while Glu461 was proposed to be the acid/base catalyst (*54*).

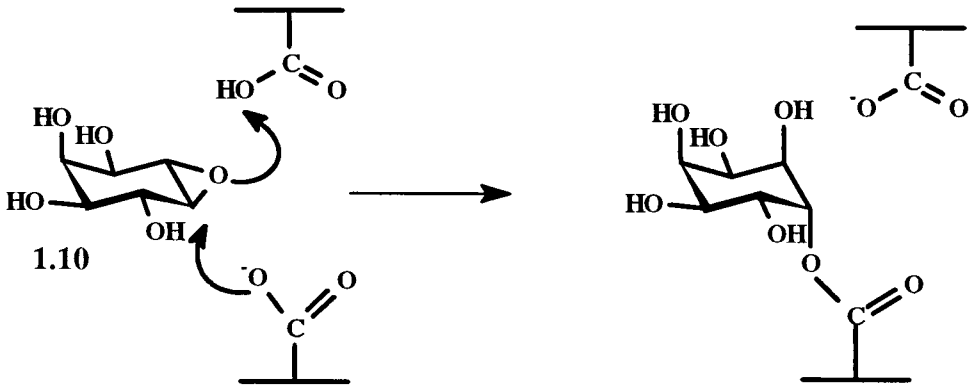

Figure 1.9 Mechanism of inactivation of β*-galactosidase by conduritol C cis-epoxide (**1.10**). (The residues involved in protonation and nucleophilic attack may not necessarily be the catalytic residues in the normal mechanism).*

ii. 2-Deoxy-2-fluoro glycosides

The 2-deoxy-2-fluoro glycosides have proven to be extremely valuable in providing evidence for the existence of a covalent glycosyl-enzyme intermediate in several retaining glycosidases and in identifying the catalytic nucleophile. The presence of an electron withdrawing fluorine at C-2 inductively destabilizes the oxocarbenium ion-like transition states of both the glycosylation and deglycosylation steps. The replacement of the hydroxyl group at C-2 also results in the disruption of important hydrogen bonding interactions which stabilize the transition state. Together, this results in a decrease of 10^5 to 10^8 fold in the rates of both glycosylation and deglycosylation (*30, 55*). However, the presence of a good leaving group

(typically 2,4-dinitrophenolate (DNP) or fluoride) helps to accelerate the glycosylation step, resulting in the accumulation of the glycosyl-enzyme intermediate. This trapped glycosyl-enzyme intermediate is catalytically competent and can be turned over in the presence of a suitable acceptor to give fully active enzyme. This strategy has been used successfully to identify the catalytic nucleophiles for many glycosidases (Table 1.1).

Table 1.1 Glycosidases that have been Inactivated and their Nucleophiles Identified with 2-Deoxy-2-Fluoro Glycosides

Glycosidase	Family	2-Deoxy-2-Fluoro Glycoside[1]	Reference
Agrobacterium sp. β-glucosidase	1	DNP2FβGlu	(*56*)
Bacillus circulans/subtilis xylanase	11	DNP2FβX2	(*57*)
Candida albicans exo-β-(1,3) glucanase	5	DNP2FβGlu	(*58*)
Cellulomonas fimi exoglycanase	10	DNP2FβC	(*59*)
Clostridium thermocellum CelC endoglucanase	5	DNP2FβC	(*60*)
E. coli β-galactosidase	3	DNP2FβGal	(*54*)
Fusarium oxysporum endoglucanase I	7	DNP2FβC	(*61*)
Human acid β-glucocerebrosidase	30	2FβGluF	(*62*)
Human lysosomal β-galactosidase	35	DNP2FβGal	(*63*)
Sweet almond β-glucosidase	1	2FβGluF	(*64*)
Thermoanaerobacterium saccharolyticum β-xylosidase	39	DNP2FβX	(*65*)

[1] DNP2FβGlu = 2,4-dinitrophenyl-2-deoxy-2-fluoro-β-D-glucopyranoside; DNP2FβGal = 2,4-dinitrophenyl-2-deoxy-2-fluoro-β-D-galactopyranoside; DNP2FβC = 2,4-dinitrophenyl-2-deoxy-2-fluoro-β-D-cellobioside; DNP2FβX2 = 2,4-dinitrophenyl-2-deoxy-2-fluoro-β-D xylobioside; DNP2FβX = 2,4-dinitrophenyl-2-deoxy-2-fluoro-β-D-xylopyranoside; 2FβGluF = 2-deoxy-2-fluoro-β-D-glucosyl fluoride.

The first nucleophile to be identified in this manner was Glu358 of *Agrobacterium* β-glucosidase (Abg) (*56*) (Figure 1.10). The reaction of Abg with 2,4-dinitrophenyl-2-deoxy-2-fluoro-β-D-glucopyranoside (DNP2FβGlu) (**1.11**) resulted in a glycosyl-enzyme intermediate whose half life was over 500 hours (*56*). The extended lifetime of this intermediate allowed its covalent nature and α-linkage to be proven by ^{1}H and ^{19}F NMR (*56, 66*). The identity of the nucleophile was conclusively demonstrated by inactivation of the enzyme with [1-^{3}H]-DNP2FβGlu, digestion with pepsin, isolation of the radiolabelled peptide and Edman sequencing (*56*).

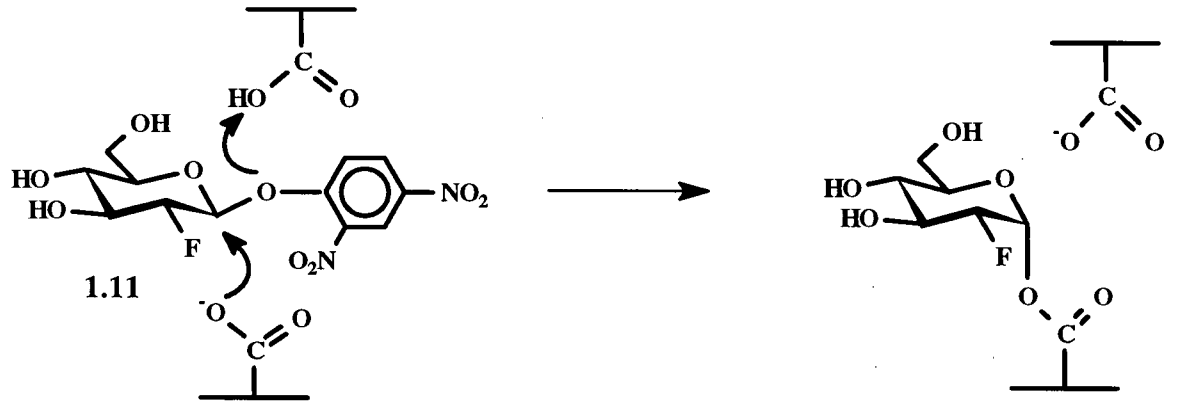

Figure 1.10 Identification of the active site nucleophile of Agrobacterium sp. β*-glucosidase using DNP2F*β*Glu (**1.11**)*

The long-lived nature of 2-deoxy-2-fluoro glycosyl enzyme intermediates has proven useful for crystallographic studies of the inactivator bound at the enzyme active site. Such a glycosyl-enzyme intermediate was observed for the retaining β-1,4 glycanase from *C. fimi* (Cex) co-crystallized in the presence of DNP-2-deoxy-2-fluoro-cellobioside (DNP2FβC) (*67*). Cleavage of the mechanism based inactivator, DNP2FβC, by Cex released dinitrophenol, permitting the formation of a covalent fluorocellobiosyl-enzyme species with Glu233, the

catalytic nucleophile. The resulting α-D-glucopyranosyl linkage to Glu233 was also supported by ^{19}F NMR studies.

From the list of glycosidases whose nucleophiles have been identified using 2-fluoro-sugars, it is obvious that this strategy has worked well for β-glycosidases, but has been less successful for α-retaining glycosidases or α-glycosyl transferases. For example, 2-deoxy-2-fluoro-α-maltosyl fluoride was found to act as a slow substrate for human pancreatic α-amylase and rabbit muscle glycogen debranching enzyme rather than as an inactivator (*68*). Apparently, the deglycosylation step for an α-glycosyl transferase is not slowed sufficiently by the substitution of fluorine at C-2 to allow accumulation of an intermediate. This may also indicate a fundamental difference in mechanism and charge development between β- and α-glycosidases (*26, 68*). Furthermore, the replacement of fluorine at C-2 makes this type of inhibitor less useful for those enzymes whose substrates are not amenable to substitution at that position (e.g. an *N*-acetylhexosaminidase). A solution to these problems was recently developed in our laboratory in an effort to provide a broader approach to the labelling of both β- and α-retaining glycosidases without compromising specificity through substitution of any ring hydroxyl, as detailed below.

iii. 5-Fluoro glycosides

5-Fluoro glycosides with a good leaving group such as fluoride might be expected to accumulate a 5-fluoro glycosyl-enzyme intermediate similar to the 2-deoxy-2-fluoro glycosyl-enzyme intermediate. A fluorine at C-5 in a pyranose ring is in an analogous position to the fluorine at C-2 as they are both adjacent to centers of developing positive charge. In the case of the 5-fluoro compound, the electron withdrawing fluorine is adjacent to the developing

positive charge of the ring oxygen while in the corresponding 2-deoxy-2-fluoro case, the fluorine is closest to the developing charge at C-1. It has been suggested through modelling studies that the greatest difference in partial charge between the ground state and the developing transition state actually occurs at O-5 rather than C-1 (*69, 70*). Therefore, if O-5 has the greatest positive charge development in the transition state then substitution of a fluorine at C-5 rather than at C-2 would serve to destabilize the transition state to a greater extent. This is further magnified since the fluorine at C-5 replaces a hydrogen while that at C-2 replaces a significantly electronegative oxygen. Thus, on electronic grounds, 5-fluoro glycosides might prove more advantageous than 2-deoxy-2-fluoro glycosides in trapping a glycosyl-enzyme intermediate. In addition, some of the reduction in the rates of glycosylation and deglycosylation with 2-deoxy-2-fluoro glycosides presumably results from the disruption in binding interactions as a consequence of the removal of the C-2 hydroxyl group. In comparison, substitution of the hydrogen at the 5-position with a relatively small fluoro moiety might be expected to result in less severe disruptions in binding affinity as the C-2 hydroxyl group is unaltered. Hence, for a given enzyme, the degree to which the glycosyl-enzyme intermediate will accumulate depends upon the relative importance of how a particular substitution affects the binding affinity for the substrate versus the charge development at the transition state. These considerations may provide a further means to manipulate the formation and breakdown of a glycosyl-enzyme intermediate.

The utility of the 5-fluoro strategy towards retaining β-glycosidases was first demonstrated using the two 5-fluoro epimers, 5-fluoro-β-D-glucosyl fluoride (5FβGluF, **1.12**) and 5-fluoro-α-L-idosyl fluoride (5FαIdoF, **1.13**) as inhibitors for *Agrobacterium* sp. β-glucosidase (*71*) (Figure 1.11). Incubation of either epimer with Abg resulted in a time-

dependent inactivation of the enzyme. This inactivation was shown to be active site-directed as protection from inactivation was provided by appropriate inhibitors known to bind at the active site. The competence of the glycosyl-enzyme intermediate was demonstrated by the recovery of activity after the enzyme was freed of excess inactivator. Mass spectral analysis of the intact protein incubated with either inactivator (5FβGluF or 5FαIdoF) demonstrated the attachment of one 5-fluoro glycosyl moiety per enzyme unit. Through additional mass spectrometry experiments involving the use of neutral loss methodology (see Section 2.3.4.1), the catalytic nucleophile, Glu358, was confirmed to be the site of attachment.

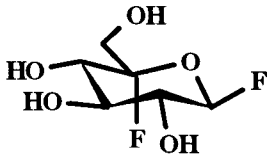

1.12

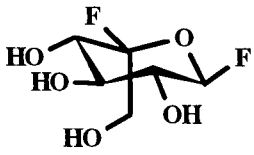

1.13

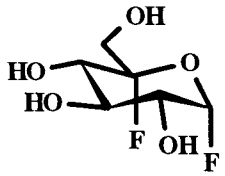

1.14

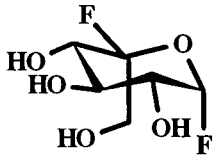

1.15

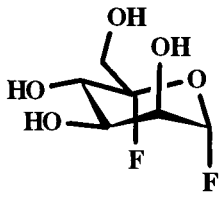

1.16

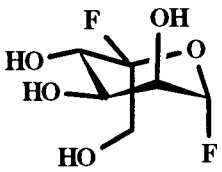

1.17

*Figure 1.11 Structures of 5-fluoro glycosides: 5F-β-D-GluF (**1.12**), 5F-α-L-IdoF (**1.13**), 5F-α-D-GluF (**1.14**), 5F-β-L-IdoF (**1.15**), 5F-α-D-ManF (**1.16**) and 5F-β-L-GulF (**1.17**). (Note: the compounds are not necessarily shown in their preferred conformation).*

The 5-fluoro approach proved useful in identifying the nucleophiles of several retaining α-glycosidases which had not previously been labelled by treatment with 2-deoxy-2-fluoro glycosides. Examples of α-glycosidases inactivated by 5-fluoro glycosides and their nucleophiles identified include (with the appropriate 5-fluoro glycoside in brackets): Yeast α-

glucosidase-Asp214 (5-fluoro-α-D-glucosyl fluoride (5FαGluF, **1.14**) and 5-fluoro-β-L-idosyl fluoride (5FβIdoF, **1.15**)) (*71*), jack bean α-mannosidase-Asp{numbered sequence not yet determined} (5-fluoro-α-D-mannosyl fluoride (5FαManF, **1.16**) and 5-fluoro-β-L-gulosyl fluoride (5FβGulF, **1.17**)) (Figure 1.11) (*72*).

iv. 2,2-Dihalo glycosides

In parallel with the evolution of the 5-fluoro strategy to overcome the limitations of the 2-deoxy-2-fluoro methodology, another set of mechanism based inactivators, the 2,2-dihalo glycosides, was developed. The relative ineffectiveness of 2-deoxy-2-fluoro glycosides in inactivation of α-glycosidases or glycosyl transferases was presumed to be a consequence of relatively rapid turnover of the glycosyl-enzyme intermediate preventing accumulation. To overcome this problem, it was proposed that the turnover of the intermediate could be further retarded by the introduction of a second halogen at C-2 (Figure 1.12). As the substitution of an additional halogen at C-2 would further slow the formation of the intermediate, the introduction of an extremely good leaving group, such as chloride or trinitrophenolate, was necessary.

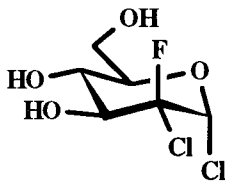

1.18

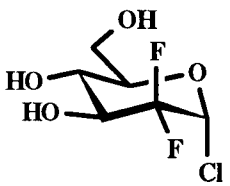

1.19

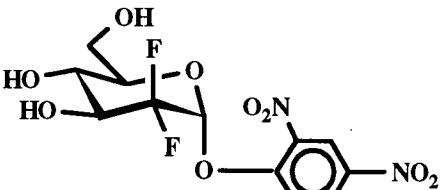

1.20

*Figure 1.12 Structures of 2,2-dihalo glycosides: 2-chloro-2-deoxy-2-fluoro-α-D-glucopyranosyl chloride (**1.18**), 2,2-difluoro-α-D-arabino-hexopyranosyl chloride (**1.19**) and 2,4,6-trinitrophenyl-2-deoxy-2,2-difluoro-α-D-arabino-hexopyranoside (**1.20**)*

A series of 2,2-dihalo-glycosides employing a chloride leaving group was synthesized and these were evaluated as potential inactivators of yeast α-glucosidase and jack bean α-mannosidase. Both 2Cl2FαGluCl (**1.18**) and 2,2FαAraCl (**1.19**) inactivated yeast α-glucosidase, but neither inactivated jack bean α-mannosidase despite the similarities in their mechanisms (*73*). The competitive inhibitor, deoxynojirimycin, protected α-glucosidase from inactivation by both **1.18** and **1.19**, thereby providing evidence for active site directed inactivation. After a prolonged period of incubation, no reactivation of yeast α-glucosidase activity was observed (over 10 days at 37°C for **1.18** in the presence of buffer and over 3 days at 37°C for **1.19** in the presence of buffer or with α-methyl glucoside as a possible transglycosylation acceptor), suggesting an extremely stable, long-lived glycosyl-enzyme intermediate in both cases.

Trinitrophenolate was also used as the leaving group in a pair of difluoro glycosides. TNP2,2FαGlu (**1.20**) was found to act as an inactivator of yeast α-glucosidase (*74*). This inactivation was determined to be active site-directed through protection experiments with 1-deoxynojirimycin (*68*). The corresponding trinitrophenyl difluoromaltoside derivative (structure not shown) was found to inactivate human pancreatic α-amylase (*68*). These results are significant in that they provide further evidence for the accumulation of a glycosyl-enzyme intermediate in retaining α-glycosidases and α-glycosyl transferases.

v. 4-Deoxy glycosides

Another strategy which has proven useful for identifying the catalytic nucleophile of several α-glycosyl transferases takes advantage of the key difference in the acceptor between the transferases and the glycosidases during the deglycosylation step. Whereas the

glycosidases utilize water as an acceptor, the transferases use the hydroxyl group of a second sugar molecule. For example, if the transferase of interest catalyzes the elongation of an oligosaccharide chain through the formation of an α-1,4 link, then the 4-hydroxyl group on the acceptor sugar acts as a nucleophile. Therefore, removal of the 4-hydroxyl group on the second substrate molecule will prohibit transfer and should result in accumulation of the intermediate, thereby allowing subsequent identification of the attachment site. The most suitable substitutions for the non-reducing 4-hydroxyl group are hydrogen (deoxy sugar) or fluorine (deoxy-fluoro sugar).

This approach was adopted to trap the intermediate formed with glycogen debranching enzyme, a retaining α-glycosyl transferase (*75*). The substrate employed, 4-deoxy-α-maltotriosyl fluoride (4DαG3F, **1.21**) contains a reactive fluoride leaving group, facilitating formation of the intermediate. However, the absence of an acceptor group 4-hydroxyl on the second substrate molecule results in accumulation of the intermediate, thereby allowing subsequent identification of the attachment site as Asp549 (Figure 1.13).

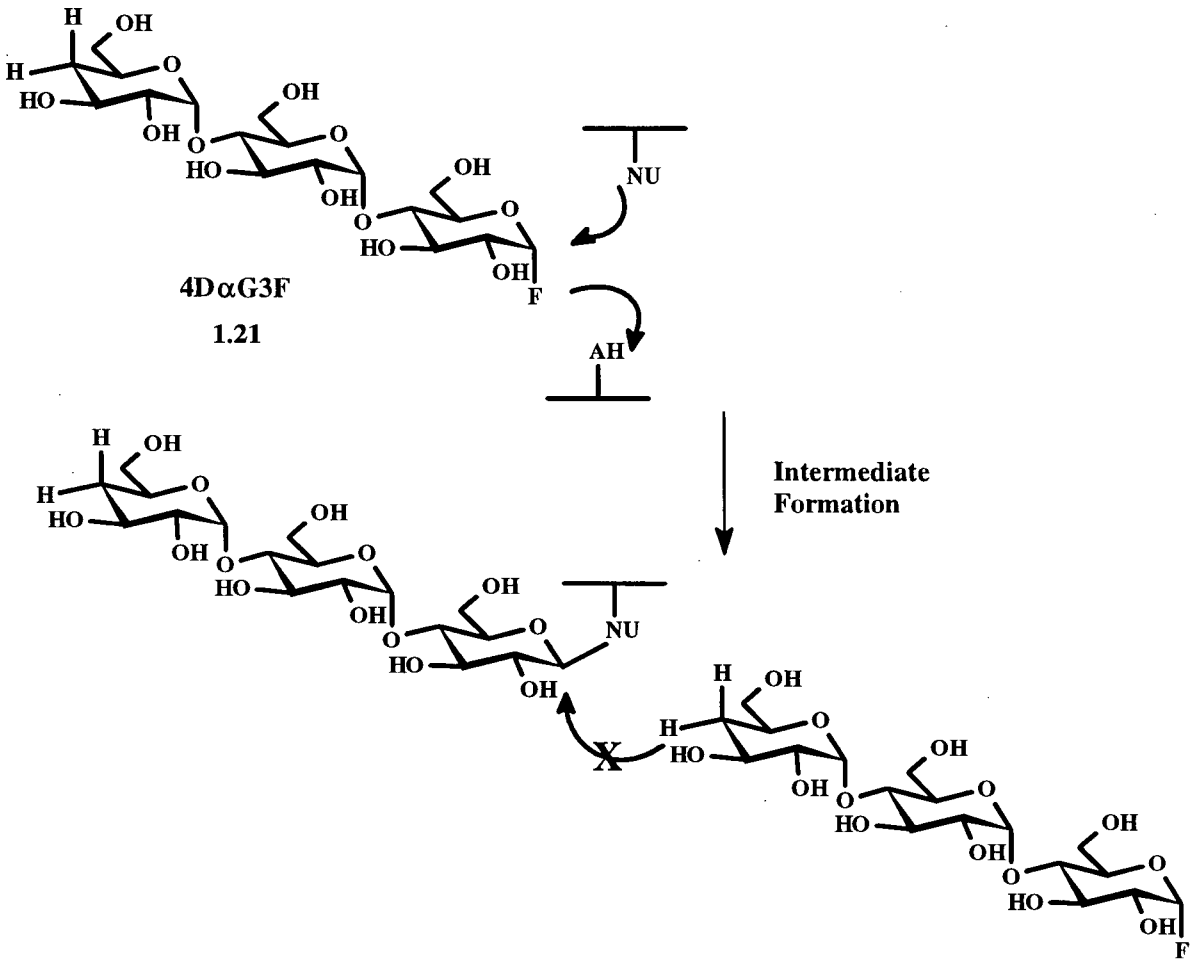

*Figure 1.13 General mechanism for the accumulation of a glycosyl-enzyme intermediate on a glycosyl transferase using an incompetent substrate, 4DαG3F (**1.21**)*

1.5 AIMS OF THIS THESIS

1.5.1 Overview

The focus of this thesis is the investigation of the chemical mechanisms of two enzymes involved in metabolizing polysaccharides, glycogen phosphorylase and cyclodextrin glycosyltransferase. Glycogen phosphorylase is the enzyme responsible for the degradation of glycogen, the body's storehouse of glucose. In contrast, the function of cyclodextrin glycosyltransferase is to convert starch to cyclic compounds and related glucose polymers.

While these enzymes catalyze the formation of two different products, both reactions are α-glycosyl transfers involving similar substrates. In an effort to further probe the nature of the reaction intermediate for both of these enzymes, modified substrates will be synthesized which can be used to "trick" each enzyme into catalyzing only the first half of its normal reaction. Through a combination of kinetic analysis, mass spectrometry, X-ray crystallography and NMR spectroscopy it is hoped that proof of the nature of the intermediate can be provided for both enzymes.

1.5.2 Specific Aims

1. *What is the nature of the intermediate in cyclodextrin glycosyltransferase?* This study follows a similar approach to that employed for the labelling and identification of the catalytic nucleophile of glycogen debranching enzyme. Through the use of 4-deoxy-α-maltotriosyl fluoride (**1.21**), a substrate which contains a good leaving group and which can therefore undergo the first step (glycosylation), but not the second step (deglycosylation), it should be possible to trap an intermediate, thereby allowing subsequent identification of the attachment site and hopefully structural analysis.

2. *What is the nature of the intermediate in glycogen phosphorylase?* The aim of this study is to probe the nature of the reaction intermediate in glycogen phosphorylase through the use of an incompetent analogue of glycogen, 4-deoxymaltohexaose in the presence of the co-substrate glucose-1-phosphate. The absence of the 4-hydroxyl group at the acceptor end of the sugar should prevent turnover of the intermediate, hopefully allowing it to be trapped. Through comparative studies with potato α-glucan phosphorylase, it is hoped that evidence of the nature of the reactive intermediate can be obtained.

CHAPTER 2

A MECHANISTIC STUDY OF CYCLODEXTRIN GLYCOSYLTRANSFERASE

2.1 GENERAL INTRODUCTION

2.1.1 Cyclodextrins

Cyclodextrins were first isolated in 1891 by Villiers as degradation products of starch and they were later characterized as cyclic oligosaccharides in 1904 by Schardinger (*76*). In this century there has been an ever-increasing interest in exploring the properties of cyclodextrins for their widespread use in many industrial applications.

α-, β-, and γ-cyclodextrins contain 6, 7 or 8 glucose units respectively linked α-1,4 to form a ring which contains no free 4-hydroxyl groups (Figure 2.1). They form inclusion complexes with smaller molecules which fit into their 5-8 Å cavity. These complexes are of interest because their hydrophilic exterior makes them readily soluble in water while their hydrophobic interior can stabilize many insoluble molecules. As a result, cyclodextrins can have important applications in the pharmaceutical, pesticide, foodstuff, and cosmetic industries (*77*). Moreover, the inclusion process provides many advantages to the stabilization of the encapsulated molecules, such as protection from light and atmosphere, improvement to solubility which is useful in creams and emulsifiers, as well as an improvement in handling and storage in a powder form. In addition, cyclodextrins, either free or in modified forms, are known to catalyze reactions such as ester hydrolysis, decarboxylation and oxidation and thus, they have been studied as enzyme models.

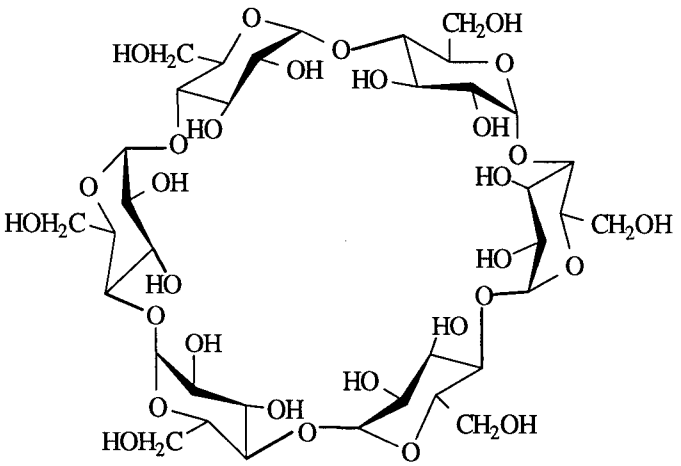

2.1

Figure 2.1 α-*Cyclodextrin*

2.1.2 Cyclodextrin Glycosyltransferases

The industrial production of cyclodextrins from starch is carried out enzymatically by a group of enzymes known as the cyclodextrin glycosyltransferases or CGTases. Over thirteen organisms, mostly *Bacillus* species, are now known to produce CGTases. As a result, increased effort has been made towards cloning and overexpressing the CGTase genes, as the industrial demand for cyclodextrins escalates. CGTases are classified as α, β, or γ according to the type of cyclodextrin formed initially. As the reaction continues, the other two forms of cyclodextrins are usually also synthesized. The enzymatic synthesis of cyclodextrins thus results in a mixture of products requiring lengthy and costly isolation and purification. A better understanding of the mechanism of action of CGTase is therefore required so that modifications to the synthetic method can be made which will increase the overall yield of the desired cyclodextrin. The enzyme used in this study, β-CGTase from *Bacillus circulans* 251, is currently used in the large scale production of β-cyclodextrin, a product which has

numerous industrial applications (*77*). Consequently, a detailed investigation of the three-dimensional structure of the enzyme and the mechanism of its transglycosylation reaction has been undertaken in an effort to improve yields and specificity, as follows.

2.1.3 Mechanism of Action

Cyclodextrin glycosyltransferases degrade starch into both linear or cyclic oligosaccharides by four distinct reactions. The main one is a cyclization reaction which generates a mixture of α-, β-, and γ-cyclodextrins. Other reactions catalyzed include disproportionation, linearization, and hydrolysis (Figure 2.2). Reaction in each case proceeds with retention of anomeric configuration and is believed to involve a two-step double displacement mechanism (see Section 1.3). In addition to the two active site carboxylates functioning as the nucleophile and general acid/base catalyst, a third conserved carboxylate is believed to function by modulating the ionization state of the other catalytic residues and producing a more favourable electronic environment for stabilization of the positively charged transition state.

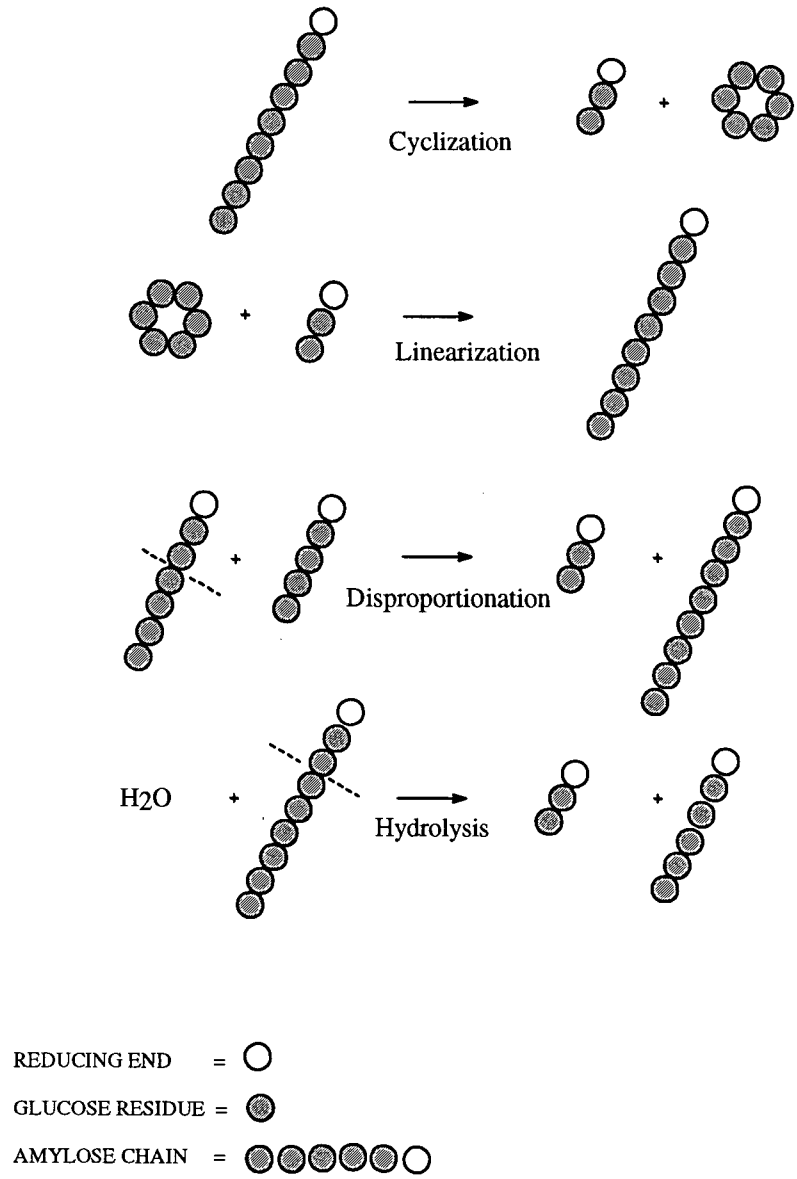

Figure 2.2 The reactions catalyzed by cyclodextrin glycosyltransferase. The glucose residues are linked together in an α-1,4 fashion.

2.1.4 Structural Information

Extensive progress has been made in recent years in elucidating the identity and function of the catalytic carboxylates in many α-glucosidases and α-glycosyl transferases by means of kinetic analysis, site-directed mutagenesis, and X-ray crystallography (see Section 1.4). The nucleotide sequence and 2.0 Å crystal structure of *B. circulans* 251 CGTase have

been reported (*78*) (Figure 2.3). The 75 kDa enzyme contains 686 amino acids folded into five domains, labelled A - E. Domains A - C are, together, structurally similar to the α-amylases. The active site of CGTase is located at the N-terminal side of the $(\beta/\alpha)_8$ barrel of domain A. The E-domain has been implicated in starch binding and is held in position with respect to domains A - C through an interconnecting region of β-sheet (domain D). On the basis of a structure of the enzyme complexed with acarbose (*79*), a potent inhibitor of α-amylases (K_i = 10 μM for pig pancreatic α-amylase (*80*)) and CGTases (K_i = 0.06 μM) (*81*)), and of complexes with natural substrates such as maltoheptaose and α-cyclodextrin (*82*), as well as a complex with a maltononaose inhibitor (*83*), the catalytic residues have been identified as Asp229, Glu257, and Glu328 (*Bacillus circulans* 251 numbering). In addition, sequence alignments with other members of the α-amylase family (Family 13) have shown that these three carboxylates are completely conserved within the consensus regions and align with other carboxylates which have already been identified as the catalytic residues (*9*). From these results, Glu257 was proposed to be the acid/base catalyst, Asp229 the catalytic nucleophile and Asp328 the third stabilizing residue as noted earlier. By means of site directed mutagenesis, three mutants, Asp229Asn, Glu257Gln and Asp328Asn, have been constructed and studied (*82*). All showed drastically reduced activities using natural substrates. In order to gain insight into the mode of substrate binding a double mutant, Asp229Asn/Glu257Gln, was constructed and crystallized in the presence of α-cyclodextrin and its three-dimensional structure solved (*82*). This structure showed Asp229 at a distance of 2.8 Å from the C-1 atom, thus close enough to act as the nucleophile, while Glu257 and Asp328 were somewhat farther away. A similar picture of substrate binding has been derived from structural studies on α-amylases (*80, 84-87*). Definitive identification and confirmation of the covalent nature

of the intermediate, however, requires that a reaction intermediate be trapped and characterized.

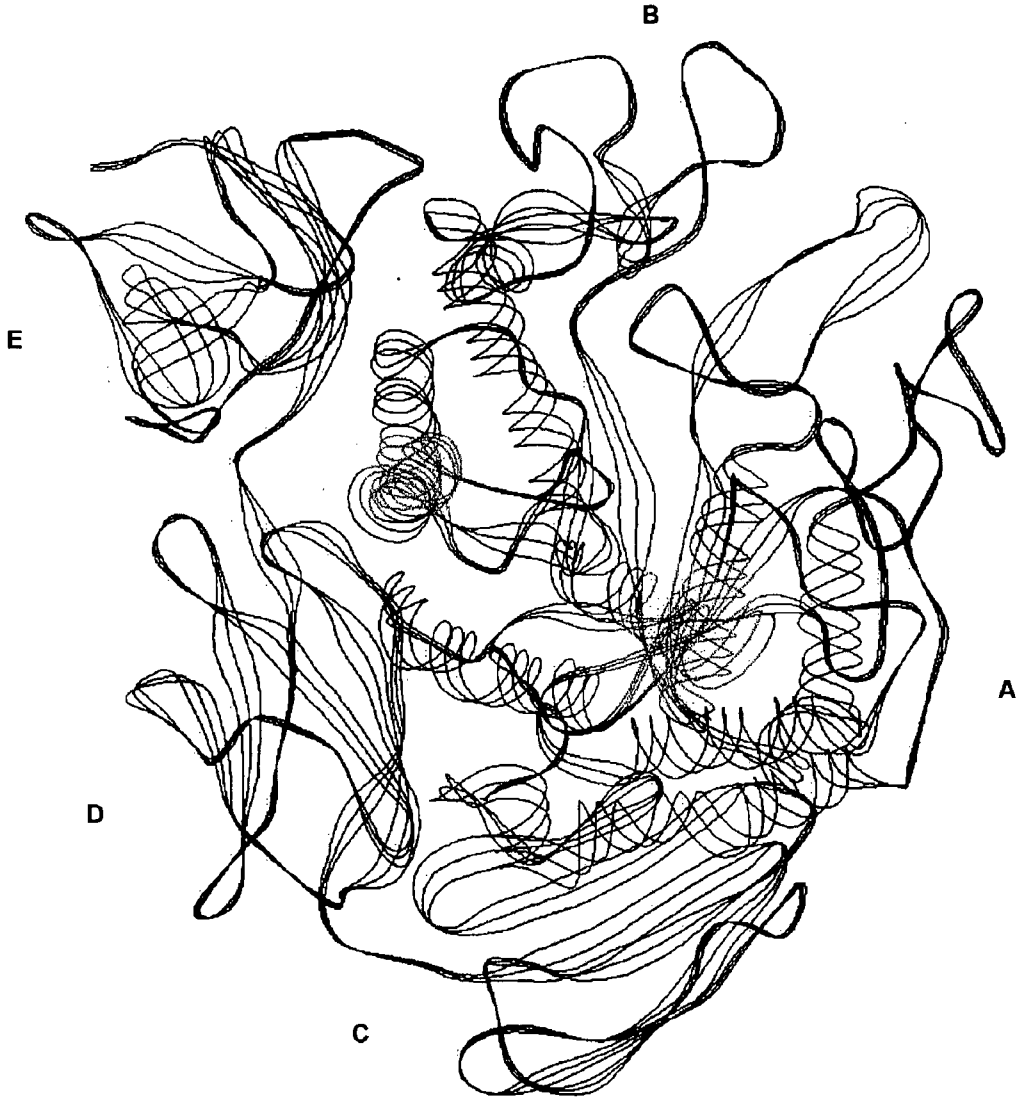

Figure 2.3 Stereo ribbon drawing of CGTase from B. circulans 251 (78). The domains of CGTase are labelled A-E.

2.2 THE SPECIFIC AIMS OF THIS STUDY

1. Can α-maltotriosyl fluoride act as a satisfactory substrate for CGTase? Previous evidence suggests that other glycosyl fluorides can act as good donors for CGTases in enzymatic synthetic reactions (*88*), but their activity has not been subject to kinetic analysis. Therefore, it seemed likely that α-maltotriosyl fluoride could be developed as a substrate for CGTase. The reaction could be easily assayed by following the enzyme catalyzed release of fluoride in a time-dependent fashion using an ion-selective fluoride electrode.

2. Can 4-deoxy-α-maltotriosyl fluoride (4DαG3F) act as an incompetent substrate for CGTase and be used to trap a covalent glycosyl-enzyme intermediate and provide proof of the identity of the nucleophile? The basis for this approach comes from the success of the strategy employed to trap the intermediate of glycogen debranching enzyme where 4DαG3F (**1.21**) was used because it could undergo the first step, formation of the glycosyl-enzyme intermediate, but not the second, transglycosylation to a second molecule of substrate (see Section 1.4.4.1) (*75*). The aim of this study was to apply a similar approach to the labelling and identification of the catalytic nucleophile of CGTase. Moreover, the use of 4DαG3F in crystallographic studies of the covalent intermediate bound to CGTase should provide valuable information concerning the mechanism of action of CGTase.

3. What are the mechanistic consequences of mutating the proposed acid/base catalyst, Glu257, and nucleophile, Asp229? Mutants have been constructed in which Glu257 has been replaced with a glutamine or an alanine and Asp229 has been replaced with an asparagine or an alanine (*82*). Kinetic studies indicated that these mutants had a much reduced level of

activity with the natural substrate, starch (*82*). In this study, the mutants will be evaluated using the synthetic glycosyl fluoride substrates, α-maltotriosyl fluoride and 4-deoxy-α-maltotriosyl fluoride, and the products of the reactions analyzed by HPLC. In addition, a kinetic analysis in the presence and absence of azide will be completed. This study, modeled after the method developed for β-glycosidases (*24, 89*) will be applied here for the first time to a retaining α-glycosyl transferase to probe the roles of Asp229 and Glu257.

4. What is the nature of the strong inhibition provided by the naturally occurring pseudotetrasaccharide, acarbose? Acarbose is known to be a potent inhibitor of CGTase (K_i = 0.06 μM) (*81*), but structural studies have cast doubt upon whether or not it is a transition state analogue (*79*). A useful way of determining whether a particular inhibitor is truly a transition state analogue or is just a fortuitously tight binding inhibitor involves probing the effects of modifications to the enzyme-substrate and enzyme-inhibitor complexes. One way in which such modifications can be achieved is to generate a series of modified enzymes, mutated at sites thought to play key roles in binding and catalysis. A number of CGTase mutants have previously been generated in the search for a CGTase with improved properties for the industrial production of cyclodextrins (*90, 91*). Therefore, this approach will be applied to CGTase by measuring k_{cat}/K_m values for both α-glucosyl fluoride and α-maltotriosyl fluoride and K_i values for acarbose with a series of active site mutants. The degree of correlation obtained from logarithmic plots of k_{cat}/K_m values versus K_i values for each substrate will provide an indication as to whether acarbose is truly a transition state analogue or not.

2.3 RESULTS AND DISCUSSION-PART 1

2.3.1 α-Glycosyl Fluorides as Substrates for Wild-Type CGTase

2.3.1.1 Synthesis of glycosyl fluorides

The glycosyl fluorides were synthesized by two different procedures as described in Section 4.1.2. The method adopted from Junnemann et al. (*92*) provides the most efficient route to all of the three glycosyl fluorides, α-maltotriosyl fluoride (αG3F), α-maltosyl fluoride (αG2F), or α-glucosyl fluoride (αGF), used in this study. The synthesis of α-maltotriosyl fluoride from maltotriose is shown in Scheme 2.1.

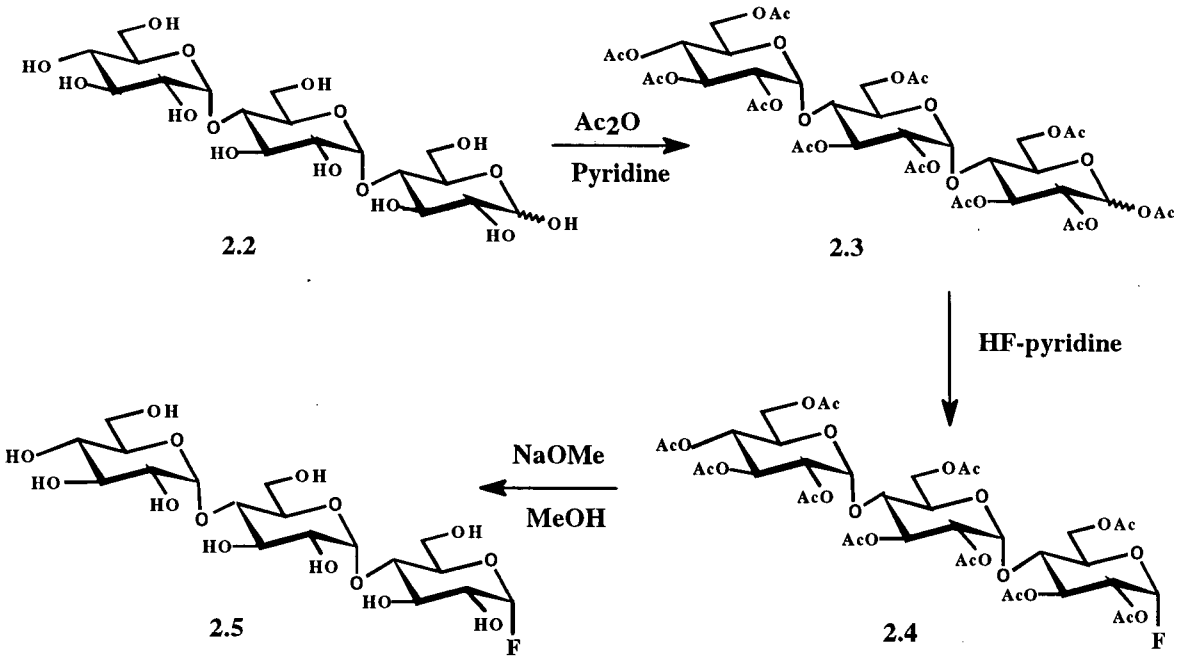

*Scheme 2.1 The synthesis of α-maltotriosyl fluoride (**2.5**) from maltotriose (**2.2**)*

2.3.1.2 Kinetic evaluation of α-glycosyl fluorides as substrates for wild-type CGTase

It was first necessary to evaluate whether or not glycosyl fluorides could act as reasonable substrates for CGTase. The enzyme-catalyzed release of fluoride could be followed in a continuous fashion by measuring the concentration of fluoride over time with a fluoride ion-selective electrode as described in Section 4.2.2. α-Maltotriosyl fluoride proved to be a good substrate for CGTase as shown in Table 2.1 (k_{cat} = 275 s^{-1} and K_m = 2.5 mM). This compares very well with an activity of 280 units/mg (where 1 unit of activity is defined as the amount of enzyme able to produce 1 μmol of βCD/min/mg of protein), which corresponds to a k_{cat} of 350 s^{-1} for the natural substrate, starch (*82*). Thus, although CGTase cannot normally use a trisaccharide as a substrate, the presence of the fluoride at the anomeric position as a good leaving group is sufficient to replace the transition state stabilization ordinarily provided by interactions between the enzyme and the oligosaccharide leaving group. Thus it serves as an activated substrate and eliminates the need for a longer oligosaccharide.

Table 2.1 Kinetic Constants Determined for the Reaction of *B. circulans* 251 Wild-Type CGTase with α-Glycosyl Fluorides

Substrate [1]	**K_m (mM)**	**k_{cat} (s^{-1})**	**k_{cat}/K_m ($mM^{-1}s^{-1}$)**
αG3F	2.5	275	111
αG2F	10.9	314	28.8
αGF	32.5	333	10.2

[1] Graphical representation of data is shown in Appendix B, Figure B-1.
Average errors in kinetic parameters: K_m (+/- 5 - 7%) and k_{cat} (+/- 5 %).

As shown in Figure 2.4, because CGTase can catalyze four different reactions, numerous products could arise from the reaction of CGTase with αG3F; however, the dominant process is expected to be transglycosylation. Thus, α-maltotriosyl fluoride acts as a glycosyl donor, forming a maltotriosyl-enzyme intermediate which can then react with another equivalent of α-maltotriosyl fluoride to form α-maltohexaosyl fluoride (αG6F) and so on to yield βCD and αG2F from αG9F.

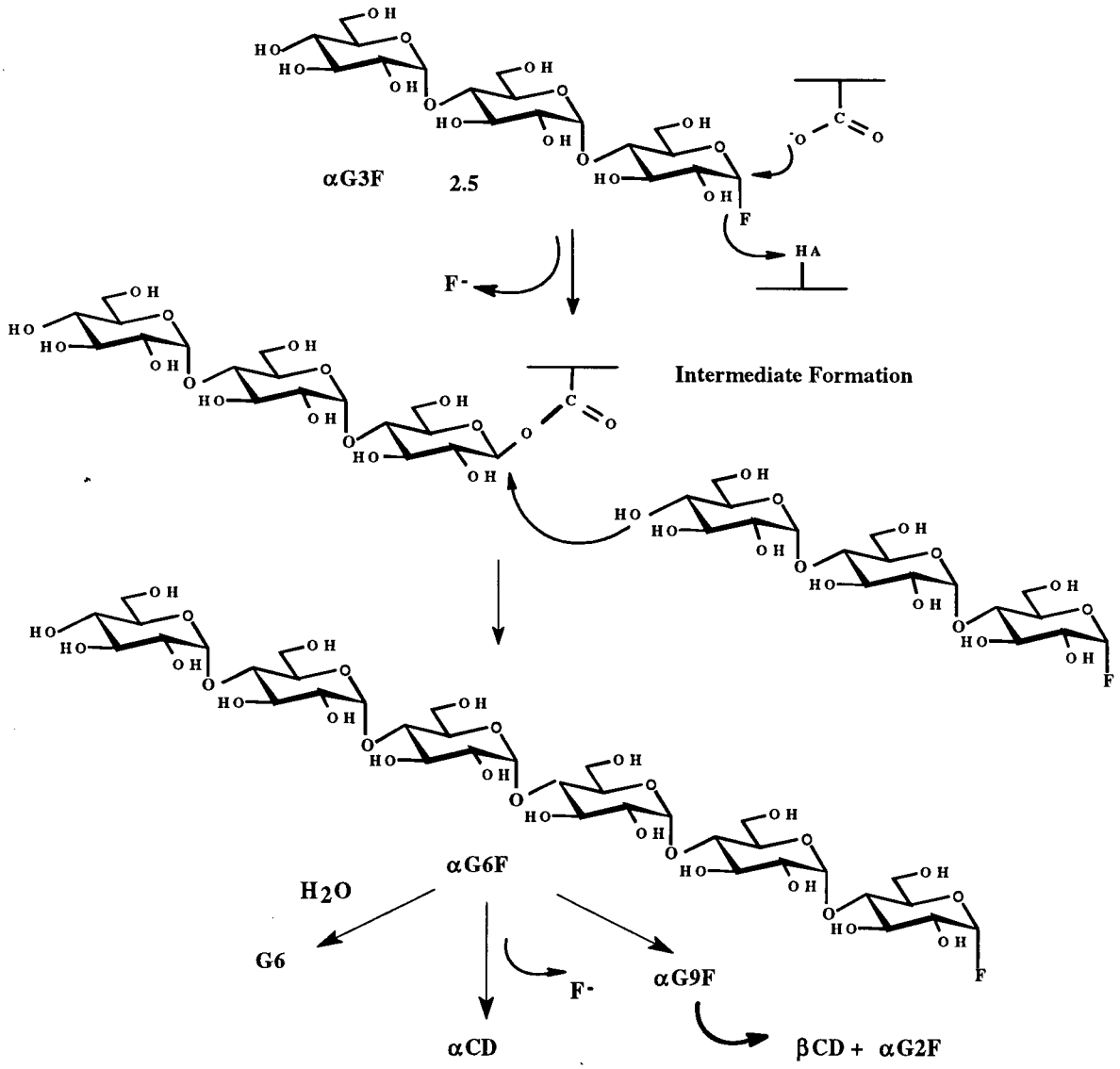

Figure 2.4 Possible reaction products resulting from the CGTase catalyzed reaction of αG3F

In order to investigate the types of products synthesized from αG3F by CGTase over time, reaction mixtures were subjected to HPLC analysis using a Dynamax-NH_2 linked silica HPLC column linked to an electrospray mass spectrometer. The dominant reaction occurring is, as predicted, transglycosylation to produce βCD (Figure 2.5A). After 1 h, the major products were βCD and a mixture of primarily longer oligosaccharides arising from a variety of cyclization, linearization and disproportionation reactions (Figure 2.5B). Thus, the dominant reaction occurring is shown to be transglycosylation to produce longer malto-oligosaccharyl fluorides, followed by cyclization, rather than direct hydrolysis to yield G3.

Two other glycosyl fluorides were investigated as substrates for *B. circulans* CGTase. As seen in Table 2.1, both α-glucosyl fluoride (αGF) and α-maltosyl fluoride (αG2F) served as substrates, but with reduced efficiencies compared to αG3F, as seen in k_{cat}/K_m values. Interestingly, the k_{cat} values for the three substrates were similar indicating that, once bound, there was no particular advantage in a longer oligosaccharide: the progressive decrease in k_{cat}/K_m arose from changes in K_m values. While the lower K_m values for the longer substrates most likely reflect an increase in affinity due to the presence of the additional sugar residues, they could also, to some extent, reflect an increase in the rate of the glycosylation step relative to deglycosylation as sugar residues are added, with the consequence of reduced K_m values. An equivalent situation was observed with the exoglycanase Cex from *Cellulomonas fimi* when substrates of different sizes were studied (*27*). Whatever the substrate employed, due to the transglycosylation processes occurring, over an extended period of time βCD was the major product observed as seen in Figure 2.5C for the reaction of CGTase with αG2F and Figure 2.5D for the reaction of CGTase with αGF. Therefore, because αG3F showed the

best binding to CGTase and was readily available, it was chosen as the standard substrate with which to assay the enzyme.

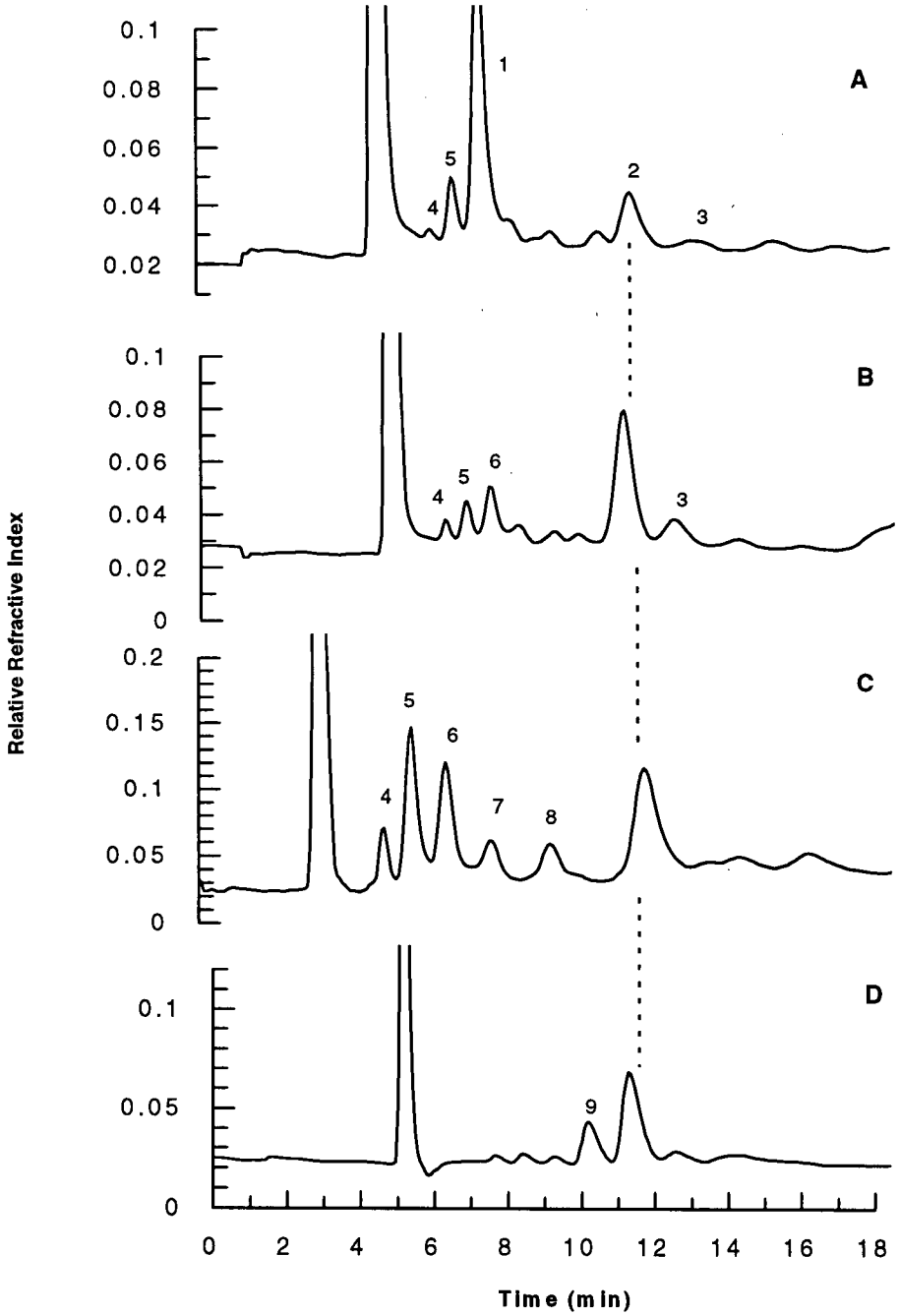

Figure 2.5 HPLC analysis of the products of the reaction of wt CGTase with (A) αG3F after 15 min reaction time, (B) αG3F after 1 h reaction time, (C) αG2F after 1 h reaction time, (D) αGF after 1 h reaction time. (1 = αG3F, 2 = βCD, 3 = γCD, 4 = αGF, 5 = αG2F, 6 = G, 7 = G2, 8 = G3, 9 = αCD). Conditions: Dynamax column, 0.8 mL/min 60/40 CH_3CN/H_2O.

2.3.2 4-Deoxy-α-Maltotriosyl Fluoride as an Incompetent Substrate for Wild-Type CGTase

2.3.2.1 Synthesis of 4-deoxy-α-maltotriosyl fluoride

The synthesis of 4-deoxy-α-maltotriosyl fluoride (**1.21**) was adapted from the method of Lindhorst et al. (*93*). The sequence of reactions and reagents employed for the transformations was identical to that used previously (Scheme 2.2). However, modifications in reaction times and temperatures for several of the steps resulted in significant improvements in yields. In particular, the yield of the HF-pyridine anomerization step was increased from 64% to 80%. Although it is possible to obtain the α-fluoro anomer directly from the per-*O*-acetylated oligosaccharide by reaction with HF-pyridine as shown in Scheme 2.1, such a procedure is not effective for the fluorination of the per-*O*-acetylated 4-deoxymaltotriose (**2.11**). Substitution of the non-reducing 4-hydroxyl group with a hydrogen results in the α-1,4 bond linking that sugar and the middle sugar becoming more susceptible to hydrolysis than in the parent compound, maltotriose. This is consistent with the 27 fold faster hydrolysis of 4-deoxy glycosides observed previously (*94*). This hydrolysis reaction is less significant when the 4-deoxy sugar is first fluorinated with DAST to give an α/β mixture followed by treatment with HF-pyridine at a lower temperature to yield the α-anomer.

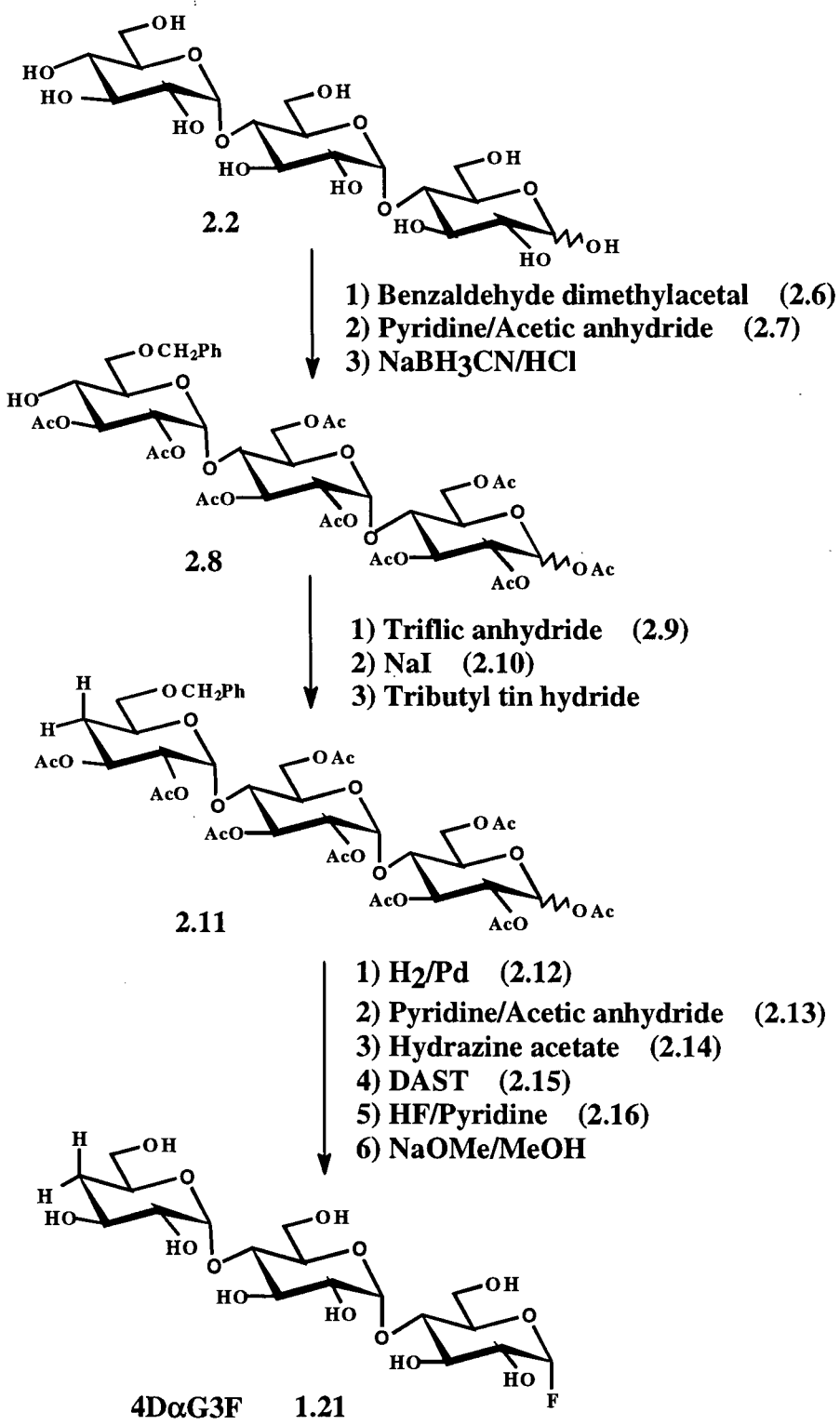

Scheme 2.2 Synthesis of 4-deoxy-α-maltotriosyl fluoride

2.3.2.2 Evaluation of 4-deoxy-α-maltotriosyl fluoride as an incompetent substrate for wild-type CGTase

Based upon the findings with αG3F it was assumed that 4-deoxy-α-maltotriosyl fluoride (4DαG3F) should function as an incompetent substrate for CGTase as its nucleophilic 4-hydroxyl was missing, allowing the 4-deoxymaltotriosyl-enzyme intermediate to form but then no further transglycosylation to occur as shown in Figure 2.6.

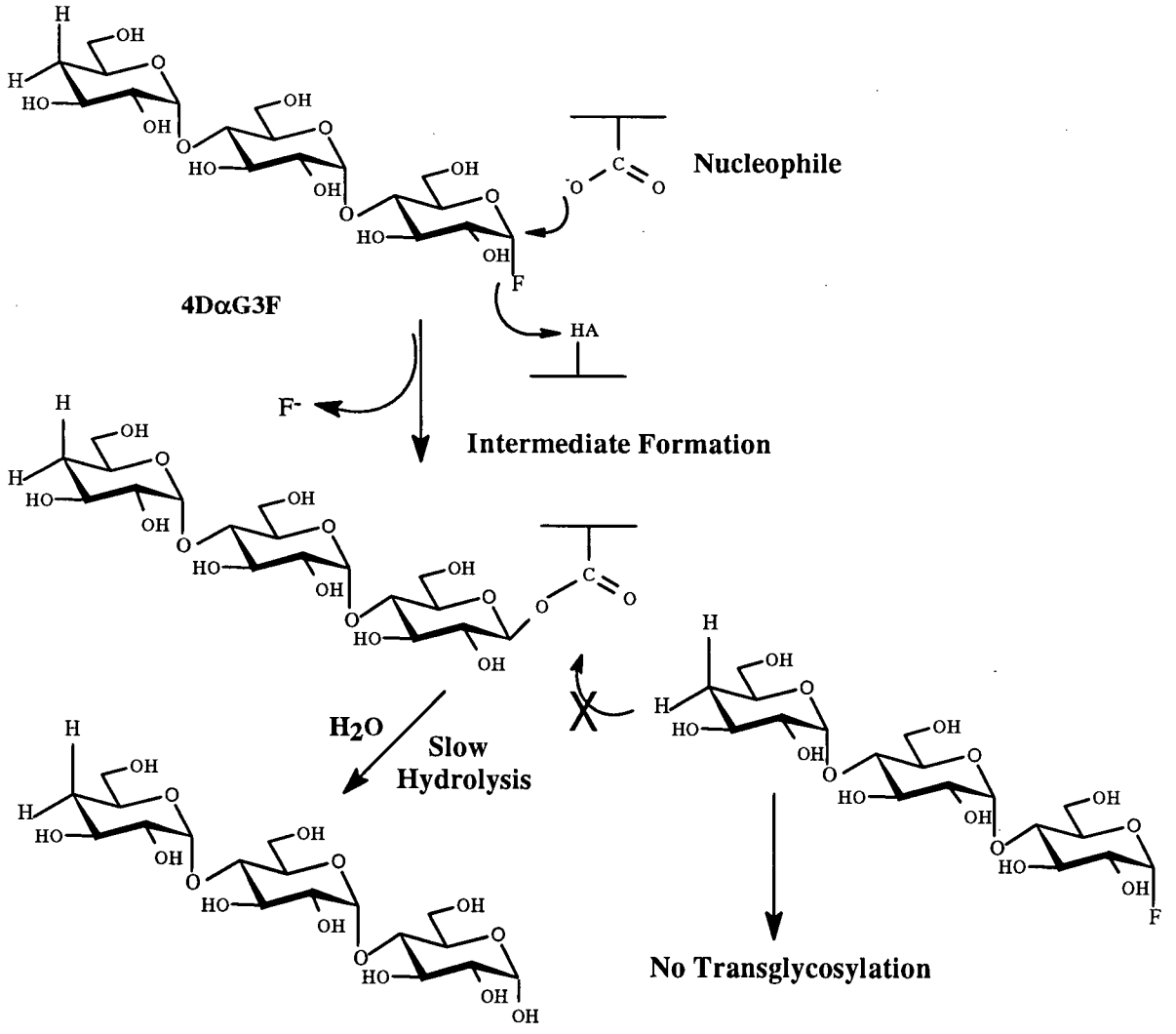

Figure 2.6 Mechanism for the accumulation of an intermediate on CGTase in the presence of 4DαG3F and subsequent turnover via hydrolysis

However, as seen in Table 2.2, 4DαG3F does indeed act as a substrate, albeit slow, indicating that the enzyme intermediate still does turnover to a significant extent. The question of how this turnover occurs was resolved by HPLC analysis of reaction products as shown in Figure 2.7. 4-Deoxymaltotriose (4DG3) was the major product, resulting from simple hydrolysis of the maltotriosyl-enzyme intermediate (Figure 2.7A). However, over time, although the retention times of the peaks did not change, small amounts of the disproportionation products, G1, G2, and 4DG2 were detected by ES-MS, arising from cleavage within the oligosaccharide moiety (Figure 2.7B).

Table 2.2 Kinetic Constants Determined for the Reaction of *B. circulans* 251 Wild-Type CGTase with 4-Deoxy-α-Glycosyl Fluorides

Substrate [1]	K_m (mM)	k_{cat} (s^{-1})	k_{cat}/K_m ($mM^{-1}s^{-1}$)
4DαG3F	0.073	2.0	27.5
4DαG2F	1.3	8.8	6.76
αG3F [2]	2.5	275	111
αG2F [2]	10.9	314	28.8

[1] Graphical representation of data is shown in Appendix B, Figure B-1.
[2] Reported previously in Table 2.1 and presented here for comparison purposes.

Kinetic analysis gave a K_m value of 0.073 mM, which is approximately 35 times lower than that for αG3F (Table 2.2). In terms of strength of binding, αG3F and 4DαG3F are probably not structurally different enough to cause such differences in K_m values. Instead, because K_m is not only a reflection of the strength of binding of a substrate, but also represents a combination of individual rate constants for the reaction, such a decrease in K_m probably

reflects a change in the relative ratios of the rate constants for the separate steps of the reaction (see Appendix A). The removal of the 4-hydroxyl group prevents transfer to this position, thus should result in a decrease in k_3, the rate constant for the second chemical step in the reaction. This is also reflected in the lower k_{cat} value (reduced over 100 fold) for 4DαG3F consistent with reaction occurring only via the hydrolysis pathway. The equivalent disaccharide substrate, 4-deoxy-α-maltosyl fluoride (4DαG2F) was also tested as a substrate for wt CGTase. The K_m value for 4DαG2F was reduced 8 fold from that of αG2F, while the k_{cat} was reduced 35 fold. HPLC analysis of the products of the reaction of wt CGTase with 4DαG2F revealed that hydrolysis was the dominant process to yield 4-deoxymaltose (4DG2), with a small amount of disproportion to yield 4-deoxyglucose (4DG) and glucose (G) (Figure 2.7C). Unfortunately, the relatively short half life, $t_{1/2}$ = 0.5 s (4DαG3F) or $t_{1/2}$ = 0.1 s (4DαG2F) of either intermediate precluded any investigation by mass spectrometry necessitating some additional measures to increase its lifetime.

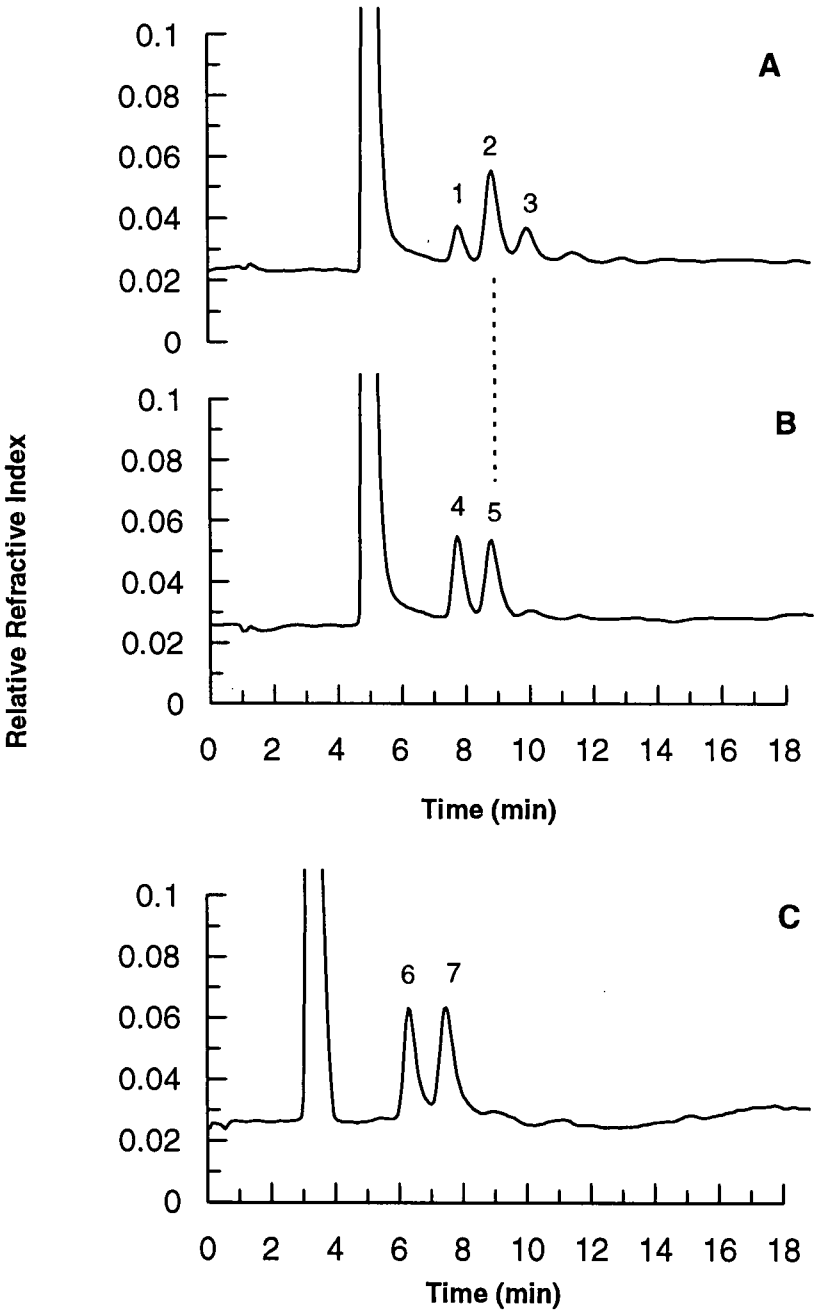

*Figure 2.7 HPLC analysis of the products of the reaction of wt CGTase with (**A**) 4DαG3F after 15 min reaction time, (**B**) 4DαG3F after 1 h reaction time, (**C**) 4DαG2F after 1 h reaction time. (1 = 4DαG3F, 2 = 4DG3, 3 = 4DG4, 4 = G/4DG2, 5 = G2/4DG3, 6 = 4DG, 7 = G/4DG2). Conditions: Dynamax column, 0.8 mL/min 60/40 CH_3CN/H_2O. (Note: Profiles A and B cannot be directly overlapped with C as two separate columns were used).*

2.3.3 Investigation of Glu257Gln and Glu257Ala CGTase

A solution to the problem of the still relatively fast hydrolysis of the accumulating intermediate lay in a mutant of the presumed acid/base catalyst, Glu257. Two mutants at position 257, Glu257Gln and Glu257Ala, had been previously generated by our collaborators at the University of Groningen. In earlier work with cellulases and β-glucosidase (*25, 89*), it had been shown that by removing the acid/base catalyst and using a substrate such as a glycosyl fluoride with a good leaving group the intermediate could be readily accumulated. This occurs because the leaving group does not need acid catalysis, thus, despite the absence of an acid catalyst, the first step is still fast. However, since that side chain also serves as the general base catalyst for the second step, deglycosylation is slowed, allowing an accumulation of the intermediate. Thus, it was believed that the combination of a presumed acid/base catalyst mutant of CGTase, such as Glu257Gln or Glu257Ala, with an incompetent substrate such as 4DαG3F should provide a means to accumulate an intermediate of longer lifetime.

2.3.3.1 α-Maltotriosyl fluoride as a substrate for Glu257Gln and Glu257Ala CGTase

As a first step, turnover of the substrate, αG3F, by Glu257Gln was investigated. Using the fluoride electrode to monitor the time dependent release of fluoride ion, αG3F was found to be a substrate for Glu257Gln CGTase as shown in Table 2.3, but with significantly reduced k_{cat} and K_m values. The k_{cat} was reduced almost 300 fold and K_m was reduced 7 fold compared with wild-type, thus k_{cat}/K_m was reduced 40 fold.

The K_m value for αG3F with Glu257Ala was found to be almost 2 fold lower than that of the wt CGTase. This reduction in K_m likely reflects the accumulation of an intermediate. However, the K_m value for αG3F with Glu257Ala is 4 fold higher than the K_m measured for

Glu257Gln CGTase. This might reflect a disruption in binding affinity resulting from the substitution of a glutamic acid with an alanine. In comparison, the substitution of a glutamic acid residue with a glutamine is likely to result in less severe disruptions in binding affinity. These differences in the K_m values between the two Glu257 mutants may also reflect a change in the relative ratio of rate constants for the 2 steps of the reaction. Reductions of about 5 fold in k_{cat} for Glu257Ala from that obtained for Glu257Gln and 1.5 x 10^3 fold from wild-type were observed. These reductions are about average when compared with the activities measured for similar mutations in β-glycosidases. For example, only a 70-100 fold reduction in activity was noted upon mutating the acid/base catalyst (Glu172) in *B. circulans* β-xylanase to Gln (*95*). However, k_{cat} reductions in the range of 200 to 2000 fold from wild-type have been measured for similar mutations in other β-retaining glycosidases (*25, 89*).

Table 2.3 Kinetic Parameters for the Reaction of *B. circulans* Glu257Gln and Glu257Ala CGTase with α-Glycosyl Fluorides

Enzyme	Substrate [1]	K_m (mM)	k_{cat} (s^{-1})	k_{cat}/K_m ($mM^{-1}s^{-1}$)
wt [2]	αG3F	2.5	275	111
wt [2]	4DαG3F	0.073	2.0	27.5
wt [2]	4DαG2F	1.3	8.8	6.76
Glu257Gln	αG3F	0.37	1.0	2.70
Glu257Ala	αG3F	1.6	0.18	0.11
Glu257Gln	4DαG3F	0.027	0.6	22.2
Glu257Gln	4DαG2F	0.33	1.1	3.33

[1] Graphical representation of data is shown in Appendix B, Figure B-2.
[2] Reported previously in Tables 2.1 and 2.2 but presented here for comparison purposes.

HPLC analysis of products of the reaction catalyzed by Glu257Gln showed a slightly different pattern to that seen with the wild-type enzyme. Although βCD was the main cyclization product obtained, considerably more enzyme catalyzed hydrolysis occurred, producing maltotriose. In addition, a lower percentage of disproportionation products was obtained, indicating a change in the reactions catalyzed (Figure 2.8A). HPLC analysis of the products of the reaction of Glu257Ala with αG3F showed that an almost equivalent amount of transglycosylation product, αCD, and hydrolysis product, G3, were made (Figure 2.8B).

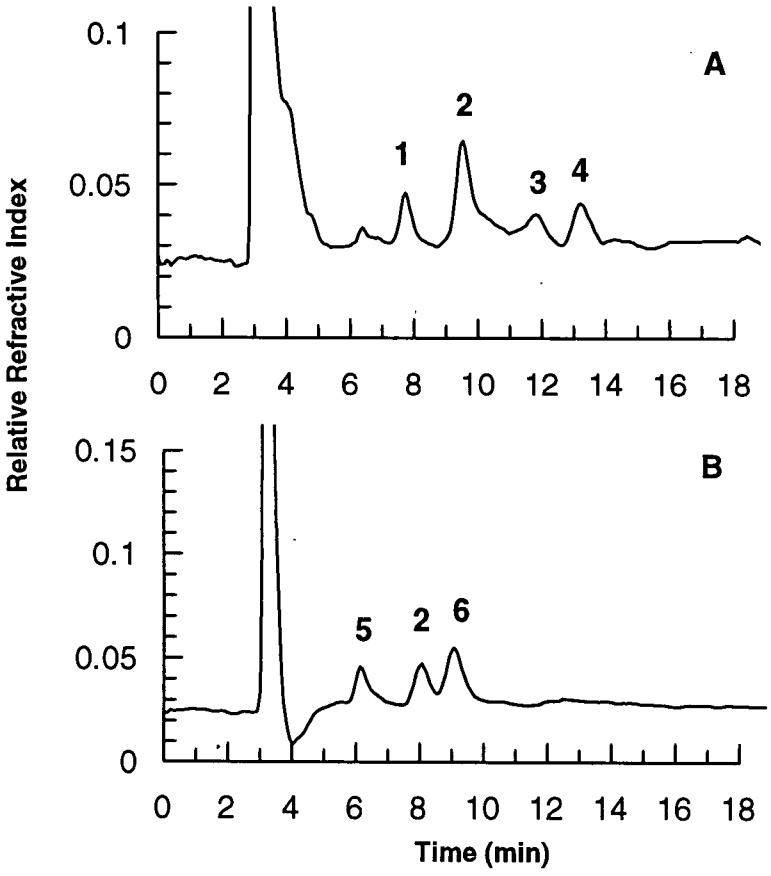

Figure 2.8 HPLC analysis of the reaction products of the acid/base catalyst mutants with αG3F. (A) Glu257Gln and αG3F after 1 h reaction time, (B) Glu257Ala and αG3F after incubation overnight (1 = G2, 2 = G3, 3 = G4, 4 = βCD, 5 = αG3F, 6 = αCD). Conditions: Dynamax column, 0.8 mL/min 60/40 CH_3CN/H_2O. (Note: profiles A and B cannot be directly overlapped as two separate columns were used).

2.3.3.2 4DαG3F and 4DαG2F as incompetent substrates for Glu257Gln

The Glu257Gln mutant was chosen as an initial point from which to begin our investigations with the incompetent substrates 4DαG3F and 4DαG2F as the substitution of a glutamic acid residue with a glutamine is likely to result in less severe binding disruptions than substitution with an alanine. Mutation of the acid/base catalyst, Glu257, to Gln resulted in a reduction of 2.7 fold in K_m for 4DαG3F and 3.9 fold in K_m for 4DαG2F (Table 2.3). The value of K_m for 4DαG3F was reduced over 10 fold when compared with the reaction of Glu257Gln CGTase with αG3F. It seems likely that these reductions in the values of K_m are due to the accumulation of a glycosyl-enzyme intermediate. The k_{cat} value for 4DαG3F was reduced by a factor of 3.3 fold over that for the wild-type enzyme while the k_{cat} value for 4DαG2F was reduced 8 fold indicating a surprisingly small apparent contribution of Glu257 to the general base catalyzed hydrolysis pathway. This finding is further discussed in Section 2.3.6. Interestingly, the k_{cat} values for αG3F and 4DαG3F with Glu257Gln are very similar, consistent with the idea that the reaction occurring is primarily hydrolysis and not transglycosylation in both cases. The half life ($t_{1/2}$) of the 4DG3-enzyme intermediate was estimated to be 1.1 s from the k_{cat} value. HPLC analysis of the products of the reaction of Glu257Gln CGTase with 4DαG3F showed only 4DG3 as a major product (Figure 2.9A) and essentially no disproportionation products, even after overnight incubation. This is in contrast to the disproportionation observed with wt CGTase and 4DαG3F (Figure 2.7B). Similarly, the only product of the reaction of Glu257Gln CGTase with 4DαG2F was that arising from the hydrolysis of the starting material (Figure 2.9B).

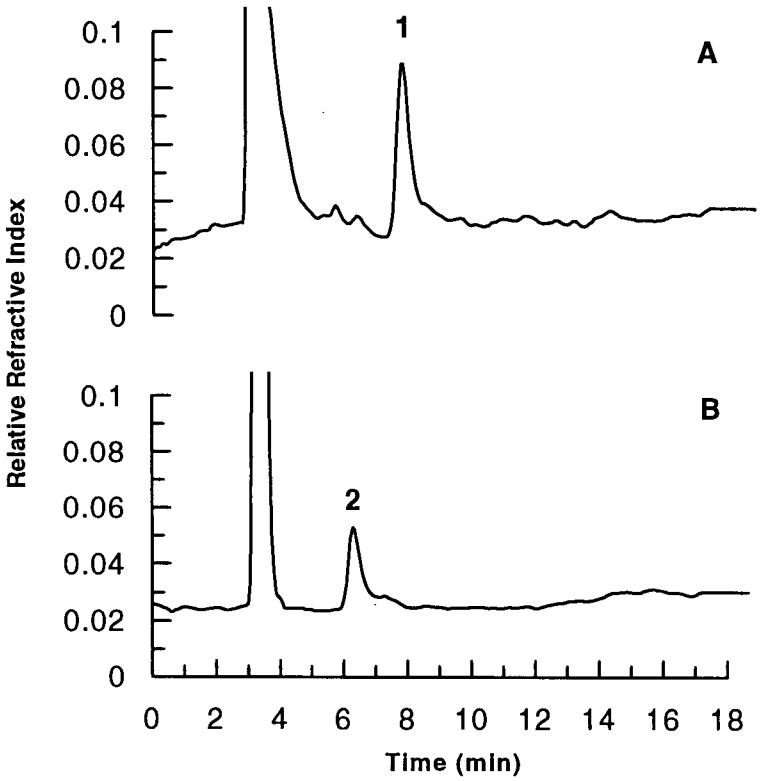

Figure 2.9 HPLC analysis of the reaction products of Glu257Gln CGTase with (A) 4DαG3F after 1 h reaction time, (B) 4DαG2F after 1 h reaction time (1 = 4DG3, 2 = 4DG2). Conditions: Dynamax column, 0.8 mL/min 60/40 CH_3CN/H_2O.

2.3.4 Mass Spectrometric Evidence for a Covalent Enzyme-Substrate Intermediate

Upon incubation of Glu257Gln CGTase (Figure 2.10A) with an excess of 4DαG3F an increase in molecular weight equivalent to a 4DG3 moiety on the intact protein {(74,513 + 471) +/- 5 Da} was observed by ES-MS (Figure 2.10B). The equivalent disaccharide, 4DαG2F also acted as an incompetent substrate and similar ES-MS analysis of Glu257Gln CGTase incubated with 4DαG2F revealed a mass increase of {(74,513 + 309) +/- 5 Da} consistent with the formation of a 4DG2-enzyme complex (Figure 2.10C). The turnover rate for the reaction of αG3F with Glu257Gln was also low enough that accumulations of both a G3 moiety on the intact protein {(74,513 + 487) +/- 5 Da}, and a G6 moiety {(74,513 + 973) +/- 5 Da} were observed by ES-MS (Figure 2.10D).

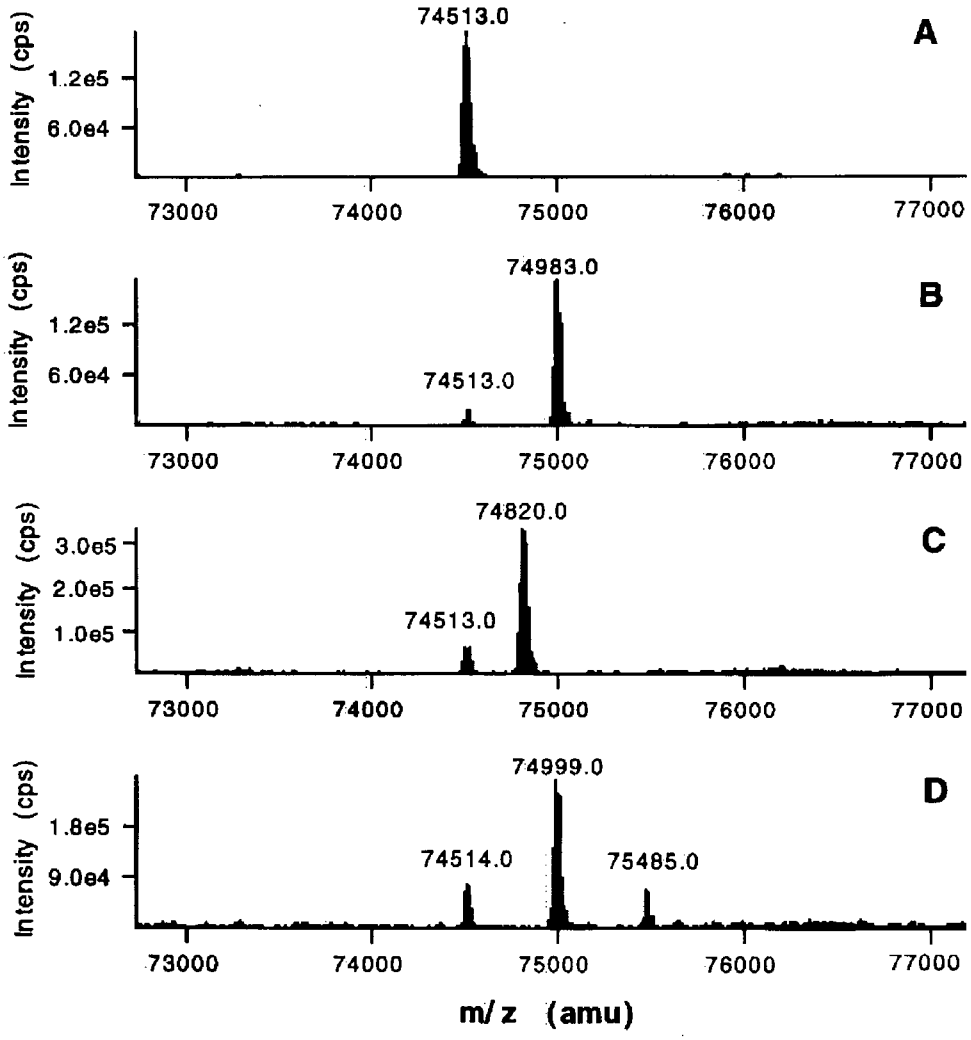

Figure 2.10 Electrospray mass spectra of (A) intact Glu257Gln CGTase (3 mg/mL) incubated for 5 min with (B) 4DαG3F (62.5 mM), (C) 4DαG2F (62.5 mM), and (D) αG3F (62.5 mM).

2.3.4.1 Identification of the peptide containing the nucleophile

Identification of the attachment site of the 4-deoxy-maltotriosyl label was achieved by labelling, peptic digestion, and neutral loss tandem mass spectrometry (*57*). In this mass spectrometry technique, ions are subjected to limited fragmentation by collisions with an inert gas (nitrogen) in a collision cell located between the two mass analyzers Q1 and Q3. Because the ester linkage between the inhibitor and the peptide is one of the more labile linkages present, facile homolytic cleavage of this bond occurs resulting in the loss of the sugar as a neutral species, with the peptide retaining its original charge. The mass spectrometer is then set so that Q1 and Q3 are scanned in a linked manner such that only those ions that lose the mass of the lost sugar moiety can pass through both quadrupoles and be detected.

The 4DG3-labelled Glu257Gln mutant and a control (not exposed to 4DαG3F) were digested using pepsin. The resulting peptide mixtures were separated by reverse phase HPLC using the ES-MS as a detector, revealing a large number of peptides (Figure 2.11A). The peptide with the 4DG3 label was located by MS/MS analysis using the neutral loss experiment. The spectrometer was first scanned in the neutral loss mode searching for a peptide which loses a neutral species of 471 Da, which corresponds to the mass of the 4-deoxy-maltotriosyl label. However, no significant peaks were detected. When the spectrometer was scanned for the mass loss of m/z 235.5, corresponding to the loss of a sugar from a doubly charged peptide, two strong peaks were observed, labelled peptides 1 and 2 (Figure 2.11B). These 2 peaks, having retention times of 35.75 min and 37.5 min and m/z values of 1075.5 Da and 1140.5 Da respectively, were not seen in the control digest (Figure 2.11C) and presumably represent two different 4-deoxy-maltotriosyl-labelled peptides. Because the doubly charged labelled peptides have m/z values of 1075.5 Da (Figure 2.11D)

and 1140.5 Da (Figure 2.11E), the singly charged unlabelled peptides must have masses of 1679 [(2 x 1075.5) - 2 - 471 + 1 H] and 1809 [(2 x 1140.5) - 2 - 471 + 1 H]. A computer generated search of all possible peptides in the Glu257Gln CGTase mutant yielded 18 possible peptides with molecular weight 1679 +/- 2 Da and 34 possible peptides with molecular weight of 1809 +/- 2 Da. Of these, 7 sets of peptides contained overlapping amino acid sequences. It is assumed that the two peptides arise from different modes of proteolysis of the same labelled protein since only a single oligosaccharide was initially attached. When CGTase was incubated with 4DαG2F, digested and analyzed by neutral loss, the same 2 peptides were found to be labelled (data not shown). Because of the large size of the labelled peptides, their definitive identification by MS/MS was precluded since good fragmentation was not achieved.

2.3.4.2 Identification of the catalytic nucleophile

As shown in Figure 2.11, the peptides were readily separable by HPLC and so, after purification, their sequences were determined by Edman degradation. As shown in Table 2.4, sequences of ^{229}DAVKHMPFGWQKSF^{242} for peptide 1 and ^{229}DAVKHMPFGWQKSFM^{243} for peptide 2 were obtained, clearly indicating, as expected, that they are overlapping peptides. The catalytic nucleophile must be an amino acid which is common to both peptides and by analogy with other glycosidases and glycosyl transferases is either a glutamate or aspartate (*9, 11, 46*). The only carboxylic amino acid contained within these sequences is Asp229 suggesting that this is indeed the catalytic nucleophile. As shown in Table 2.5, Asp229 is completely conserved among members of Family 13.

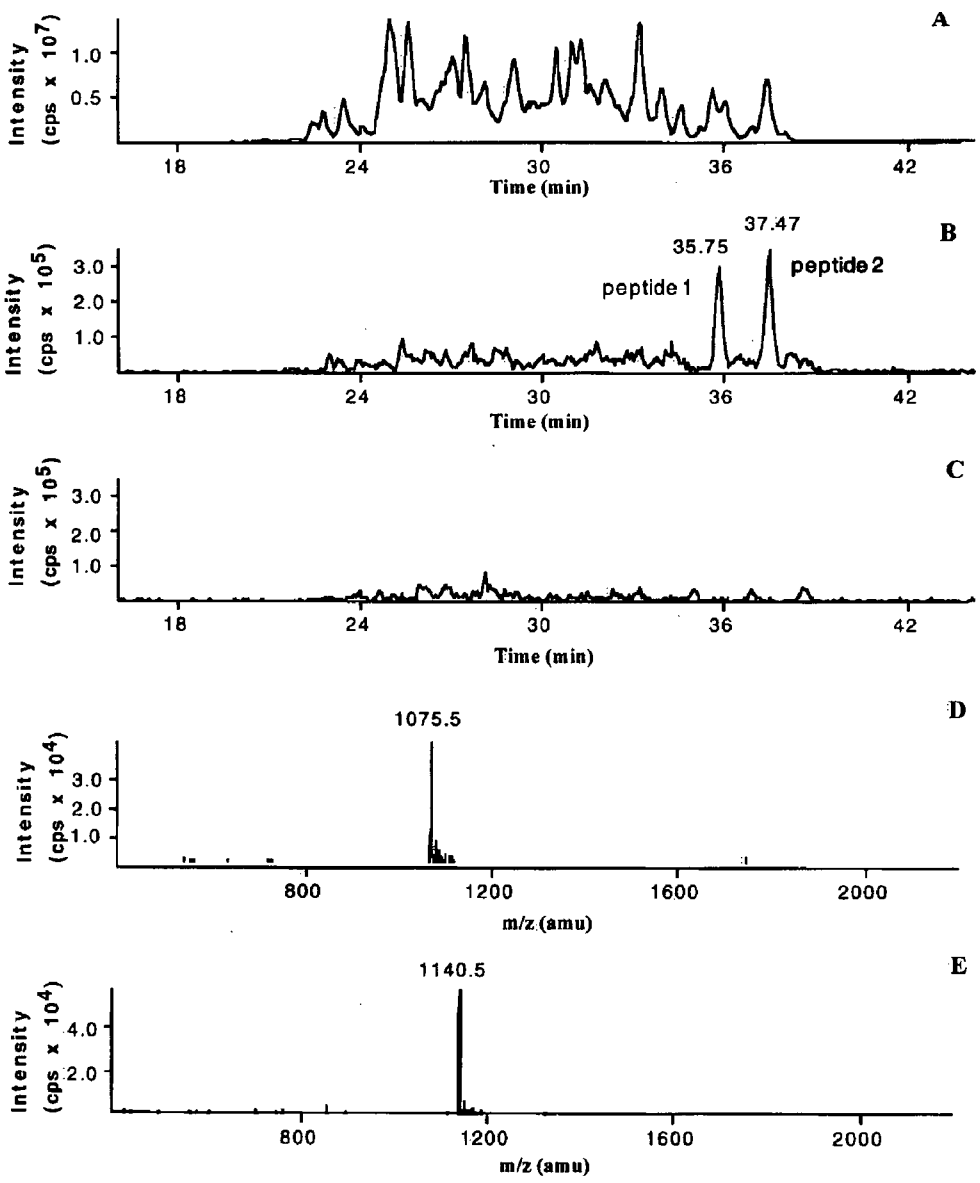

Figure 2.11 Electrospray mass spectrometry experiments on Glu257Gln CGTase proteolytic digests: (A) labelled with 4DαG3F, total ion chromatogram in normal MS mode; (B) labelled with 4DαG3F, TIC in neutral loss mode; (C) unlabelled, in neutral loss mode; (D) mass spectrum of peptide 1 in panel B; (E) mass spectrum of peptide 2 in panel B.

Table 2.4 Edman Degradation of Glu 257Gln CGTase active site peptides 1 and 2

	peptide 1				peptide 2		
cycle	**PTH derivative**	**Yield (pmol)**	**cDNA**	**cycle**	**PTH derivative**	**Yield (pmol)**	**cDNA**
1	Asp	42	Asp	1	Asp	43	Asp
2	Ala	60	Ala	2	Ala	32	Ala
3	Val	91	Val	3	Val	44	Val
4	Lys	20	Lys	4	Lys	10	Lys
5	His	3	His	5	His	2	His
6	Met	24	Met	6	Met	7	Met
7	Pro	9	Pro	7	Pro	2	Pro
8	Phe	19	Phe	8	Phe	4	Phe
9	Gly	20	Gly	9	Gly	2	Gly
10	Trp	19	Trp	10	Trp	3	Trp
11	Gln	6	Gln	11	Gln	5	Gln
12	Lys	2	Lys	12	Lys	2	Lys
13	Ser	2	Ser	13	Ser	Q	Ser
14	Phe	Q	Phe	14	Phe	Q	Phe
				15	Met	Q	Met

Q = qualitative assignment

Table 2.5 Conserved Active Site Sequence Regions for some Members of Family 13 Glycosidases and Glycosyl Transferases

***B. circulans* CGTase numbering**[1]	**224**	**253**	**320**
CGTase (*B. circulans*)	DGIRM**D**AVK	FTFG**E**WFL	QVTFIDNH**D**
CGTase (*B. macerans*)	DGIRF**D**AVK	FTFG**E**WFL	MVTFIDNH**D**
α-amylase (human pancreas)	AGFRL**D**ASK	FIFQ**E**VID	ALVFVDNH**D**
α-glucosidase (yeast)	DGFRL**D**ASK	MRVG**E**VAH	ATTYIENH**D**
glycogen debranching enzyme (rabbit muscle)	QGVRL**D**NCH	YVVA**E**LFT	ALFMDITH**D**
Pullulanase (*Klebsiella pneumonia*)	DGFRF**D**LAS	YFFG**E**GWD	VVNYVSKH**D**

[1] The residues that are bold face correspond to the 3 conserved active site carboxylates.

In addition to defining the role of Asp229 as the catalytic nucleophile, these results also help to clarify the available X-ray structural data on the functions of the three conserved carboxylates in CGTase. In native CGTase, a strong hydrogen bond (2.5 Å) exists between Glu257 and Asp328 (*78, 96*), indicating that one of the carboxylates is protonated, most probably Glu257. In the structure with acarbose bound (*79*), the hydrogen bond between Asp328 and Glu257 is broken, and the Glu257 side chain moves to within hydrogen bonding distance of the glycosidic oxygen of the scissile bond. Thus, it was suspected that Glu257 is the proton donor that initiates the reaction. In the same structure of CGTase complexed with acarbose, Asp229 is at 2.8 Å from the C-1 atom and is thus close enough to act as either a nucleophile or acid/base catalyst. However, Asp229 lies on the opposite side of the substrate binding cleft to the other two key carboxylates and thus was proposed to fulfill the role of

nucleophile. The trapping of a covalent glycosyl-enzyme intermediate on Asp229 conclusively identifies it as the nucleophile. Therefore, although in this case, Asp229 had been correctly assigned the role of nucleophile and Glu257, the role of acid/base catalyst, crystallographic data alone are not always sufficient to definitively identify catalytic carboxylates.

2.3.5 Crystallographic Evidence for a β-Linked Covalent Glycosyl-Enzyme Intermediate for CGTase

The mechanism of reaction of CGTase at the catalytic site was further probed by obtaining a crystal structure of Glu257Gln reacted with 4DαG3F. This data was collected by our collaborators, Dr. Bauke Dijkstra and Mr. Joost Uitdehaag, University of Groningen, the Netherlands. Crystals of *B. circulans* 251 Glu257Gln CGTase were grown in the presence of 5% maltose as reported previously (*78*). Maltose is essential for the formation of the crystals. However, as maltose would act as a good acceptor for the elongation of 4DαG3F, it was necessary to first wash the crystals repeatedly to remove all traces of maltose before exposing them to 4DαG3F. However, washing with buffer containing no maltose resulted in cracking of the crystals. Therefore, the crystals were washed with 1% 4-deoxymaltose (4DG2). The crystals retained the structural stability gained from having a disaccharide moiety bound, yet the potential for elongation was eliminated. Finally, the crystal was soaked for a brief period in 125 mM 4DαG3F and frozen to 100K for data collection.

Upon refinement to 1.8 Å, a 4DG3 moiety was observed to be bound in the -1, -2 and -3 subsites (we are using the nomenclature recently proposed by Davies et al. where the site of cleavage is positioned between the -1 and +1 subsites and the nonreducing sugar is located in the -3 subsite, see Figure 2.12) (*97*). The nucleophile, Asp229, was observed to make a β-

covalent bond to the C-1 anomeric carbon (Figure 2.13). In addition, a 4DG2 moiety was observed to be bound in two of the acceptor sites, +1 and +2. This is the first 3D structure of such a covalent intermediate for any α-1,4 retaining glycosyl transferase or α-glycosidase (see Figure 2.14A for a view of the entire protein as well as two views of the active site region, Figures 2.14B & C). In addition, it is the first time that both donor and acceptor oligosaccharides have been crystallographically observed bound at the active site of CGTase.

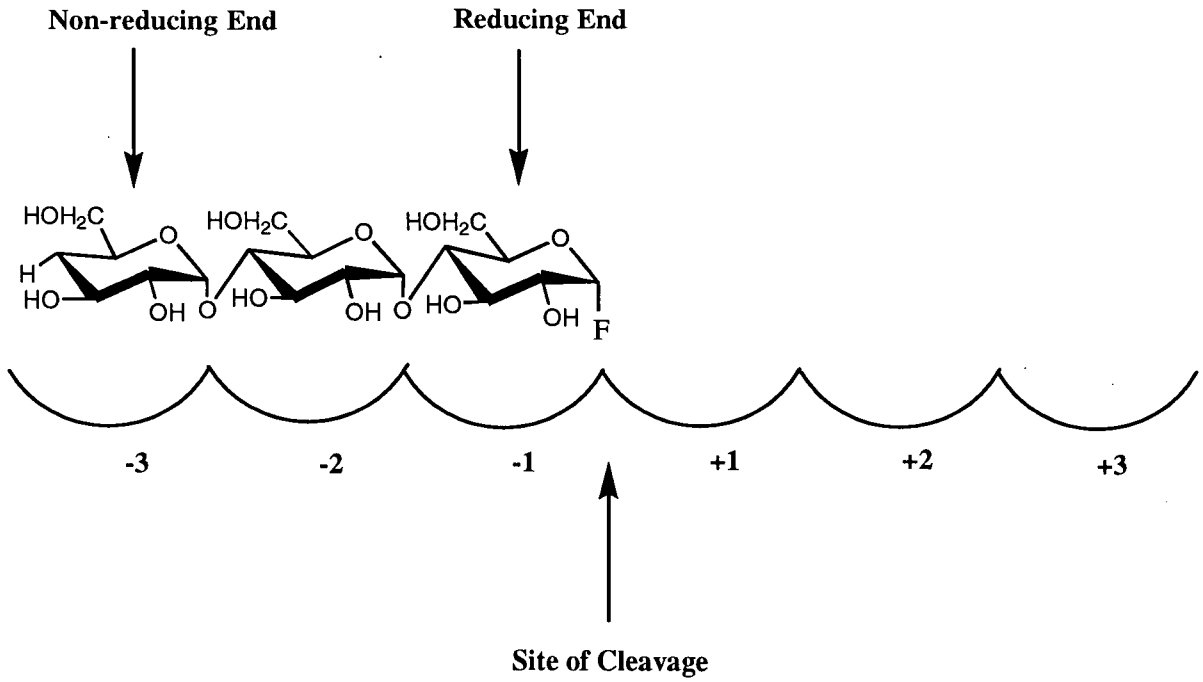

Figure 2.12 The binding of 4DαG3F to CGTase showing subsites labelled according to (97) with the site of cleavage positioned between the -1 and +1 subsites.

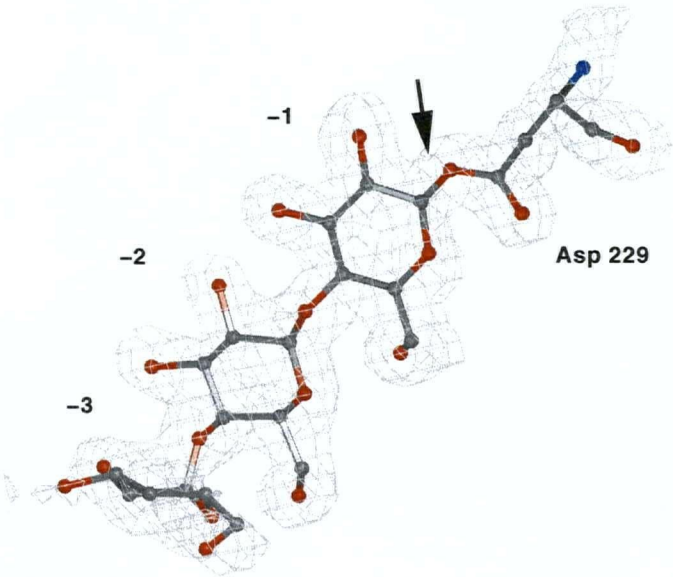

Figure 2.13 Electron density of the 4-deoxymaltotriosyl moiety covalently bound to Asp229 of Glu257Gln CGTase. The arrow indicates the glycosyl-enzyme covalent bond.

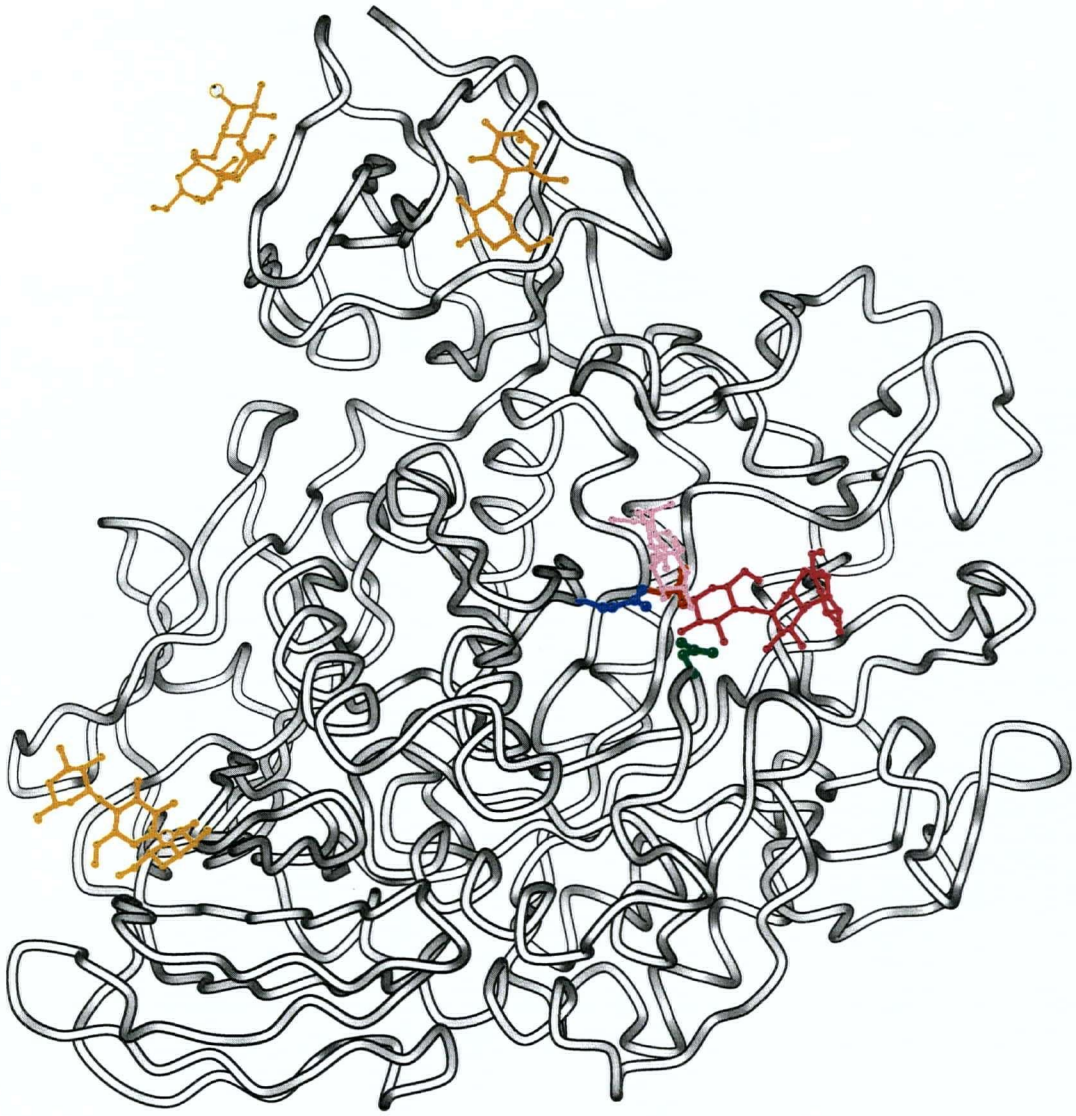

Figure 2.14 (A) Full view of the 4-deoxymaltotriosyl Glu257Gln CGTase crystal structure determined to 1.8 A resolution. The crystal was grown in the presence of maltose, washed with 4DG2, and then soaked with 4DαG3F prior to data collection. The three conserved carboxylates are highlighted; Gln257 (blue), Asp229 (red), and Asp328 (green). The 4-deoxymaltotriosyl moiety is shown in purple, the 4-deoxymaltose is shown in pink. One 4-deoxymaltose (yellow) and two 4-deoxymaltotrioses (yellow) are also observed to be bound in the three maltose binding sites on the surface of the protein.

B

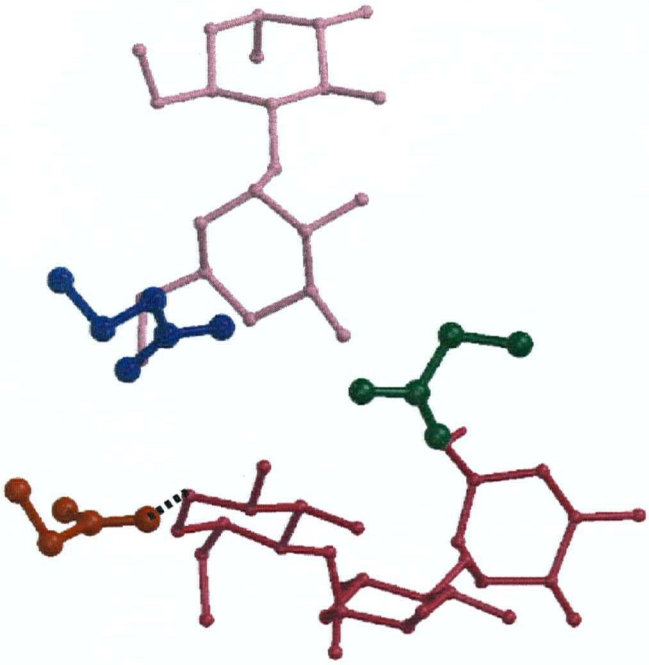

C

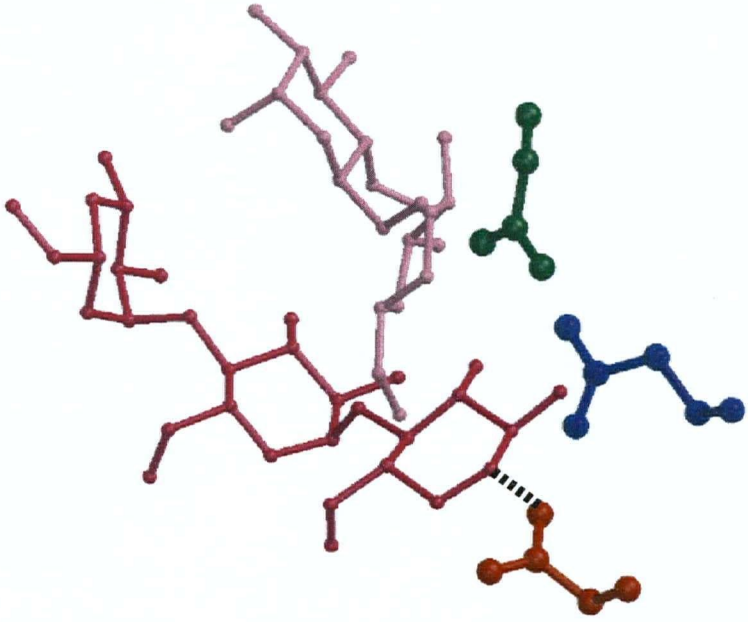

Figure 2.14 (B & C) Two views of the active site region of the 4−deoxymaltotriosyl Glu257Gln CGTase crystal structure. The nucleophile, Asp229 (red), the acid/base catalyst Gln (blue) and the third carboxylate residue, Asp328 (green) are highlighted. The covalent bond between Asp229 and C−1 of the 4−deoxymaltotriosyl moiety (purple) is represented as a dotted line. The 4−deoxymaltose is shown in pink.

Interestingly, the saccharide to which the covalent bond is made is in an undistorted $^4C_1$ chair conformation. This is in agreement with the crystallographic studies recently completely for the β-retaining glycosidase, Cex, with a covalently bound 2-fluorocellobioside substrate (*67, 98*). In this crystal structure, determined to 1.8 Å resolution, the nucleophile forms a covalent bond to the C-1 anomeric carbon of the saccharide in the -1 subsite. The covalently bound saccharide was clearly observed to adopt a $^4C_1$ chair conformation.

Much of the driving force for the departure of the leaving group and subsequent formation of a covalent glycosyl-enzyme intermediate is believed to come from the ability of the ring oxygen to donate electrons. The theory of stereoelectronic control proposes that such reactions are favoured for conformations in which the non-bonding electrons on the ring oxygen lie antiperiplanar to the leaving group (*99*). In the normal $^4C_1$ conformation, the axial leaving group of an α-glycoside is positioned antiperiplanar to the non-bonding electrons of the ring oxygen while the equatorial leaving group of β-glycosides is not in such an antiperiplanar configuration. Hence, it has been proposed that for β-glycosidases, the saccharide unit bound at the -1 site must adopt a twist boat conformation before catalysis can occur so that the leaving group can be positioned in an antiperiplanar configuration to the lone pair on the ring oxygen. In contrast, an α-substrate inherently satisfies the antiperiplanar requirement of configuration deemed necessary by stereoelectronic theory. Therefore, on this basis, it might be predicted that an α-glycosidase would initially bind its substrate in an undistorted chair conformation. However, this argument is a subject of contention and is not generally accepted (*100*). Until recently, the available experimental evidence could neither support nor exclude the possibility of a distorted saccharide conformation upon binding. The best experimental evidence from which to answer these questions comes from crystallographic

studies in which oligosaccharides are observed to be bound in both the -1 and +1 subsites and thus, they bind across the point of catalytic cleavage.

There now exist several examples of crystal structures of β-glycosidases with saccharides noncovalently bound across the catalytic site. A complex of *Serratia marcescens* chitobiase with di-*N*-acetylglucosamine has been obtained to 1.9 Å resolution (*101*). The disaccharide is observed to span the catalytic site and the sugar in the -1 site appears to adopt a twist boat conformation. Other evidence comes from the crystal structure of the retaining endoglucanase I from *Fusarium oxysporum* in the presence of a nonhydrolyzable thiooligosaccharide substrate analogue (*102*). In this case, the pyranose ring at the point of potential enzymatic cleavage was clearly distorted from the standard $^4C_1$ chair conformation toward a twist boat conformation. Until recently, no comparison could be made to an α-glycosidase or α-glycosyl transferase complexed with a noncovalently bound substrate spanning the catalytic site.

Preliminary crystallographic results have been obtained for a double mutant, D229N/E257Q, from *B. circulans* 251 CGTase complexed with maltononaose to 2.0 Å resolution (Mr. J. Uitdehaag, personal communication). This oligosaccharide was observed to span the -1 and +1 subsites and the saccharide in the -1 site was clearly distorted. This is in disagreement with the predictions from stereoelectronic theory that α-glycosidases will not distort the substrate upon binding. However, it is not unreasonable to assume that both β- and α-retaining glycosidases and glycosyl transferases may distort the substrate upon binding in order to more easily assume the presumed half chair conformation of the oxocarbenium ion-like transition state.

2.3.6 Further Analysis of Glu257Gln CGTase: A New Mechanism for a Glycosyl Transferase

As discussed in Section 2.3.3.2 for Glu257Gln CGTase, the k_{cat} values for 4DαG3F and 4DαG2F with Glu257Gln CGTase are 3.3 and 8 fold lower than with wt CGTase and the reaction is proceeding through hydrolysis not transglycosylation. This very small change in k_{cat} as a consequence of mutating the acid/base catalyst was very surprising, previous work having shown that mutation of the acid/base catalyst in other glycosidases results in a much larger drop in k_{cat}. For example, a 200 to 2000 fold drop in k_{cat} was observed upon mutating the acid/base catalyst in *C. fimi* exoglycanase and *Agrobacterium sp.* β-glucosidase (*25, 89*). The small rate decrease observed in the case of CGTase could be due to a decreased requirement for general base catalysis. However, this seems very unlikely since transglycosylation with normal substrates is not similarly affected; the Glu257Gln mutant uses αG3F as a substrate about 300 fold more slowly than does wild-type CGTase (Section 2.3.3.1). A change in mechanism, or of reaction catalyzed, seems more likely. One possibility is that another sugar hydroxyl now acts as nucleophile in a transglycosylation process, but this seems unlikely since, were this to be the case, such a process would have likely dominated in the reaction of αG3F with Glu257Gln CGTase. Another possibility is that the β-linked intermediate ordinarily formed might undergo hydrolysis by attack at the ester center rather than at the sugar anomeric center when general base catalytic assistance for the latter process is removed: as is shown in Figure 2.15. Such a process would require approach of a water molecule to the ester center. Inspection of the structure reveals that this is indeed possible (Dr. B. W. Dijkstra, personal communication). The consequence would be a smaller difference between the k_{cat} values for the wild-type enzyme and those for the mutant. It

should be simple to distinguish between these two mechanistic possibilities by HPLC analysis of reaction products using HPLC conditions which allow identification of the product anomeric stereochemistry without causing mutarotation.

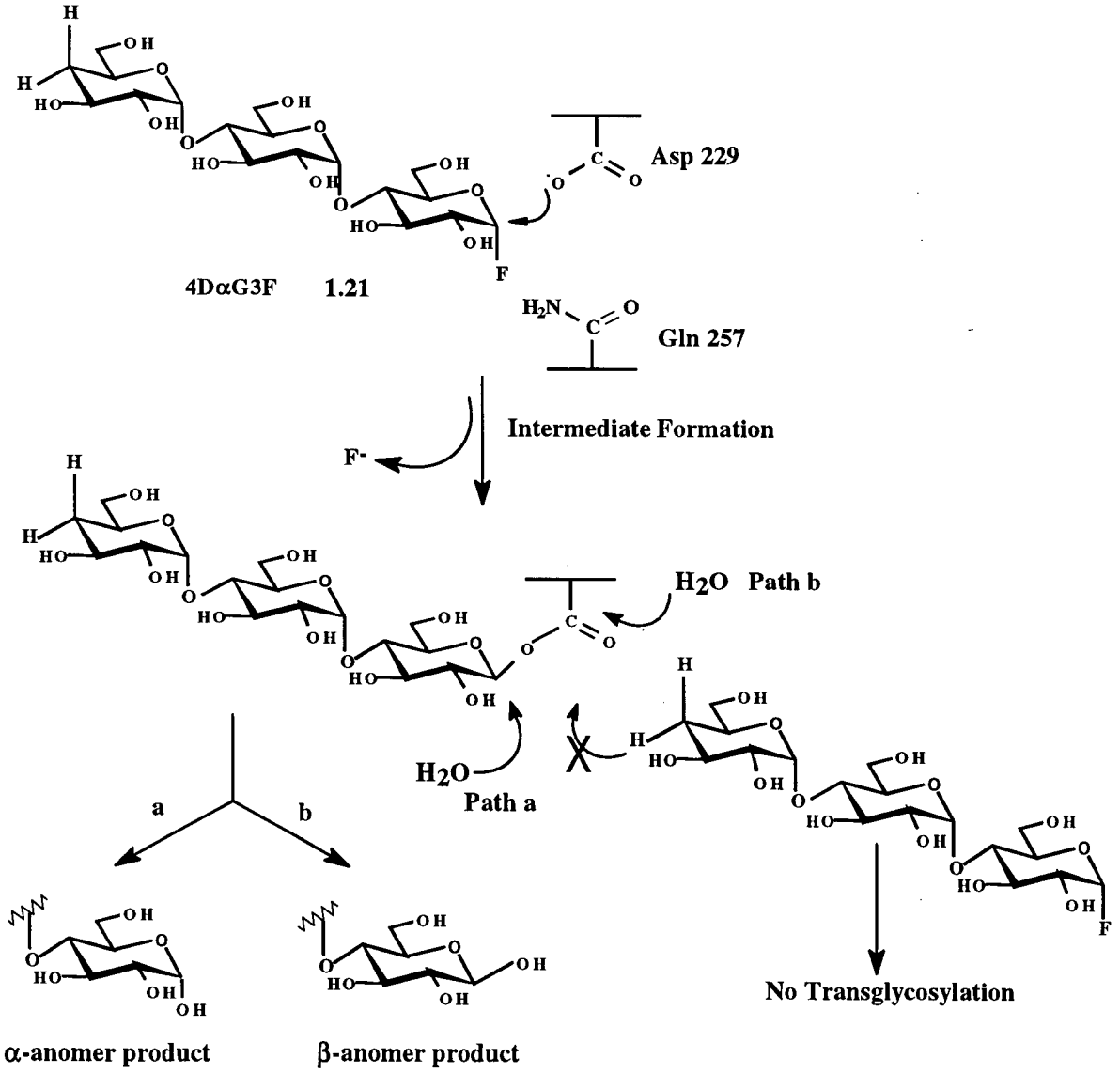

*Figure 2.15 Proposed mechanism for hydrolysis of the covalent glycosyl-enzyme intermediate in Glu257Gln CGTase. (**a**) Attack of H_2O at the anomeric center to give α-product, (**b**) Attack of H_2O at the ester center to give β-product.*

2.3.6.1 HPLC Analysis of Reaction Products

The Waters Dextropak column has been shown to separate the α and β anomers of malto-oligosaccharides when run in deionized water (*103*). As shown in Figure 2.16A, hydrolysis of 4DαG3F by Glu257Gln CGTase over a 5 minute period results in only the β-isomer of 4DG3, with no α anomer, or transfer products. After time, mutarotation occurs to give a mixture of both α and β products, with the final product mixture reflecting a typical 60/40 distribution of β and α anomers (Figure 2.16B). It is important to note that these peaks were definitively identified as the α and β anomers of 4DG3 in three ways. First, an authentic sample of equilibriated 4DG3, when injected onto the Dextropak column produced two peaks with identical retention times. Second, the molecular weight of each peak is identical and corresponds to the weight of 4DG3. Third, only one peak, which corresponds in mass and retention time to 4DG3, appears when the same reaction mixture is analyzed on the Dynamax column (see Figure 2.9A). A similar scenario is observed in Figure 2.16C for the reaction of Glu257Gln and 4DαG2F where the initial product obtained is β-4DG2, which later mutarotates giving a mixture of α and β isomers (Figure 2.16D). Since the glycosyl-enzyme intermediate formed must have the β-configuration, this means that hydrolysis must proceed via attack of water on the acyl center. This is the first time such a mechanism has been observed for a glycosidase. The appearance of this mechanism was a consequence of removal of two of the required elements of the normal process; the attacking nucleophile and the general base catalyst for this process. Removal of the general base catalyst did not, however, disable the alternative ester hydrolysis pathway since this residue would be inappropriately positioned for that mechanism.

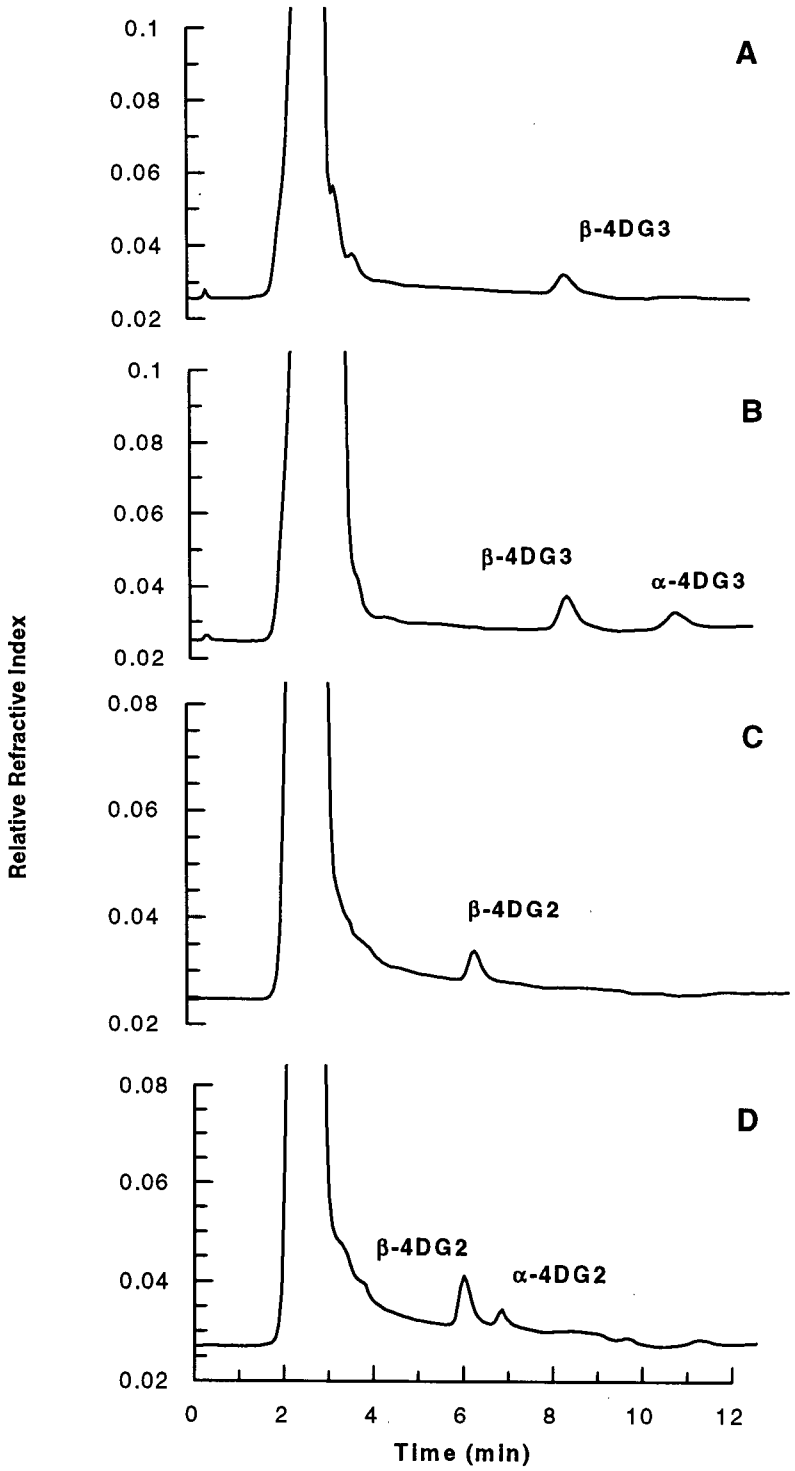

*Figure 2.16 HPLC analysis of the products of the reaction of Glu257Gln CGTase with (**A**) 4DαG3F after 2 min, (**B**) 4DαG3F after 20 min, (**C**) 4DαG2F after 2 min, (**D**) 4DαG2F after 20 min. Conditions: Dextropak column, 1 mL/min H_2O.*

A mechanism involving nucleophilic attack by an active site carboxylate followed by hydrolysis of the ester to regenerate the enzyme is well precedented in other enzyme systems. Interestingly, these are all enzymes involved in remediation of environmental contaminants such as epoxide hydrolases and dehalogenases. For the epoxide hydrolases, the first step is presumed to involve nucleophilic attack of a carboxylic acid to open the epoxide, leading to the formation of an ester intermediate as shown in Figure 2.17 (*104*). Subsequently, water hydrolyzes the ester with general base catalysis to release the diol product. Haloalkane dehalogenase and (4-chlorobenzoyl) coenzyme A dehalogenase have been shown to operate through similar mechanisms (*105-110*). Interestingly, epoxide hydrolase and bacterial haloalkane dehalogenase share sequence identity and a common catalytic motif while (4-chlorobenzoyl) coenzyme A dehalogenase does not show any active site homology nor similarity in crystal structure and appears to be connected to the other two enzymes solely by the similar use of an active site carboxylate to mediate hydrolytic substitution at a carbon center (*106, 111, 112*).

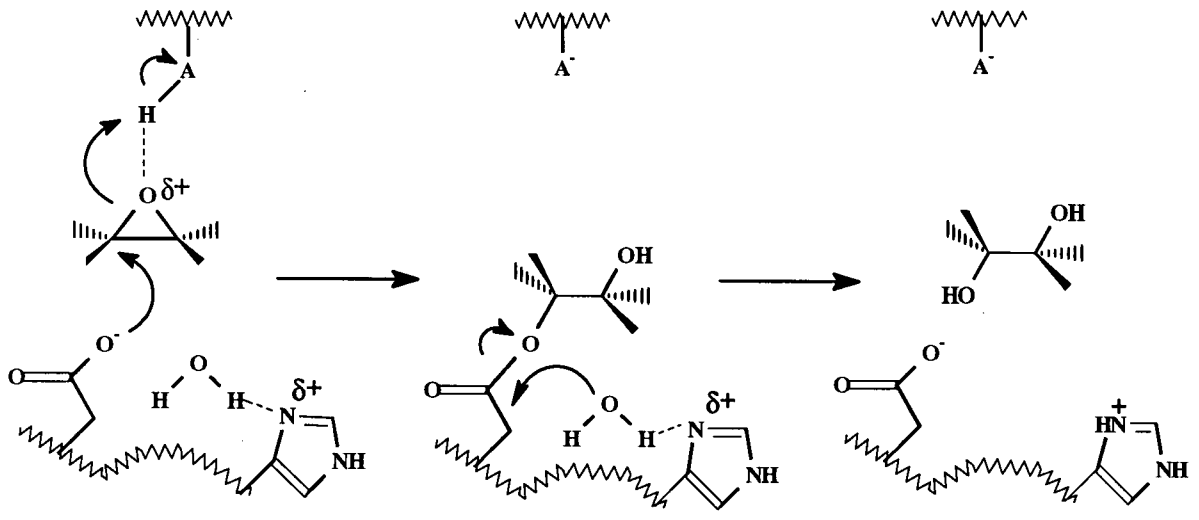

Figure 2.17 Mechanism for a soluble epoxide hydrolase showing water attack at the ester center rather than the reaction center. Adapted from (104).

It is interesting to speculate why such a mechanism is not ordinarily seen in glycosidases, but is seen in enzymes involved in bioremediation. An attractive possibility is that some evolutionary primitive glycosidases did indeed use such a mechanism. However, such a mechanism carries with it an inherent danger since esterolytic attack on this intermediate by an alternative nucleophile such as ammonia would result in conversion of the active site acid to an amide thereby rendering the enzyme inactive. Enzymes adopting such a mechanism within a relatively uncontrolled environment would have ultimately been selected against in favour of 'safer' mechanisms. However, such evolutionary primitive enzymes as the dehalogenases or epoxide hydrolases might not have yet reached this stage of refinement.

2.3.7 Kinetic Analysis of Asp229Asn and Asp229Ala CGTase

In order to further probe the role of the catalytic nucleophile, a kinetic analysis of two mutants, Asp229Asn and Asp229Ala, from *B. circulans* CGTase was performed. Values of k_{cat} and K_m for αG3F with Asp229Asn are 2000 and 30 fold lower than for the wild-type CGTase (Table 2.6). This compares with a reduction of 300 and 7 fold respectively for the Glu257Gln mutant when assayed with the same substrate. Using starch as a substrate and assaying for βCD formation, the k_{cat} value for Asp229Asn was found to be 2.3×10^4 fold lower than that of the wild-type enzyme (*82*). These reductions in activity observed for Asp229Asn CGTase (2×10^3 - 2.3×10^4 fold depending on the substrate analyzed) are about average when compared with those observed for the analogous nucleophile mutants in other members of Family 13 glycosyl transferases and hydrolases. For example, when assayed for β-cyclodextrin forming activity, the mutant Asp229Asn from an alkalophilic *Bacillus* CGTase showed a 10^3 fold lower activity compared with wild-type (*113*). On the other hand, when

the equivalent residue to Asp229 (Asp176) in *Bacillus subtilis* α-amylase was mutated to Asn, a 10^5 fold lower activity against starch was measured (*114*). However, even though the low level of activity measured for Asp229Asn is within the range expected from equivalent studies on other related α-glycosidases and α-glycosyl transferases, concerns are present about whether the activities actually measured are true activities of the mutant or are due to contamination, as discussed below.

αG3F was found to be a substrate for Asp229Ala but with a k_{cat} value almost 2 fold lower compared with Asp229Asn and 3.3×10^3 fold lower compared with wild-type CGTase (Table 2.6). This reduction in activity is comparable to that noted for the same mutation in *B. circulans* strain 8 CGTase where a 1000 fold drop in activity compared to wt was measured (*96*). The K_m value for αG3F with Asp229Ala was 160 fold higher than the corresponding K_m measured for Asp229Asn CGTase and 8 fold higher than the K_m measured for wild-type. The reason for this high K_m value is not clear. It is possible that the substitution of aspartate with alanine may disrupt a binding interaction that normally exists between the aspartate and the substrate (hence the large K_m value). Possibly the asparagine replacement engages in more effective hydrogen bonding.

Table 2.6 Kinetic Parameters for the Reaction of *B. circulans* Asp229Asn and Asp229Ala CGTase with α-Maltotriosyl Fluoride

Mutant	Substrate [1]	K_m (mM)	k_{cat} (s^{-1})	k_{cat}/K_m ($mM^{-1}s^{-1}$)
Asp229Asn	αG3F	0.10	0.14	1.4
Asp229Ala	αG3F	16.1	0.083	0.0052
Glu257Gln [2]	αG3F	0.37	1.0	2.70
wt [2]	αG3F	2.5	275	111

[1] Graphical representation of data is shown in Appendix B, Figure B-2.
[2] Reported previously in Tables 2.1 and 2.3 and presented here for comparison purposes.

The residual activity exhibited by the Asp229Asn and Asp229Ala mutants may be attributed to several factors. One, it is possible that the preparation of either of the mutant enzymes may be contaminated with a small percentage of wild-type enzyme or another CGTase mutant. This contamination could be derived from translational misincorporation or through physical contamination during the purification of Asp229Asn or Asp229Ala. In some cases, it may be possible to determine whether the low level of activity is due to wild-type enzyme contamination. Such an experiment would involve measuring the rate of inactivation of the mutant with a mechanism based inactivator. If complete inactivation of the enzyme is observed according to a rate constant essentially identical to that measured with wild-type enzyme, then the observed activity can probably be attributed to wild-type contamination. Typically, such a contaminant would be a very minor component (0.01% to 0.1% or less) and thus, by ES-MS, only the intact mass for the mutant would be observed. Therefore, if the inactivated mutant enzyme sample (containing a wt contaminant) is analyzed by ES-MS, the mass of the mutant should remain unchanged, indicating that the loss in activity could not be

due to derivatization of the mutant enzyme but rather was due to derivatization of the wild-type enzyme. Such experiments were performed on the acid/base catalyst mutant of Cex with the inactivator DNP-2-deoxy-2-fluoro-β-cellobioside to show that the residual activity measured for the mutant could be attributed to a wild-type contaminant (*89*). An analogous set of experiments could not be performed on Asp229Asn or Asp229Ala because it was not possible to locate a mechanism based inactivator for CGTase (2 potential candidates: 5FGluαF (**1.14**) and 5FβIdoF (**1.15**) (see Section 1.4.4.1), were not found to act as inactivators for CGTase, but rather as weak reversible inhibitors, data not shown). An alternative to these types of experiments would be the use of sub-stoichiometric (relative to the enzyme) amounts of a tight-binding reversible inhibitor to titrate out a suspected wild-type contaminant. However, in order for a reversible inhibitor to be effective for these purposes, it must bind very tightly to the wild-type enzyme and the potent α-glycosidase inhibitor acarbose (see Figure 2.22) did not prove useful in this regard as the K_i value for wild-type enzyme was 0.2 μM (see Table 2.7). Therefore, in order to effectively inhibit all of the wild-type contaminant, it would be necessary to use an inhibitor concentration at least 5-10 times the K_i value (1-2 μM). In turn, the concentration of mutant enzyme would have to be at least 5-10 times this value (10-20 μM), a relatively high concentration of enzyme. This experiment was not attempted due to the limited supply of the mutant enzymes. Regardless, it is unlikely that in either case, the residual activity exhibited by the Asp229 mutants is due to a wild-type contaminant because for Asp229Asn, the K_m value measured is so low (0.1 mM) compared with that of the wild-type enzyme (2.5 mM) and for Asp229Ala, the measured K_m is so high (16.1 mM) compared to that of the wild-type enzyme. However, it is not possible to exclude contamination by another mutant.

HPLC analysis of the reaction products of the Asp229 mutant CGTases with αG3F provides some insight into the questions surrounding this residual activity (Figure 2.18). The initial product observed from the reaction of Asp229Asn with αG3F was G3, presumably resulting from simple hydrolysis of αG3F (Figure 2.18A). After longer incubation times, αCD and βCD and the smaller disproportionation products, G and G2, were also obtained (Figure 2.18B). HPLC analysis of the products of the reaction of Asp229Ala with αG3F showed that G2 was the major product, but a significant amount of transglycosylation to yield βCD was still observed (Figure 2.18C). Whether this activity can be attributed to Asp229Asn or Asp229Ala or is a consequence of some other factor is unclear. The formation of both αCD and βCD are predicted to result from a reaction involving retention of configuration and a covalent glycosyl-enzyme intermediate. The mutation of Asp229 to Asn or Ala should eliminate the possibility that this residue will participate in the formation of a covalent glycosyl-enzyme intermediate and instead, another residue may be taking over the role of nucleophile. It has been speculated from crystallographic studies that the third active site carboxylate (Asp328) may be in a position to partially take over for the nucleophile (*82*), although its orientation and distance to the anomeric carbon make this unlikely. If Asp328 was fulfilling the role of nucleophile, it might be predicted that accumulation of a covalent intermediate could be observed by ES-MS, especially given the low K_m value measured. Upon incubation of Asp229Asn or Asp229Ala with αG3F or 4DαG3F, the mass of the protein remained unchanged, thus providing no support for the accumulation of an intermediate (data not shown). It is also possible in the case of Asp229Asn that the asparagine side chain may be able to partially fulfill the role of nucleophile by properly orientating a water molecule for attack at the anomeric center. However, it is also possible

that the enzyme responsible for the production of these transglycosylation products may be a minor component and thus it would not be possible to observe its derivatization by ES-MS. Another explanation may be that the mutant enzyme is employing an alternative mechanism to catalyze the reaction which does not involve the formation of a covalent intermediate.

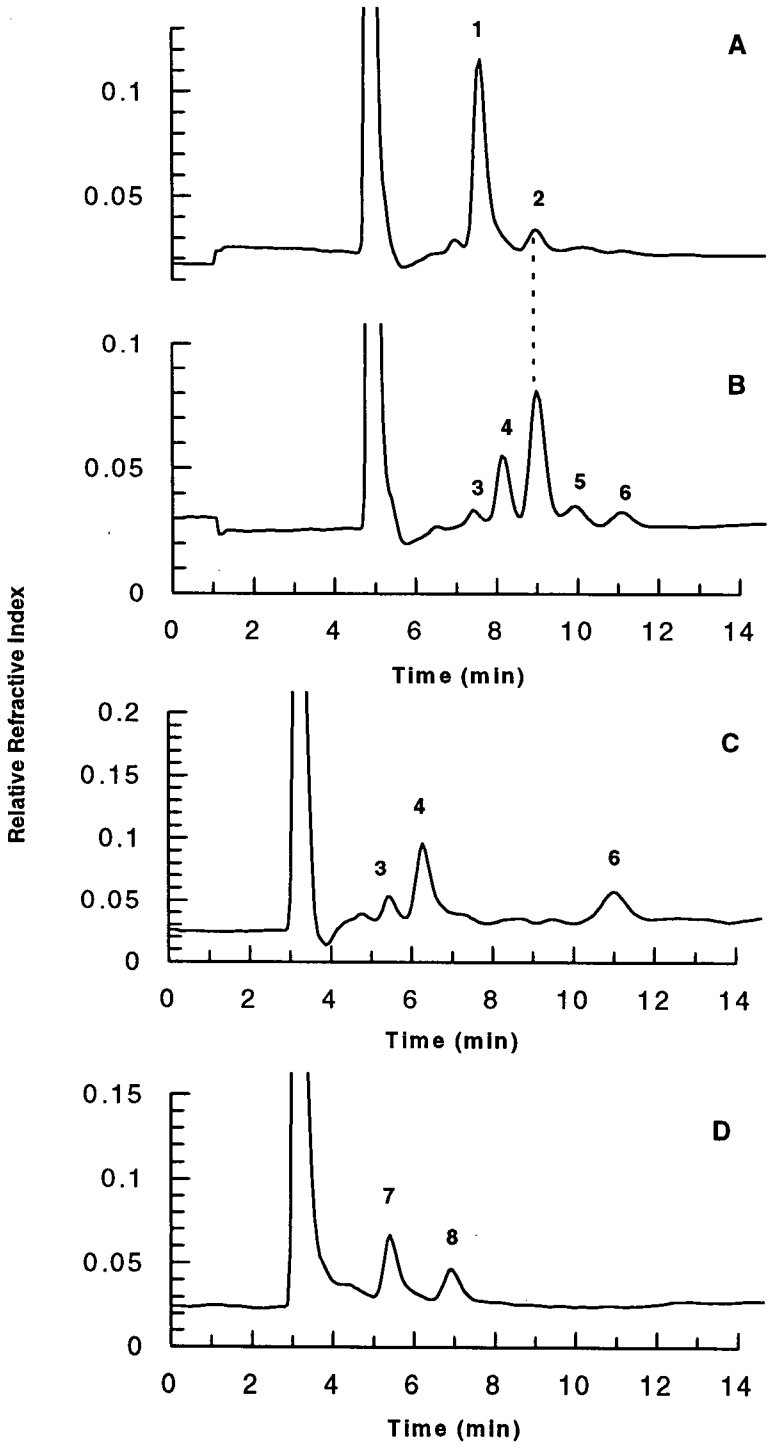

Figure 2.18 HPLC analysis of the reaction products of (A) Asp229Asn and αG3F after 30 min reaction time, (B) Asp229Asn and αG3F after 4 h reaction time, (C) Asp229Ala and αG3F after incubation overnight (D) Asp229Asn and 4DαG3F after 4 h reaction time (1 = αG3F, 2 = G3, 3 = G, 4 = G2, 5 = αCD, 6 = βCD, 7 = 4DαG3F, 8 = 4DG3). Conditions: Dynamax column, 0.8 mL/min 60/40 CH_3CN/H_2O. (Note: profiles A and B could not be directly overlapped with either C or D because different columns were used).

The latter possibility was investigated by incubating Asp229Asn with 4DαG3F, a substrate for which no transglycosylation should be possible. The products were analyzed by HPLC using a variety of column which is capable of separating α and β anomers of malto-oligosaccharides as previously discussed in Section 2.3.6 (*103*). As shown in Figure 2.19A, after 5 min, the initial product formed was β-4DG3, which mutarotates over time to form an α/β mixture (Figures 2.19B and C). This is presumably forming through an inverting mechanism which does not involve a covalent intermediate as shown in Section 1.3, Figure 1.3. It is important to note that the only product being made is 4DG3 as shown in Figure 2.18D when the identical reaction was analyzed on the Dynamax column and the mass of peak 8 was determined by ES-MS. It is also important to note that no accumulation of any intermediate could be observed by ES-MS when 4DαG3F and Asp229Asn were incubated together (data not shown). This is not unreasonable as an inverting mechanism does not involve the formation of a covalent glycosyl-enzyme intermediate. This is the first time that such a change in mechanism resulting from mutation of the nucleophile has been reported for a retaining α-glycosidase or α-glycosyl transferase. It appears that the mutant only adopts such an inverting mechanism under conditions when the transglycosylation pathway has been shut down, in this case by deoxygenation of the acceptor.

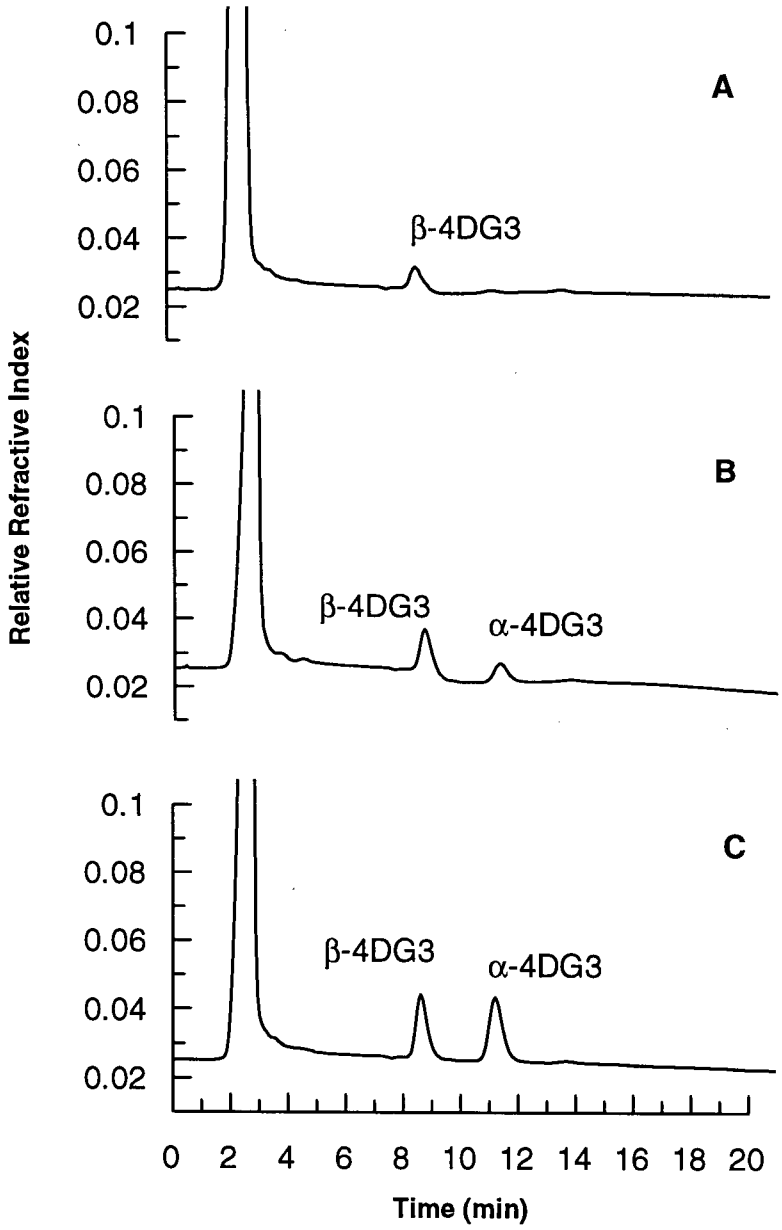

*Figure 2.19 HPLC analysis of the products of the reaction of Asp229Asn with 4DαG3F. (**A**) after 5 min, (**B**) after 30 min, (**C**) after 90 min. Conditions: Dextropak column, 1 mL/min H_2O. (Note: the starting material, 4DαG3F elutes at approximately 60 min).*

A similar experiment to the one employed with Asp229Asn was also completed with Asp229Ala in an effort to ascertain whether or not this mutant was operating via inversion under conditions in which no transglycosylation was possible. That is, Asp229Ala was incubated with 4DαG3F and the reaction products analyzed by HPLC using the Dextropak

column to separate anomers. Only one peak, which corresponded to the starting material, 4DαG3F, could be detected by HPLC (data not shown). No peaks corresponding to the predicted hydrolysis products, α-4DG3 and/or β-4DG3, could be detected. In fact, no product of any kind could be detected, even when the sample had incubated with enzyme for up to 48 hours or the concentration of enzyme was increased 4 times. Although a detailed kinetic analysis was not performed to determine K_m and k_{cat} values for Asp229Asn or Asp229Ala with 4DαG3F, an estimate of the turnover times can be obtained from the HPLC analysis. As shown in Figure 2.19A, after a reaction time of 5 min, product had been generated from the reaction of Asp229Asn with 4DαG3F (estimated turnover time, less than 5 min). However, as Asp229Ala was incubated with 4DαG3F for up to 48 hours with no evidence of product formation, the turnover time for Asp229Ala with 4DαG3F must be at least 3000 min. Thus an upper limit on k_{cat} of 0.00033 min^{-1} can be assigned. It is not clear why Asp229Ala is so slow at catalyzing the hydrolysis of 4DαG3F compared with Asp229Asn, but it is possible that Asp229Ala is not stable at room temperature for long periods of time. Another explanation could be that an asparagine side chain may be better adapted to orient a water molecule for attack at the anomeric center through a potential hydrogen bond. On the other hand, an alanine side chain cannot function as a hydrogen bond donor or acceptor and in fact, the hydrophobic methyl side chain of an Ala residue may decrease the probability that water can approach the anomeric center of the substrate for attack.

2.3.8 Further Analysis of the Alanine Mutants of the Acid/Base Catalyst and the Nucleophile of CGTase

As discussed previously, the acid/base catalyst and nucleophile are primarily identified through site directed mutagenesis, kinetic analysis and X-ray crystallography. However, in cases in which there are no crystal structures available, it is often difficult to specifically assign each carboxylate. For example, conclusive identification of the acid/base catalyst cannot always be made from analysis of kinetic data on selected mutants. Although mutagenesis of the acid/base catalyst usually results in a less severe drop in activity than the corresponding mutation of the nucleophile, it often becomes difficult to distinguish between the acid/base catalyst and the third conserved carboxylate in the active site from kinetic data alone. A strategy was developed by MacLeod et al. to overcome these limitations (*24, 89*). It was noted that the addition of azide to mutants missing either the active site nucleophile or acid/base catalyst substantially increased turnover rates and resulted in the formation of glycosyl azide products. No such azide adducts are formed with a mutant of another conserved carboxylate, even though rate enhancements are observed. Substitution of the conserved carboxylates with an alanine residue is preferred because it presumably generates additional space in the active site region of the substrate for the approach of azide. The azide products are usually identified by chromatography or ^{1}H NMR. It is predicted that if the glycosyl azide has the same stereochemistry as the starting material then the mutated residue is assigned as the acid/base catalyst (Figure 2.20A). If the glycosyl azide has the opposite stereochemistry to that of the starting material then the mutated residue is identified as the nucleophile (Figure 2.20B). This approach has proven useful for identifying the acid/base catalyst of Cex from *C. fimi*, Abg, *E. coli* β-galactosidase, and *B. subtilis* xylanase (*25, 89,*

95, 115). However, such an approach had not yet been applied to any retaining α-glycosyl transferases or α-glycosidases. Therefore, the objective of this study was to test the validity of this approach with CGTase.

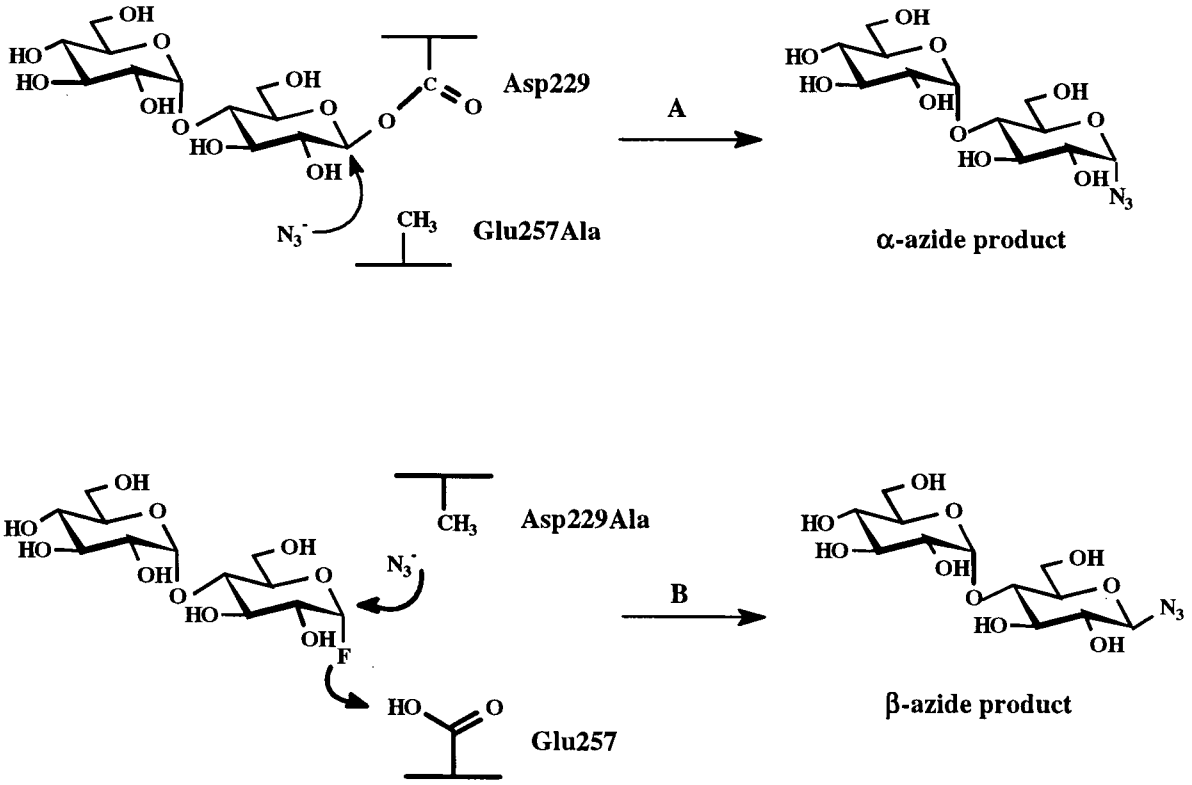

Figure 2.20 Expected products for the reaction of αG2F and azide with the alanine mutants of (A) the acid/base catalyst (Glu257) and (B) the nucleophile (Asp229).

2.3.8.1 Effect of Added Nucleophiles on the Reaction Rates of CGTase mutants

Among the CGTase mutants tested: Glu257Ala, Glu257Gln, Asp229Ala, and Asp229Asn, only Glu257Ala showed an increase (1.8 times) in the catalyzed rate of fluoride release from αG3F upon the addition of azide. Presumably, substitution with a glutamine residue at the same position does not generate enough space for azide to approach the substrate. This rate enhancement was not improved by using formate or acetate in place of

azide. In comparison, the alanine mutants of both the acid/base catalyst and the nucleophile of β-glycosidases generally show increases in rate of between 10^2 to 10^4 fold upon the addition of azide (*25, 89*).

2.3.8.2 Identification of the reaction products of Glu257Ala CGTase with αG3F and azide

Upon incubation of Glu257Ala CGTase with αG3F and azide, the predicted products should be α-maltotriosyl azide, maltotriose and α-cyclodextrin (the latter two are based on the usual products of the reaction of Glu257Ala with αG3F-see Figure 2.8B). Glu257Ala was incubated with αG3F and azide and left to react overnight, the enzyme was removed and the products of the reaction were analyzed by ^{1}H NMR and ES-MS and compared with a control reaction. As shown in Figure 2.21B, when azide was included in the reaction a new doublet appears at δ = 5.75 ppm (peak 6). This peak is absent in the control reaction which did not include azide in the mixture (Figure 2.21A). This chemical shift is in the region for an α-anomer of a glycosyl azide. As well, the coupling constant of 4.2 Hz compares well with what is expected for an α-linked product, and is not large enough to be a β-azide product (coupling is typically in the range of 8 - 10 Hz for a β-linked product) (*25*). The molecular weight of the product (360, M + NH_4^+) corresponds to that of α-maltotriosyl azide. The other anomeric peaks are attributed to the following: δ = 5.92 ppm (dd, 1 H, $J_{1,2}$ = 3.8 Hz, $J_{1,F}$ = 53 Hz, β-H-1, αG3F, peaks 1 and 2), δ = 5.61 (m, 2 H, H-1' & H-1'', G3 and αG3F, peak 3), δ = 5.45 ppm (dd, 1-H, $J_{1,2}$ = 4.2 Hz, β-H-1, G3. peak 4) and δ = 5.27 ppm (dd, 1 H, $J_{1,2}$ = 3.3 Hz, β-H-1, αCD, peak 5). The production of G3 and αCD from the reaction of Glu257Ala with αG3F were predicted from the previous HPLC analysis (Figure 2.8B). The generation of an azide product which has the same configuration as the starting material

therefore confirms the identity of Glu257 as the acid/base catalyst. This is the first case in which this approach has been used to confirm the identity of the acid/base catalyst of an α-glycosyl transferase. Therefore, although in this case large rate enhancements were not obtained after adding azide, it is possible that the principle of the approach may prove useful for distinguishing the acid/base catalyst from the other conserved carboxylates in α-retaining enzymes where actual trapping of an intermediate has not yet been achieved.

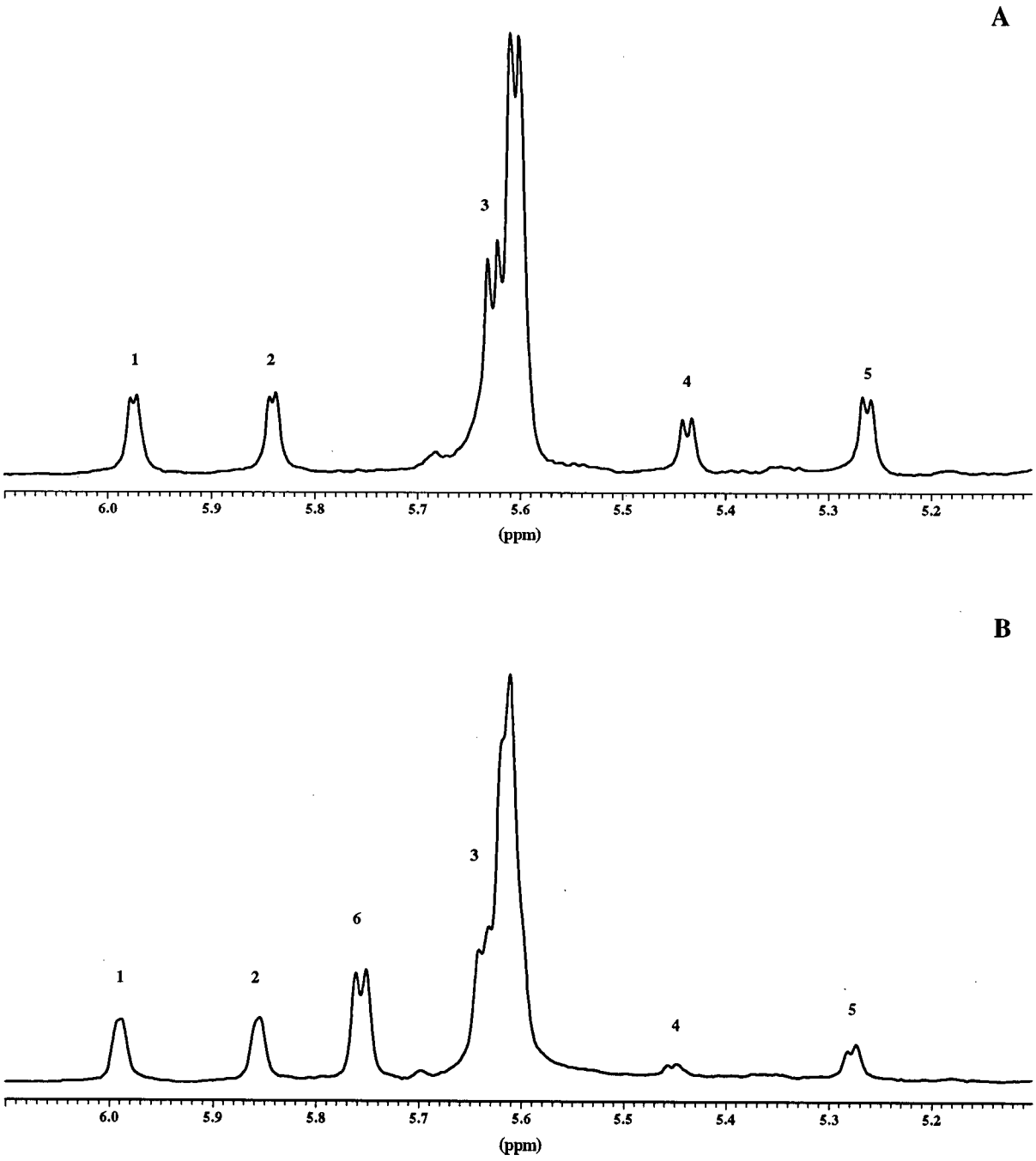

Figure 2.21 ^{1}H *NMR spectra (anomeric region) of the products of the reaction of Glu257Ala with αG3F after overnight incubation (**A**) in the absence of azide and (**B**) in the presence of 250 mM azide. (peak 1 = αG3F, peak 2 = αG3F, peak 3 = αG3F & G3, peak 4 = G3, peak 5 = αCD, peak 6 =* $\alpha G3N_3$*).*

2.3.9 Conclusions-Part 1

Confirmation of the identity of the nucleophile of *B. circulans* 251 CGTase as Asp229 was achieved using a unique combination of site directed mutagenesis, an incompetent substrate and mass spectrometry (*116*). This work has also provided the first concrete evidence for a covalent glycosyl-enzyme intermediate for *B. circulans* 251 CGTase and the first 3-D structure of such an intermediate for any α-glycosidase or α-glycosyl transferase. In two other cases evidence of a covalent glycosyl-enzyme intermediate in Family 13 glycosidases/glycosyl transferases has been obtained from rapid trapping studies with natural substrates. Low temperature ^{13}C NMR experiments have given evidence for the formation of a β-linked covalent adduct between maltotetraose and porcine pancreas α-amylase involving an aspartic acid (*48*). Other evidence for a stabilized intermediate comes from experiments with *Streptococcus sobrinus* α-glycosyl transferase where an aspartic acid was identified as the catalytic nucleophile by rapidly denaturing a reaction mixture of enzyme and radiolabelled sucrose and isolating the labelled peptide (*46, 47*). In one other Family 13 enzyme, yeast α-glucosidase, two mechanism-based glycosidase inactivators, 5-fluoro-α-*D*-glucosyl fluoride (**1.14**) and 5-fluoro-β-*L*-idosyl fluoride (**1.15**), were used in conjunction with mass spectrometry to identify the catalytic nucleophile as Asp214 (the homologous residue), thereby also confirming the existence of a covalent intermediate (*71*) (see Section 1.4.4.1).

The use of 4DαG3F in crystallographic studies of the covalent intermediate bound to CGTase provided valuable information towards understanding the mechanism of reaction of CGTase at the catalytic site. Not only was the existence of a covalent intermediate confirmed but information about the conformation of the sugar in the covalently bound state was

obtained. In addition, the nature of the binding of the acceptor sugar was examined and should provide an improved understanding of the processes occurring at the reaction site. This will help to clarify the contributions of other residues to substrate binding and product specificity and could prove useful in the future in creating enzymes which produce specific types of cyclodextrin product.

2.4 RESULTS AND DISCUSSION-PART 2

2.4.1 Investigation of Acarbose as a Transition State Analogue for CGTase

As discussed in Section 1.4.3, transition state analogues can be used to probe enzyme mechanisms. Transition state analogues should bind tightly to the enzyme as they are able to recruit the binding interactions normally intended for stabilization of the reaction transition state. A useful way of determining whether a particular inhibitor is truly a transition state analogue or is just a fortuitously tight binding inhibitor involves probing the effects on modifications to the interactions between the enzyme and inhibitor and then probing the effects of equivalent modifications to the enzyme/substrate complex at the transition state. The measurement of K_i values quantifies enzyme and inhibitor interactions while the measurement of k_{cat}/K_m values quantifies enzyme-substrate interactions at the transition state. If these modifications result in a good correlation between the inhibitor K_i values and the substrate k_{cat}/K_m values then it can be concluded that the inhibitor is indeed a transition state analogue. This approach has been reviewed recently (*117*). Such modifications can be effected in two ways. One way involves the synthesis and kinetic evaluation of a series of modified substrates with the wild-type enzyme, along with measurement of K_i values for the identically modified inhibitors. The other approach involves the construction of a series of

mutant enzymes, preferably mutated at sites thought to play a role in substrate recognition and catalysis, then measurement of k_{cat}/K_m and K_i values with each mutant for a single substrate and transition state analogue inhibitor respectively. The choice of approach depends primarily upon whether it is easier to generate mutant enzymes or modified substrates and inhibitors. The former approach has been used to demonstrate that a series of phosphonamidate peptide derivatives are indeed true transition state analogue inhibitors for zinc peptidases and thermolysin (*118, 119*). Similarily nojiritetrazoles were shown by this method to be true transition state analogues for a range of glycosidases (*39*), while 1-deoxynojirimycin and castanospermine were shown not to be transition state analogues for *Agrobacterium sp.* β-glucosidase but rather, tight binding, fortuitous inhibitors (*120*). The latter approach has been applied to rat carboxypeptidase A (*119, 121*) and glucoamylase (*122*). It seemed possible that such an approach could be applied to interactions of cyclodextrin glycosyltransferase with the inhibitor acarbose, because of the wealth of active site mutants already generated in attempts to modulate product specificity and binding (*90, 91*). This might provide insight into some surprising findings concerning the binding mode of acarbose to CGTase deduced crystallographically (*79*).

Acarbose is a naturally occurring pseudo-tetrasaccharide inhibitor of a range of α-glucosidases and glycosyl transferases including pig pancreatic α-amylase (K_i = 10 μM) (*123*) and α-glucoamylase (K_i = 0.001 nM) (*124*). Acarbose is currently used in a clinical setting for the treatment of diabetes (*125-127*). Acarbose consists of a valienamine moiety at the non-reducing end linked via an α-1,4 NH bond to a maltotriosyl derivative (Figure 2.22). The valienamine moiety mimics the flattened glucosyl residue believed to exist in the transition state. The exocyclic amine moiety is in a position analogous to the anomeric oxygen and its

protonation would place a positive charge in a similar location to that which would be generated upon protonation of the glycosidic bond.

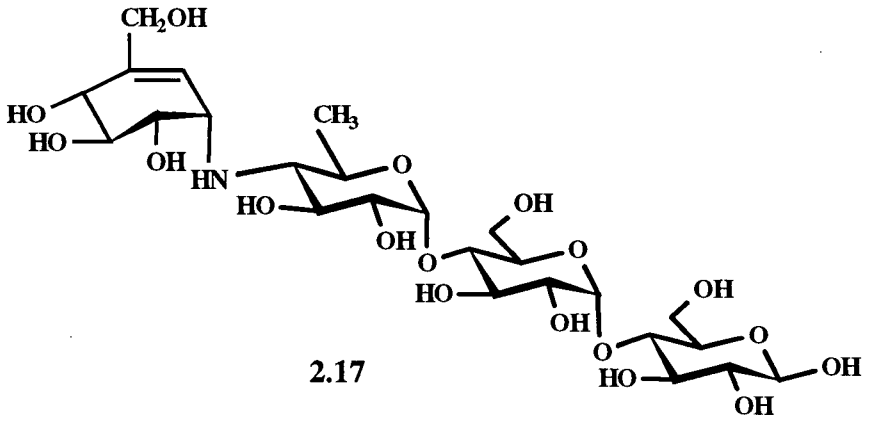

2.17

Figure 2.22 Acarbose

Recently, the 2.5 Å crystal structure of CGTase with acarbose bound at the active site was reported (*79*) as well as a structure of CGTase with a bound maltononaose inhibitor apparently derived from condensation of maltopentaose and acarbose (*83*). Interestingly, the mode of binding of acarbose appeared to be different from that in previously reported structures of complexes of acarbose with other α-glycosyl transferases/hydrolases, namely, glucoamylase, porcine pancreatic α-amylase, *Aspergillus oryzae* α-amylase (*80, 128, 129*) and a thermostable CGTase (*130*) since the valienamine moiety, generally thought to mimic the glycosyl cation-like transition state, does not appear to be bound in the -1 site in the case of CGTase (we are using the universal nomenclature system recently proposed (*97*) in which cleavage occurs between the -1 and +1 subsites). Rather it was interpreted to be bound in the -2 site, with the 6-deoxyglucosyl moiety bound in the -1 site and its glycosidic oxygen at the site of cleavage.

In an effort to investigate the interactions of acarbose with CGTase, we have screened a range of active site mutants which are believed to be responsible for governing a wide range of product specificities (Figure 2.23). Two substrates, α-maltotriosyl fluoride and α-glucosyl fluoride were used in this analysis allowing the determination of accurate kinetic parameters using the fluoride electrode as discussed in Section 2.3.1.2.

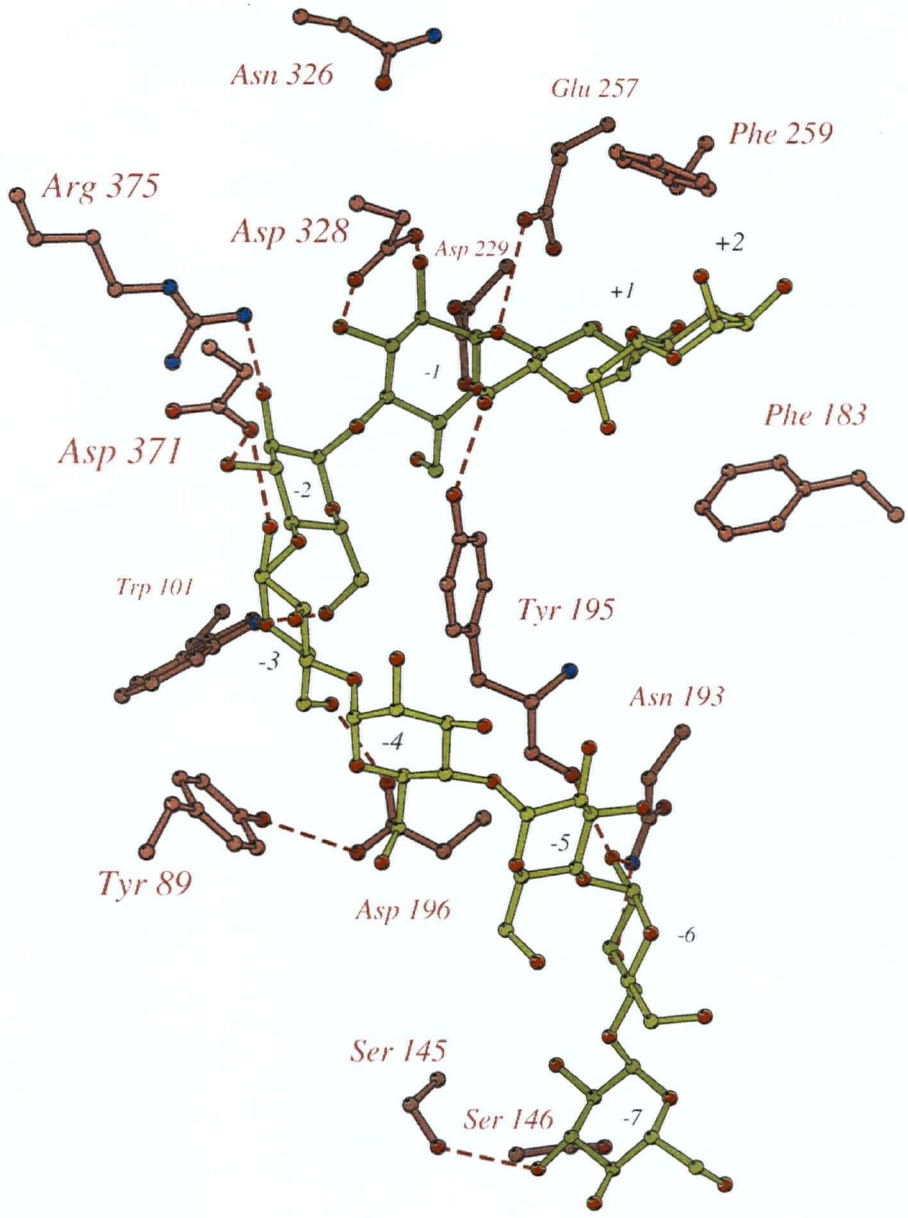

Figure 2.23 Schematic representation of the active site of CGTase complexed with maltononaose (diagram kindly supplied by Dr. B. Dijkstra and Mr. J. Uitdehaag, University of Groningen, the Netherlands, from the unpublished data of a crystal structure of a D229N/E257Q double mutant complexed with maltononaose. For simplicity, D229 and E257 have not been modeled in as mutated and maltononaose residues are modeled in as undistorted chairs. Many of the residues believed to play important roles in catalysis are included in the diagram. The positions at which mutants were made and later used in this study include: Tyr195, Ser145, Ser146, Asp371, Asn193, and Asn326).

2.4.2 Kinetic Analysis of Active Site Mutants of CGTase using Glycosyl Fluorides as Substrates

As reported previously, both αG3F and αGF are convenient substrates for CGTase since the enzyme-catalyzed release of fluoride can be easily assayed using an ion-selective fluoride electrode. Even though CGTase otherwise prefers longer oligosaccharides, a short one, such as αGF, can be used if a good leaving group, such as fluoride, is provided. When the release of fluoride from αGF is followed using the fluoride electrode a slow reaction rate is observed over a lengthy induction period, but this rate gradually increases with time, as is shown in Figure 2.24. It seemed likely that this behaviour was a consequence of a transglycosylation reaction between two molecules of αGF producing α-maltosyl fluoride which acts as a better donor or acceptor, thereby more rapidly reacting to give αG3F and so on. The lack of such an induction period when αG3F was used as substrate certainly supports this hypothesis (data not shown). Further evidence that longer oligosaccharides serve as better acceptors was obtained by monitoring the reaction with αGF in the presence of different malto-oligosaccharides. As seen in Figure 2.24, inclusion of maltotriose considerably shortens the lag period while maltotetraose shortens it yet further. When maltohexaose is added, no lag phase at all was observed. Since, in this study, we were interested in the reaction of αGF, only the initial slope was used in our kinetic evaluation.

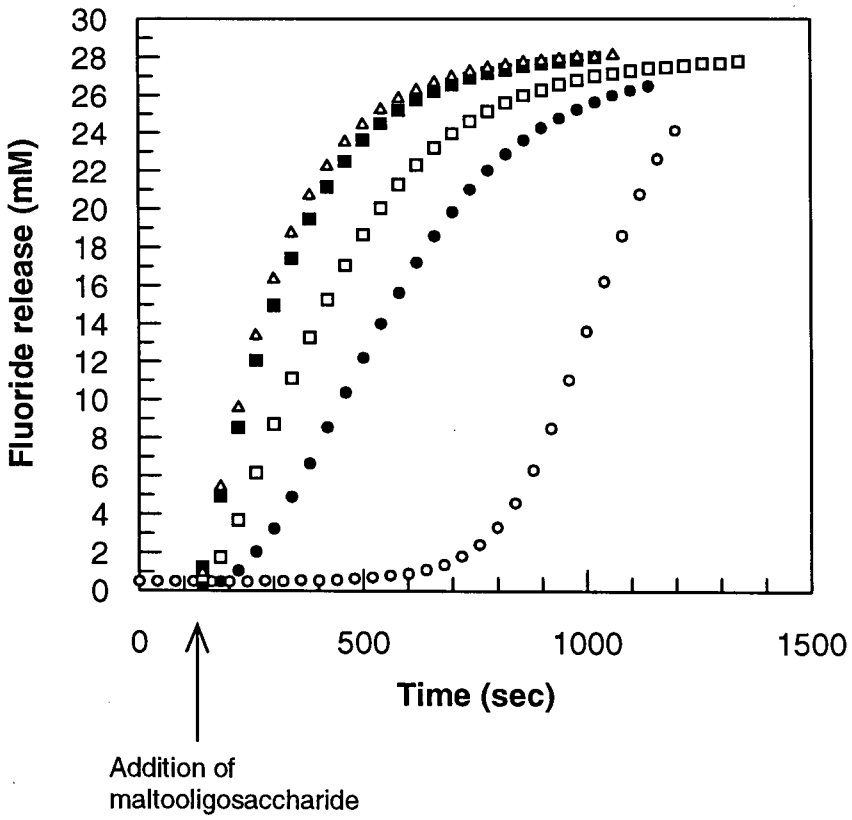

Figure 2.24 Reaction of D371N CGTase with αGF (28 mM) and various acceptors showing fluoride release over time. Concentrations of acceptors used were: ○ = D371N + αGF only (no added acceptor); ● = 30 mM G3; □ = 30 mM G4; ■ = 30 mM G5; Δ = 30 mM G6.

As shown in Table 2.7, a wide variety of mutations within the active site have been generated in an effort to determine the effects that a particular alteration has on the enzyme catalyzed reaction. All of the mutants tested were able to utilize αG3F as a substrate, albeit to varying extents, with k_{cat} values ranging from 275 s^{-1} to 0.0093 s^{-1}; a spread of almost 3 x 10^4 fold. Interestingly K_m values for all the mutants studied were greater than that for the wild-type enzyme indicating varying degrees of disruption of binding interactions. The degree of weakening of binding ranged from very small (< 2 fold) in the cases of the Y195F and S145E mutants, to very large (80 fold) in the case of the Y195G mutant. This very small effect with

the S145E mutant is consistent with the observation that this residue interacts only with the sugar residue in the -7 site (*83*). αG3F will not bind in that site, thus effects should be minimal. The presence of very disparate effects with the Y195F and Y195G mutants is also consistent with the role of Y195. Y195 is thought to be the key amino acid in the active site which the cyclodextrin product wraps around during formation and it may also be largely responsible for helping to exclude water molecules from the active site, thus preventing hydrolysis (*83*). Its hydroxyl group is thought to hydrogen bond to the sugar in the +1 site, while the aromatic ring provides important interactions with the rest of the substrate, especially the sugar in the -1 site (*83*). Since αG3F does not occupy the +1 site, minor consequences of removing that hydrogen bond are reasonable, yet complete removal of the side chain is clearly highly deleterious.

Mutations within the CGTase system produced an even larger range of effects on the enzyme-catalyzed reaction of the shorter, monosaccharide substrate, αGF; the k_{cat} values spanned from 330 s^{-1} to 0.0002 s^{-1}, a range of 1.6 x 10^6 fold. Effects on K_m ranged from a small disruption in binding (<1.5 fold) for the Y195F mutant to significant changes in binding (25 fold) for the Y195G mutant. Effects on k_{cat}/K_m consequently ranged over 4.1 x 10^7 fold. Similar structure/activity correlations to those observed with αG3F are apparent. That is, the proximity of Y195 and N326 to the -1 subsite make them important residues for optimal binding of the substrate. N326 is known to sit in a key position in the active site and kinetic analysis on mutants modified at the equivalent residue in a thermostable CGTase showed drastic changes in pH optima upon mutation (*130*). Therefore, mutations at these positions result in the largest disruptions in binding affinity and rate reductions.

Since this enzyme is a transferase, therefore ultimately requiring interactions in both the glycone and aglycone sites, care must be exercised in the interpretation of the kinetic parameters of these various mutants in terms of localized binding interactions. This is particularly true when the rate-determining step for each substrate/mutant pair is not known. If formation of the glycosyl-enzyme is rate limiting then interactions in the negative (-1, -2 etc) sites will likely be the most important. If however, the second, transglycosylation, step is rate-limiting, then interaction with the positive (+1, +2 etc) sites could be equally important. This uncertainty is largely sidestepped if values of k_{cat}/K_m are interpreted since this second order rate constant, known as the specificity constant, reflects only the first irreversible step. For CGTase, as shown with various glycosidases (*26, 27, 34*), it is reasonable to assume that this is the first, glycosylation step, thus changes in this parameter reflect changes in interactions in the negative sites.

Table 2.7 Kinetic Parameters for the Reaction of α-Glucosyl Fluoride and α-Maltotriosyl Fluoride with CGTases (wt and mutants) and for Inhibition by Acarbose

	α-Glucosyl fluoride[1]			α-Maltotriosyl fluoride			Acarbose
CGTase	K_m (mM)	k_{cat} (s^{-1})	k_{cat}/K_m (s^{-1} mM^{-1})	K_m (mM)	k_{cat} (s^{-1})	k_{cat}/K_m (s^{-1} mM^{-1})	K_i (mM)
wt	32.3 [2]	330 [2]	10.2 [2]	2.5 [2]	275 [2]	110 [2]	0.0002
Y195F	40.0	123	3.075	4.0	7.8	1.95	0.00036
Y195L	100	0.60	0.006	11.6	0.47	0.041	0.0176
Y195G	800	2×10^{-4}	2.5×10^{-7}	200	0.046	0.00023	0.341
N326Q	400	4.8×10^{-3}	1.2×10^{-5}	12.2	0.0093	0.00076	0.106
S145E	60	100	1.67	3.37	175	51.9	0.001
S146P	250	0.16	6.4×10^{-4}	16.5	7.75	0.470	0.025
D371N	74	1.35	0.0182	18.6	214	11.5	0.010
N193G	50	0.54	0.0108	7.65	57.6	7.52	0.005

[1] The data is graphically displayed in Appendix B, Figures B-3 to B-8.
[2] Reported in Table 2.1.

2.4.3 Inhibition of CGTase Mutants by Acarbose

Inhibition constants for acarbose were measured with each of the CGTase mutants, and these are also presented in Table 2.7. In three cases, including the weakest and strongest binding examples, the K_i value was determined from a full analysis using a range of substrate and inhibitor concentrations as is shown for Y195G CGTase in Figure 2.25. Inhibition was strictly competitive in each case. In the other cases, K_i values were determined from data obtained at a series of inhibitor concentrations using a fixed concentration of substrate as

described in Section 4.2.3. The mutant enzymes all bound to acarbose, but less tightly than does wild type CGTase, with widely varying affinities ranging from a K_i of 0.2 μM for wild-type to 341 μM for Y195G CGTase. This large loss of affinity upon removal of the Y195 side chain is again consistent with the key role played by this residue.

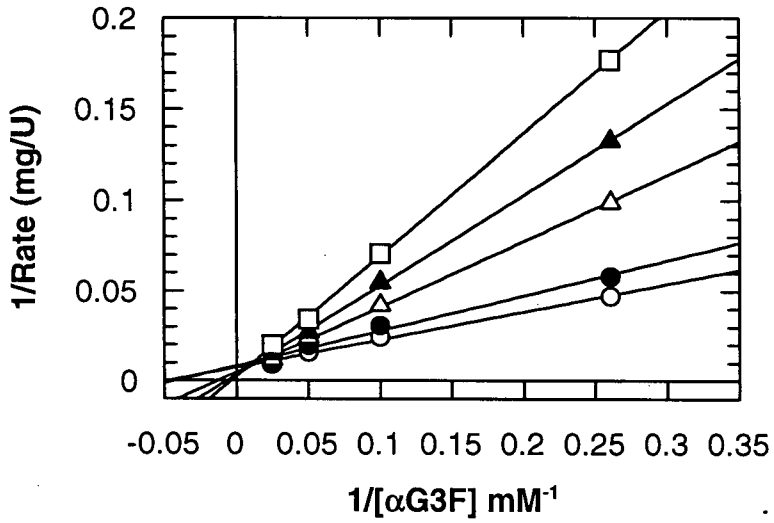

Figure 2.25 Lineweaver Burke plot for Y195G CGTase with αG3F as substrate and acarbose as inhibitor. Concentrations of acarbose used were: ○ = 0 μM; ● = 38 μM; Δ = 200 μM; ▲ = 384 μM; □ = 770 μM. (Units are μmol of F- released/min).

2.4.4 How Good a Transition State Analogue Inhibitor is Acarbose?

Some measure of the degree to which acarbose mimics the reaction transition state is provided by the plot of log (K_m/k_{cat}) for αG3F versus log K_i for acarbose in Figure 2.26A. A respectable correlation (solid line $\rho = 0.90$) is observed with a slope of 1.61 clearly indicating a substantial degree of mimicry. Changes in binding interactions to the inhibitor therefore correlate quite well with changes in transition state binding interactions with substrate. Not surprisingly there is also some mimicry of ground state binding interactions as revealed by the

correlation of log K_m for the substrate αG3F with log K_i for acarbose in Figure 2.27A. A correlation coefficient of $\rho = 0.90$ is again observed, but the slope, 0.47, is approximately three times smaller than the correlation with log (K_m/k_{cat}).

Interestingly, the correlation seen between log (K_m/k_{cat}) for αGF and log K_i for acarbose is considerably better, with $\rho = 0.98$ and a slope of 2.2, as shown in Figure 2.26B. This very strong correlation clearly indicates that acarbose is binding as a transition state analogue. Again, some ground state mimicry was observed, the plot of log K_m versus log K_i for acarbose having a slope of 0.4 and $\rho = 0.93$ (Figure 2.27B).

The better correlation observed for αGF than αG3F is completely consistent with the binding modes of these substrates and of acarbose, as shown in Figure 2.28. The only occupied subsite common to the substrate and to acarbose is, in fact, the -1 subsite, assuming that acarbose binds in that mode. Thus the effects of mutations upon interactions at that site will dominate the correlation. Such effects will be particularly large if the mutation directly removes interactions at that site. In addition, changes in interactions at that site resulting from more remote mutations will also be sensed. However, mutations at more remote sites which do not have an effect upon interaction at that site will not be sensed. Thus mutations affecting only interactions at the +1, +2, and +3 sites will affect the binding of acarbose but will not necessarily affect K_m/k_{cat} values for the two substrates. This will result in scatter in the plot shown (Figure 2.26A). Similarly mutations affecting interactions in the -2 and -3 sites will affect K_m/k_{cat} values for αG3F, but not K_i values for acarbose, thus adding additional scatter to that correlation. The -2 and -3 sites are not directly probed by αGF, hence the improved correlation.

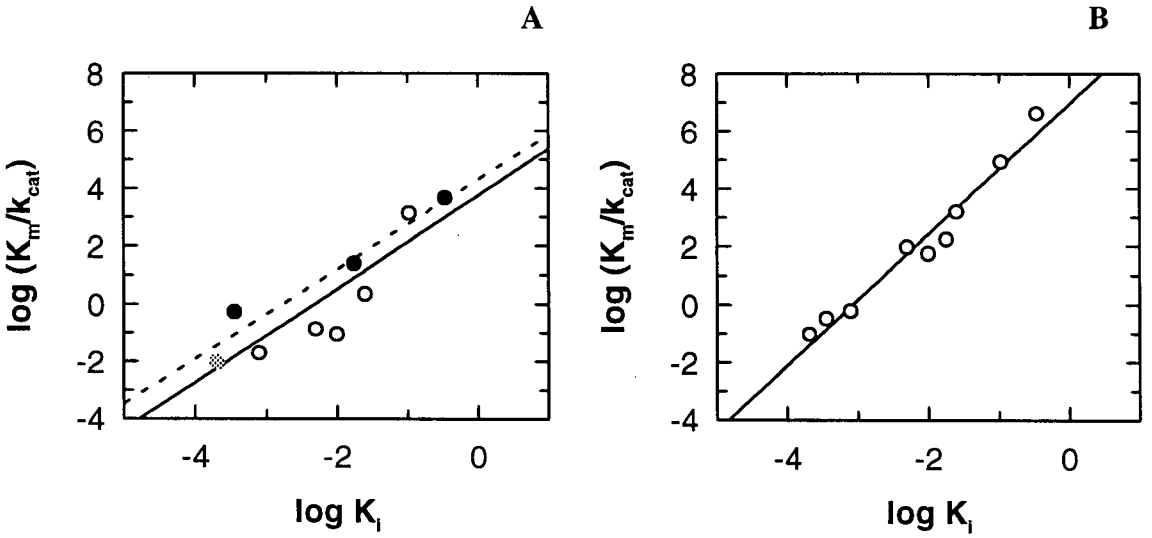

Figure 2.26 Linear free energy relationship between kinetic parameters for the inhibitor acarbose and glycosyl fluoride substrates with a series of mutants of CGTase. (A) log (K_m/k_{cat}) for αG3F vs log K_i for acarbose; (B) log (K_m/k_{cat}) for αGF vs log K_i acarbose. (Filled circles represent Tyr mutants. Grey shaded circle represents wild-type CGTase. The dotted line in A indicates the best fit line through Y195 mutants and wt. The solid line is the best fit line through all the data).

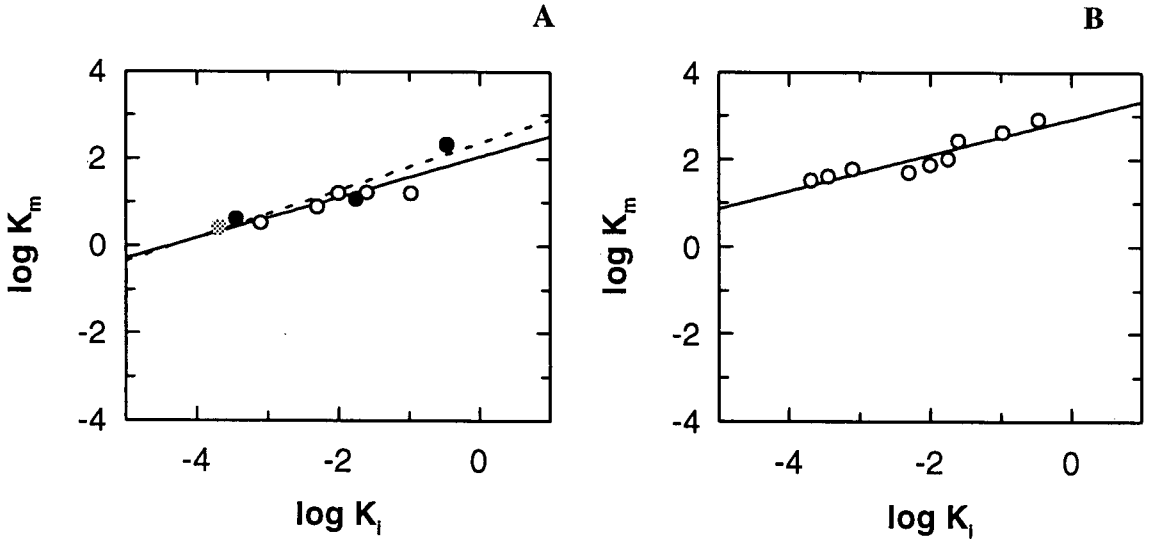

Figure 2.27 Linear free energy relationship between kinetic parameters for the inhibitor acarbose and glycosyl fluoride substrates with a series of mutants of CGTase. (A) log K_m for αG3F vs log K_i for acarbose; (B) log K_m for αGF vs log K_i for acarbose. (Filled circles represent Tyr mutants. Grey shaded circle represents wild-type CGTase. The dotted line in A indicates the best fit line through Y195 mutants and wt. The solid line is the best fit line through all the data).

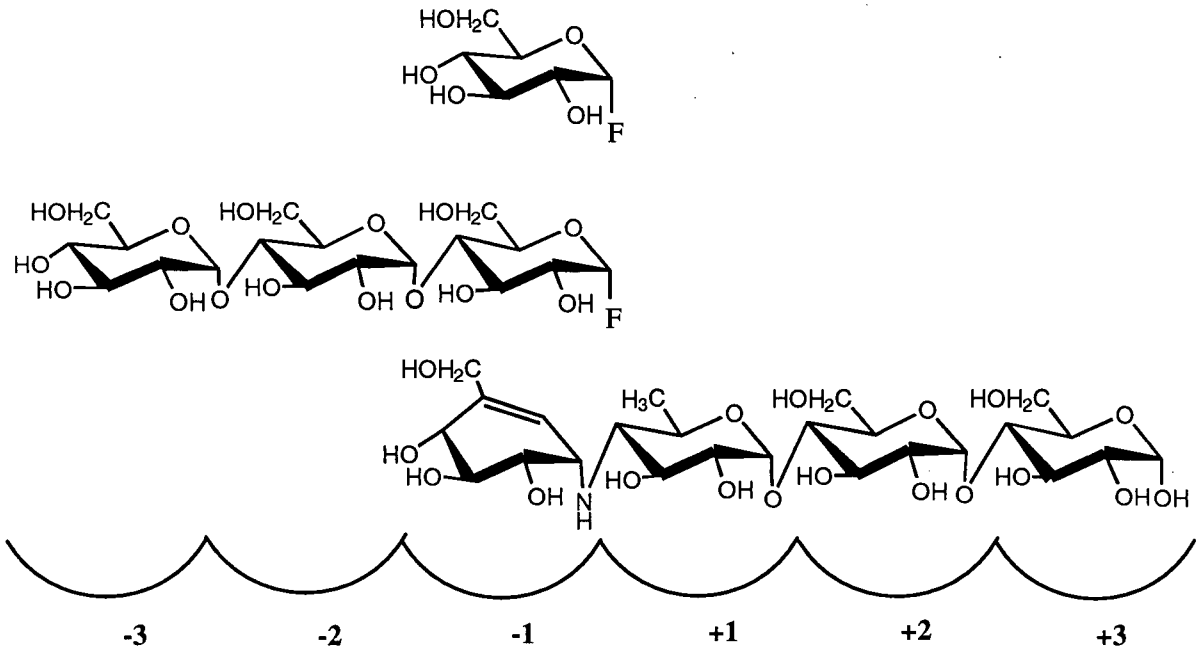

Figure 2.28 Structure of the pseudotetrasaccharide, acarbose, positioned in the subsites of CGTase in the 'amylase' mode with the relative binding positions of αG3F and αGF shown above. The cleavage site is positioned between subsite -1 and +1.

Another measure of the importance of probing equivalent interactions with the substrate and with the inhibitor is obtained by selecting data only for mutants which directly affect interactions at the common (-1) subsite. The only amino acid residue mutated which fully fits that requirement is Tyr195. Indeed, as shown with the filled circles in Figure 2.26A and 2.27A, when only such data are considered, a much better correlation (dotted line ρ = 0.97, slope = 1.55, Figure 2.26A; dotted line ρ = 0.96, slope = 0.54, Figure 2.27A) is observed, consistent with the interactions observed crystallographically.

2.4.5 Conclusions-Part 2

The excellent correlation seen between log (K_m/k_{cat}) for turnover of αGF by a series of CGTase mutants and log K_i for acarbose for each of these same mutants provides convincing evidence that acarbose functions as a transition state analogue inhibitor for this enzyme. It seems probable that the majority of the binding interactions providing this very high affinity are associated with the valienamine moiety. Since acarbose also contains a trisaccharide portion it is not surprising that it also shows some ground state mimicry as revealed in the plot of log K_m versus log K_i. However, the considerably smaller slope observed in this plot reflects the lower degree of mimicry. These results are consistent with expectations regarding the structure of the transition state for this retaining transferase. It is also of importance to note that a similar correlation ($\rho = 0.88$) between the affinity (K_a) for acarbose and the catalytic efficiency (k_{cat}/K_m) for maltose was recently reported for the inverting α-glycosidase, glucoamylase (*122*). These results therefore provide further support for the notion that transition states for inverting and retaining glycosidases are quite similar in character (*13, 131*).

The conclusive evidence that acarbose could act as a transition state analogue for CGTase contradicted the binding mode of acarbose observed crystallographically. As discussed previously, the valienamine moiety was observed bound in the -2 site instead of the -1 site (*79*). This was in contrast to the binding mode of acarbose observed in all of the other structures of related enzymes such as glucoamylase, porcine pancreatic α-amylase, *Aspergillus oryzae* α-amylase and a thermostable CGTase (*80, 128-130*). As well, it seemed unlikely that the portions of acarbose believed to be responsible for its transition state mimicry, the valienamine moiety and the exocyclic nitrogen, would be positioned in the -2

subsite, instead of in the -1 subsite, the site of cleavage (Figure 2.28). Faced with these findings, our collaborator, Dr. B. Dijkstra, has re-examined the binding mode of acarbose to CGTase using the original data set (*79*) as well as obtaining new (2.2 Å resolution) crystallographic data for CGTase complexed with acarbose. This is particularly important since, at the time of publication of the first structure (*79*), it was not realized that acarbose may undergo a transglycosylation reaction in the crystal, adding a glucose residue to the valienamine (*83*). Both experiments confirmed that the valienamine moiety is in fact bound in the -1 subsite and not the -2 site as they had previously reported (Dr. B. Dijkstra and Mr. J. Uitdehaag, personal communication). As shown in Figure 2.29, in the re-refined structure, a re-arranged acarbose moiety was observed and the electron density for a sugar 6-hydroxyl group was present at subsites -2, -1 and +2, but not at subsite +1. Thus, on this basis, acarbose is bound with its 6-deoxy glucose unit in subsite +1 and consequently the valienamine moiety is bound in the -1 subsite. It is possible that the low resolution (2.5 Å) obtained for the original structure may have contributed to the assignment of the valienamine moiety in the wrong site.

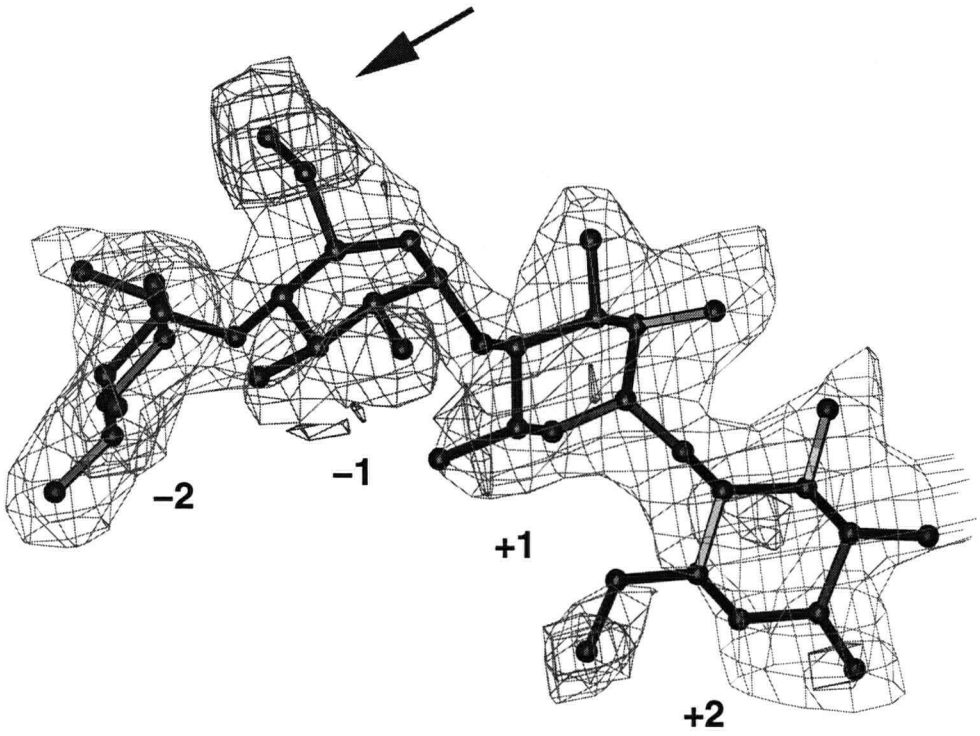

Figure 2.29 Electron density for a re-arranged acarbose bound to B. circulans 251 CGTase from the re-refined data set (unpublished data kindly supplied by Dr. B. Dijkstra and Mr. J. Uitdehaag, University of Groningen, the Netherlands). The numbers indicate the subsites and the arrow indicates the 6-hydroxyl group of the valienamine moiety.

CHAPTER 3

A MECHANISTIC STUDY OF RABBIT MUSCLE GLYCOGEN PHOSPHORYLASE

3.1 GENERAL INTRODUCTION

3.1.1 Function and Role

α-Glucan phosphorylases (α-1,4-glucan-orthophosphate transferase; E.C. 2.4.1.1), catalyze the phosphorolytic cleavage of polysaccharides such as starch and glycogen to produce α-D-glucose-1-phosphate (G1P), a key metabolic intermediate (Figure 3.1). Homologs of phosphorylase are present in diverse species ranging from yeast to potato to human. Two of the most extensively studied forms of phosphorylase are the rabbit muscle and potato enzymes. Many of the eukaryotic enzymes function as cooperative homodimers and are often, but not always, under the control of phosphorylation and allosteric effectors. A covalently bound pyridoxal phosphate (PLP) cofactor is important for the activity of all α-glucan phosphorylases. As the objective of this work is to investigate the mechanism of rabbit muscle glycogen phosphorylase and compare the results to those from analogous experiments performed on potato phosphorylase, the similarities and differences between the two enzymes will be highlighted in this introduction.

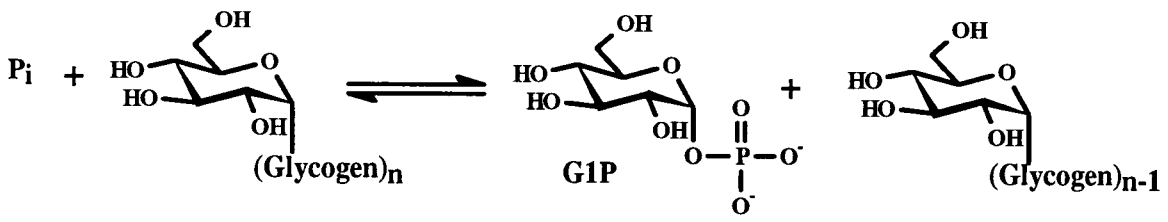

Figure 3.1 The reaction catalyzed by glycogen phosphorylase (for potato phosphorylase the preferred polysaccharide substrate is starch)

3.1.2 Allostery

Rabbit muscle glycogen phosphorylase, which was first isolated in 1936 by Cori & Cori, is a complex enzyme whose activity is strictly controlled by a number of allosteric effectors and by covalent modification (*132*). The enzyme can exist in two distinct forms, phosphorylase *a* and *b*. Phosphorylase *b* is converted to the *a* form through the action of phosphorylase kinase, which phosphorylates the enzyme at Ser14. A phosphatase dephosphorylates the phosphate at Ser14, thereby converting phosphorylase *a* back to the *b* form. Phosphorylase *b* exists in two conformational states, the inactive T state and the active R state. These two states are regulated by the allosteric binding of effectors such as AMP and inhibitors such as ADP, ATP, glucose, and glucose-6-phosphate. Phosphorylase *a*, on the other hand, exists almost exclusively in the more active R state and it is found to be active in the absence of AMP. In contrast, the action of potato phosphorylase is not regulated by any of the covalent or allosteric effectors that modify the activity of rabbit muscle glycogen phosphorylase. Thus, potato phosphorylase represents a model system for studying the mechanism of phosphorolytic cleavage since the process of catalysis can be separated from complicated regulatory controls.

3.1.3 Structural Information

The average weight of the phosphorylase monomer is between 90,000 Da and 110,000 Da depending on its source. The molecular weight of rabbit muscle glycogen phosphorylase is 97,444 Da while potato phosphorylase is 103,916 Da. The overall sequence homology of rabbit muscle phosphorylase to potato phosphorylase is approximately 50%, however, there is a higher degree of homology (> 75%) among the key active site residues (*133, 134*). The

highest region of homology is the pyridoxal phosphate binding site. The area of lowest homology is the N-terminal end, the region responsible for much of the allosteric regulation in muscle phosphorylase.

Rabbit muscle glycogen phosphorylase can exist either as a homodimer or a homotetramer depending on the extent of enzyme activation. In the absence of all effectors, phosphorylase *a* is present as a tetramer while phosphorylase *b* is present as an inactive dimer. When phosphorylase *b* is activated by AMP, the dimers associate into tetramers. In the presence of glycogen, both tetrameric phosphorylase *a* and *b*, dissociate into active R state dimers. Potato phosphorylase exists as a dimer.

The X-ray crystal structures of the four basic conformational states of the muscle enzyme: T state glycogen phosphorylase *b* (*135*), T state phosphorylase *a* (*136*), R state phosphorylase *b* (*137, 138*), and R state phosphorylase *a* (*139*), have all been determined (see Figure 3.2 for a representative example). These studies have identified the location of the primary ligand binding sites. The catalytic site is located in a deep cleft near the boundary between the N-terminal and C-terminal domains and is composed of 3 distinct subsites. The first is specific for binding the glucosyl portion of glucose-1-phosphate (G1P) and as such, glucose can also bind here. The second subsite consists of a pocket that binds the phosphate moiety of G1P or free orthophosphate (Pi). The third subsite is responsible for the binding of the cofactor pyridoxal phosphate. Additionally, crystallographic studies on phosphorylated and unphosphorylated forms of rabbit muscle glycogen phosphorylase and forms complexed with substrates and effectors have provided detailed information about the nature of the structural changes occurring after allosteric activation (for useful reviews see (*140-142*)). A

direct comparison cannot be made to potato phosphorylase as the preliminary crystal structure, first reported in 1984 by Hecht et al., has never been published *(143)*.

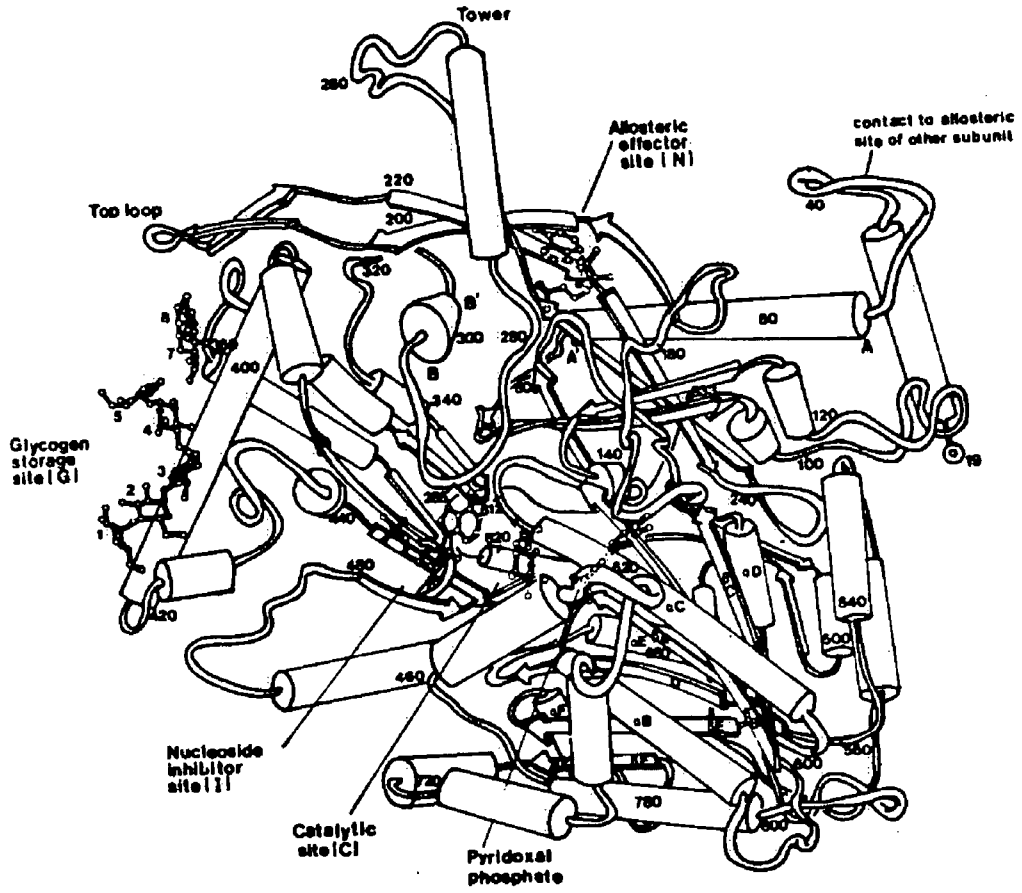

Figure 3.2 X-ray structure of rabbit muscle glycogen phosphorylase b monomer from McLaughlin et al. (144). α-Helices and β-strands are represented by cylinders and arrows, respectively.

3.1.4 The Catalytic Mechanism of Phosphorylase

To date, the catalytic mechanisms of both muscle and potato phosphorylase remain unclear. However, previous studies have indicated that despite their phylogenetic separation, the two enzymes exhibit similar substrate specificities. This was quantified by the excellent linear free energy relationships (ρ = 0.998 and ρ = 0.999, slope = 1.0 and slope = 1.2) observed when the V_{max}/K_m value for each of a series of deoxy and deoxyfluoro analogues of G1P for the muscle enzyme were plotted logarithmically versus the same parameters for the potato enzyme (*145*). This high degree of correlation indicates that very similar hydrogen-bonding interactions between the enzyme and the substrate must be present at the transition states for the two enzymic reactions, consistent with the high degree of active site homology.

Two key features of the reaction suggest that it has similarities to the double displacement mechanism of many retaining α-glycosidases and α-glycosyl transferases (see Section 1.3). Such a mechanism accounts for the observed retention of configuration at the anomeric center and the cleavage of the anomeric carbon-oxygen bond (*7*). General features of the double displacement mechanism which would apply to phosphorylase are general acid catalyzed glycosidic bond cleavage, stabilization of the glycosyl moiety through a covalent bond, and general base catalyzed attack at the anomeric carbon by the 4-hydroxyl at the non-reducing end of the acceptor glucan (Figure 3.3). The most likely candidate for the nucleophilic side chain is a carboxylate but so far its identity remains unknown. Other notable features of the catalytic mechanism of phosphorylase include the presence of the cofactor, pyridoxal phosphate, and the fact that the enzyme catalyzes a bi-substrate reaction.

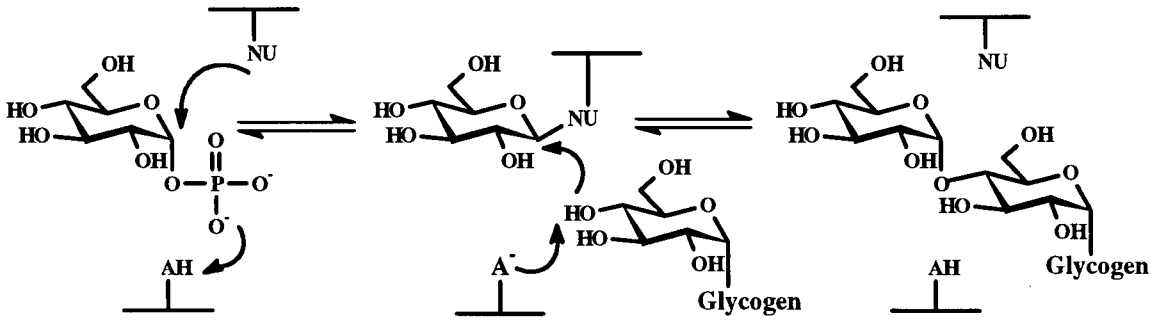

Figure 3.3 The proposed double displacement mechanism for glycogen phosphorylase

3.1.5 Evidence for Oxocarbenium Ion-Like Transition States

There is experimental evidence for the existence of an oxocarbenium ion-like transition state in the mechanism of phosphorylase. Work by Street et al. on a series of G1P analogues in which sugar hydroxyls were individually replaced by hydrogen or fluorine determined that a linear free energy relationship existed between the rate constants for the enzymic reaction and those for the spontaneous, acid-catalyzed hydrolysis (*30*). This experiment was highlighted in Section 1.4.3. Since the spontaneous hydrolysis of G1P is known to proceed through an intermediate with positive charge development on the glucosyl ring, the observation of a reasonable correlation between rates of the two reactions indicates a similar development of positive charge between the two transition states. These results are inconsistent with any truly concerted mechanism as proposed by Klein et al. (*146*) while they are compatible with a less concerted mechanism involving substantial departure of the leaving group prior to attack (*30*).

Another strategy for defining the charge development at the transition state involves kinetic isotope effect measurements. Two studies have been completed on muscle phosphorylase with conflicting results. By measuring the phosphorylase-catalyzed rates of both a C-1 protio and C-1 deuterio G1P, an α-secondary deuterium kinetic isotope effect of

k_H/k_D = 1.10 was determined by Tu et al. (*147*). This would be consistent with a mechanism involving sp^2 hybridization at the transition state of the rate determining step. Later Firsov et al. used doubly labelled G1P substrates to measure the kinetic isotope effect on both the forward and reverse directions of the reaction (*148*). The kinetic isotope effects measured in this manner were found to be unity (k_H/k_D = 1.0; k_H/k_T = 1.0). This result was more consistent with an S_N2 type transition state. However, kinetic isotope effect measurements only provide insights into transition states of chemical steps if that step is rate determining. They tell nothing of value if the rate determining step is the interconversion of a ternary complex, as is likely with phosphorylase.

As discussed in Section 1.4.3, the use of transition state analogues which are believed to mimic the transition state of the natural substrate has also provided support for an oxocarbenium ion-like transition state in muscle phosphorylase as well as information on the orientation of the catalytic residues. Two such examples are D-glucono-(1,5)-lactone (**1.6**) and nojirimycin tetrazole (NJT) (**1.8**), both of which are bound tighter by the enzyme in the presence of Pi (*149, 150*). In addition, crystallographic studies on the T and R state forms of muscle phosphorylase *b* complexed with nojirimycin tetrazole and phosphate have proven useful for further defining the phosphate binding site (*150*). A schematic representation of the active site of muscle phosphorylase with NJT bound is shown in Figure 3.4. Although this structure may not provide an accurate representation of the active site in its native state, it is interesting to note that there are no carboxylate residues located in the proximity of NJT and Pi which could fulfill the role of nucleophile. The closest candidate appears to be the main chain carbonyl oxygen of His377 which is located adjacent to the C-1 carbon of NJT and may provide a means of stabilizing a charged intermediate (*150*).

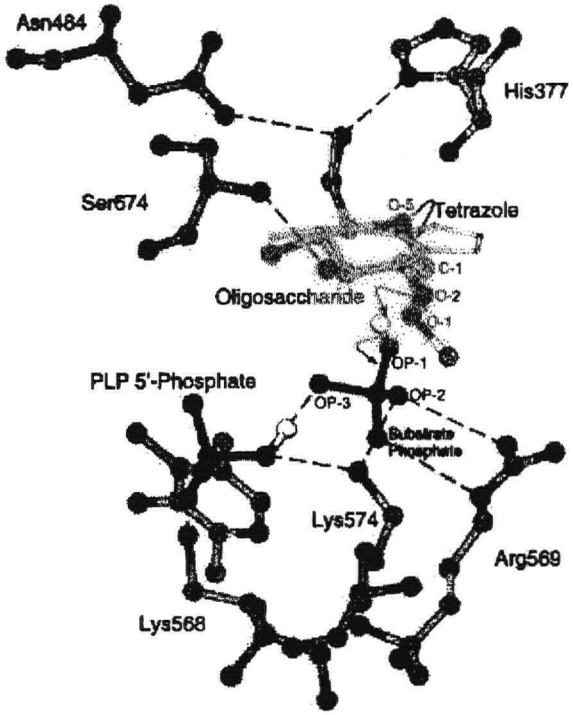

Figure 3.4 Schematic diagram of the catalytic site of glycogen phosphorylase b in the presence of nojirimycin tetrazole and phosphate. Taken from Mitchell et al. (150).

3.1.6 The Role of Pyridoxal Phosphate in Catalysis

Each subunit of phosphorylase contains one molecule of pyridoxal phosphate (PLP) which is covalently bound as a Schiff base to a lysine residue (Figure 3.5). Pyridoxal phosphate is covalently bound to Lys680 and Lys652 in muscle and potato phosphorylase respectively. When PLP is removed from the muscle enzyme, activity is lost but can be regained through reconstitution with PLP (*151*).

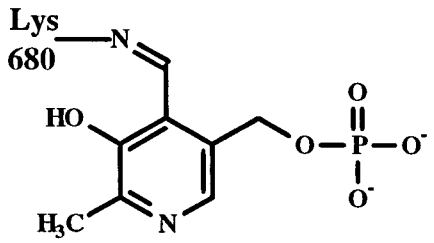

Figure 3.5 Pyridoxal phosphate shown covalently linked to Lys680 in rabbit muscle phosphorylase

The role of PLP in the reaction catalyzed by phosphorylase is unique in PLP-containing enzymes because very little loss in activity is observed when the imine linkage that connects the pyridoxal to the enzyme is reduced. In an effort to determine which components of the PLP moiety are essential for catalytic activity, many analogues of PLP have been synthesized and reconstituted into phosphorylase (for a review see (*152*)). It was found that the phosphate part of the pyridoxal phosphate must be present and be in a dianionic form to confer catalytic activity. The aldehyde functionality at the 4-position was found to be essential for proper cofactor binding. All other components of the pyridoxal phosphate moiety were less essential for activity.

3.1.6.1 PLP as an acid/base catalyst?

Largely on the basis of ^{31}P NMR studies coupled with evidence from kinetic studies with glycosidic substrates lacking a phosphate moiety (such as glucal and heptenitol), it has been suggested that PLP functions as an acid/base catalyst (*153-156*). As shown in Figure 3.6, PLP is proposed to protonate the phosphate moiety of the G1P and then assist in departure of the leaving group. However, substantial experimental evidence now exists to suggest that PLP does not behave as an acid/base catalyst.

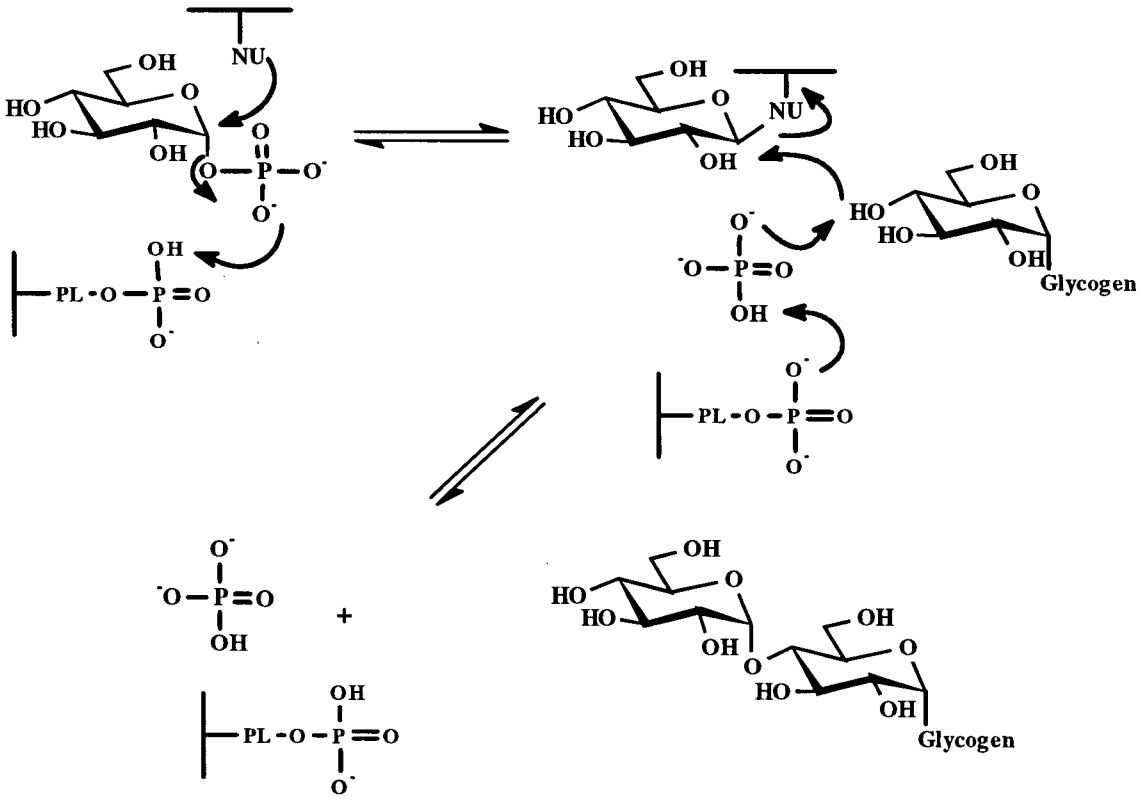

Figure 3.6 The proposed mechanism for glycogen phosphorylase with PLP acting as an acid/base catalyst

Evidence against the involvement of PLP as an acid catalyst comes from studies with muscle phosphorylase reconstituted with pyridoxal, an enzyme derivative which is only active in the presence of activator anions which bind in place of the missing phosphate moiety.

When fluorophosphate (pK_2 = 4.8) and phosphite (pK_2 = 6.6) were used as replacement anions, both were shown to be equally good activators of phosphorylase activity (*157*). The relatively low pK_a of fluorophosphate essentially ensures that it binds to phosphorylase in a dianionic form and remains dianionic throughout the experiment. Moreover, measurement of the pH dependence of catalysis by both fluorophosphate- and phosphite- activated pyridoxal phosphorylase showed very similar pH profiles regardless of the activator anion used, indicating that no significant differences exist between the two enzyme systems (*158*). However, based on the differences in the pK_2 values of these phosphate analogues, a large difference in their pH profiles would be expected if the coenzyme phosphate was involved in an essential proton transfer step. Thus, it was unlikely that PLP could function as an acid/base catalyst.

Nonetheless, it is possible that the behaviour of the pyridoxal-reconstituted phosphorylase complexed with noncovalently bound phosphate analogues may not reflect that of the PLP cofactor found in the native enzyme. Therefore, some researchers question the validity of these experiments. In fact, recent X-ray crystallographic studies of pyridoxal-reconstituted phosphorylase complexed with either phosphite, phosphate or fluorophosphate, glucose and IMP showed that the anions bind at the catalytic site in a similar but not identical position to that of the cofactor phosphate group in the native enzyme (phosphorus to phosphorus distance is 1.0 Å) (*159*).

To overcome the possible limitations of the earlier experiments two phosphonate analogues of pyridoxal phosphate, pyridoxal 5′-methylene phosphonic acid (**3.1**) and pyridoxal 5′-difluoromethylene phosphonic acid (**3.2**) were synthesized and reconstituted into apo-phosphorylase and their kinetic behaviour analyzed (Figure 3.7) (*160*). These analogues

incorporate all of the requirements essential for catalytic activity as well as phosphonic acid groups which differ significantly in their pK_a values. In addition, X-ray crystallographic studies of glycogen phosphorylase reconstituted with pyridoxal 5′-methylene phosphonic acid (**3.1**) have demonstrated that this analogue binds to the enzyme in an essentially identical mode to that of the native cofactor (*161*). Despite their significant differences in phosphonic acid pK_a values (a difference of 3 pK_a units), the pH dependences of V_{max}, K_m, and V_{max}/K_m were found to be similar for both systems (*160*). These results reaffirm the idea that PLP does not function as an essential acid/base catalyst and instead remains dianionic throughout catalysis.

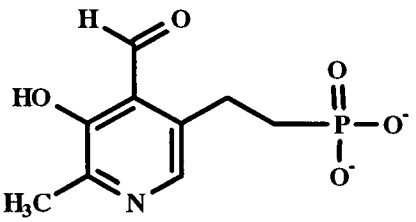

3.1

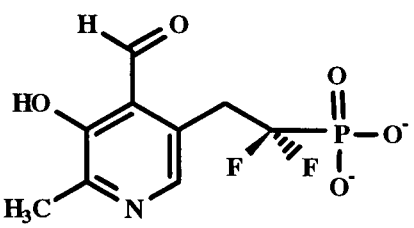

3.2

*Figure 3.7 Structures of the phosphonate PLP analogue (**3.1**) and difluorophosphonate PLP analogue (**3.2**)*

3.1.6.2 PLP as an electrophilic catalyst?

While these experimental results suggest that PLP is not involved in an essential proton transfer, they do not exclude PLP from acting in an electrophilic role. It is possible that the PLP moiety can act as an electronic sink to promote the departure of the phosphate leaving group and to electronically stabilize the intermediate long enough to permit the attack of the incoming acceptor nucleophile (Figure 3.8). In this model, it is proposed that the phosphate of PLP is distorted into a trigonal bipyramid with the empty apical position oriented

towards the substrate phosphate (see (*152, 162*)). The interaction of the substrate phosphate with the phosphate of the pyridoxal may help to promote the departure of the leaving group. This type of mechanism was probed by reconstituting pyridoxal phosphorylase with oxyanions of early transition metals such as molybdate, tungstate and vanadate which can all adopt trigonal bipyramidal configurations (*163*). Therefore, if a distorted phosphate is formed during the reaction then one or more of these metals may inhibit the reaction by competing for the cofactor phosphate binding site. Although molybdate was found to bind some 13 times more tightly to the enzyme than phosphate, this evidence is insufficient to fully support the proposed electrophilic mechanism.

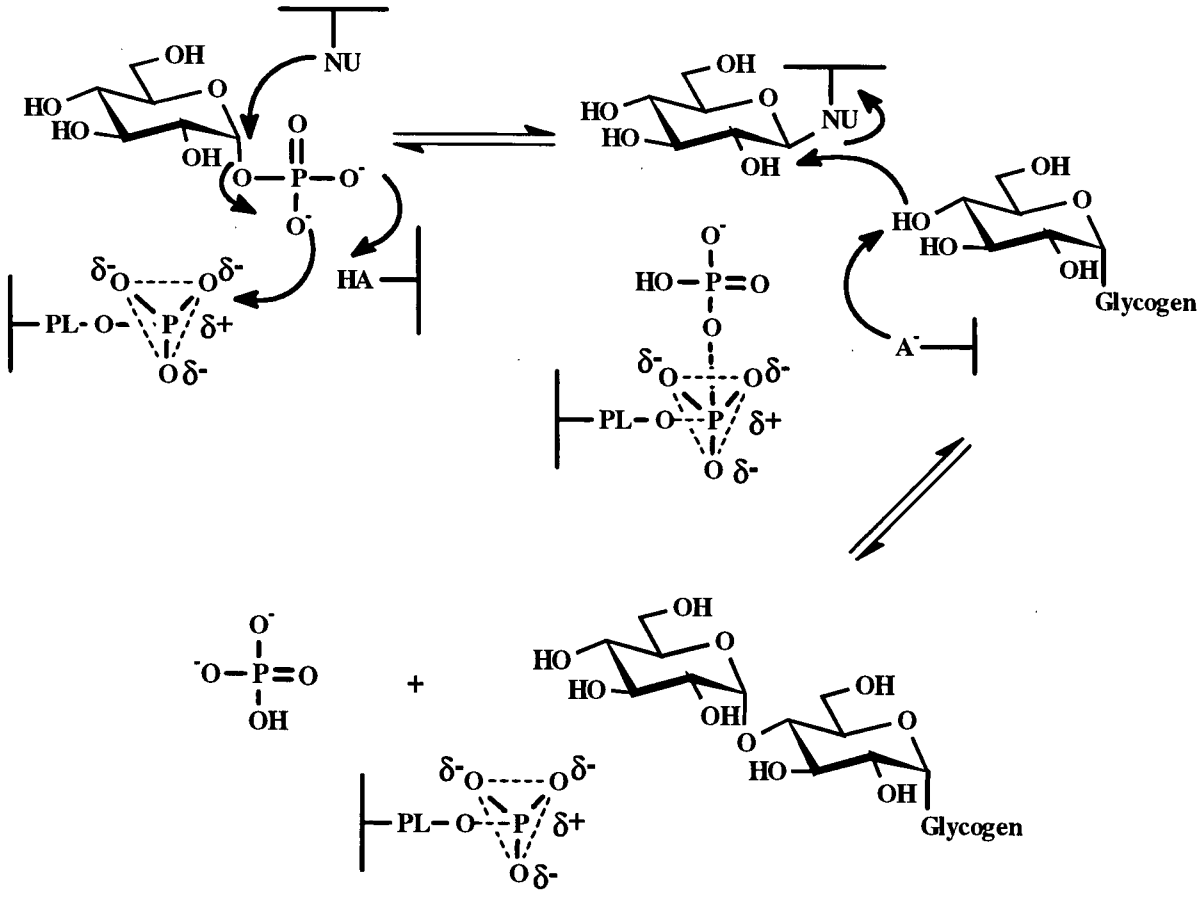

Figure 3.8 The proposed mechanism for glycogen phosphorylase with PLP acting as an electrophilic catalyst

An alternative role for a dianionic cofactor phosphate might be in destabilization of the ground state enzyme-substrate complex through electrostatic interactions (*160*). This could result in catalysis if the enzyme-substrate binding energy were used to enforce the close binding of the substrate and cofactor phosphate. This electronic destabilization could then be released at the transition state through a change in position of the substrate phosphate.

3.1.7 Kinetic Mechanism

Through initial velocity measurements, inhibition studies, and equilibrium isotope exchange reactions, rabbit muscle glycogen phosphorylase and potato phosphorylase have been shown to follow a rapid equilibrium random Bi-Bi kinetic mechanism (Figure 3.9) (muscle: (*164-166*), potato: (*149*)). In this model, an active ternary complex cannot be formed until all substrates (G1P or Pi and glycogen/starch or oligosaccharide) are present. The rate determining step for both enzyme systems is believed to be the interconversion of the ternary complex. In order to simplify interpretation of the kinetic data, in most studies (including those reported in this thesis), the model may be simplified to that of a single substrate system by utilizing one of the substrates at saturating concentrations (for example, glycogen).

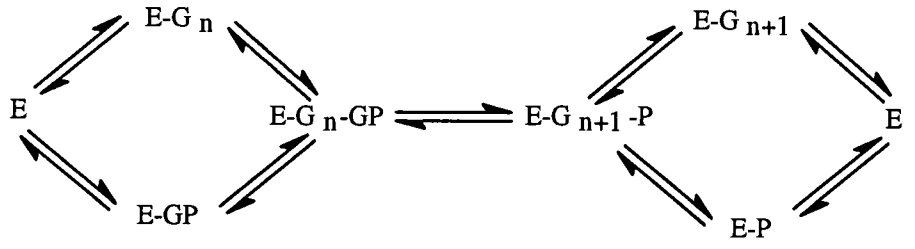

Figure 3.9 The rapid equilibrium random Bi-Bi kinetic mechanism for glycogen phosphorylase. E = enzyme, G_n = glycogen, GP = G1P, P = orthophosphate, E-G_n = enzyme-glycogen complex, E-GP = enzyme-G1P complex, E-G_n-GP and E-G_{n+1}-P are the enzyme-substrate ternary complexes. The same mechanism applies to potato phosphorylase where starch would be the preferred substrate over glycogen.

3.1.8 The Nature of the Glycosyl-Enzyme Intermediate: Covalent or Stabilized Ion Pair?

As discussed previously, both muscle and potato phosphorylases catalyze a two substrate reaction: glycogen or starch plus phosphate or G1P, depending upon the direction of the reaction. On the other hand, the otherwise analogous sucrose phosphorylase functions through a ping-pong mechanism, in which half-reactions are catalyzed. Therefore, sucrose can bind to the enzyme and transfer the glucosyl moiety to a suitably placed enzymatic nucleophile before the acceptor molecule (Pi in this case) binds to the enzyme and completes the transfer. Voet and Abeles were able to capture the glycosyl-enzyme intermediate using radiolabelled sucrose and rapid acid denaturation (*44*). Therefore, in order to attempt similar experiments on muscle or potato phosphorylase, suitable substrates which would allow the formation of the enzyme ternary complex but prevent enzymic turnover of the enzyme-substrate intermediate would first have to be developed.

In 1977, Kokesh and Kakuda published a set of experimental results which provide some evidence for a long lived intermediate in the catalytic mechanism of potato phosphorylase (*167*). In the presence of α- or β-cyclodextrin (see Figure 2.1), an oligosaccharide mimic, it is possible to prevent an α-glucosyl transfer because of the absence of any free 4-hydroxyl groups in the cyclodextrin ring. Kokesh and Kakuda showed that an ^{18}O labelled oxygen that had been incorporated into one of the non-bridging positions in the phosphate moiety of G1P could be enzymatically exchanged to the bridging position only in the presence of cyclodextrin (Figure 3.10). This confirmed that the ternary complex (oligosaccharide and G1P or Pi) must be formed before enzymatic turnover can occur. Also, although these experiments do not define the type of intermediate formed, covalent or ion-

pair, they do provide some evidence for an intermediate which has a sufficiently long lifetime to allow for rotation of the phosphate moiety.

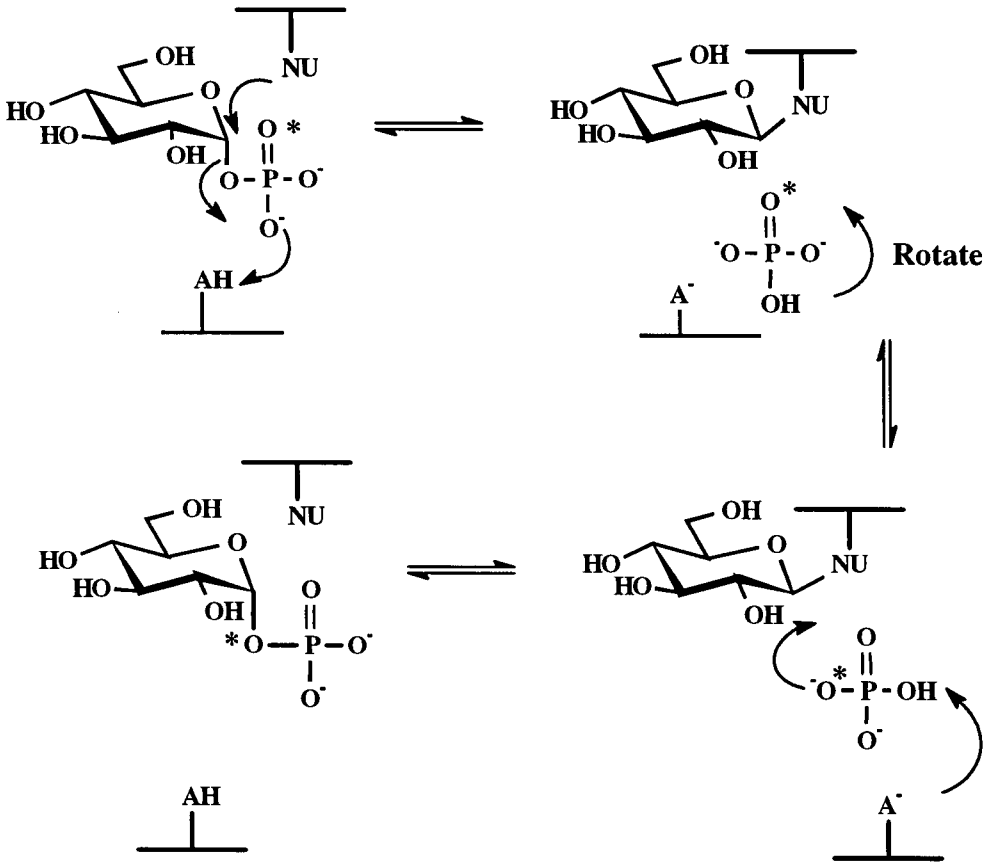

Figure 3.10 Positional isotope exchange catalyzed by potato phosphorylase in the presence of cyclodextrin (structure not shown). (indicates an ^{18}O label).*

3.2 THE SPECIFIC AIMS OF THIS STUDY

While there is currently very little disagreement on the general features of the reaction catalyzed by phosphorylase, three major questions remain, namely: does the reaction involve a glycosyl-enzyme intermediate; what is the active site binding mode of oligo- or polysaccharide substrates; and what is the mechanistic role of the essential active site cofactor PLP? The objective of this work is to provide insight into the first two questions.

1. *What is the nature of the intermediate in the reaction catalyzed by phosphorylase?* In order for phosphorylase to catalyze its reaction, both components must be present, glycogen or starch plus phosphate or G1P, for an active ternary complex to form and turnover to occur. Therefore, in order to form and hopefully trap a glycosyl-enzyme intermediate, some form of incompetent oligo- or polysaccharide analogue is required which is sufficiently close in structure to the natural substrate to bind, but which cannot act as a glycosyl acceptor. As discussed previously, cyclodextrins satisfy this requirement in that they have no free 4-hydroxyl group and indeed they have been used to activate potato phosphorylase in a positional isotope exchange (PIX) reaction in which the bridging and non-bridging oxygen atoms of G1P were observed to scramble (see Section 3.1.8) (*167*). However, because the tunnel shaped active site cleft of muscle phosphorylase cannot accommodate such a cyclic structure other alternatives must be sought. Previously, analogues of glycogen have been constructed in which the non-reducing terminal ends of the glucan chains had been enzymatically capped with 4-deoxy or 4-deoxyfluoro glucose moieties (*168*). Unfortunately, it proved impossible to completely (> 99%) cap all of the chain ends, hence a low level of transfer (1%) was still observed, making further experiments impossible. Therefore, the need existed for malto-oligosaccharides selectively deoxygenated at the 4-hydroxyl of the non-reducing end sugar to explore the mechanism of phosphorylase more closely.

The objective of this project was to chemoenzymatically synthesize two such analogues, 4-deoxymaltopentaose (4DG5) and 4-deoxymaltohexaose (4DG6). This will be accomplished by elongating 4-deoxy-α-maltotriosyl fluoride (**1.21**) with maltotriose (**2.2**) using the transferase activity of glycogen debranching enzyme. Attempts will be made to provide evidence for a covalent glycosyl-enzyme intermediate using mass spectrometry and

rapid acid denaturation experiments. Furthermore, analogous PIX experiments to the one previously reported for potato phosphorylase in the presence of G1P and α-cyclodextrin will be attempted using both muscle and potato phosphorylase. In place of cyclodextrin, 4-deoxymaltopentaose or 4-deoxymaltohexaose will be used as oligosaccharide mimics. Glucose-1-phosphate selectively labelled with ^{18}O in the bridging position (anomeric oxygen) will be prepared using a new chemical synthesis. ^{31}P NMR will be used to follow the extent of isotope exchange.

2. *What is the nature of the binding mode of oligosaccharide to phosphorylase?* A detailed kinetic analysis of the interaction of 4DG5 and 4DG6 with both muscle and potato phosphorylase will be completed in order to gain insight into this question. In addition, the 4-deoxy-oligosaccharides will be used as a means to probe the high binding affinity previously measured for rabbit muscle glycogen phosphorylase with 4-deoxy-glycogen (*168*). To date, no X-ray crystal structure of an oligosaccharide bound to the active site of rabbit muscle glycogen phosphorylase has ever been obtained. It is hoped that 4-deoxymaltohexaose could prove useful in attempts to crystallographically observe enzyme/oligosaccharide complexes.

3.3 RESULTS AND DISCUSSION

3.3.1 Malto-Oligosaccharides as Substrates for Phosphorylase

Despite their similarities in structural and kinetic properties, affinities for substrate glucans differ widely between the muscle and potato phosphorylases (*134, 169*). Muscle phosphorylase prefers highly branched oligosaccharides such as glycogen while potato phosphorylase has a higher affinity for linear oligosaccharides. Although these differences in

affinities have already been characterized to some extent, they often vary with the assay method and the enzyme source. Therefore, it was first necessary to obtain an independent set of kinetic parameters for maltopentaose (G5) and maltohexaose (G6) under our operating conditions. This would then allow the kinetic data determined for the modified malto-oligosaccharides, 4DG5 and 4DG6, to be compared more consistently with the kinetic parameters determined for the standard substrates, G5 and G6.

The kinetic parameters for the reaction of rabbit muscle glycogen phosphorylase with maltopentaose and maltohexaose in both the synthetic and degradation directions were determined (Table 3.1). As observed previously (*170*), the K_m values for G1P with muscle phosphorylase in the presence of G5 and G6 were 4 - 5 fold higher than those determined in the presence of glycogen. Similarly, K_m values for phosphate were 2 - 3 fold lower in the presence of glycogen than oligosaccharides. The K_m values were 100 fold lower for the linear oligosaccharides with potato phosphorylase than with the muscle enzyme. This is entirely consistent with the preference of the potato enzyme for linear oligosaccharides as noted previously (*134*).

Table 3.1 Kinetic Parameters Determined for Rabbit Muscle and Potato Phosphorylase with Malto-Oligosaccharides as Substrates

Synthesis Direction		*Muscle*		*Potato*	
Variable	**Constant**[1]	**V_m (U/mg)**	**K_m (mM)**	**V_m (U/mg)**	**K_m (mM)**
G1P	α-glucan[2]	54.9	1.7	32.3	1.9
α-glucan[2]	G1P	--	0.079[3]	--	0.046[3]
G1P	G5	35.0	8.0	30.1	1.6
G1P	G6	40.7	7.1	--	--
G5	G1P	86.1	35	20.7	0.33
G6	G1P	130.5	79.3	--	--
Degradation Direction		*Muscle*		*Potato*	
Pi	α-glucan[2]	30.3	2.40	7.9	1.9
α-glucan[2]	Pi	--	--	--	--
Pi	G5	27	6.2	7.2	2.1
Pi	G6	28.3	5.4	--	--
G5	Pi	32.5	17.6	7.2	0.23
G6	Pi	34.4	15.3	--	--

[1] Experimental data is displayed in a graphical format in Appendix B (Figures B-9, B-10, B-11) along with the concentrations of the constant components used (U = units = μmol/min).
[2] Glycogen was used for muscle phosphorylase and starch for the potato enzyme.
[3] Values reported previously by Fukui et al. (*134*). These values were calculated on the basis of the molar concentration of the non-reducing ends of each glucan.
Average errors in kinetic parameters: synthesis direction: K_m (+/- 10 %), V_m (+/- 5 %), degradation direction: K_m (+/- 10 %), V_m (+/- 5 %).

As the products from the elongation of the malto-oligosaccharides are themselves substrates for phosphorylase, it was necessary to ensure that the extension of the malto-oligosaccharide primer was minimal during the assay time. For example, the kinetic parameters determined for G5 in the synthesis direction should reflect the enzyme catalyzed conversion from G5 to G6 rather than that from G6 to G7, and so on. The chain length

extensions of the primer were calculated from the ratio of moles of Pi released versus moles of malto-oligosaccharide originally present (*169*). In all experiments, the total percentage of malto-oligosaccharides elongated by one glucose unit ranged from 0.1-1.0%. This concentration of higher oligosaccharides will not significantly affect the kinetic parameters determined.

3.3.2 Synthesis and Purification of 4-Deoxymaltopentaose and 4-Deoxymaltohexaose

As muscle phosphorylase requires a minimum of 5 glucose units in order to bind the oligosaccharide, it is necessary to use, at the very least, maltopentaose as a building block with which to synthesize an incompetent substrate (*169*). However, as maltopentaose and longer oligosaccharides are expensive to buy and difficult and costly to synthetically modify, a shorter oligosaccharide such as maltotriose would provide a more accessible starting material. Through enzymatic means it is possible to elongate maltotriose using the transferase activity of glycogen debranching enzyme (Glyx) (*171*). In addition, it has been well established that glycogen debranching enzyme can catalyze the elongation of glycosyl fluorides such as α-maltotriosyl fluoride to produce the hexasaccharide, α-maltohexaosyl fluoride (*68*). As it was of interest to obtain a malto-oligosaccharide in which the 4-hydroxyl group of the non-reducing end sugar had been replaced with a smaller non-nucleophilic group such as hydrogen (deoxy), 4-deoxy-α-maltotriosyl fluoride (4DαG3F, **1.21**) was chosen as the donor sugar. This was chemically synthesized as described previously in Section 2.3.2.1. When incubated with the acceptor sugar, maltotriose, 4-deoxymaltohexaose (4DG6, **3.3**) as well as 4-deoxymaltopentaose (4DG5, **3.4**) were produced (Figure 3.11). The accumulation of 4DG5 presumably results from the disproportionation reaction also shown in Figure 3.11 (*172*).

Both 4DG5 and 4DG6 were easily purified from the reaction mixture by preparative HPLC using a Dextropak column, as shown in Figure 3.12. The yields varied depending on the length of reaction and the activity of the enzyme. The reaction was stopped when the yield of 4DG6 had been maximized. Typical yields were 43% 4DG6 and 45% 4DG5.

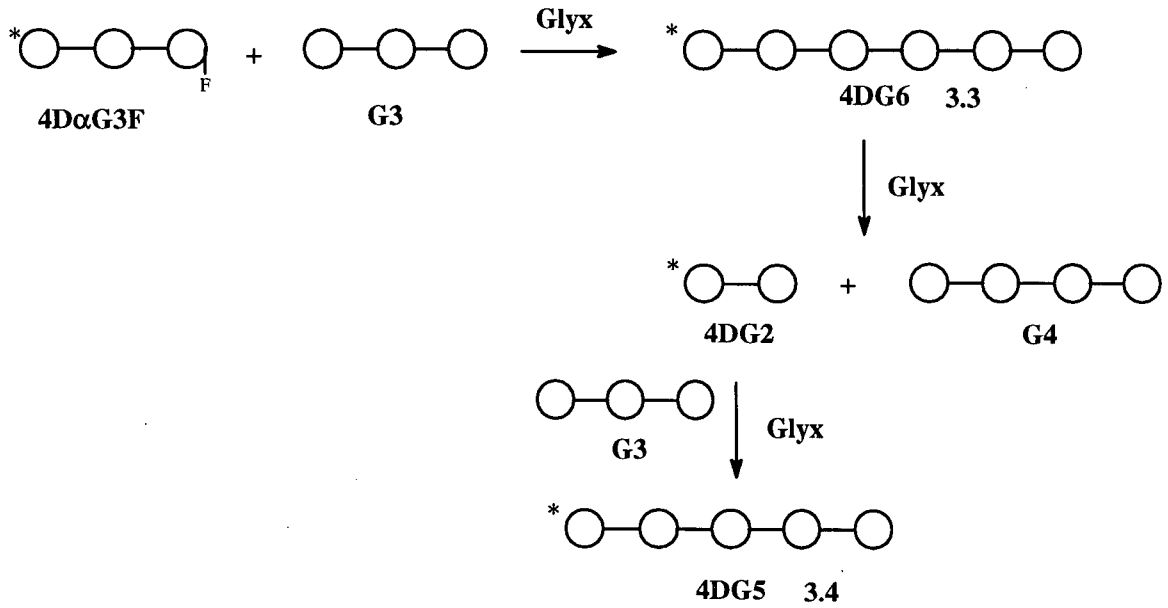

*Figure 3.11 Synthesis of 4DG5 and 4DG6 from 4DαG3F and G3 using glycogen debranching enzyme (Glyx). Each circle represents a glucose moiety linked α-1,4 to the adjacent glucose moiety. The * indicates this non-reducing sugar contains a 4-deoxy moiety.*

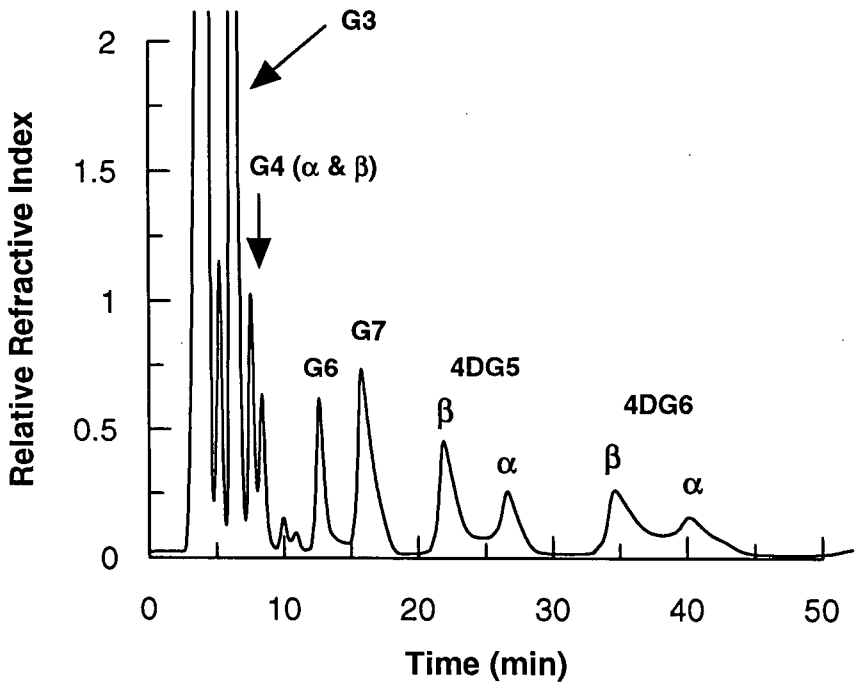

Figure 3.12 HPLC profile of the products of the reaction of glycogen debranching enzyme with 4DαG3F and G3 after 48 h reaction time (Reaction mixture: [4DαG3F] = 22 mM, [G3] = 40.3 mM, [Glyx] = 5.5 mg/mL). Conditions: Dextropak column, 7 mL/min, 100 % H_2O.

3.3.3 4-Deoxymaltopentaose and 4-Deoxymaltohexaose as Incompetent Substrates for Phosphorylase

Because of the limited supply of both 4DG5 and 4DG6, and because approximately equivalent amounts of each were available, 4DG6 was used for the experiments with muscle phosphorylase and 4DG5 was used for the experiments with potato phosphorylase. The binding modes of 4DG6 or 4DG5 to muscle and potato phosphorylase were determined by completing a full inhibition analysis in both the synthetic and degradation directions (see Appendix A for a review on the determination of the mode of inhibition from a graphical analysis). As seen in Figures 3.13A and C, and Figures 3.14A and C, 4DG6 and 4DG5 were found to competitively inhibit binding of maltopentaose (G5) in both the synthetic and

degradation directions for muscle and potato phosphorylase. This indicates that the 4-deoxy-oligosaccharide is competing with maltopentaose for the same binding sub-sites in both directions of catalysis. On the other hand, 4DG6 or 4DG5 were found to bind noncompetitively with respect to either G1P or Pi (Figures 3.13B and D and Figures 3.14B and D). This indicates that the 4-deoxy-oligosaccharides and G1P or Pi were binding simultaneously to the enzyme at independent sites. Thus, these results suggest that the 4-deoxy-oligosaccharides are binding in the substrate acceptor sites.

The K_i values measured for 4DG6 and muscle phosphorylase were approximately 40 fold lower than the K_m value measured for maltohexaose (Tables 3.1 and 3.2). A smaller difference in binding affinity was observed when 4DG5 was tested as an oligosaccharide analogue for potato phosphorylase in either reaction direction. The K_i values were about 10 fold lower compared with the K_m values for maltopentaose.

In the degradation direction (with Pi as the co-substrate), the 4-deoxy-oligosaccharides were also tested as substrates with both enzymes. Over the time period monitored (5 min), the enzyme-catalyzed phosphorolysis of the 4-deoxy-oligosaccharides was negligible. This is consistent with the slow rate of muscle or potato phosphorylase catalyzed turnover of 4-deoxy-glucose-1-phosphate compared with G1P (V_m/K_m decreased almost 500 and 300 fold respectively) *(30, 145)*.

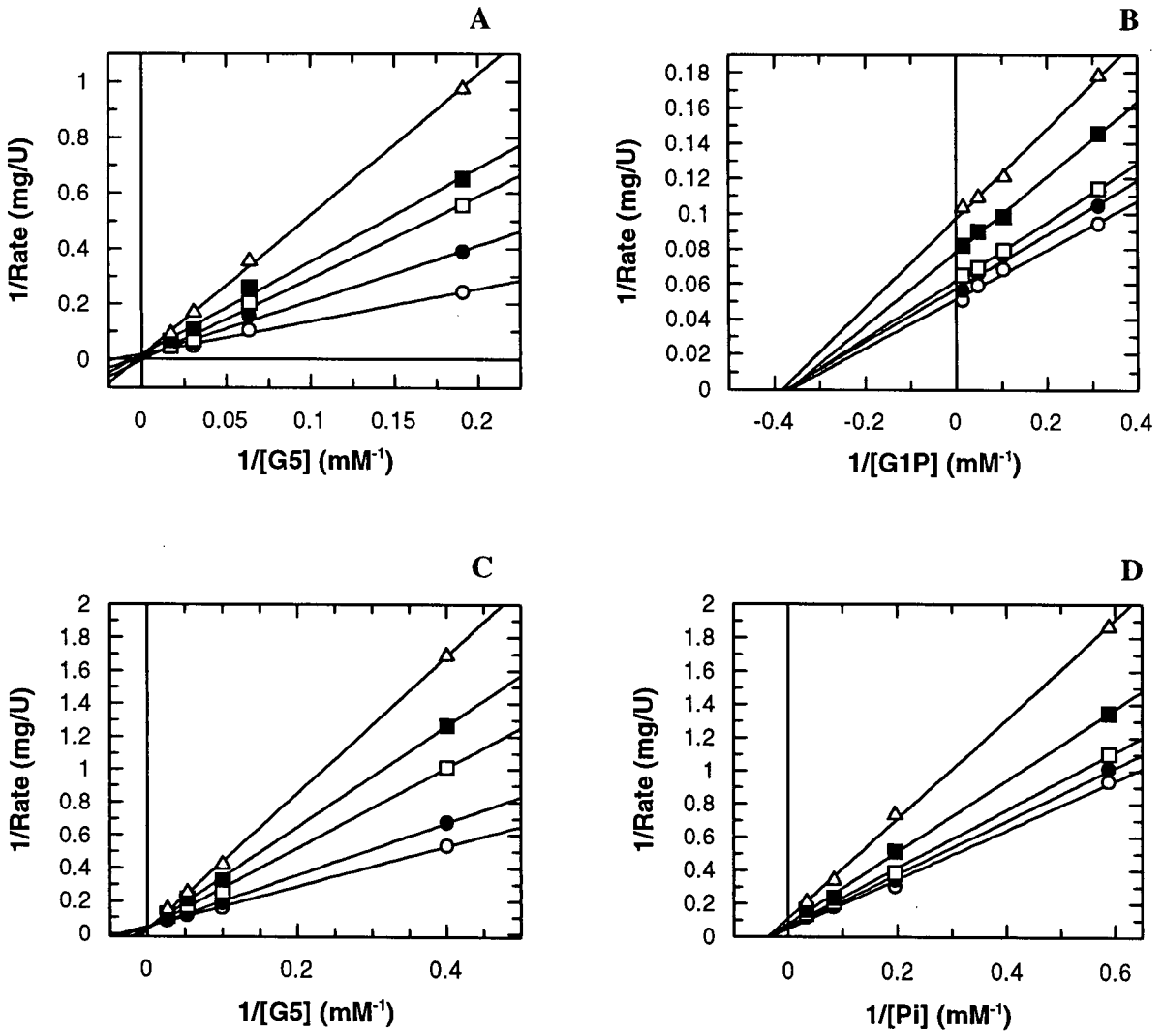

Figure 3.13 Lineweaver Burke plots for the inhibition of muscle phosphorylase by 4DG6 (I). **(A)** [G1P] = 72.6 mM, [enz] = 0 .103 μM, [I]: ○ = 0 mM; ● = 0.0125 mM; □ = 0.025 mM; ■ = 0.06 mM; Δ = 0.125 mM, **(B)** [G5] = 33.5 mM, [enz] = 0.039 μM, [I]: ○= 0 mM; ● = 0.0125 mM; □ = 0.025 mM; ■ = 0.06 mM; Δ = 0.125 mM, **(C)** [Pi] = 23.8 mM, [enz] = 0.040 μM, [I]: ○ = 0 mM; ● = 0.046 mM; □ = 0.093 mM; ■ = 0.232 mM; Δ = 0.465 mM, **(D)** [G5] = 20 mM, [enz] = 0.040 μM, [I]: ○ = 0 mM; ● = 0.046 mM; □ = 0.093 mM; ■ = 0.232 mM; Δ = 0.465 mM.

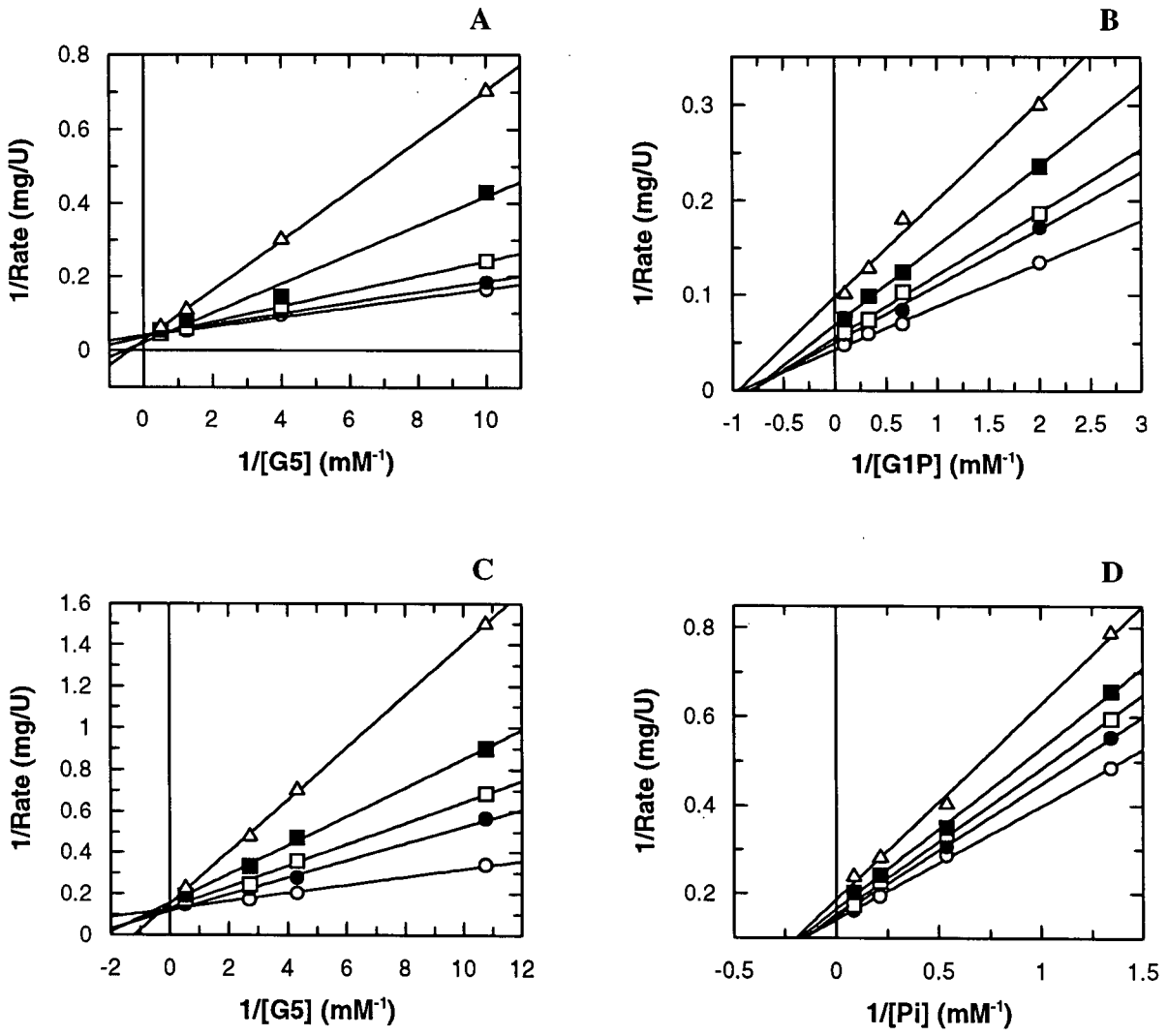

Figure 3.14 Lineweaver Burke plots for the inhibition of potato phosphorylase by 4DG5 (I). **(A)** [G1P] = 10.0 mM, [enz] = 0.145 μM, [I]: ❍ = 0 mM; ● = 0.685 mM; □ = 1.37 mM; ■ = 3.43 mM; Δ = 6.85 mM, **(B)** [G5] = 0.9 mM, [enz] = 0.145 μM, [I]: ❍ = 0 mM; ● = 0.650 mM; □ = 1.21 mM; ■ = 3.03 mM; Δ = 6.05 mM, **(C)** [Pi] = 11.6 mM, [enz] = 0.049 μM, [I]: ❍ = 0 mM; ● = 0.535 mM; □ = 2.14 mM; ■ = 3.75 mM; Δ = 5.36 mM, **(D)** [G5] = 2.79 mM, [enz] = 0.049 μM, [I]: ❍ = 0 mM; ● = 0.598 mM; □ = 1.20 mM; ■ = 2.99 mM; Δ = 5.98 mM.

Table 3.2 Inhibition Parameters Determined for Rabbit Muscle Phosphorylase (4-Deoxymaltohexaose) and Potato Phosphorylase (4-Deoxymaltopentaose)

Synthesis Direction	*Muscle*		*Potato*	
Variable substrate	G1P	G5	G1P	G5
K_i (mM)	6.4	2.1	0.1	0.04
Inhibition mode[1]	noncompetitive	competitive	noncompetitive	competitive
Degradation Direction	*Muscle*		*Potato*	
Variable substrate	Pi	G5	Pi	G5
K_i (mM)	7.4	2.5	1.0	0.06
Inhibition mode[1]	noncompetitive	competitive	noncompetitive	competitive

[1] See Figures 3.13 and 3.14 and Appendix A for determination of the mode of inhibition.

It is unclear why there is an increase in binding affinity when the 4-hydroxyl at the non-reducing end of an oligosaccharide substrate is replaced by hydrogen. One possible explanation could relate to the concept that enzymes have evolved to bind the substrate weakly and the transition state tightly (*29, 173*). This may indicate that the non-reducing end 4-hydroxyl group is involved in an unfavourable binding interaction in the ground state, though a strong one in the transition state. By removing this hydroxyl group and replacing it with a hydrogen, this unfavourable ground state interaction is removed, resulting in tighter binding. The higher binding affinity of the 4-deoxy-oligosaccharides compared to the parent oligosaccharides (approximately 40 and 10 fold decreases in K_m to K_i for the muscle and potato enzyme respectively) corresponds to an increase in Gibbs free energy of binding of about 2.2 kcal/mol and 1.3 kcal/mol in each case. This may be considered a minimum estimate of the true binding strength associated with a particular substitution. This is because the observed increase in binding energy represents the difference between the available binding

energy and whatever binding energy is used to bring about other activation processes (*174*). A similar difference in binding affinities was previously reported for 4-substituted glycogen analogues versus unmodified glycogen. Both 4-deoxy-glycogen and 4-deoxy-4-fluoro-glycogen were found to be reasonable inhibitors of muscle phosphorylase and from their approximate K_i values, it was estimated that they bound some 100 fold more tightly than glycogen itself (*168*).

The relatively high binding affinity of muscle phosphorylase for 4DG6 may prove useful in using this modified substrate to determine the mode of oligosaccharide binding to phosphorylase in the crystalline state. Recently, the crystal structure of *E. coli* maltodextrin phosphorylase co-crystallized with maltohexaose was solved to 3.0 Å, providing the first structure of an oligosaccharide bound at the catalytic site of an α-glucan phosphorylase (*175*). Despite the fact that maltohexaose was used in the crystallization conditions, only two glucose units were observed to be bound at the catalytic site (at subsites +1 and +2) (Figure 3.15). Thus, no oligosaccharide was observed bound in subsites 3 and 4, although 2 sugars were modeled into these sites. As well, no sugar was observed bound at subsite -1 (the catalytic site), although this subsite is known to have a high specificity for D-glucopyranose sugars. Therefore, little could be inferred about the positioning of key catalytic residues at the active site with oligosaccharide present in its normal binding mode. Specifically, the orientation of the active site residues obtained from this structure provided no new clues as to the possible identity of a carboxylate which could be properly positioned to act as a catalytic nucleophile, as required by a double displacement type mechanism. *E. coli* phosphorylase is similar to potato phosphorylase in that it exhibits no allosteric control and has a higher affinity for linear oligosaccharides than for glycogen and other branched polysaccharides.

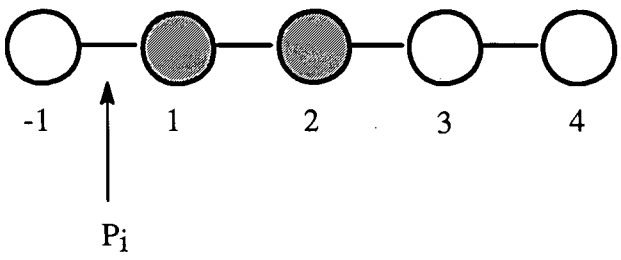

Figure 3.15 A schematic representation of the glucosyl subsites for E. coli phosphorylase. Phosphorolysis takes place between subsite -1 and 1, thus the non-reducing end of the chain would be at subsite -1 and the reducing end would be at subsite 4. The shaded circles represent the sites at which glucose units were observed crystallographically. Adapted from (175).

Difficulties in obtaining a similar structure for muscle phosphorylase lie in the relatively low affinity of the active site for oligosaccharide (K_m = 20 mM) compared with the glycogen storage site (K_m = 1 mM) (*170*). However, the higher binding affinity exhibited by phosphorylase for 4DG6 might provide a means to crystallographically observe oligosaccharide bound at the enzyme active site. As well, the modification of the non-reducing end of the oligosaccharide will prevent further elongation by phosphorylase. Preliminary crystallization studies were carried out by our collaborator, Professor L. N. Johnson, at the University of Oxford. R state rabbit muscle phosphorylase *b* crystals were soaked in sodium tartrate containing 50 mM G1P and 50 mM 4DG6 for 24 hours. After refinement to 2.9 Å resolution, there was no clear evidence for either G1P or oligosaccharide bound at the catalytic site. However, oligosaccharide was observed to be bound at the glycogen storage site, although only the density corresponding to a disaccharide was defined, probably indicating that the other sugars were disordered (personal communication, Professor L. N. Johnson). Possible modifications to the oligosaccharide analogue such as increasing its

length and/or incorporating a branch point may make it feasible to repeat these crystallization studies in the future (see Section 3.5).

3.3.4 Physical Evidence for a Covalent Glycosyl-Enzyme Intermediate

3.3.4.1 Electrospray mass spectrometry experiments

As discussed previously, electrospray mass spectrometry (ES-MS) can be a powerful technique for detecting glycosyl-enzyme intermediates. If deglycosylation is the rate limiting step, it might be possible to observe a covalent glucosyl-enzyme intermediate by ES-MS after incubating muscle phosphorylase with 4DG6, G1P and AMP. The expected molecular weight of holo-muscle phosphorylase is 97,444 Da. However, the PLP cofactor (MWt = 228) is lost under the acidic conditions employed for mass spectral analysis, thus the experimentally determined mass of 97,213 +/- 10 Da corresponds well to the expected mass of the apo-enzyme, 97,213 Da (Figure 3.16A). The experimental approach used to probe the existence of a glycosyl-enzyme intermediate involved incubating phosphorylase with 4DG6, AMP, and G1P for a defined length of time under standard pH conditions, followed by injection of the mixture onto an HPLC column placed in line with the mass spectrometer. The HPLC column was necessary to remove interfering buffer salts. If a glucosyl moiety was covalently bound to the enzyme, an increase of approximately 163 Da to the intact mass should be observed. Under certain conditions some evidence was obtained for a higher molecular weight species with an average increase of approximately 238 Da higher than the intact mass (Figure 3.16B). This increase in mass was observed under several different experimental conditions including those when D-glucal or 6-deoxy-D-glucose-1-phosphate were used in place of G1P as a way to slow down the turnover of the intermediate (*30*). However this mass increase was greater

than that expected and was not reproducible. Indeed, the higher molecular weight species may represent holo-phosphorylase (enzyme with the PLP cofactor still covalently attached). It is possible that by incubating the enzyme with the substrates or substrate analogues, the imine linkage of the PLP moiety may be stabilized to an extent, resulting in a slower rate of imine hydrolysis under the acidic conditions employed for the mass spectral analysis. Experiments run under the same conditions using G5 instead of 4DG6 as an oligosaccharide activator did not result in such an accumulation of a higher molecular weight species (Figure 3.16C).

The limitation of these experiments may reside in the fact that the glycosyl-enzyme intermediate is not stable for the length of time necessary for the mixture to be eluted from the HPLC column (approximately 10 min). In an effort to shorten the time it took the sample to reach the mass spectrometer, the solution was introduced into the MS through direct injection, essentially reducing the injection time from 10 min to less than 1 min and leaving the enzyme in contact with ligands right up until the ionization process. This experiment used the high mass detector of Professor D. Douglas, Department of Chemistry, University of British Columbia, since m/z values greater than 2,500 were formed. Unfortunately, using a direct injection technique, it is not possible to introduce a high concentration of salts, especially phosphate, into the mass spectrometer because they diminish the signal resolution. Therefore, under the conditions necessary for the accumulation of a glycosyl-enzyme intermediate (AMP, G1P or other derivative (glucal) and Pi plus oligosaccharide), a high level of signal interference was observed, rendering this technique unsatisfactory for this purpose.

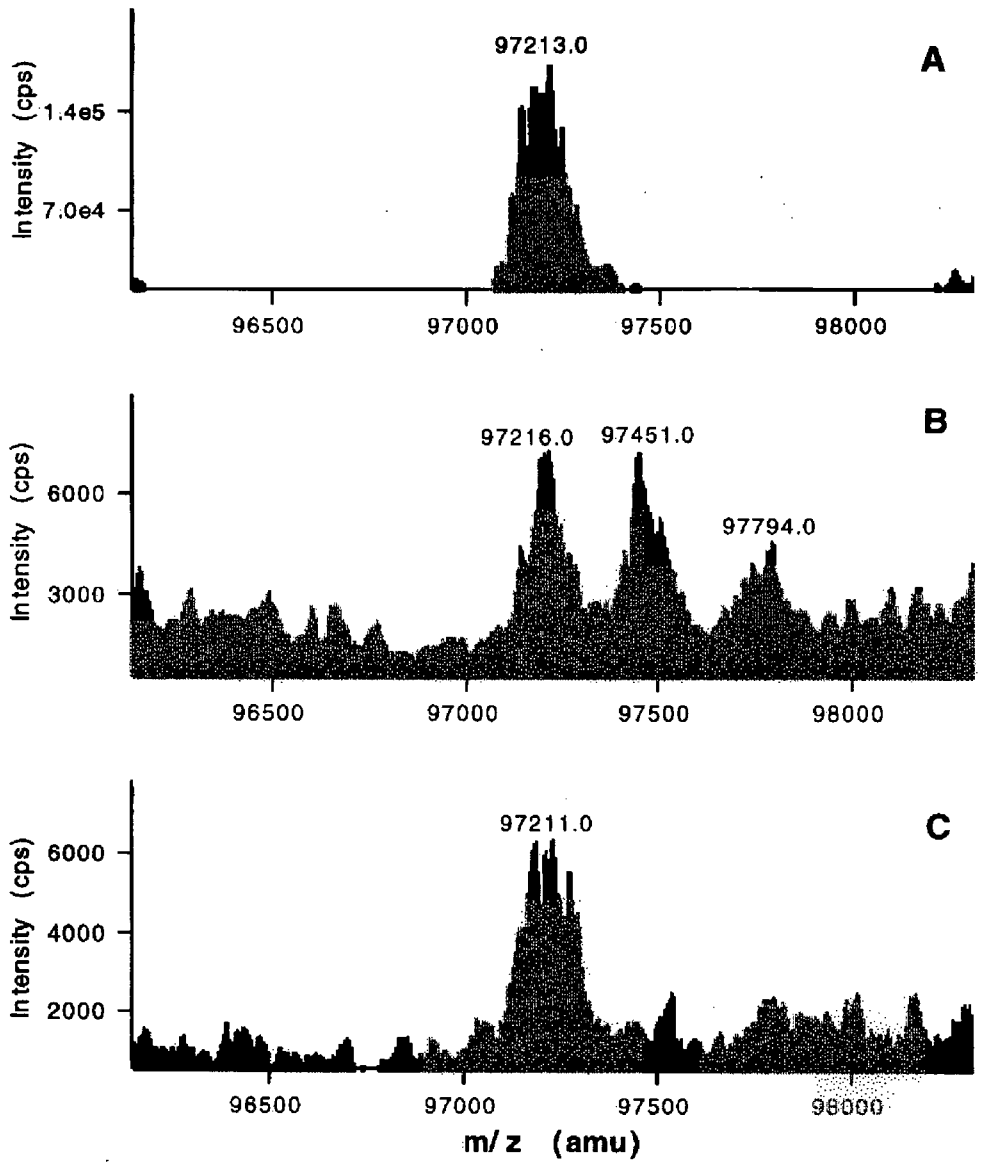

*Figure 3.16 Electrospray mass spectra of muscle phosphorylase. (**A**) Native phosphorylase, (**B**) Phosphorylase incubated in the presence of 4DG6, AMP, and G1P, (**C**) Phosphorylase incubated in the presence of G5, AMP, and G1P.*

Another mass spectrometry strategy which was employed to search for evidence of a glycosyl-enzyme intermediate was comparative peptide mapping. In these experiments, phosphorylase was incubated in the presence and absence of 4DG6, G1P and AMP for a defined length of time and then digested into peptides under acid conditions using pepsin. The resulting peptides were separated by HPLC and detected by ES-MS. The peptide profile obtained in the presence of 4DG6 was compared to the peptide profile obtained in its absence, although no differences between the two could be identified. The large number of peptides generated from such a sizeable protein, many of which co-elute, probably limits the success of this type of experiment.

Analogous types of experiments were attempted with potato phosphorylase. The molecular weight of potato phosphorylase is 103,916 Da, but as with muscle enzyme, the PLP cofactor is lost during mass spectral analysis, thus a mass of 103,685 Da is expected. The intact enzyme was found to have a molecular weight of 103,679 +/- 11 Da, which corresponds well to the anticipated mass (Figure 3.17A). The mass spectrum in Figure 3.17B is typical of the results obtained after potato phosphorylase was incubated with 4DG5 and G1P and analyzed by HPLC-MS as described above for the muscle enzyme. Based on the mass spectra, there is no obvious accumulation of a higher molecular weight species which might provide evidence for a covalent glycosyl-enzyme intermediate. Similar comparative peptide mapping experiments to those described above for the muscle enzyme did not result in the identification of a labelled peptide, though again the intermediate may not be stable under the conditions required for the protein digestion and analysis. While these results did not demonstrate the existence of a covalently bound glycosyl-enzyme species, they do not exclude

the possibility. It is probable that the intermediate turns over too rapidly to accumulate and be detected in this fashion.

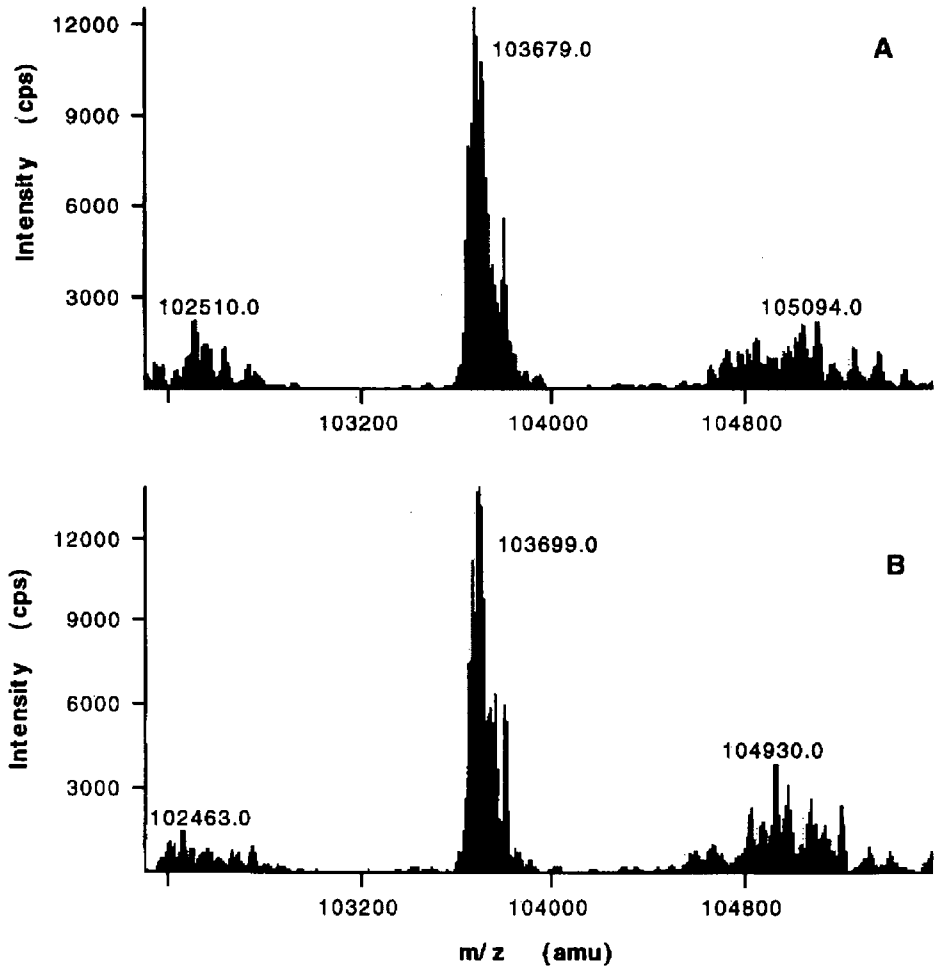

Figure 3.17 Electrospray mass spectra of potato phosphorylase. (A) Native potato phosphorylase, (B) Potato phosphorylase incubated in the presence of 4DG5 and G1P.

3.3.4.2 Rapid acid denaturation experiments in the presence of ^{14}C-G1P

An alternative technique which has been used with some success for trapping a glycosyl-enzyme intermediate in other glycosidases and glycosyl transferases is rapid acid denaturation (see Section 1.4.4.1). Such an experiment proved useful in trapping a covalent intermediate on sucrose phosphorylase (*44*). This type of experiment was attempted here by using either 4DG6 (muscle) or 4DG5 (potato) to form the ternary complex in the presence of ^{14}C-G1P as a radiolabelled tracer. Reactions of ^{14}C-G1P with muscle phosphorylase were initiated by addition of the enzyme to buffered reaction mixtures containing AMP and 4DG6. An aliquot of ^{14}C-G1P was added and the mixture was incubated for 5 min at room temperature. The reactions were terminated by the addition of cold 5% TCA to precipitate the enzyme and then the protein was spun down in a microcentrifuge at 4°C. The protein pellet was washed three times with 2.5% TCA and then dissolved in 0.1 M NaOH and counted for radioactivity. No more than three washes were deemed to be necessary to bring the counts in the supernatant down to baseline levels (Figure 3.18A). Compared with the control (no oligosaccharide activator was present, thus no active ternary complex should form), the levels of radioactivity associated with the protein pellet were approximately 50% of what would be expected if every equivalence of phosphorylase was bound with a ^{14}C-glucose moiety (Figure 3.18B). This was observed regardless of whether 4DG6 or G5 was used to activate the enzyme. Duplicate experiments gave similar percentages of incorporation.

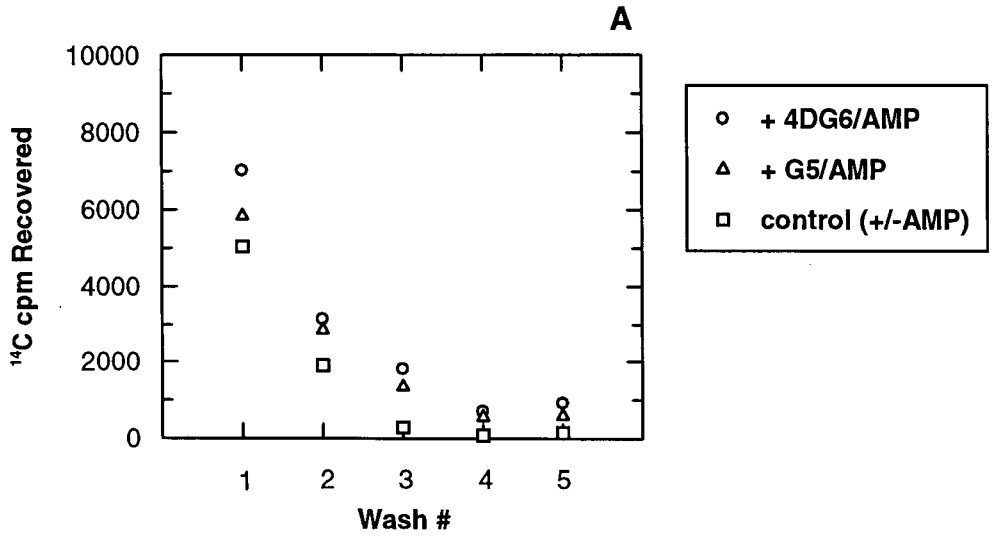

Figure 3.18A Plot of ^{14}C CPM in the supernatant versus wash # for the rapid acid denaturation of muscle phosphorylase in the presence of ^{14}C-G1P. The phosphorylase is precipitated by the addition of 5% TCA and washed with portions of 2.5% TCA.

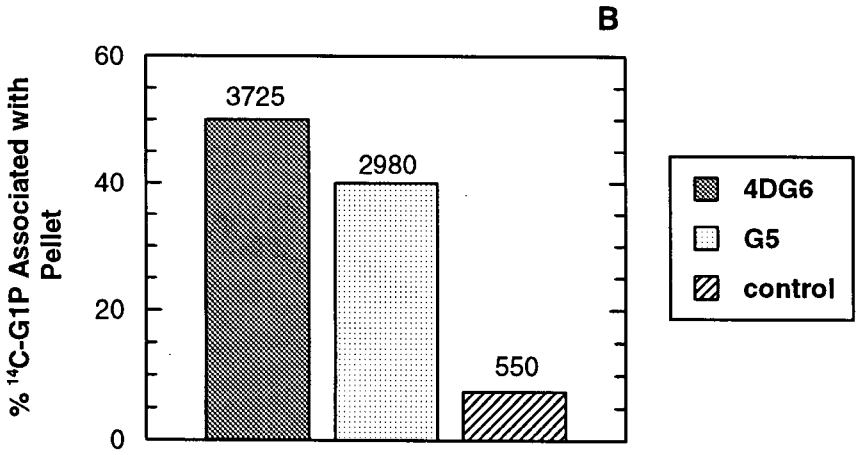

Figure 3.18B CPM measured in the precipitate for muscle phosphorylase incubated in the presence of ^{14}C-G1P and various effectors and then precipitated and washed three times. If every equivalence of phosphorylase was bound with a ^{14}C-glucosyl moiety then approximately 7450 cpm should be associated with the protein pellet. The numbers on top of the bars represent the cpm counted for each pellet after 3 washes.

Analogous experiments were performed on potato phosphorylase under identical denaturation conditions. Similar percentages of ^{14}C-G1P were found to be associated with the protein as were measured for muscle phosphorylase (Figure 3.19). Again these experiments were performed in duplicate and were found to be reproducible. However, there is always the possibility that the presence of oligosaccharide enhances the entrapment of ^{14}C-G1P within the precipitated protein, giving misleading results. Further, even if correct, this type of experiment does not distinguish as to the nature of the associated species, covalent or noncovalent (such as an ion-pair). If the intermediate is covalent in nature and is stable for an extended period of time, it may be useful to treat the denatured protein pellet with a protease such as pepsin. The peptides generated could be separated by HPLC and counted for radioactivity which may indicate that a covalent glucosyl moiety is bound to the peptide. Due to a limited supply of 4-deoxy-oligosaccharides and time, this type of experiment was not attempted but may be pursued in the near future.

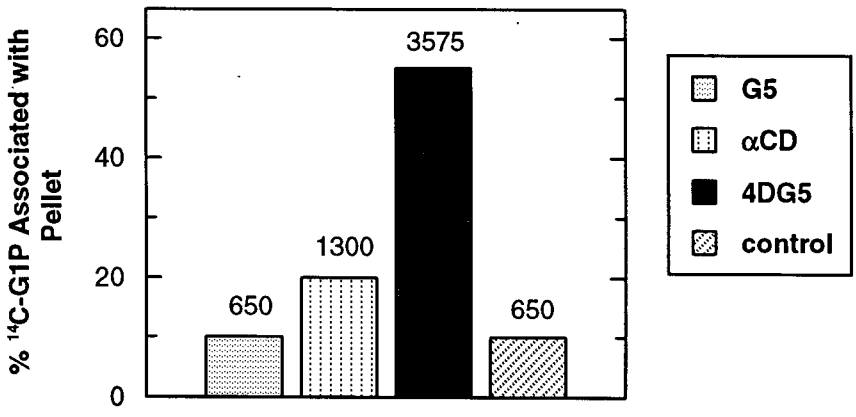

Figure 3.19 CPM measured in the precipitate for potato phosphorylase incubated in the presence of ^{14}C-G1P and various effectors and then precipitated and washed three times. If every equivalence of potato phosphorylase was bound with a ^{14}C-glucosyl moiety then approximately 6500 cpm should be associated with the protein pellet. The numbers on the top of the bars represent the cpm counted for each pellet after 3 washes.

3.3.5 Positional Isotope Exchange

The technique of positional isotope exchange (PIX) (for a review see (*176*)) has been applied to a variety of enzyme-catalyzed reactions to probe the existence of short lived intermediates (*177-179*). The PIX technique can be used to probe the mechanisms of enzymes such as phosphorylases in which the carbon-oxygen bond at the anomeric center of G1P is cleaved by looking at rearrangement reactions in the absence of the second substrate. If the phosphate that is released after enzymatic cleavage of G1P has the opportunity to rotate before reformation of the glucose-1-phosphate moiety, then exchange of a non-bridging oxygen and the anomeric oxygen should occur. The only way in which such a positional isotope exchange might be induced in phosphorylase is to include an oligosaccharide analogue in the reaction mixture that allows a ternary complex to form without turning over. The technique of using a substrate analogue to induce a PIX reaction was demonstrated by Kokesh and Kakuda with potato phosphorylase as described in Section 3.1.8. The degree of isotope exchange was measured by first hydrolyzing the remaining G1P with alkaline phosphatase, followed by treatment with acid to precipitate out phosphate and quantifying the extent of exchange using mass spectrometry (*167*). In recent years it has become easier to monitor the extent of positional isotope exchange through the use of high resolution ^{31}P NMR. It is well documented that substitution of ^{18}O-P for ^{16}O-P causes small upfield shifts in the resulting ^{31}P signal (*180, 181*). Thus, by simply measuring the difference in intensities of the two resonances in the ^{31}P NMR spectrum, the exchange can be measured in a nondestructive manner. The ^{18}O labelled G1P will be incubated with both potato and muscle phosphorylase in the presence of 4DG5 or 4DG6 in an attempt to demonstrate enzyme catalyzed positional isotope exchange using ^{31}P NMR. A new chemical synthesis of glucose-1-phosphate

exclusively labelled with approximately 80% ^{18}O in the bridging position was developed as follows for this purpose.

3.3.5.1 Synthesis of glucose-[1-^{18}O]-phosphate

The labelled α-glucose-1-phosphate was chemically prepared from 2,3,4,6-tetra-*O*-acetyl-α-D-glucopyranosyl bromide (**3.6**) in 5 steps (Scheme 3.1). This provides an alternative to the previously published enzymatic synthesis of G1P labelled with ^{18}O in a non-bridging oxygen position (*182*). Unfortunately, it was not possible to directly convert the glycosyl bromide to the labelled intermediate using $H_2{}^{18}O$ under Koenigs Knorr conditions because the ^{18}O label also became incorporated into the C-2 acetate group through a neighbouring group participation reaction (Scheme 3.2). This resulted in only 40% incorporation of ^{18}O at the anomeric oxygen, a percentage which is not sufficient for the NMR experiments. To circumvent this problem, the bromide was first hydrolyzed using H_2O/acetone under standard Koenigs-Knorr conditions, then the ^{18}O label was incorporated into the anomeric position by heating **3.7** in $H_2{}^{18}O/CH_3CN$ for 14-16 hours overnight. This labelled material (**3.8**) was then reacted with diphenylchlorophosphate to stereospecifically incorporate an α-phosphate group (*183*). This was followed by two deprotection steps to yield the labelled product (**3.11**), α-D-glucose-[1-^{18}O]-phosphate (G-[1-^{18}O]-P). Electrospray mass spectrometry confirmed an 80% incorporation of ^{18}O in the product. Figure 3.21A shows the ^{31}P NMR signals for the ^{18}O-labelled G1P product. The ^{31}P signal of the ^{18}O labelled material is shifted 0.017 ppm upfield (peak 2) of the unlabelled material (peak 1). The relative height of the two peaks confirms the incorporation ratio of 80% ^{18}O to 20% ^{16}O.

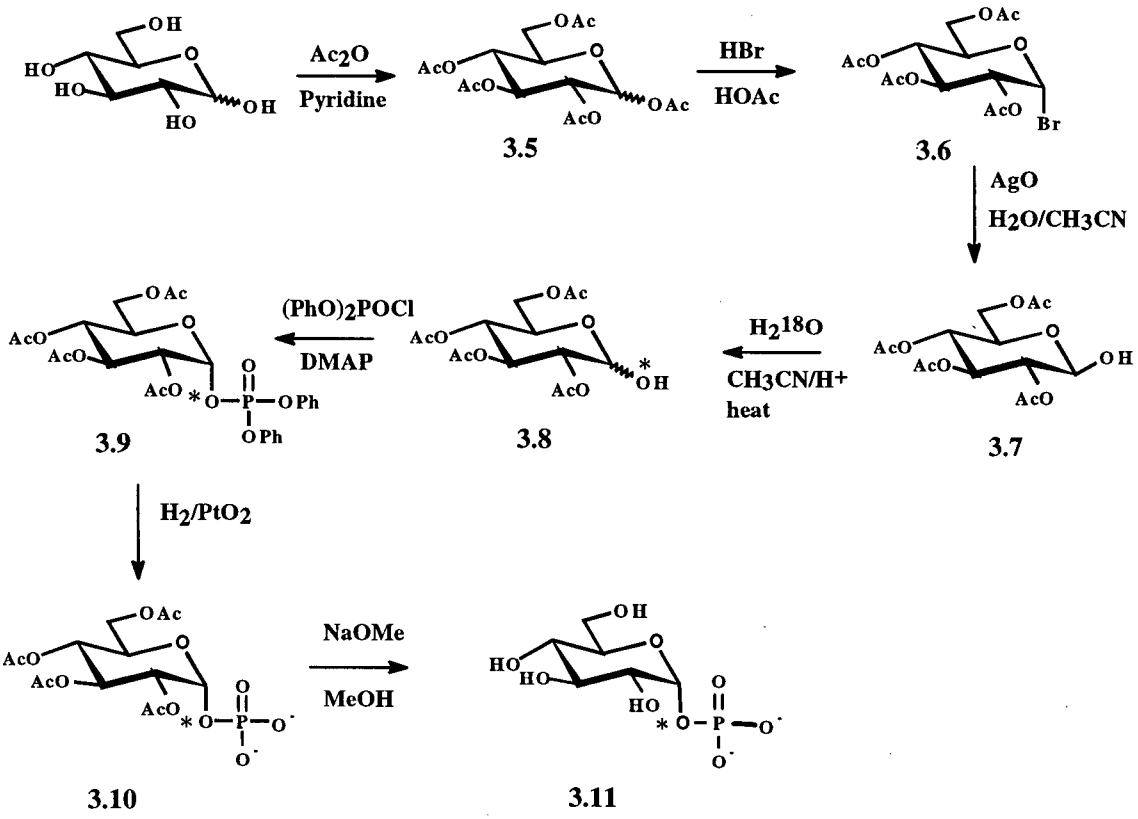

Scheme 3.1 Synthesis of glucose-[1-^{18}O]-phosphate (indicates ^{18}O incorporation)*

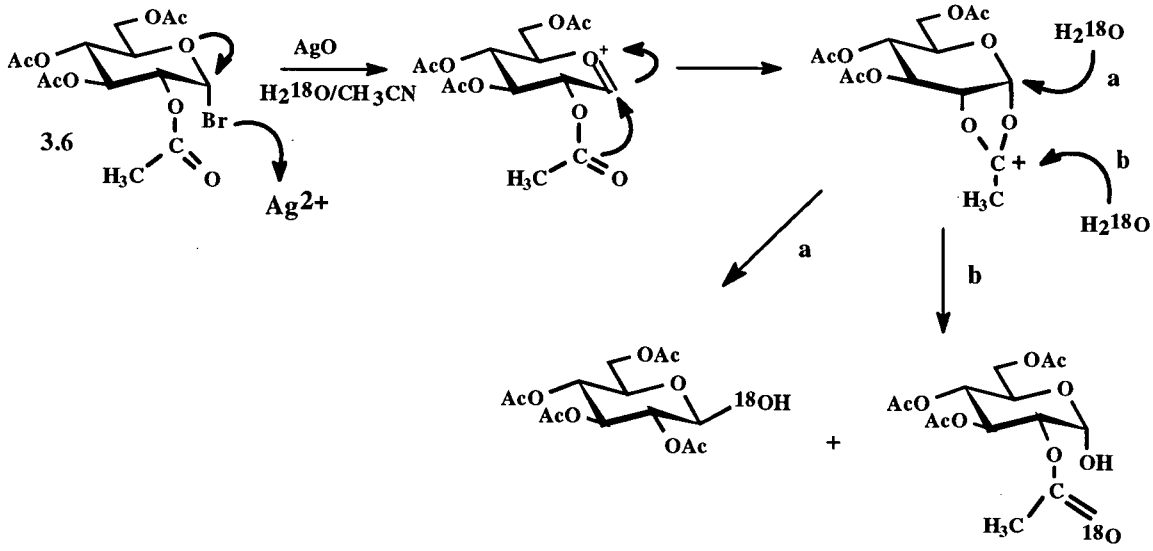

Scheme 3.2 Incorporation of ^{18}O into the C-2 acetate of glucose-1-phosphate

3.3.5.2 Positional isotope exchange catalyzed by potato phosphorylase

As shown in Figure 3.20, 4DG5 should not act as an acceptor for the reaction of potato phosphorylase with G1P. Instead, assuming that the lifetime of the intermediate is long enough, it may be possible for positional isotope exchange to occur through rotation of the phosphate moiety. Potato phosphorylase was incubated with 4DG5 and G-[1-^{18}O]-P and the reaction was followed by ^{31}P NMR. Selected time points are shown in Figures 3.21A-D after 0, 4, 8, and 14 hours of enzymatic treatment. A new signal at 0.010 ppm upfield from the ^{31}P-^{18}O signal of the starting material is evident (peak 3). This signal could be attributed to the phosphate from a G1P moiety in which an ^{18}O label has been scrambled into a non-bridging position. However, the signal appearing at 1.08 ppm must be factored into this conclusion. This signal was assigned to free orthophosphate through a comparison to the ^{31}P NMR of a Pi standard solution and quantification of the Pi in the NMR tube using the Fiske-Subbarow assay as described in Section 4.3.3. The isotopic distribution of 80/20 (^{18}O/^{16}O) in the Pi peak (peaks 5 and 4) clearly indicates that this phosphate was derived from the ^{18}O labelled G1P starting material. The production of Pi could be due to a contaminating enzyme, such as a phosphatase, in the potato phosphorylase preparation, or it could indicate that potato phosphorylase has an inherent hydrolytic activity. This latter possibility is unlikely based on the fact that when G1P and enzyme were incubated together Pi was found to accumulate to the same extent as in the NMR experiment. Given that potato phosphorylase is not likely to be conformationally active under the conditions of the control experiment (as no oligosaccharide was present), the production of Pi probably resulted from the action of another enzyme.

The necessary consequence of the release of this labelled Pi, however, is that potato phosphorylase will now catalyze the phosphorolytic cleavage of the 4DG5 through the normal degradation pathway, resulting in the production of 4-deoxy-glucose-[1-^{18}O]-phosphate (4DG-[1-^{18}O]-P) and G4. Any contaminating starch or malto-oligosaccharides in the potato phosphorylase preparation could also act as substrates for the reaction with Pi giving rise to another source of labelled G1P. In this newly formed 4DG-[1-^{18}O]-P, it is three times more likely that the ^{18}O will end up in a non-bridging position than a bridging position. Since the ^{31}P NMR shifts of the phosphate groups in G1P and 4DG1P are the same (*184*), the appearance of peak 3 (shifted upfield by 0.010 ppm) is most likely due to the formation of 4DG-[1-^{18}O]-P. Therefore, the PIX observed is most likely occurring through this unwanted pathway rather than through that sought.

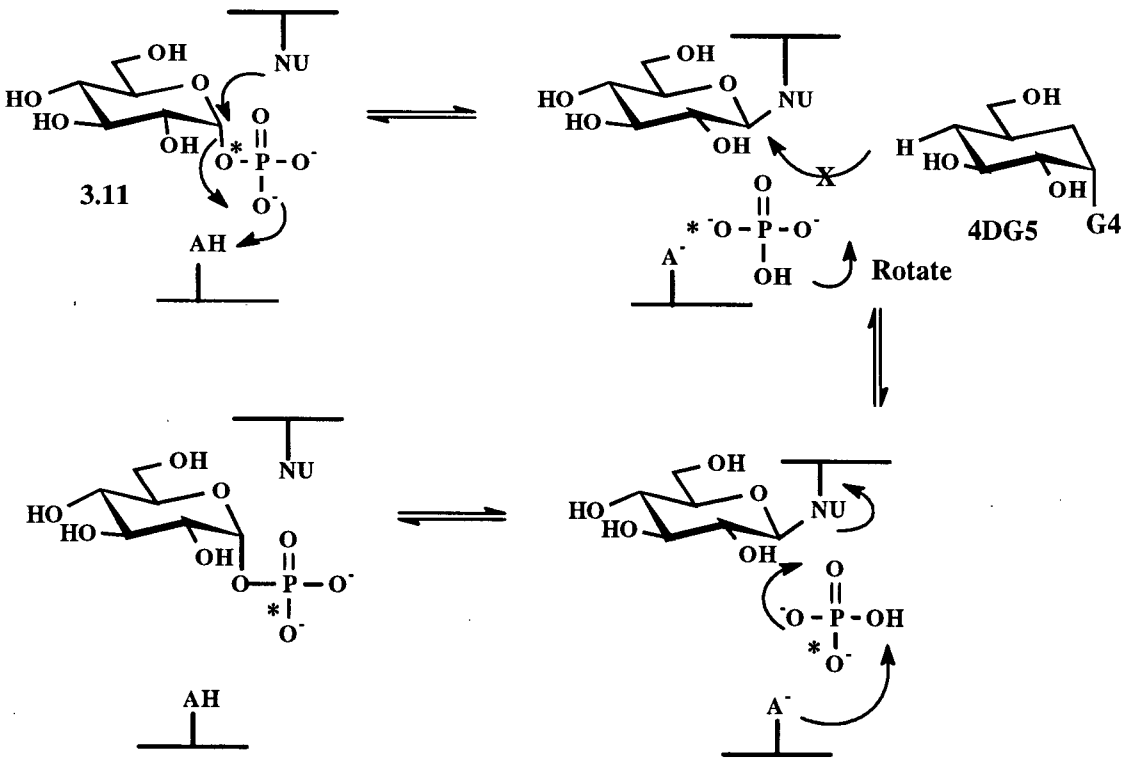

*Figure 3.20 Proposed mechanism for potato phosphorylase positional isotope exchange of G-[1-^{18}O]-P (**3.11**) in the presence of 4DG5*

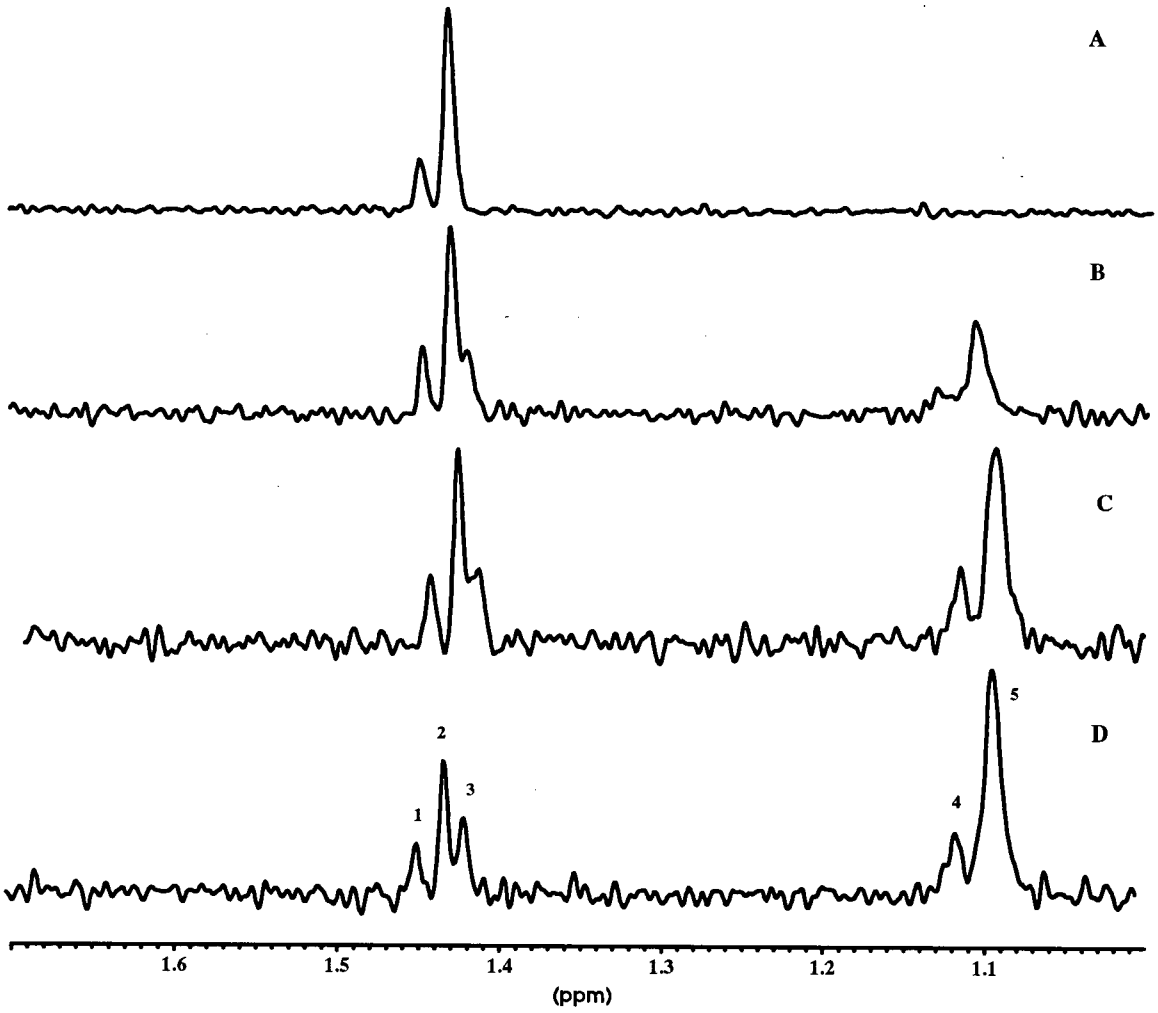

Figure 3.21 ^{31}P *NMR spectra of the products of the reaction of potato phosphorylase, G-[1-*^{18}O*]-P and 4DG5. Time after the addition of enzyme:* ***(A)*** *0 h,* ***(B)*** *4 h,* ***(C)*** *8 h,* ***(D)*** *14 h. Peaks 1,2 & 3: G1P and/or 4DG1P, Peak 1 =* ^{31}P*-bridging* ^{16}O*, Peak 2 =* ^{31}P*-bridging* ^{18}O*, Peak 3 =* ^{31}P*-non-bridging* ^{18}O*; Peak 4 & 5: Pi (*H_3PO_4*), Peak 4 = 20%* $H_3P^{16}O_4$*, Peak 5 = 80%* $H_3P^{16}O_3{}^{18}O$*.*

A similar NMR experiment to that described above was carried out using α-cyclodextrin as an incompetent substrate in place of 4DG5. This allowed the use of ^{31}P NMR as a way to substantiate the earlier results of Kokesh and Kakuda (*167*). As differences in kinetic parameters tend to exist depending on the preparation of potato phosphorylase, it was first necessary to confirm the extent and mode of inhibition afforded by α-cyclodextrin. As shown in Table 3.3, α-cyclodextrin was found to be a competitive inhibitor with respect to maltopentaose and noncompetitive with respect to G1P or Pi. It is not clear, however, why K_i values measured are so much higher than that of 0.016 mM for αCD measured previously for the potato phosphorylase-catalyzed elongation of starch with G1P (*185*).

A very similar set of ^{31}P NMR spectra to those shown previously in Figure 3.21 for incubation with 4DG5 were obtained for potato phosphorylase plus G-[1-^{18}O]-P in the presence of αCD, including the appearance of free Pi (data not shown). Since the same preparation of potato phosphorylase was used, it is likely that a contaminating enzyme is again responsible for the production of Pi. In this case, the Pi released should not react with the αCD, as this is a completely inert substrate analogue. It is, however, still possible that the Pi could react with any contaminating linear oligosaccharides or starch to produce G1P. The obvious complications behind this experiment therefore make it impossible to come to a conclusion at this time. It is interesting to note that when Kokesh and Kakuda performed the same set of experiments, 36.4% Pi was produced in the control reaction (potato phosphorylase and G1P only), indicating that their mixture was also likely contaminated with another enzyme (*167*).

Table 3.3 Inhibition Parameters Determined for Potato Phosphorylase with α-Cyclodextrin

Synthesis Direction		
Variable substrate	G1P	G5
K_i (mM)	0.122	0.099
Inhibition mode[1]	noncompetitive	competitive
Degradation Direction		
Variable substrate	Pi	G5
K_i (mM)	0.919	0.254
Inhibition mode[1]	noncompetitive	competitive

[1] See Appendix B, Figure B-12 for a graphical representation of the data.
Average error in K_i (+/- 10 %).

A similar set of ^{31}P NMR experiments was attempted using muscle phosphorylase and 4DG6 (5 mM) as an oligosaccharide activator. However, no positional isotope exchange was observed under the experimental conditions used (data not shown). One explanation could be that the concentration of 4DG6 was not sufficient to fully saturate the enzyme. Interestingly, no production of Pi was observed in these experiments. This implies that there was no contaminating enzyme capable of Pi production present in the muscle phosphorylase preparation or that muscle phosphorylase does not have any inherent hydrolytic activity.

3.4 THE SEARCH FOR POSSIBLE INHIBITORS AND INACTIVATORS OF PHOSPHORYLASE

The mechanistic details of the reaction catalyzed by glycogen phosphorylase have been difficult to define, in part because the enzyme is highly substrate specific. However, some previous studies have been completed with reagents which inactivate phosphorylase through chemical modifications of amino acid residues (*186-189*). Although these reagents are generally nonspecific, they have provided some information on residues important in catalysis and allosteric activation. Our ultimate goal was to find an inactivator which is active site directed and which can be used to label and identify a putative nucleophile (see Section 1.4.4).

As discussed in Section 1.4.4.1, 5-fluoro glycosides have proved successful in trapping an intermediate and identifying the nucleophile of some α-retaining glycosidases including yeast α-glucosidase (*71*) and jack bean α-mannosidase (*72*). In addition, α-glucosyl fluoride (αGF) acts as a reasonable inhibitor of muscle phosphorylase (*190*). The inhibition by αGF was competitive with respect to G1P and Pi and the K_i values of 0.2 mM and 0.4 mM were approximately one order of magnitude lower than the K_m values for G1P and Pi. In addition, in the presence of a suitable primer and orthophosphate, the glucosyl moiety of αGF can be slowly transferred to an oligosaccharide primer by both muscle and potato phosphorylase (muscle (10 mM Pi): V_{max} = 1 x 10^{-4} μmol/min/mg, K_m = not determined; potato (10 mM Pi): V_{max} = 1 x 10^{-3} μmol/min/mg, K_m = 9 mM) (*191*)). The competition of αGF for the same binding sites as G1P and Pi suggested that the 5-fluoro glycosides may bind in a similar manner and so 5FαGluF (**1.14**) and 5FβIdoF (**1.15**) were investigated as potential inactivators of muscle phosphorylase. 5FαGluF was not found to act as an inactivator but only weakly inhibited the enzyme (K_i = 5 mM) (see Appendix B, Figure B-14). However, 5FβIdoF was

found to slowly inactivate muscle phosphorylase with a k_i = 0.0010 min^{-1} and K_i = 33.4 mM in the presence of AMP and glycogen (Figures 3.22A & B).

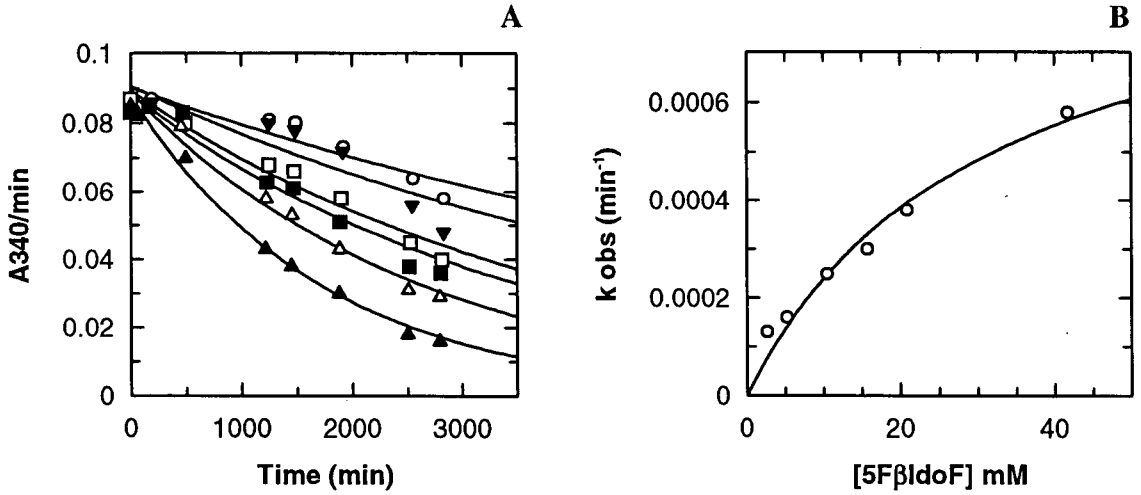

Figure 3.22 Inactivation of muscle phosphorylase with 5FβIdoF. (A) [enz] = 0.093 mg/mL; [AMP] = 1 mM; [glycogen] = 0.5%; [5FβIdoF]: ○ = 2.60 mM; ▼ = 5.22 mM; □ = 10.43 mM; ■ = 15.65 mM; Δ = 20.86 mM; ▲ = 41.72 mM. (B) Replot of k_{obs} for determination of k_i and K_i. Rates measured in the degradation direction using the PGM/G6PDH coupled assay system. Errors in k_i and K_i are +/- 20 %.

At one concentration of 5FβIdoF (20 mM), the rate of inactivation was measured in the presence and absence of AMP (Figure 3.23A). No detectable differences between the two rates were measured. This is somewhat surprising because if the mechanism for inactivation is the same for both allosteric forms of the enzyme, it seems likely that the active site residue responsible for the inactivation would be better positioned in one conformation than in the other. This might be expected to result in a difference in the rate of inactivation depending on the presence of AMP.

To test for the active site directed nature of the 5FβIdoF inactivation, phosphorylase was inactivated in the presence of glucose, which is known to reversibly bind to the active site. At the concentration of glucose employed (8 mM, 2 x K_D) approximately 50%

protection was afforded (Figure 3.23B). The k_{obs} determined in the presence of glucose (0.00018 min^{-1}) agrees well with the calculated rate of inactivation in the presence of 8 mM glucose (k_{obs} = 0.00017 min^{-1}). Although this suggests that 5FβIdoF reacts at the active site, it does not exclude the possibility that it is also reacting at other sites on the enzyme. Mass spectral analysis of inactivated enzyme (> 80% inactivated) suggested that the sample was composed of many species of many molecular weights (data not shown). Accurate molecular weights of the adducts could not be calculated from the data. Furthermore, some precipitation was observed at high concentrations of inactivated enzyme. This may suggest that some of the species observed in the mass spectra resulted from the partial degradation of the protein over the long periods required for inactivation. Comparative peptide mapping of inactivated versus native phosphorylase did not provide any more conclusive results as to the identity of the labelled residue (data not shown).

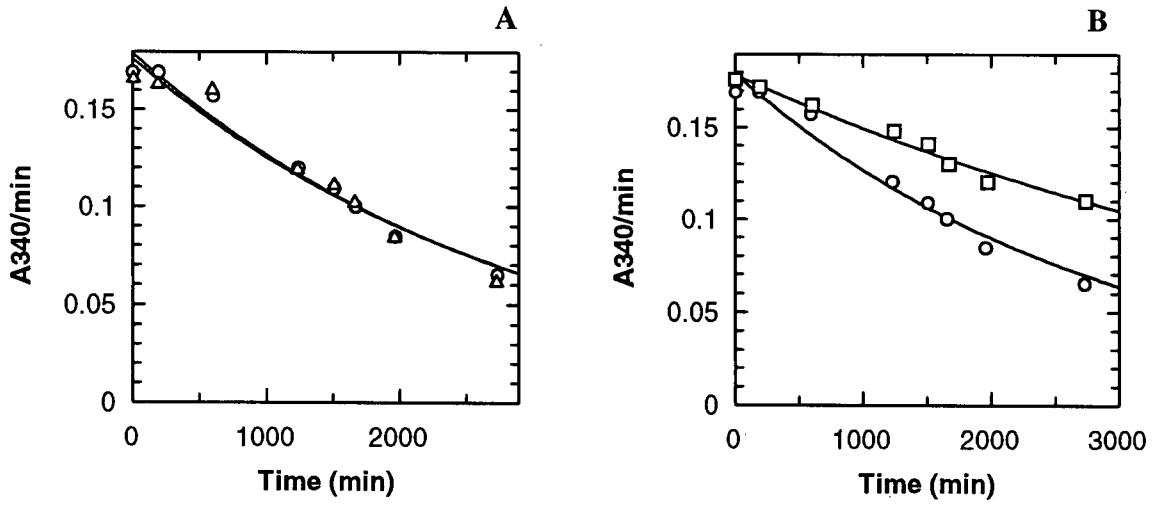

Figure 3.23 (A) Inactivation of muscle phosphorylase with 5FβIdoF in the presence and absence of AMP ([enz] =0.093 mg/mL; [glycogen] = 0.5%; Δ = 20 mM 5FβIdoF; O = 20 mM 5FβIdoF + 1 mM AMP). (B) Inactivation of muscle phosphorylase in the presence (k_{obs} = 0.00018 min^{-1}) and absence (k_{obs} = 0.00034 min^{-1}) of glucose ([enz] = 0.093 mg/mL; [glycogen] = 0.5%; □ = 20 mM 5FβIdoF + 8 mM glucose; O = 20 mM 5FβIdoF). Rates measured in the degradation direction using the PGM/G6PDH coupled assay system.

Potato phosphorylase was not inactivated by either 5FβIdoF or 5FαGluF after incubation for up to 48 h with 20 mM of either inactivator. Instead, the 5-fluoro glycosides were found to be weak reversible inhibitors with K_i values of 4 mM (5FαGluF) and 26 mM (5FβIdoF) when measured in the degradation direction (these values were determined from RFK_i measurements, see Appendix B, Figure B-14). Therefore, these 5-fluoro glycosides were not investigated further.

Some other inhibitors were surveyed for their ability to inhibit muscle phosphorylase (Figure 3.24). If a suitably tight binding inhibitor was identified, the possibility exists for examining its mode of binding in the crystalline state as with nojirimycin tetrazole (Section 3.1.5).

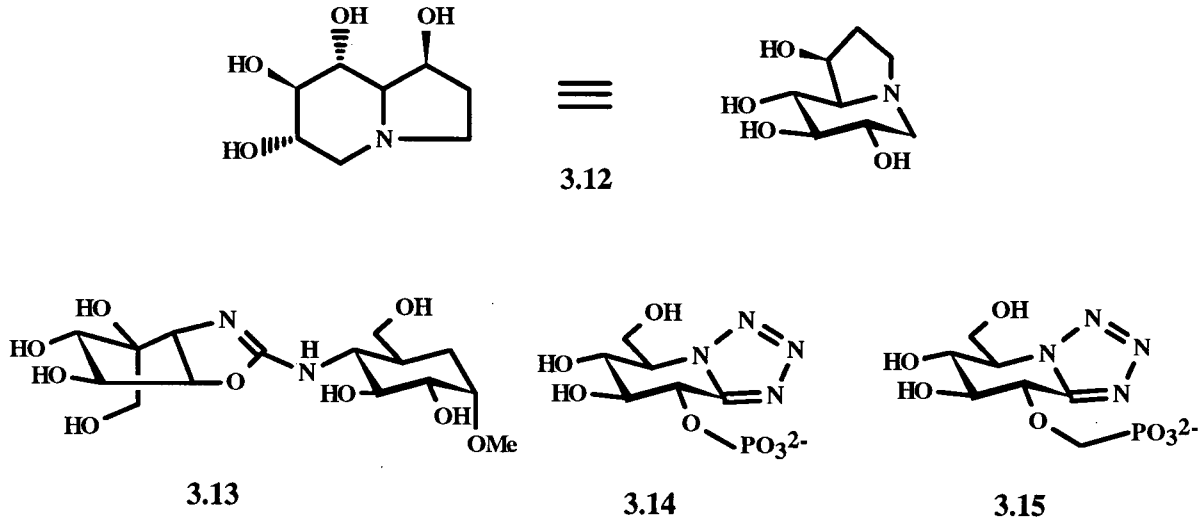

*Figure 3.24 Compounds investigated as potential inhibitors of muscle phosphorylase: castanospermine (**3.12**), (1-4) trehazoloid pseudodisaccharide (**3.13**), nojirimycin tetrazole-2-O-phosphate (**3.14**), nojirimycin tetrazole-2-O-methyl phosphonate (**3.15**).*

The natural product castanospermine (**3.12**) is a well known potent inhibitor of several β-glycosidases (*37*). Although it inhibits α-glucosidase from yeast rather weakly (K_i = 1.5 mM), it has been shown to inhibit other types of α-glucosidases more strongly (K_i = 0.015 μM, rice α-glucosidase and K_i = 0.1 μM, rat liver α-glucosidase) (*37*). Castanospermine was tested as an inhibitor of muscle phosphorylase and was found to inhibit phosphorylase with a K_i of 0.3 mM in the presence of Pi, but it only inhibited phosphorylase weakly in the synthesis direction (K_i = 15 mM) as shown in Table 3.4.

The (1-4) trehazoloid pseudodisaccharide (**3.13**) was previously found to be a good inhibitor of yeast α-glucosidase (K_i = 9.3 μM) (*192*). In an effort to achieve more efficient and selective inhibition, the trehazoloid was designed to incorporate both the glycone and algycone portions of a substrate. From a range finder K_i measurement, the trehazoloid was found to inhibit phosphorylase weakly with a K_i = 10 mM (degradation direction) (Table 3.4).

Table 3.4 Compounds Investigated as Inhibitors of Muscle Phosphorylase

Compound	**K_i (mM)[1] Synthesis Direction**	**K_i (mM)[1] Degradation Direction**
Castanospermine (**3.12**)	15	0.3
Trehazoloid (**3.13**)	--[2]	10
NJT-2-O-Pi (**3.14**)	7	5.5
NJT-2-O-CH_2-Pi (**3.15**)	12	3

[1] These values were determined from RFK_i measurements (see Appendix B, Figures B-13 and B-14). The synthesis direction is in the presence of G1P and the degradation direction is in the presence of Pi.
[2] Not measured.

Recently, a very successful inhibitor of muscle phosphorylase was identified and used in crystallographic studies to examine the binding mode of phosphate as described in Section 3.1.5 (*150*). Nojirimycin tetrazole (**1.8**) exhibited competitive inhibition with respect to G1P yielding a K_i value of 700 μM. When assayed in the degradation direction in the presence of Pi, a K_i value of 53 μM was determined. Thus, the presence of Pi dramatically increased the enzyme's affinity for the inhibitor and Pi was seen to bind in close proximity to the 2-hydroxyl (*150*). Therefore, it was proposed that by incorporating a properly positioned phosphate group directly into the nojirimycin tetrazole moiety, an even tighter binding inhibitor may result. Hence, nojirimycin tetrazole-2-O-phosphate (**3.14**, NJT-2-O-Pi) was synthesized by our collaborator, Dr. A. Vasella, Organic Chemistry Institute, Zurich, and then tested as an inhibitor of muscle phosphorylase. Unfortunately, the incorporation of a phosphate group into nojirimycin tetrazole drastically weakened binding (RFK_i = 5.5 mM) compared with the parent compound, nojirimycin tetrazole, complexed with free Pi (K_i = 53 μM) (*150*). It is possible that the covalently bound Pi group is not optimally positioned for effective binding. Therefore, in an effort to modify this distance, the derivative nojirimycin tetrazole-2-O-methyl phosphonate (**3.15**, NJT-2-O-CH_2-Pi) was synthesized by Dr. A. Vasella. The incorporation of an additional CH_2 linker at the 2-position did not result in any significant improvement in binding affinity (K_i = 3 mM) over that seen for NJT-2-O-Pi (K_i = 5.5 mM).

3.5 CONCLUSIONS

The nature of the glucosyl-enzyme intermediate in the mechanism of phosphorylase still remains a mystery. Although the experiments attempted in this thesis have not yet provided a clear resolution to this question, some of the mass spectrometric and denaturation experiments suggest that a covalent intermediate may exist. More important, perhaps, is the experimental approach taken in an attempt to answer this question. The concept of using a 4-deoxy-oligosaccharide as an incompetent substrate analogue in an effort to effect the accumulation of an intermediate is applied here for the first time to muscle and potato α-glucan phosphorylases. In addition, the investigation of the kinetic parameters for 4DG5 and 4DG6 with both muscle and potato phosphorylase has provided some insight into the phenomenon of tight binding observed previously with the modified glycogen analogues.

A possible improvement which could be made to this method is to incorporate a branch point into a 4-deoxy-oligosaccharide. Phosphorylase may well have a higher affinity for such a branched oligosaccharide, a property which may, in turn, provide a better chance of trapping a glucosyl-enzyme intermediate. Previous kinetic studies with muscle phosphorylase and a variety of semi-synthetic branched oligosaccharides concluded that, on average, the branch point oligosaccharide was bound 5 fold tighter than the corresponding linear oligosaccharide (*193*). In this thesis, preliminary work in this direction was pursued through the purification of the branch point oligosaccharide, DP5 (**3.16**) (Figure 3.25). Using this branched oligosaccharide as a core, it was hoped that the non-reducing ends could be blocked with a 4-deoxy sugar by using the transferase activity of CGTase or Glyx (Figure 3.26).

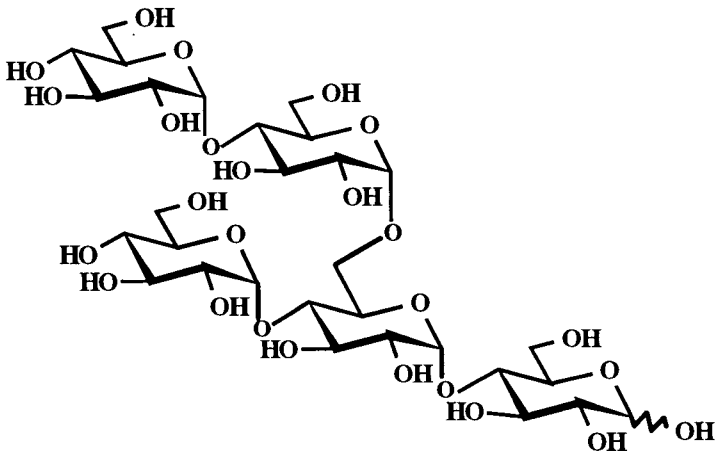

*Figure 3.25 Structure of the branch point pentasaccharide, DP5 (**3.16**)*

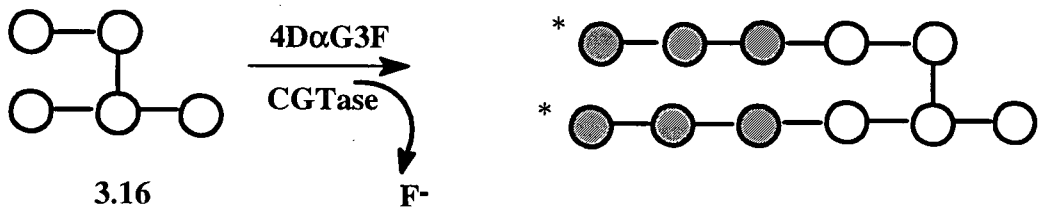

*Figure 3.26 The proposed elongation of DP5 by CGTase in the presence of 4DαG3F, to yield a DP5 core (open circles) elongated on each branch by a 4-deoxy-maltotriosyl moiety (shaded circles, the * indicates the non-reducing 4-hydroxyl group).*

Two problems were encountered which limited the success of this approach. One, the yield of DP5 from the enzymatic degradation of amylopectin using a commercial α-amylase, Termamyl, was very low (< 5%). However, after extensive purification, a small amount of DP5 was obtained for initial elongation trials. Using various donors such as 4DαG3F, 4DαG2F, 4DG6, αG3F, αG2F, G4, G5 and so on, neither CGTase (wt or Glu257Gln) or Glyx proved effective at elongating the DP5 core. Only minor amounts of the desired products were isolated. The majority of the products had instead resulted from the extensive

enzymatic disproportionation of the reactants. Future avenues of research might include chemical derivatization of a larger branch point oligosaccharide which could be used directly for kinetic analysis. Another option, once a branch point core is in hand, is to search for other enzymes which would be more effective in incorporating modified sugars into the non-reducing ends of the branch point. A mutant transferase enzyme, which has reduced hydrolytic and disproportionation activities, might prove useful in this regard.

CHAPTER 4

MATERIALS AND METHODS

4.1 SYNTHETIC PROCEDURES

4.1.1 General

a. Analytical methods

^{1}H NMR spectra were recorded on the following instruments at the indicated field strengths: a Bruker AC-200 at 200 MHz, a Varian XL-300 at 300 MHz, or a Bruker WH-400 at 400 MHz. ^{13}C NMR spectra were recorded on a Varian XL-300 spectrometer at 75 MHz. ^{19}F NMR spectra were recorded on a Bruker AC-200 multinuclear spectrometer operating at a frequency of 188 MHz. ^{31}P NMR spectra were recorded on a Bruker AC-200 multinuclear spectrometer operating at a frequency of 81 MHz. ^{1}H NMR chemical shifts are internally referenced to $CDCl_3$ or MeOH and for samples dissolved in D_2O, the spectra are externally referenced to 2,2-dimethyl-2-silapentane-5-sulphonate (δ = 0.015 ppm), ^{13}C NMR spectra are proton decoupled and shifts are internally referenced to $CDCl_3$ or MeOH or for samples dissolved in D_2O, a drop of MeOH is added as a reference. ^{19}F NMR shifts are referenced to $CFCl_3$, although the samples were externally referenced to trifluoroacetic acid (δ = -76.53 ppm). ^{31}P NMR chemical shifts are externally referenced to 10% H_3PO_4 in D_2O (δ = 0.00 ppm).

Desorption chemical ionization (DCI) mass spectra were recorded on a Delsi Nermag R10-10C single quadrupole mass spectrometer using ammonia as the chemical ionization gas. Electrospray mass spectra were recorded on a Sciex API-300 mass spectrometer using direct flow injection. The samples were introduced in 100% MeOH by a syringe pump driven at 5 μL/min in the presence of 5 mM ammonium acetate as an ionization agent.

Thin layer chromatography (TLC) was performed using plates (silica gel 60 F_{254}, Merck) with visualization under UV light or after charring with 10% H_2SO_4 in MeOH or ammonium molybdate-H_2SO_4 solution in MeOH. Column chromatography was performed under elevated pressure using Kieselgel 60 (230-400 mesh).

Microanalyses were performed by Mr. Peter Borda in the microanalytical laboratory at the Department of Chemistry, University of British Columbia.

b. Solvents and reagents

Solvents and reagents were either of reagent, certified, spectral, or HPLC grade. Dry solvents were prepared as follows. Dichloromethane was distilled over calcium hydride. Dimethylformamide was predried over magnesium sulphate overnight and then distilled under reduced pressure over 4 Å sieves. Benzene was distilled over calcium hydride. Acetonitrile was distilled over calcium hydride and stored over 3 Å molecular sieves. Methanol was distilled over magnesium with iodine and THF was distilled over sodium and benzophenone.

The ^{18}O enriched water (95-98% ^{18}O) was purchased from Cambridge Isotope Laboratories. "Amberlyst" brand resin, "15 dry" (containing less than 1.5% water) was kindly donated by Rohm and Haas Canada. Chelex (200-400 mesh, Na^+ form) and Dowex 50 W H^+ Amberlite resin were from BioRad. Maltose and maltotriose were obtained from Sigma. All other chemicals were purchased from Aldrich Chemical Company and used without further purification.

c. Compounds synthesized and provided by colleagues

The compounds which were not synthesized in this thesis were: 4-deoxymaltose (4DG2) and 4-deoxy-α-maltosyl fluoride (4DαG2F) which were prepared by Dr. Thisbe

Lindhorst, and 5F-α-D-glucosyl fluoride (5FαGluF) and 5F-β-D-idosyl fluoride (5FβIdoF), which were prepared by Dr. John McCarter.

4.1.2 Synthesis of α-glycosyl fluorides

The three α-glycosyl fluorides used in this study (αGF, αG2F, and αG3F) were originally synthesized via a five step procedure which involved selective deprotection of the anomeric acetate, followed by two fluorination steps. However, the more direct method of Junnemann et al. was later adopted (*92*). Both methods are detailed below.

4.1.2.1 General five step procedure for the synthesis of α-glycosyl fluorides

a. Acetylation

The sugar was dissolved in pyridine and acetic anhydride was added in excess (typical volume ratio was pyridine to acetic anhydride 3:2). The reaction mixture was stirred overnight at room temperature (for glucose) or at 50-60°C (for maltose or maltotriose). The reaction mixture was diluted into ice-water and extracted with dichloromethane, and dried over $MgSO_4$. The product was purified by column chromatography or crystallized from ethyl acetate (EtOAc)/hexanes.

b. Selective deacetylation with hydrazine acetate

The per-*O*-acetylated glycoside was selectively deprotected at the anomeric center using hydrazine acetate. The sugar was dissolved in DMF, the solution warmed to 50°C and hydrazine acetate (1.1 equiv.) was added. The reaction was stirred for 15 min at 50°C and then for 30 min at room temperature. The mixture was then diluted into EtOAc, washed two

times with H_2O and dried over $MgSO_4$. After removing the solvent by rotary evaporation, the product was purified by column chromatography.

c. Fluorination of selectively deprotected glycosides

The glycoside was dissolved in dry CH_2Cl_2 and the solution was cooled to 0^0C under N_2. Diethylaminosulphur trifluoride (DAST) (2.5 equiv.) was diluted with CH_2Cl_2 and slowly added dropwise, the solution was warmed to room temperature and stirred for 18 hours. The reaction mixture was worked up by quenching with MeOH, followed by evaporation *in vacuo*. The product was then dissolved in CH_2Cl_2, washed with saturated aqueous $NaHCO_3$ and H_2O, dried ($MgSO_4$) and purified by column chromatography.

d. Anomerization of the glycosyl fluoride with HF-pyridine

The glycosyl fluoride was placed in a plastic screw capped vial and cooled to -78°C under N_2. An aliquot of HF-pyridine was added using a plastic syringe and the reaction mixture was stirred at -78°C for 20 min, then allowed to warm to room temperature and stirred for one further hour. The mixture was diluted with CH_2Cl_2, washed with ice-water, saturated aqueous $NaHCO_3$ and water, then dried over $MgSO_4$. After removing the solvent, the mixture was purified by column chromatography.

e. Deacetylation with sodium methoxide in methanol

To the glycosyl fluoride dissolved in dry methanol was added a catalytic amount of a freshly prepared sodium methoxide solution in dry methanol (typically 0.02 M). The reaction mixture was stirred at room temperature under N_2 until the reaction was judged to be complete by TLC (usual reaction time was overnight for G3 and G2 and 2-3 h for G). The

reaction mixture was neutralized by the addition of a small amount of Dowex 50 W H^+ Amberlite resin (Bio-Rad), then the resin removed by filtration and the solvent evaporated *in vacuo* and the mixture was purified by column chromatography.

4.1.2.2 Three step synthesis of α-glycosyl fluorides

The following work was adapted from the method of Junnemann et al. (*92*). Details are provided for the synthesis of α-maltotriosyl fluoride (αG3F).

2,3,4,6,2′,3′,4′,6′,2″,3″,4″,6″-Undeca-*O*-acetyl-α-maltotriosyl fluoride (2.4). Maltotriose per-*O*-acetate (*194*) **2.3** (2.5 g, 2.59 mmol) was added directly to a plastic vial at -78°C containing 20 mL HF-pyridine and the reaction was stirred under a blanket of N_2 for 20 min. The reaction mixture was allowed to warm to room temperature and stir for a further 2 to 3 h, then diluted with CH_2Cl_2 and washed with H_2O, saturated aqueous $NaHCO_3$ and H_2O, and dried ($MgSO_4$). Evaporation *in vacuo* followed by column chromatography (1.5:1 EtOAc:hexanes) yielded **2.4** (1.45 g, 60%) as a white solid. **^{1}H NMR data** ($CDCl_3$, 400 MHz) *selected data only*: δ 5.67 (dd, 1 H, $J_{1,F}$ 52.9, $J_{1,2}$ 3.9 Hz, H-1), 5.39 (d, 1 H, $J_{1',2'}$ 3.8 Hz, H-1′), 5.36 (d, 1 H, $J_{1'',2''}$ 3.8 Hz, H-1″). **^{19}F NMR data** ($CDCl_3$, 188 MHz): δ -149.2 (dd, $J_{1,F}$ 52.9, $J_{2,F}$ 26.0 Hz, F-1).

α-Maltotriosyl fluoride (2.5). Compound **2.4** (1.45 g, 1.57 mmol) was deprotected with NaOMe following the general procedure detailed above. Purification was achieved by adsorbing the reaction mixture to silica followed by flash chromatography (7:2:1 EtOAc:MeOH:H_2O) to give pure α-maltotriosyl fluoride (αG3F) **2.5** (630 mg, 80%) as a colourless gum. Lyophilization afforded **2.5** as a white solid. **^{1}H NMR data** (D_2O, 400

MHz) *selected data only*: δ 5.67 (dd, 1 H, $J_{1,F}$ 52.9, $J_{1,2}$ 3.9 Hz, H-1), 5.39 (d, 1 H, $J_{1',2'}$ 3.8 Hz, H-1′), 5.36 (d, 1 H, $J_{1'',2''}$ 3.8 Hz, H-1″). **^{19}F NMR data** (D_2O, 188 MHz): δ -150.4 (dd, $J_{1,F}$ 52.9, $J_{2,F}$ 26.0 Hz, F-1). **MS data** (DCI): Calculated for $C_{18}H_{31}FO_{15}$ 521.46 ($M + NH_4^+$), found 522 ($M + NH_4^+$). Anal. calculated for $C_{18}H_{31}FO_{15}\cdot H_2O$: C 41.22, H 6.34, found: C 41.25, H 6.61.

4.1.3 Synthesis of 4-deoxy-α-maltotriosyl fluoride (4DαG3F)

The compound 4-deoxy-α-maltotriosyl fluoride was synthesized according to Lindhorst et al. (*93*) with some modifications to reaction times, temperatures, and methods of purification.

4′-*O*-(4,6-*O*-Benzylidene-α-D-glucopyranosyl)-maltose (2.6). Maltotriose (11.5 g, 22.8 mmol) was dissolved in dry DMF (200 mL) containing ρ-toluenesulfonic acid (40 mg) and benzaldehyde dimethylacetal (3.7 mL, 24.7 mmol). The mixture was placed on a rotary evaporator under vacuum at 70°C for 8 h in order to remove the MeOH formed during the reaction. The yield of the reaction was consistently around 50% (TLC: 7:2:1 EtOAc:MeOH:H_2O). The DMF was evaporated *in vacuo* and the entire mixture was used in the next step without further purification.

1,2,3,6,2′,3′,6′-Hepta-*O*-acetyl-4′-*O*-(2,3-di-*O*-acetyl-4,6-*O*-benzylidene-α-D-glucopyranosyl)-maltose (2.7). The hemiacetal mixture **2.6** was dissolved in pyridine (130 mL) and acetylated using acetic anhydride (40 mL). The reaction mixture was stirred overnight at 50-60°C, then diluted with CH_2Cl_2, washed with saturated aqueous $NaHCO_3$ and H_2O, and dried over $MgSO_4$. The solvent was removed by co-evaporation with toluene.

Column chromatography yielded pure **2.7** (10 g, 45%, mixture of anomers) as a white solid. **^{1}H NMR data** ($CDCl_3$, 400 MHz) *selected data only*: δ 7.35 (m, 5 H, aromatic), 6.21 (d, $J_{1,2}$ 3.7 Hz, H-1α), 5.72 (d, $J_{1,2}$ 8.1 Hz, H-1β), 5.10-5.50 (m, 6 H, H-1′, H-1″, H-3, H-3′, H-3″, PhC*H*). **MS data** (DCI): Calculated for $C_{43}H_{54}O_{25}$ 988.91 ($M + NH_4^+$), found 989 ($M + NH_4^+$).

1,2,3,6,2′,3′,6′-Hepta-*O*-acetyl-4′-*O*-(2,3-di-*O*-acetyl-6-*O*-benzyl-α-D-glucopyranosyl)-maltose (2.8). To a solution of **2.7** (3 g, 3.0 mmol) in dry THF (100 mL) was added $NaBH_3CN$ (1.8 g, 30 mmol). Under N_2, a saturated solution of HCl gas in dry diethyl ether (approximately 50 mL) was added dropwise until the pH of the solution remained acidic. The reaction was complete (TLC: 1.5:1 EtOAc:hexanes) after 1 h at room temperature. The mixture was diluted into dichloromethane and washed with water, aqueous $NaHCO_3$ and saturated NaCl solution and dried ($MgSO_4$), then the solvent was removed by rotary evaporation to give a yellow oil. Purification was achieved by column chromatography (1.5:1 EtOAc:hexanes) to yield **2.8** (2.5 g, 85%) as a white solid. **^{1}H NMR data** ($CDCl_3$, 400 MHz) *selected data* β *anomer only*: δ 7.30 (m, 5 H, aromatic), 5.70 (d, 1 H, $J_{1,2}$ 8.0 Hz, H-1), 5.10-5.50 (m, 5 H, H-1′, H-1″, H-3, H-3′, H-3″), 4.90 (dd, 1 H, $J_{1,2}$ 8, $J_{2,3}$ 9 Hz, H-2), 4.75 (dd, 1 H, $J_{1″,2″}$ 4, $J_{2″,3″}$ 10 Hz, H-2″), 4.70 (dd, 1 H, $J_{1′,2′}$ 4, $J_{2′,3′}$ 10 Hz, H-2′). 4.50 (s, 2 H, PhCH_2), 2.70 (s, 1 H, 4″-OH), 1.9-2.1 (9 s, 27 H, 9 OAc). **MS data** (DCI): Calculated for $C_{43}H_{56}O_{25}$ 990.93 ($M + NH_4^+$), found 991 ($M + NH_4^+$).

1,2,3,6,2′,3′,6′-Hepta-*O*-acetyl-4′-*O*-(2,3-di-*O*-acetyl-6-*O*-benzyl-4-deoxy-4-iodo-α-D-galactopyranosyl)-maltose (2.10). Compound **2.8** (2 g, 2.1 mmol) was dissolved in dry CH_2Cl_2 (100 mL) containing 2 mL pyridine and cooled to -10°C under N_2. Triflic anhydride

(0.5 mL, 2.73 mmol) was added dropwise and the reaction allowed to stir at room temperature. After 30 min (TLC: 2:1 EtOAc:hexanes), the reaction was deemed complete. The mixture was diluted into CH_2Cl_2 and washed with H_2O, aqueous $NaHCO_3$ and H_2O, then dried over $MgSO_4$ and the solvent removed *in vacuo* to give **2.9**. The resulting syrup was dissolved in dry DMF and stirred with NaI (1.5 g, 10 mmol) overnight. The 4″-iodo compound could not be distinguished from the 4″-triflate (**2.9**) by TLC analysis. The reaction mixture was diluted with CH_2Cl_2 and then washed with H_2O, the combined aqueous phases were extracted three times with CH_2Cl_2. The organic layers were dried over $MgSO_4$, evaporated and purified by column chromatography (1:1 EtOAc:hexanes) to yield **2.10** (1.70 g, 75%) as a white foam. **^{1}H NMR data** ($CDCl_3$, 400 MHz) *selected data* β-*anomer only*: δ 7.3-7.4 (m, 5 H, aromatic), 5.70 (d, 1 H, $J_{1,2}$ 8.1 Hz, H-1), 5.33 (d, 1 H, $J_{1'',2''}$ 4.3 Hz, H-1″), 5.32 (m, 1 H, $J_{2',3'}$ 10.3 Hz, H-3′), 5.25 (dd, 1 H, $J_{2,3}$ 8.9, $J_{3,4}$ 9.1 Hz, H-3), 5.20 (d, 1 H, $J_{1',2'}$ 3.9 Hz, H-1′), 5.15 (dd, 1 H, $J_{1'',2''}$ 4.3, $J_{2'',3''}$ 10.7 Hz, H-2″), 4.92 (dd, 1 H, $J_{1,2}$ 8.1, $J_{2,3}$ 8.9 Hz, H-2), 4.75 (bd, 1 H, $J_{3'',4''}$ 3.3 Hz, H-4″), 4.68 (dd, 1 H, $J_{1',2'}$ 3.9, $J_{2',3'}$ 10.3 Hz, H-2′), 4.50 (m, 3 H, PhCH_2, H-6a′), 4.41 (m, 2 H, H-3″, H-6a), 4.10-4.20 (m, 2 H, H-6b, H-6b′), 3.85-3.95 (m, 3 H, H-4, H-4′, H-5′), 3.80 (m, 1 H, H-5), 3.40-3.50 (m, 3 H, H-5″, H-6a″, H-6b″), 1.9-2.1 (m, 27 H, 9 OAc). **MS data** (DCI): Calculated for $C_{43}H_{55}IO_{24}$ 1100.83 (M + NH_4^+), found 1101 (M + NH_4^+).

1,2,3,6,2′,3′,6′-Hepta-*O*-acetyl-4′-*O*-(2,3-di-*O*-acetyl-6-*O*-benzyl-4-deoxy-α-D-*xylo*-hexopyranosyl)-maltose (2.11). To a solution of **2.10** (1.5 g, 1.38 mmol) in dry benzene (100 mL) was added tributyl-tinhydride (1.85 mL, 6.9 mmol) and a catalytic amount of AIBN (2,2′-azobis(2-methylpropionitrile)). The reaction mixture was refluxed and TLC analysis

(1:1 EtOAc:hexanes) revealed that the reaction was complete after 1.5 h. The reaction mixture was evaporated to dryness, redissolved in CH_3CN, and washed three times with hexanes. After evaporation of solvent, the product was purified using column chromatography (1:1 EtOAc:hexanes) to yield **2.11** (1.2 g, 92%) as a colourless oil. **^{1}H NMR data** ($CDCl_3$, 400 MHz): *selected data* β-*anomer only*: δ 7.2-7.4 (m, 5 H, aromatic), 5.71 (d, 1 H, $J_{1,2}$ 8.1 Hz, H-1), 5.39 (d, 1 H, $J_{1'',2''}$ 3.9 Hz, H-1″), 5.35 (dd, 1 H, $J_{2',3'}$ 10.6, $J_{3',4'}$ 9.1 Hz, H-3′), 5.25 (t, 1 H, $J_{2,3}$ 8.8, $J_{3,4}$ 8.9 Hz, H-3), 5.25 (d, 1 H, $J_{1',2'}$ 4.1 Hz, H-1′), 5.15 (ddd, 1 H, $J_{2'',3''}$ 10.6, $J_{3'',4''e}$ 4.9 Hz, H-3″), 4.95 (dd, 1 H, $J_{1,2}$ 8.1, $J_{2,3}$ 8.8 Hz, H-2), 4.78 (dd, 1 H, $J_{1'',2''}$ 3.9, $J_{2'',3''}$ 10.6 Hz, H-2″), 4.70 (dd, 1 H, $J_{1',2'}$ 4.1, $J_{2',3'}$ 10.6 Hz, H-2′), 4.54, 4.52 (2 d, 2 H, PhCH_2), 4.1-4.5 (m, 4 H, H-6a, H-6b, H-6a′, H-6b′), 3.8-4.0 (m, 5 H, H-4, H-4′, H-5, H-5′, H-5″), 3.45 (m, 2 H, H-6″a, H-6″b), 2.15 (ddd, 1 H, H-4″e), 1.9-2.1 (m, 27 H, 9 OAc), 1.70 (ddd, 1 H, H-4″a). **MS data** (DCI): Calculated for $C_{43}H_{56}O_{24}$ 974.93 ($M + NH_4^+$), found 975 ($M + NH_4^+$).

1,2,3,6,2′,3′,6′-Hepta-*O*-acetyl-4′-*O*-(2,3-di-*O*-acetyl-4-deoxy-α-D-*xylo*-hexopyranosyl)-maltose (2.12). To a solution of **2.11** (1.0 g, 1.05 mmol) in MeOH (30 mL) and EtOAc (30 mL) was added a catalytic amount of Pd catalyst (10% on charcoal). The mixture was hydrogenated overnight. The solution was gravity filtered and the solvent was removed *in vacuo* to yield **2.12** (0.86 g, 95%) as a clear oil. The compound was used without further purification for the next step.

1,2,3,6,2′,3′,6′-Hepta-*O*-acetyl-4′-*O*-(2,3,6-tri-*O*-acetyl-4-deoxy-α-D-*xylo*-hexopyranosyl)-maltose (2.13). Compound **2.12** was dissolved in pyridine (20 mL), acetic anhydride (2 mL) was added and the solution was reacted overnight at room temperature. The mixture was diluted with CH_2Cl_2, washed with H_2O, saturated aqueous $NaHCO_3$ and H_2O, and then dried ($MgSO_4$). After removing the solvent by rotary evaporation, the mixture was purified by column chromatography (2:1 EtOAc:hexanes) to yield **2.13** (0.82 g, 91%) as a clear glass. **^{1}H NMR data** ($CDCl_3$, 400 MHz) *selected data* β-*anomer only*: δ 5.38 (d, 1 H, $J_{1'',2''}$ 3.6 Hz, H-1″), 5.34 (dd, 1 H, H-3′), 5.32 (d, 1 H, $J_{1,2}$ 7.7 Hz, H-1), 5.25 (dd, 1 H, $J_{2,3}$ 8.9, $J_{3,4}$ 9.1 Hz, H-3), 5.20 (d, 1 H, $J_{1',2'}$ 4.2 Hz, H-1′), 5.13 (ddd, 1 H, $J_{3'',4''e}$ 4.9 Hz, H-3″), 4.9 (dd, 1 H, $J_{2,3}$ 8.9 Hz, H-2), 4.75 (dd, 1 H, $J_{1'',2''}$ 3.6, $J_{2'',3''}$ 9.6 Hz, H-2″), 4.70 (dd, 1 H, $J_{1',2'}$ 4.2, $J_{2',3'}$ 10.3 Hz, H-2′), 1.9-2.1 (m, 31 H, 10 OAc, H-4″e). 1.57 (ddd, 1 H, H-4″a). **MS data** (DCI): Calculated for $C_{38}H_{52}O_{25}$ 926.84 ($M + NH_4^+$), found 927 ($M + NH_4^+$).

2,3,6,2′,3′,6′-Hexa-*O*-acetyl-4′-*O*-(2,3,6-tri-*O*-acetyl-4-deoxy-α-D-*xylo*-hexopyranosyl)-maltose (2.14). The 4-deoxy-per-*O*-acetate **2.13** (0.62 g, 0.68 mmol) was dissolved in DMF (10 mL) and heated to 50°C. Hydrazine acetate (0.070 g, 0.75 mmol) was added and the reaction mixture was stirred for a further 10 min at 50°C and 20 min at room temperature, after which time the reaction had gone to completion (TLC: 2:1 EtOAc:hexanes). The mixture was worked up by diluting in EtOAc, washing with H_2O, and drying over $MgSO_4$. After purification by column chromatography, **2.14** was obtained in 96% yield (0.57 g).

2,3,6,2′,3′,6′-Hexa-*O*-acetyl-4′-*O*-(2,3,6-tri-*O*-acetyl-4-deoxy-α-D-*xylo*-hexopyranosyl)-α- and β-maltosyl fluoride (2.15). Compound **2.14** (0.52 g, 0.60 mmol) was dissolved in dry CH_2Cl_2 (10 mL) at 0^0C under N_2 and a solution of DAST (0.16 mL, 1.2 mmol) in 5 mL CH_2Cl_2 was added. The reaction mixture was stirred for 15 h at room temperature after which time TLC analysis (2:1 EtOAc:hexanes) deemed it to be complete. The reaction was quenched by the addition of MeOH and the solvent was evaporated to give a yellow oil. The oil was dissolved in CH_2Cl_2 and washed two times each with aqueous $NaHCO_3$ and H_2O, followed by evaporation *in vacuo*. Purification by column chromatography yielded **2.15** (0.38 g, 73%) as a white foam. **^{1}H NMR data** ($CDCl_3$, 400 MHz) *selected data only*: δ 5.63 (dd, $J_{1,F}$ 53, $J_{1,2}$ 2.7 Hz, H-1α), 5.57 (dd, $J_{2,3}$ 10, $J_{3,4}$ 8.8 Hz, H-3α), 5.25 (d, $J_{1'2'}$ 4.0 Hz, H-1′), 5.17 (dd, $J_{1,F}$ 51.3, $J_{1,2}$ 4.8 Hz, H-1β), 5.15 (ddd, H-3″), 4.92 (ddd, $J_{1,2}$ 4.8, $J_{2,3}$ 8.5, $J_{2,F}$ 6.1 Hz, H-2β), 4.8 (dd, $J_{1'',2''}$ 4.0, $J_{2''3''}$ 10.5 Hz, H-2″β), 4.70 (dd, $J_{1',2'}$ 4.0, $J_{2'3'}$ 10.2 Hz, H-2′β), 2.0-2.2 (9 s, 9-OAc and H-4″eβ). 1.57 (q, H-4″aβ). **^{19}F NMR data** ($CDCl_3$, 188 MHz): δ -131.89 (β), -149.17 (α). **MS data** (DCI): Calculated $C_{36}H_{49}FO_{23}$ 886.77 ($M + NH_4^+$), found 887 ($M + NH_4^+$).

2,3,6,2′,3′,6′-Hexa-*O*-acetyl-4′-*O*-(2,3,6-tri-*O*-acetyl-4-deoxy-α-D-*xylo*-hexopyranosyl)-α-maltosyl fluoride (2.16). The α/β fluoride **2.15** (0.31 g, 0.35 mmol) was placed in a plastic vial and cooled under N_2 to -78°C for 10-20 min. An aliquot (5 mL) of HF-pyridine was added and the reaction was kept at -78°C for 20 min and at -20°C for 2 h. The reaction mixture was diluted with CH_2Cl_2 and quenched with saturated aqueous $NaHCO_3$, the organic layer was washed with water, dried ($MgSO_4$) and the solvent was removed by evaporation. Purification by column chromatography (1:1 EtOAc:hexanes) yielded **2.16** (0.25 g, 80%) as a

white solid. **^{1}H NMR data** ($CDCl_3$, 400 MHz) *selected data only*: δ 5.63 (dd, 1 H, $J_{1,F}$ 53.2, $J_{1,2}$ 2.6 Hz, H-1), 5.53 (dd, 1 H, $J_{2,3}$ 10.0, $J_{3,4}$ 9.5 Hz, H-3), 5.35 (m, 2 H, $J_{1'',2''}$ 4.1 Hz, H-1'', H-3'), 5.28 (d, 1 H, $J_{1',2'}$ 4.0 Hz, H-1'), 5.15 (ddd, 1 H, H-3''), 4.84 (ddd, 1 H, $J_{2,F}$ 23, $J_{1,2}$ 2.6, $J_{2,3}$ 10.0 Hz, H-2), 4.78 (dd, 1 H, $J_{1'',2''}$ 4.1, $J_{2'',3''}$ 10.4 Hz, H-2''), 4.70 (dd, 1 H, $J_{1',2'}$ 4.0, $J_{2',3'}$ 10.4 Hz, H-2'), 1.9-2.1 (8 s, 28 H, 9 OAc and H-4''e), 1.58 (q, 1 H, H-4''a). **^{19}F NMR data** ($CDCl_3$, 188 MHz): δ -149.026 (α) (dd, $J_{1,F}$ 53.2, $J_{2,F}$ 26.0 Hz, F-1). **MS data** (DCI): Calculated $C_{36}H_{49}FO_{23}$ 886.77 ($M + NH_4^+$), found 887 ($M + NH_4^+$).

4'-*O*-(4-Deoxy-α-D-*xylo*-hexopyranosyl)-α-maltosyl fluoride (1.21). To a solution of **2.16** (70 mg, 0.081 mmol) in dry MeOH (10 mL) was added a 200 µl aliquot of a freshly prepared NaOMe solution (0.05 M). The reaction mixture was stirred overnight at room temperature and then neutralized with a minimal amount of ion exchange resin (Bio-Rad Dowex 50W-X 12, 50-100 mesh, H^+ form). If necessary, the reaction was purified by column chromatography (7:2:1 EtOAc:MeOH:H_2O) to yield the final product **1.21** (4DαG3F) (38 mg, 96%) as a clear oil. The oil was lyophilized to give an amorphous white solid. **^{1}H NMR data** (D_2O, 400 MHz) *selected data only*: δ 5.65 (dd, 1 H, $J_{1,F}$ 53.6, $J_{1,2}$ 2.8 Hz, H-1), 5.3-5.4 (2 d, 2 H, $J_{1'2'}$ 4.0, $J_{1'',2''}$ 4.0 Hz, H-1', H-1''), 3.4-4.1 (dd, 1 H, $J_{1',2'}$ 4.0, $J_{2',3'}$ 9.7 Hz, H-2'), 1.95 (ddd, 1 H, $J_{3'',4''e}$ 4.8, $J_{4''e,4''a}$ 12.0, $J_{4''e,5''}$ 2.0 Hz, H-4''e), 1.40 (q, 1 H, $J_{3'',4''a}$ 12.0, $J_{4''a,4''e}$ 12.0, $J_{4''a,5''}$ 12.0 Hz, H-4-a''). **^{19}F NMR data** (D_2O, 188 MHz): δ -150.4 (dd, $J_{1,F}$ 53.6, $J_{2,F}$ 26.0 Hz, F-1). **MS data** (DCI): Calculated for $C_{18}H_{31}FO_{14}$ 505.46 ($M + NH_4^+$), found 506 ($M + NH_4^+$). Anal. calculated for $C_{18}H_{31}FO_{14}\cdot 2H_2O$: C 41.06, H 6.70, found: C 41.25, H 6.61.

4.1.4 Enzymatic Synthesis of 4-Deoxymaltopentaose and 4-Deoxymaltohexaose

To 1 equiv. of 4DαG3F (**1.21**) (11 mg, 2.25 x 10^{-5} mol) in 200 mM sodium citrate buffer (700 μL), pH 6.0 was added 1.8 equiv. maltotriose (20 mg, 4.03 x 10^{-5} mol) and glycogen debranching enzyme (300 μL, 5 U/mL, 18.3 mg/mL, in 100 mM citrate buffer, 1 mM EDTA, 1 mM DTT, pH 6.0, see Section 4.3.2 for purification of glycogen debranching enzyme). The progress of the reaction was checked at 24 h by injecting a small sample of the reaction mixture (10 μL) onto an analytical Waters Dextropak HPLC column (8 x 100 mm) and eluting with a mobile phase of 100% double deionized water at 0.8 mL/min. The products were identified using a refractive index detector and relative yields were determined by the integration of peak areas. The progress of the reaction was continuously monitored by analytical HPLC as described above until the yield of 4DG6 was optimized. On average, the reaction was stopped after 40-48 h with a typical yield of 45% 4DG5 (**3.4**) (8 mg) and 43% 4DG6 (**3.3**) (9 mg). The reaction was terminated by passing the solution through a 100,000 molecular weight cut off filter (Amicon) to recover the enzyme.

Purification of Reaction Products: The reaction mixture was loaded onto a large Waters Dextropak column (10 x 250 mm) and eluted at 7 mL/min with a solvent system of 100% double deionized water. Fractions containing 4DG5 and 4DG6 as well as any remaining starting material (4DαG3F) were pooled and concentrated by evaporation and then a small sample was injected onto the analytical column to assess purity. The final products were lyophilized to give white solids. **MS data** (MALDI): Calculated for $C_{30}O_{25}H_{52}$ 835.72 (4DG5 + Na^+), found 835.7 (4DG5 + Na^+), calculated for $C_{36}O_{30}H_{62}$ 997.86 (4DG6 + Na^+), found 997.2 (4DG6 + Na^+); ES-MS: calculated for $C_{30}O_{25}H_{52}$ 830.7 (4DG5 + NH_4^+), found

831 (4DG5 + NH_4^+), calculated for $C_{36}O_{30}H_{62}$ 992.9 (4DG6 + NH_4^+), found 993 (4DG6 + NH_4^+).

4.1.5 Synthesis of Glucose-[1-^{18}O]-Phosphate

2,3,4,6-Tetra-*O*-acetyl-α-D-glucopyranosyl bromide (3.6). Per-*O*-acetylated glucose **3.5** (5 g) was dissolved in 20 mL of 45% acetic acid/HBr containing a few drops of acetic anhydride. The reaction was complete after stirring for 1 h at room temperature and was quenched at 4°C with $NaHCO_3$/water. The bromide **3.6** readily crystallized from ether/hexanes, yield 4.12 g (78%).

2,3,4,6-Tetra-*O*-acetyl-β-D-glucopyranose (3.7). The bromide **3.6** (4.12 g, 10.0 mmol) in acetone (10 mL) was added to 500 μL H_2O and 2 g (8.63 mmol) Ag_2O and the reaction stirred for 30 min at room temperature in the dark. The silver salts were filtered off, the solution rotary evaporated to dryness and then crystallized with EtOAc/hexanes to give a white solid **3.7** (3.15 g, 90% yield). **^{1}H NMR data** ($CDCl_3$, 200 MHz): δ 5.3 (t, 1 H, $J_{2,3}$ 10, $J_{3,4}$ 10 Hz, H-3), 5.05 (t, 1 H, $J_{3,4}$ 9, $J_{4,5}$ 9 Hz, H-4), 4.9 (dd, 1 H, $J_{1,2}$ 8.0, $J_{2,3}$ 10 Hz, H-2), 4.75 (d, 1 H, $J_{1,2}$ 8 Hz, H-1α), 4.1 (m, 2 H, H-6a, H-5), 3.8 (m, 1 H, H-6b), 2.1 (m, 12 H, 4 OAc).

2,3,4,6-Tetra-*O*-acetyl-[1-^{18}O]-α/β-D-glucopyranose (3.8). A typical ^{18}O incorporation experiment was performed as follows. 2,3,4,6-Tetra-*O*-acetyl-β-D-glucopyranose **3.7** (250 mg, 0.72 mmol) dried over P_2O_5 for 48 hours was dissolved in a mixture containing 250 μL of 95-98% $H_2{}^{18}O$ and 1.2 mL dry CH_3CN. Ten to fifteen beads of Amberlite resin (H^+ form) were added as catalyst and the solution was placed in an ampule, flooded with N_2 and sealed

off. The reaction mixture was heated for 14-16 h at 105°C, then the solvent was removed *in vacuo* and the resulting syrup was chromatographed on silica (EtOAc:hexanes 1:1) to give the ^{18}O labelled sugar **3.8** (170 mg, 68%). The extent of ^{18}O incorporation was determined by DCI (NH_4^+) mass spectrometry; typical ^{18}O incorporation being 70-80%. ^1H NMR spectra were similar to those reported for the unlabelled starting material. In practice, this compound was not isolated but used directly for the next step. **MS data** (DCI, LRMS): Calculated for $C_{14}H_{20}O_9{}^{16}O$ 366.34 (M + NH_4^+), found 366 ($C_{14}H_{20}O_9{}^{16}O$ + NH_4^+), 368 ($C_{14}H_{20}O_9{}^{18}O$ + NH_4^+) ratio of incorporation 20/80 ($^{16}O/^{18}O$).

Diphenyl (2,3,4,6-tetra-*O*-acetyl)-[1-^{18}O]-α-D-glucopyranosyl phosphate (3.9). The phosphate was produced through a modification of the procedure of Sabesan et al. (*183*). A solution of 2,3,4,6-tetra-*O*-acetyl-[1-^{18}O]-α/β-D-glucopyranose **3.8** (170 mg, 0.48 mmol) in dry dichloromethane (40 mL) containing dimethylaminopyridine (128 mg, 1.04 mmol, 2.2 equiv.) was stirred at room temperature for 15 min and then cooled to -10°C. Diphenylchlorophosphate (0.22 mL, 1.04 mmol, 2.2 equiv.) was added dropwise and the reaction mixture was stirred at -10°C for 2 hours and then allowed to warm to 4-5°C for 1 h. The mixture was diluted with CH_2Cl_2, washed with ice water, 0.5 M HCl, and saturated aqueous $NaHCO_3$. Purification by silica gel chromatography (3:2 hexanes:EtOAc) afforded 180 mg (63% yield) of **3.9** as a syrup. **^{1}H NMR data** ($CDCl_3$, 200 MHz): δ 7.30 (m, 2 x Ph), 6.06 (dd, 1 H, $J_{1,2}$ 3.8, $J_{1,P}$ 7 Hz, H-1), 5.52 (t, 1 H, $J_{2,3}$ 10, $J_{3,4}$ 10 Hz, H-3), 5.13 (t, 1 H, $J_{3,4}$ 10, $J_{4,5}$ 9 Hz, H-4), 5.02 (ddd, 1 H, $J_{1,2}$ 3.8, $J_{2,3}$ 10 Hz, H-2), 4.2 (m, 2 H, H-6a, H-5), 3.88 (m, 1 H, H-6b), 2.1 (m, 12 H, 4 OAc). **^{31}P NMR data** ($CDCl_3$, 81 MHz) proton decoupled: δ - 13.847 (P-^{16}O) and - 13.883 (P-^{18}O). **^{13}C NMR data** ($CDCl_3$, 75 MHz): δ

94.815 (d, C1-^{16}O), 94.742 (d, C1-^{18}O), 69.4 (C5), 69.0 (C3), 67.1 (C2), 60.7 (C6). **MS data** (ES): Calculated for $C_{26}H_{29}O_{12}P^{18}O$ 582.48 (M), found 582 ($C_{26}H_{29}O_{12}P^{18}O$), 600 ($C_{26}H_{29}O_{12}P^{18}O + NH_4^+$), 605 ($C_{26}H_{29}O_{12}P^{18}O + Na^+$).

2,3,4,6-Tetra-*O*-acetyl-[1-^{18}O]-α-D-glucopyranosyl phosphate (3.10). A solution of diphenyl (2,3,4,6-tetra-*O*-acetyl)-[1-^{18}O]-α-D-glucopyranosyl phosphate **3.9** (180 mg, 0.37 mmol) in 1:1 MeOH:EtOAc (20 mL) was hydrogenated (4 atm) in the presence of PtO_2 catalyst (25 mg, approximately 15% by weight) for 13-16 hours. The catalyst was removed by filtration followed by evaporation *in vacuo* to yield 100 mg of a clear syrup. Purification by preparative TLC (9:9:1 chloroform: methanol: water) afforded 95 mg of **3.10** (60% yield). **^{1}H NMR data** (MeOD, 200 MHz): δ 5.70 (dd, 1 H, $J_{1,2}$ 3.8, $J_{1,P}$ 7 Hz, H-1), 5.5 (t, 1 H, $J_{2,3}$ 10, $J_{3,4}$ 10 Hz, H-3), 5.17 (t, 1 H, $J_{3,4}$ 9, $J_{4,5}$ 9 Hz, H-4), 4.9 (ddd, $J_{1,2}$ 3.8, $J_{2,3}$ 10 Hz, H-2), 4.42 (m, 2 H, H-5 and H-6a), 4.20 (m, 1 H, H-6b), 2.1 (m, 12 H, 4 OAc). **^{31}P NMR data** (MeOD, 81 MHz) proton decoupled: δ 0.005 (P-O^{16}), - 0.012 (P-O^{18}). **^{13}C NMR data** (MeOD, 75 MHz): δ 91.335 (d, C1-^{16}O), 91.270 (d, C1-^{18}O), 70.4 (C5), 70.5 (C2), 68.1 (C3), 67.6 (C4), 61.4 (C6). **MS data** (ES): Calculated for $C_{14}H_{21}O_{12}P^{16}O$ 428.29 (M), found 429 ($C_{14}H_{21}O_{12}P^{16}O + H^+$), 431 ($C_{14}H_{21}O_{12}P^{18}O + H^+$), 453 ($C_{14}H_{21}O_{12}P^{18}O + Na^+$).

Glucose-[1-^{18}O]-phosphate disodium form (3.11) A solution of **3.10** (35 mg, 0.08 mmol) was dissolved in dry methanol under N_2 and a catalytic amount (1 mL) of a freshly prepared sodium methoxide solution (0.02 M) was added. The reaction mixture was allowed to stir overnight and was monitored by TLC (2:2:1 EtOAc:MeOH:H_2O). After dissolving the precipitated product by the addition of water (5 mL), the mixture was neutralized by the addition of a minimal amount of Amberlite resin (H^+ form) and filtered. The reaction mixture

was evaporated to dryness, redissolved in water and applied to an anion exchange column (Dowex 50W X-8 20-50 mesh, H^+ form exchanged to Na^+ form by washing resin with 1 M NaOH) equilibriated with double deionized water to yield 20 mg (81% yield) of **3.11**. **^{1}H NMR data** (D_2O, 400 MHz): δ 5.45 (dd, 1 H, $J_{1,2}$ 3.8, $J_{1,P}$ 7 Hz, H-1), 3.8 (m, 1 H, H-3), 3.51 (m, 1 H, H-2), 3.42 (t, 1 H, $J_{3,4}$ 9, $J_{4,5}$ 9 Hz, H-4), 3.7-3.8 (m, 3 H, H-5 and H-6a & b). **^{31}P NMR data** (D_2O-buffer, pH 6.3, 81 MHz) proton decoupled: δ 1.447 (P-O^{16}), 1.430 (P-O^{18}). **^{13}C NMR data** (D_2O-buffer, pH 6.3, 75 MHz): δ 94.011 (d, C1-^{18}O), 93.938 (d, C1-^{16}O), 73.2 (C5), 72.2 (C3), 72.1 (C2), 69.8 (C4), 60.7 (C6). **MS data** (ES): Calculated for $C_6H_{13}O_8P^{16}O$ 260.17 (M), found 261 ($C_6H_{13}O_8P^{16}O + H^+$), 263 ($C_6H_{13}O_8P^{18}O + H^+$), 285 ($C_6H_{13}O_8P^{18}O + Na^+$), 308 ($C_6H_{13}O_8P^{18}O + 2\ Na^+$).

4.2 ENZYMOLOGY-CYCLODEXTRIN GLYCOSYLTRANSFERASE

4.2.1 General

Wild-type and all mutant CGTases were kindly provided by Dr. B. Dijkstra and Dr. L. Dijkhuizen, University of Groningen, the Netherlands. They were purified according to the previously published method of Knegtel et al. (*82*). Pepsin was obtained from Boehringer Mannheim. All other chemicals were purchased from Sigma Chemical Company and used without further purification with the exception of acarbose which was generously provided by Miles Inc.

The kinetic parameters for the CGTase mutants Y195G, Y195F, and Y195L with αG3F were obtained by Mr. Howard Sham, an undergraduate student working under my supervision.

4.2.2 Kinetic Analysis: Determination of Kinetic Parameters for α-Glycosyl Fluorides

The reactions of CGTase (wt and mutants) with the glycosyl fluoride analogues were monitored by following the release of fluoride ion using an Orion ion selective fluoride electrode interfaced to a pH/ion selective meter (Fischer Scientific). Data were collected using the program Terminal and values of K_m and k_{cat} were calculated from the experimental rate versus substrate concentration data, using the program GraFit (*195*). In a typical experiment, an appropriate concentration of glycosyl fluoride in 50 or 100 mM citrate buffer (pH 6.0) was warmed to 30°C for 10 min (total volume = 240 μL) and the reaction initiated by adding an appropriately diluted aliquot of enzyme (typically 10 μL) in citrate buffer (final concentrations: wild-type (0.25 μg/mL), Glu257Gln (24 μg/mL), Asp229Asn (50 μg/mL), Glu257Ala (70 μg/mL), Asp229Ala (177 μg/mL)). Concentrations of enzyme used for the investigations of acarbose as a transition state analogue were as follows: (αG3F as substrate: S145E (1.1 μg/mL); S146P (13.4 μg/mL); D371N (1.7 μg/mL); N193G (1.5 μg/mL); N326Q (3.2 μg/mL); Y195G (3.2 μg/mL); Y195F (1.1 μg/mL); Y195L (1.1 μg/mL) and with αGF as substrate: S145E (19.3 μg/mL); S146P (416 μg/mL); D371N (97.3 μg/mL); N193G (65 μg/mL); N326Q (254 μg/mL); Y195G (276 μg/mL); Y195F (16.6 μg/mL); Y195L (28.1 μg/mL)). The reaction was typically followed for approximately 10 min or until 10% of the starting material was consumed. Rates were determined at 6-8 substrate concentrations ranging from 0.2 to 5 times the estimated K_m value.

4.2.3 Kinetic Analysis: Inhibition of CGTases by Acarbose

Approximate K_i values for acarbose with each mutant were first determined by measuring the rate of enzyme-catalyzed fluoride release for a single concentration of αG3F or αGF at each of a series of concentrations of acarbose (6-8 concentrations) bracketing the K_i value so determined. The enzyme concentrations were identical to those used above for the respective substrate. The observed rates were plotted in the form of a Dixon plot (1/v vs [acarbose]) and the K_i value determined (assuming competitive inhibition) from the intercept of this line with the horizontal line drawn through $1/V_{max}$. In our experience this approach consistently provides a K_i value close (within 20%) to that ultimately measured by a full analysis. Full K_i determinations were performed by measurements of V_{max} and K_m values at a series of inhibitor concentrations (typically 5 concentrations) which bracket the K_i value to be determined. The value of K_i and the mode of inhibition were determined through a direct fit of the data to expressions for each inhibition mode using the program GraFit (*195*).

4.2.4 Kinetic Analysis: Evaluation of Oligosaccharides as Acceptors

Differences in rate upon the addition of various malto-oligosaccharide acceptors were determined by measuring the initial rate of D371N CGTase (10 μL aliquot, final concentration was 97.3 μg/mL) catalyzed fluoride release using a single concentration of αGF (40 μL aliquot, final concentration was 28 mM) in 100 mM citrate buffer, pH 6.0 (final volume before the addition of oligosaccharide was 260 μL). After following the reaction for 2 min, a 20 μL aliquot of the appropriate acceptor was added and the progress of the reaction monitored. Final concentrations of G to G6 were 30 mM.

4.2.5 Kinetic Analysis: Effect of the Addition of Azide on Rate of Reaction

To a solution of αG3F (2 mM) in 100 mM citrate buffer, pH 6.0 (240 μL total volume), was added an aliquot of enzyme (10 μL, see Section 4.2.2 for concentrations) and the rate of fluoride release was followed in a similar manner as is described for the acquisition of the kinetic parameters. After a measured time period, an aliquot (10 μL) of sodium azide (final concentration: 250 mM) was added and the rate of the reaction was continually monitored.

4.2.6 Determination of the Products of Reaction of αG3F with Azide Catalyzed by Glu257Ala CGTase

To a solution of 20 mM αG3F in 200 mM citrate buffer, pH 6.0 was added Glu257Ala (0.175 μg/mL) and sodium azide (final concentration: 250 mM) and the reaction mixture incubated at room temperature for 16 hours (final volume 550 μL). In parallel, a second reaction mixture, identical to the above but without any azide present, was incubated overnight under the same conditions. The enzyme was removed from both reactions by filtering the solution through a 30,000 molecular weight cutoff filter (Amicon), followed by lyophilization to remove water. The lyophilized reaction mixtures were redissolved in D_2O and then submitted for 400 MHz ^{1}H-NMR analysis.

4.2.7 HPLC Analysis of Reaction Products

To analyze the reaction products of wild-type and mutant CGTases, each enzyme (at identical concentrations to those used in the kinetic analysis) was incubated at room temperature with the substrate of interest (at concentrations of 5 x K_m) in 50 mM citrate

buffer, pH 6.0. At specified times, 10 μL or 20 μL aliquots were removed and injected directly onto the HPLC. HPLC analysis was performed using a Dynamax 60 Å NH_2 (4.6 x 250 mm, mean particle size 5 μm) column from Rainin Instrument Co. (Woburn, Ma) linked to a Waters 410 refractive index detector (internal temperature was 40°C). A mobile phase of 60/40 CH_3CN/H_2O at a flow rate of 0.8 mL/min was used. Whenever possible, retention times were matched to authentic standards which were run under identical conditions.

4.2.8 Mass Spectrometric Analysis of Reaction Products

Mass spectra were recorded on a Sciex API 300 mass spectrometer (Sciex, Thornhill, Ontario). In each case, the reaction mixture was injected onto a Dynamax NH_2 (60 Å) HPLC column as specified above, running with a mobile phase of 65/35 CH_3CN/H_2O (to ensure maximum separation of peaks) at 0.8 mL/min. A series of two post column splitters allowed the introduction of 15% of the reaction mixture into the mass spectrometer at 50 μL/min and permitted the addition of 50/50 $MeOH/H_2O$ (containing 5 mM ammonium acetate) at 5 μL/min as an ionizer. Whenever possible, the masses of authentic standards were obtained through direct flow injection into the mass spectrometer.

4.2.9 HPLC Analysis of the Anomeric Configuration of Reaction Products

The reaction products were analyzed by incubating each enzyme (at identical concentrations to those used in the kinetic analysis) with the substrate of interest, in 100 mM citrate buffer, pH 6.0, at room temperature. Aliquots (20 μL) were removed at the specified time intervals for direct injection onto the HPLC. HPLC analysis was performed using a Waters Dextropak column (8 x 100 mm, mean particle size 4 μm) linked to a Waters 410

refractive index detector (internal temperature was 40°C). A mobile phase of 100% deionized water at 1.0 mL/min was used. Retention times were matched to those of authentic standards.

4.2.10 Labelling and Proteolysis of CGTase

Labelling of CGTase was performed by incubating Glu257Gln (10 μL, 6 mg/mL) with an excess of 4DαG3F (5 μL, 125 mM) for 10 min in 50 mM citrate buffer, pH 6.0. Proteolysis was achieved by first lowering the pH through the addition of 15 μL of 50 mM sodium phosphate buffer (pH 2) followed by immediate addition of 10 μL of pepsin (0.4 mg/mL in pH 2 buffer) and the mixture incubated at room temperature for 1 hour. ES-MS analysis and SDS-PAGE of the proteolytic digests confirmed that CGTase was completely digested under these conditions. Identical conditions were used for the labelling of Glu257Gln with 4DαG2F.

4.2.11 Electrospray Mass Spectrometry

The analyses of the protein and peptide samples were carried out using a Sciex API-300 mass spectrometer interfaced with a Michrom UMA HPLC system (Michrom Bioresources, Inc., Pleasanton, Ca). Intact CGTase (10-20 μg, wild-type, Glu257Gln (unlabelled or labelled)) was introduced into the mass spectrometer through a microbore PLRP column (1 x 50 mm) and eluted with a gradient of 20-100% solvent B at a flow rate of 50 μL/min over 5 min (solvent A: 0.06% trifluoroacetic acid, 2% acetonitrile in water; solvent B: 0.05% trifluoroacetic acid, 90% acetonitrile in water). The MS was scanned over a range of 400-2000 Da with a step size of 0.5 Da and a dwell time of 1 ms. The peptides were analyzed by loading a 10 μL sample of the pepsin digest (4.5 mg/mL) onto a C18 column

(Relasil, 1 x 150 mm) and eluted at a flow rate of 50 μL/min with a gradient of 0-60% B over 60 min. The proteolytic mixture was first examined in LC/MS mode and then in neutral loss mode.

In the single quadrupole (normal LC/MS) mode, the MS conditions were as follows: the mass analyzer was scanned over the range of 300-2400 Da with a step size of 0.5 Da, a dwell time of 1 ms, an ion source voltage (ISV) of 4.8 kV and an orifice energy (OR) of 50 V. The neutral loss spectra were obtained in the triple quadrupole mode searching for the loss of m/z 235.5 (4DG3) or 154.5 (4DG2) which corresponds to the loss of the inhibitor label from a peptide which is doubly charged. A scan range of 400 to 2200 amu was used with a step size of 0.5 amu and a dwell time of 1 ms. Other parameters are as follows: ISV = 5 kV, OR = 45 V.

4.2.12 Chemical Sequencing

The peptic digest (120 μL of 1.5 mg/mL) of the 4DG3-labelled CGTase was separated by HPLC using a Deltapak 300 Å C-18 column (3.9 x 150 mm, mean particle size 15 μm) from Waters eluted with a gradient of 0-60% B over 60 min at 700 μL/min. A 13:1 post-column splitter allowed the introduction into the mass spectrometer of a portion of the peptides to be checked for purity and the fractions containing the 4DG3-labelled peptide were collected for sequencing. Prior to solid phase sequence analysis, peptides (2-5 μg in 40% CH_3CN/0.5% TFA) were coupled to arylamine-functionalized polyvinylidene fluoride membranes (Sequelon AA, Milligen/Bioresearch) using N-ethyl-N′-(3-dimethylaminopropyl) carbodiimide. Peptide sequences were determined by solid-phase Edman degradation on a

Milligen/Bioresearch model 6600 protein sequenator using standard protocols with on-line HPLC analysis of the resulting phenylthiohydantoins.

4.3 ENZYMOLOGY-RABBIT MUSCLE AND POTATO α-GLUCAN PHOSPHORYLASE

4.3.1 General

Rabbit Muscle was purchased from Pel-Freeze Biologicals, Arkansas, U.S.A. Rabbit liver glycogen (type III) was purchased from Sigma Chemical Company and purified with BioRad AG-1X8 (200-400 mesh, Cl- form) ion exchange resin to remove nucleotides, and assayed by the method of Dische (*196*). Ammonium sulphate was purchased from Schwarz/Mann Biotech. DEAE Sephacel, G-25 Sephadex, and S-200 Sephacryl were purchased from Pharmacia Biotech. Scintillation cocktail (Ultima Gold MV) was purchased from Canberra Packard. ^{14}C-G1P in 7:3 ethanol/water was purchased from NEN and had a specific activity of 233.9 mCi/mmol. Castanospermine was kindly provided by Dr. R. Furneaux, DSIR, New Zealand, (1-4) trehazoloid pseudodisaccharide was provided by Dr. S. Knapp, Rutgers-The State University of New Jersey, and nojirimycin-2-O-phosphate and nojirimycin-2-O-methyl-phosphonate were provided by Dr. A. Vasella, Organic Chemistry Institute, Zurich, Switzerland. A sample of glycogen debranching enzyme was kindly provided by Dr. Neil Madsen and Mrs. Shirley Shechosky, University of Alberta. A sample of the α-amylase Termamyl was generously provided by Novo A/S, Denmark. All other reagents were purchased from Sigma Chemical Company and used without further purification.

Absorbance measurements were carried out on either a Pye Unicam PU 8600 or PU 8700 UV/Vis spectrometer. The PU 8600 spectrometer was equipped with a sipper cell. The PU 8700 spectrometer was equipped with a circulating water bath and thermostatted cuvette holders. In most experiments, because of limiting amounts of substrate or inhibitor, 1 cm path length microquartz black cuvettes were used.

Scintillation counting was performed on a Packard Tr 1900 liquid scintillation counter. Before each run, ^{3}H and ^{14}C standards were run to assess machine performance.

4.3.2 Enzyme Isolation and Purification

Rabbit Muscle Phosphorylase: Rabbit muscle glycogen phosphorylase *b* was prepared from rabbit muscle by the method of Fischer and Krebs using DTT in place of cysteine, and recrystallized 4 times before use (*197*). The enzyme was stored in the crystalline form under a vapour of toluene and redissolved immediately before each set of experiments into 20 mM glycerophosphate buffer containing 1 mM EDTA and 5 mM DTT, pH 6.8. The protein solution was then passed down a G-25 fine Sephadex column in order to remove the excess AMP added for the crystallization. The protein concentration was determined at 280 nm using an extinction coefficient of 1.32 mg mL^{-1} cm^{-1}.

Potato Phosphorylase: Isolation of potato tuber phosphorylase was performed by a modification of a protocol generously provided by Dr. T. Fukui, itself based on a published procedure (*198*) (see also (*145*)). The procedure is identical to that published up to and including the step involving the precipitation of potato phosphorylase using starch in ethanol. The precipitate was redissolved in buffer containing arsenate (5 mM) to enhance starch

degradation through phosphorylase catalyzed arsenolysis. The material was then loaded onto a DEAE Sephacel column equilibriated with 10 mM sodium citrate buffer, pH 6.0 at 2 mL/min and washed overnight with the same until the absorbance (280 nm) of the effluent reached baseline levels. A linear gradient of NaCl (4 L: 0-1 M) was applied to the column (2 mL/min) and 20 mL fractions were collected. Fractions were assayed and those containing phosphorylase were concentrated. This solution was then applied to a Sephacryl S200 gel filtration column equilibriated with 10 mM citrate buffer at pH 6.0 and eluted at 1 mL/min collecting 2 mL fractions. Protein concentration was determined using an extinction coefficient of 1.12 mg mL^{-1} cm^{-1}. The fractions which absorbed at 280 nm were pooled on the basis of their purity as assessed by SDS-PAGE.

Glycogen Debranching Enzyme: Glycogen debranching enzyme was purified from rabbit muscle as described previously (*199*). In addition, enzyme samples prepared by the identical method were generously donated by Dr. Neil Madsen and Mrs. Shirley Shechosky, University of Alberta. The combined enzyme activity was measured by following changes in the absorbance at 340 nm, using limit dextrin as the substrate, in a buffer of 25 mM glycylglycine, 1 mM EDTA, and 1 mM DTT at pH 7.2 at 30°C (*200*). The glucosidase activity was assayed by measuring the rate of fluoride released with αGF as the substrate in 100 mM citrate buffer, 1 mM EDTA, 1 mM DTT, pH 6.0 at 30°C using an Orion fluoride sensitive electrode (*201*).

4.3.3 General Kinetic Procedures

Kinetic Analysis-Synthesis Direction: Values of V_m and K_m were determined from the initial rates of saccharide synthesis by monitoring the release of inorganic phosphate from the substrate G1P by the procedure of Fiske & Subbarow as described by Engers (*165, 166*). All rabbit muscle phosphorylase reactions were conducted in a buffer containing 20 mM glycerophosphate (GPD), 1.5 mM EDTA, and 5 mM DTT at pH 6.8. The potato phosphorylase reactions were conducted in a buffer containing 40 mM sodium maleate, 250 mM KCl, and 0.13 mM EDTA, at pH 6.3. Reaction mixtures were 0.2 mL and were incubated at 30°C for 5 minutes. Substrate concentrations were varied between 1/5 and 5 times the K_m value ultimately determined. Typical enzyme concentrations were 2 μg/reaction mixture for muscle phosphorylase and 2.5 μg/reaction mixture for potato phosphorylase.

Kinetic Analysis-Degradation Direction: Values of V_m and K_m were determined from the initial rates of saccharide breakdown by monitoring the rate of G1P production with the phosphoglucomutase/glucose-6-phosphate dehydrogenase (PGM/G6PDH) coupled enzyme system as previously described by Engers et al. for muscle phosphorylase and by a modification of the procedure used by Suganuma et al. for potato phosphorylase (*164, 202*). Final concentrations of the coupled enzyme assay components in the cuvette were: for muscle glycogen phosphorylase; βNADP (1 mM), $Mg(OAc)_2$ (10 mM), glucose-1,6-diphosphate (1.5 μM), glycogen (0.5%), AMP (1 mM), PGM (50 μg/mL), G6PDH (3 U/mL), imidazole buffer (37.5 mM, pH 6.8), GPD buffer (20 mM, pH 6.8) and for potato phosphorylase; βNADP (1 mM), $Mg(OAc)_2$ (10 mM), PGM (100 μg/mL), G6PDH (7 U/mL), imidazole buffer (37.5 mM, pH 6.5), maleate buffer (100 mM, pH 6.5). Reactions were carried out at 30°C and

were generally followed for 5 min. Enzyme concentrations used were 1 μg/reaction mixture for muscle phosphorylase and 2.5-3 μg/reaction mixture for potato phosphorylase.

Determination of Inhibition Constants: The K_i values for 4-deoxymaltohexaose or 4-deoxymaltopentaose with each enzyme were determined by measuring the V_{max} and K_m values at a series of inhibitor concentrations (typically 5 concentrations) which bracket the K_i value to be determined in each direction of analysis. The assay conditions and enzyme concentrations employed were identical to those reported above. The data were plotted in the form of a double reciprocal plot and the value of K_i and the mode of inhibition were determined through a direct fit of the data to expressions for each inhibition mode using the program GraFit (*195*).

4.3.4 Electrospray Mass Spectrometry

The analysis of the protein and peptide samples were carried out using a Sciex AP1-300 mass spectrometer interfaced with a Michrom UMA HPLC system as described for CGTase (Section 4.2.11). Intact phosphorylase (muscle or potato, 5-20 μg, in the presence or absence of activators) was introduced into the mass spectrometer through a microbore PLRP column (1 x 50 mm) and eluted with a gradient of 20-100% solvent B at a flow rate of 50 μL/min over 11 min (solvent A: 0.06% trifluoroacetic acid, 2% acetonitrile in water; solvent B: 0.05% trifluoroacetic acid, 90% acetonitrile in water). The MS was scanned over a range of 400-2000 Da with a step size of 0.5 Da and a dwell time of 1 ms. The peptides were analyzed by loading a 10-20 μL sample of the peptide digest (4-5 mg/mL, incubated in the presence or absence of activators) onto a C18 column (Relasil, 1 x 150 mm) and eluted at a

flow rate of 50 μL/min with a gradient of 0-60% B over 75 min. The MS conditions were as follows: the mass analyzer was scanned over the range of 300-2400 Da with a step size of 0.5 Da, a dwell time of 1 ms, an ion source voltage (ISV) of 4.8 kV and an orfice energy (OR) of 50 V.

Direct flow injection mass spectrometry was carried out using a capillary flow system linked to a quadrupole mass spectrometer constructed "in house" by Dr. L. Konermann and Dr. D. Douglas as described previously (*203*). Briefly, muscle phosphorylase (2.5 mg/mL) was first exchanged into 5 mM ammonium acetate buffer at pH 6.8. Two syringes (1 mL and 0.5 mL) were advanced simultaneously by a syringe pump. One syringe (1 mL) contained 2.5 mg/mL (25 μM) phosphorylase (final concentration: 10 μM). The other syringe (0.5 mL) contained 100 mM glucal in ddH_2O (final concentration: 5 mM). Initiation of the reaction was triggered by mixing the solutions from both syringes in a reaction tee. The lengths of the reaction capillaries were similar to those described previously and the total flow rates were varied such that the minimum and maximum reaction times were 0.5 s to 1 min. The charged protein ions were generated at the exit of the reaction capillary by pneumatically assisted electrospray ionization and were analyzed as described previously by Zechel et al. (*204*). The experiment was also repeated in the presence of Pi (final concentration: 24 μM) and maltopentaose (final concentration: 3.5 mM).

4.3.5 Rapid Acid Precipitation of Glycosyl-Enzyme Intermediate and Analysis by Radiolabelling

As the commercial ^{14}C-G1P (5.14 x 10^8 dpm/μmol) sample is supplied as a solution in 7:3 ethanol/water, it was first lyophilized to remove the ethanol and then redissolved in deionized water. Purity was checked by TLC (2:2:1 EtOAc:MeOH:H_2O) prior to use.

Glycogen phosphorylase (1 mg) was first preincubated with activators (1 mM AMP and 13 mM 4-deoxymaltohexaose or 13 mM maltopentaose) in 20 mM GPD buffer, pH 6.8, for 5 min and then 10 μL of 100 mM ^{14}C-G1P (6.6 x 10^5 dpm/μmol, final concentration was 20 mM) was added to initiate the reaction. After 5 min, the reaction was quenched by the addition of 400 μL of cold 5% TCA solution in H_2O and then placed on ice. A protein pellet was immediately formed. The precipitated protein was spun at 12,000 rpm for 5 min and then the supernatant was removed and retained for counting. The pellet was washed 3 times with 400 μL of cold 2.5% TCA in H_2O and each wash was retained for counting. The pellet was redissolved in 100 μL NaOH and the entire pellet was counted for ^{14}C.

The same protocol was followed for potato phosphorylase. The enzyme (0.1 mg) was preincubated with 10 mM maltopentaose, 10 mM α-cyclodextrin or 10 mM 4-deoxymaltopentaose in 40 mM maleate buffer containing 250 mM KCl and 0.25 mM EDTA, pH 6.3 for 5 min. The reaction was initiated by the addition of 20 μl of 50 mM ^{14}C-G1P (5.14 x 10^8 dpm/μmol, final concentration 20 mM).

4.3.6 Positional Isotope Exchange Experiments

A solution of ^{18}O-labelled glucose-1-phosphate **3.11** (50 μL, 135 mM; final concentration 13 mM) in D_2O was added to 150 μL D_2O and 310 μL 80 mM maleate buffer

(in D_2O) containing 500 mM KCl, 2 mM EDTA at pH 6.3 (final buffer concentration in the NMR tube was 40 mM maleate, 250 mM KCl, 1 mM EDTA). The sample was placed in an NMR tube and approximately 20 mg of BioRad Chelex-100 resin (200-400 mesh, Na^+ form) was added to remove any metal ions which may cause broadening of the ^{31}P NMR signals. Both ^1H and ^{31}P spectra were recorded to reaffirm the purity of the glucose-1-phosphate, then a solution of the blocked oligosaccharide (final concentrations: 10.2 mM α-cyclodextrin or 4 mM 4-deoxymaltopentaose in D_2O) was added. At time zero, a solution of potato phosphorylase (20 μL of 3.8 mg/mL in 40 mM maleate buffer, 250 mM KCl, 1 mM EDTA at pH 6.3) was added and acquisition of NMR spectra was initiated. Spectra were obtained on a Bruker AC-200 multinuclear spectrometer as described previously. All spectra are externally referenced to 10% H_3PO_4 in D_2O ($\delta = 0.00$ ppm). Acquisition parameters were the following: acquisition time = 10.125 s; number of scans/experiment = 128; number of experiments = 10; DE = 388.75 Hz; P0 = 3 s (pulse width); D1 = 1 s; D2 (time between each experiment) = 3000 s. After collecting the data overnight (13 h), an aliquot of the NMR sample was removed and assayed for enzyme activity using the standard procedure provided above for potato phosphorylase in the oligosaccharide synthesis direction (see Section 4.3.3).

Similar experimental procedures were followed for the positional isotope exchange experiments with muscle phosphorylase. A solution of ^{18}O labelled glucose-1-phosphate **3.11** (100 μL, 135 mM; final concentration 22.5 mM) in D_2O was added to 125 μL D_2O and 285 μL 50 mM triethanolamine buffer (in D_2O) containing 1 mM EDTA and 5 mM DTT at pH 6.8. A solution of AMP was also added (final concentration: 1 mM). The sample was placed in the NMR tube and Chelex resin was added and the spectra were recorded as discussed previously. Then a solution of 4-deoxymaltohexaose (final concentration: 5 mM) in D_2O was

added. At time zero, a solution of muscle phosphorylase (20 μL of 10 mg/mL in 50 mM triethanolamine buffer) was added and acquisition was initiated. The acquisition parameters are identical to the ones described above for potato phosphorylase. After collecting the data overnight, an aliquot of the NMR sample was removed and assayed for enzyme activity using the standard procedure provided above for muscle phosphorylase in the oligosaccharide synthesis direction (see Section 4.3.3).

4.3.7 Kinetic Analysis: Inhibition of Muscle and Potato Phosphorylase by Various Analogues

Approximate K_i values for various analogues with muscle (phos b) or potato (pot phos) phosphorylase were determined by measuring the rate of reaction in the direction of interest for a single concentration of G1P or Pi at a series of concentrations of each analogue (5-8 concentrations bracketing the K_i value so determined). The enzyme concentrations and constant substrate concentrations were as follows for each analogue: (castanospermine (**3.12**)-synthesis direction: [glycogen] = 1%, [AMP] = 1 mM, [G1P] = 3.92 mM, [phos b] = 15 μg/mL; castanospermine (**3.12**)-degradation direction: [glycogen] = 1%, [AMP] = 1 mM, [Pi] = 3.13 mM, [phos b] = 1.5 μg/mL; (1-4) trehazoloid pseudodisaccharide (**3.13**): [glycogen] = 0.5%, [AMP] = 1 mM, [Pi] = 23.8 mM, [phos b] = 1.5 μg/mL; nojirimycin-2-O-phosphate (**3.14**) (NJT-2-O-Pi)-synthesis direction: [glycogen] = 1%, [AMP] = 1 mM, [G1P] = 2.3 mM, [phos b] = 1.4 μg/mL; nojirimycin-2-O-phosphate (**3.14**) (NJT-2-O-Pi)-degradation direction: [glycogen] = 1%, [AMP] = 1 mM, [Pi] = 3.75 mM, [phos b] = 1.4 μg/mL; nojirmycin-2-O-methyl phosphonate (**3.15**) (NJT-2-O-CH_2-Pi)-synthesis direction: [glycogen] = 1%, [AMP] = 1 mM, [G1P] = 5.77 mM, [phos b] = 10 μg/mL; nojirimycin-2-O-

methyl phosphonate (**3.15**) (NJT-2-O-CH_2-Pi)-degradation direction: [glycogen] = 1%, [AMP] = 1 mM, [Pi] = 23.8 mM, [phos b] = 1.5 μg/mL; 5FαGluF (**1.14**): [glycogen] = 0.5%, [AMP] = 1 mM, [Pi] = 23.8 mM, [phos b] = 1.5 μg/mL; 5FαGluF (**1.14**) or 5FβIdoF (**1.15**): [G5] = 2.85 mM, [Pi] = 2 mM, [pot phos] = 6 μg/mL). The observed rates were plotted in the form of a Dixon plot (1/v vs [analogue]) and the K_i value determined from the intercept of this line with the horizontal line drawn through $1/V_{max}$.

4.3.8 Preparation, Purification and Modification of the Branch Point Pentasaccharide, DP5

Enzymatic Synthesis: Amylopectin from corn (40 g) was slowly added to 200 mL boiling tap water with stirring until a homogeneous viscous solution was obtained. Immediately upon the addition of a 300 μL aliquot of α-amylase (Termamyl 120L, Novo A/S, Denmark), the viscous solution was clarified. The mixture was incubated at 60°C overnight. Any solid material remaining after overnight digestion was removed by centrifugation and then the supernatant was dialyzed overnight at room temperature against ddH_2O to remove the enzyme. The water was then removed *in vacuo* and the sugar mixture was redissolved in ddH_2O to a final concentration of approximately 0.5 mg/mL. Other sources of polysaccharide were used including rabbit muscle type III glycogen, oyster type II glycogen, and amylopectin from potato.

Purification: The reaction products of Termanyl and amylopectin were purified by preparative HPLC. Both the Dextropak column (10 x 250 mm, 7 mL/min, 100% H_2O) or Dynamax 60 Å NH_2 column (21.4 x 250 mm, mean particle size 8 μm, 7 mL/min, 60/40 CH_3CN/H_2O) were suitable for this separation. A maximum of approximately 1-2 mL of the

mixture (0.5 mg/mL) was injected at a time. The peak corresponding to the DP5 was identified by matching its retention time to that of an authentic standard kindly provided by Dr. K. Bock, the Technical University of Denmark. ^{1}H NMR and ^{13}C NMR spectra were identical to those reported previously (*205, 206*). **MS data** (ES): Calculated for $C_{30}O_{26}H_{52}$ 846.70 ($M + NH_4^+$), found 847 ($M + NH_4^+$).

Elongation: The general procedure used for the attempted enzymatic modification of DP5 was as follows. To a solution of DP5 in 100 mM citrate buffer, pH 6.0 was added an aliquot of a donor substrate in ddH_2O and an aliquot of enzyme (final volume, 30-100 μL). Some of the combinations used were as follows (enzyme, donor, DP5): wt CGTase (0.044 μg/mL), αCD (60 mM), DP5 (5.4 mM); wt CGTase (0.044 μg/mL), αG3F (60 mM), DP5 (5.4 mM); wt CGTase (0.044 μg/mL), G4 (10 mM), DP5 (6.75 mM); Glu257Gln (0.06 mg/mL), αG2F (10 mM), DP5 (5.4 mM); Glu257Gln (0.06 mg/mL), αG3F (10 mM), DP5 (5.4 mM); Glu257Gln (0.06 mg/mL), G4 (75 mM), DP5 (6.75 mM); Glu257Gln (2.7 mM), G5 (5 mM), DP5 (2.7 mM); Glu257Gln (0.24 mg/mL), 4DαG2F (20 mM), DP5 (8.4 mM); Glu257Gln (0.2 mg/mL), 4DαG3F (13.3 mM), DP5 (8.4 mM); Glu257Gln (0.12 mg/mL), αCD (60 mM), DP5 (5.4 mM); Glyx (0.37 mg/mL), αG3F (10 mM), DP5 (4.2 mM); Glyx (0.367 mg/mL), G4 (10 mM), DP5 (4.2 mM); Glyx (0.37 mg/mL), G3 (10 mM), DP5 (4.2 mM); Glyx (0.37 mg/mL), 4DαG2F (10 mM), DP5 (4.2 mM). The progress of the reaction was monitored by removing a 5 μL or 10 μL aliquot and injecting it directly onto the HPLC (Dynamax column, 4.6 x 250 mm, 1 mL/min, 60/40 CH_3CN/H_2O). The products were identified by matching retention times to authentic standards using a refractive index detector and by mass spectrometric analysis of the reaction products as described previously in Section 4.2.8.

REFERENCES

1. Varki, A. (1993) *Glycobiology 3*, 97-130.

2. Henrissat, B. (1991) *Biochem. J. 280*, 309-316.

3. Henrissat, B., and Davies, G. (1997) *Curr. Opin. Struct. Biol. 7*, 637-644.

4. Campbell, J. A., Davies, G. J., Bulone, V., and Henrissat, B. (1997) *Biochem. J. 326*, 929-939.

5. Henrissat, B., Callebaut, I., Fabrega, S., Lehn, P., Mornon, J. P., and Davies, G. (1995) *Proc. Natl. Acad. Sci. USA 92*, 7090-7094.

6. Artymiuk, P. J., Rice, D. W., Poirrette, A. R., and Willett, P. (1995) *Struct. Biol. 2*, 117-120.

7. Koshland, D. E. (1953) *Biol. Rev. 28*, 416-436.

8. Davies, G., and Henrissat, B. (1995) *Structure 3*, 853-859.

9. Svensson, B. (1994) *Plant Mol. Biol. 25*, 141-157.

10. Jespersen, H. M., MacGregor, E. A., Henrissat, B., Sierks, M. R., and Svensson, B. (1993) *J. Prot. Chem. 12*, 791-805.

11. Withers, S. G., and Aebersold, R. (1995) *Protein Sci. 4*, 361-372.

12. McCarter, J. D., and Withers, S. G. (1994) *Curr. Opin. Struct. Biol. 4*, 885-892.

13. Wang, Q., Graham, R. W., Trimbur, D., Warren, R. A. J., and Withers, S. G. (1994) *J. Am. Chem. Soc. 116*, 11594-11595.

14. Legler, G., and Bause, E. (1973) *Carbohydr. Res. 28*, 45-52.

15. Hoj, P. B., Condron, R., Traeger, J. C., McAuliffe, J. C., and Stone, B. (1992) *J. Biol. Chem. 267*, 25059-25066.

16. Naider, F., Bohak, Z., and Yariv, J. (1972) *Biochemistry 11*, 3202-3207.

17. Black, T. S., Kiss, L., Tull, D., and Withers, S. G. (1993) *Carbohydr. Res. 250*, 195-202.

18. Keresztessy, Z., Kiss, L., and Hughes, M. A. (1994) *Arch. Biochem. Biophys. 315*, 323-330.

19. Shulman, M. L., Shiyan, S. D., and Khorlin, A. Y. (1976) *Biochim. Biophys. Acta. 445*, 169-181.

20. Tull, D., Burgoyne, D. L., Chow, D. T., Withers, S. G., and Aebersold, R. (1996) *Anal. Biochem. 234*, 119-125.

21. Bombard, S., Maillet, M., and Capmau, M. L. (1995) *Carbohydr. Res. 275*, 433-440.

22. Howard, S., and Withers, S. G. (1998) *Biochemistry 37*, 3858-3864.

23. Keitel, T., Simon, O., Borriss, R., and Heinemann, U. (1993) *Proc. Natl. Acad. Sci. USA 90*, 5287-5292.

24. MacLeod, A. M., Lindhorst, T., Withers, S. G., and Warren, R. A. J. (1994) *Biochemistry 33*, 6371-6376.

25. Wang, Q., Trimbur, D., Graham, R., Warren, R. A. J., and Withers, S. G. (1995) *Biochemistry 34*, 14554-14562.

26. Kempton, J. B., and Withers, S. G. (1992) *Biochemistry 31*, 9961-9969.

27. Tull, D., and Withers, S. G. (1994) *Biochemistry 33*, 6363-6370.

28. McIntosh, L. P., Hand, G., Johnson, P. E., Joshi, M. D., Korner, M., Plesniak, L. A., Ziser, L., Wakarchuk, W., and Withers, S. G. (1996) *Biochemistry 35*, 9958-9966.

29. Pauling, L. (1946) *Chem. Eng. News 24*, 1375-1377.

30. Street, I. P., Rupitz, K., and Withers, S. G. (1989) *Biochemistry 28*, 1581-1587.

31. Percival, M. D., and Withers, S. G. (1992) *Biochemistry 31*, 498-505.

32. Sierks, M. R., Bock, K., Refn, S., and Svensson, B. (1992) *Biochemistry 31*, 8972-8977.

33. McCarter, J. D., Adam, M. J., and Withers, S. G. (1992) *Biochem. J. 286*, 721-727.

34. Namchuk, M. N., and Withers, S. G. (1995) *Biochemistry 34*, 16194-16202.

35. Lienhard, G. E. (1973) *Science 180*, 149-154.

36. Wolfenden, R. (1976) *Annu. Rev. Biophys. Bioeng. 5*, 271-306.

37. Legler, G. (1990) *Adv. Carb. Chem. Biochem. 48*, 319-385.

38. Ganem, B., and Papandreou, G. (1991) *J. Am. Chem. Soc. 113*, 8984-8985.

39. Ermert, P., Vasella, A., Weber, M., Rupitz, K., and Withers, S. G. (1993) *Carbohydr. Res. 250*, 113-128.

40. Wong, C. H., Provencher, L., Porco, J. A., Jung, S. H., Wang, Y. F., Chen, L., Wang, R., and Steensma, D. H. (1995) *J. Org. Chem. 60*, 1492-1501.

41. Sinnott, M. L., and Souchard, I. J. (1973) *Biochem. J. 133*, 89-98.

42. Withers, S. G., MacLennan, D. J., and Street, I. P. (1986) *Carbohydr. Res. 154*, 127-144.

43. Konstantinidis, A., and Sinnott, M. L. (1991) *Biochem. J. 279*, 587-593.

44. Voet, J. G., and Abeles, R. H. (1970) *J. Biol. Chem. 245*, 1020-1031.

45. Mieyal, J. J., Simon, M., and Abeles, R. H. (1972) *J. Biol. Chem. 247*, 532-542.

46. Mooser, G., Hefta, S. A., Paxton, R. J., Shively, J. E., and Lee, T. D. (1991) *J. Biol. Chem. 266*, 8916-8922.

47. Mooser, G. (1992) in *The Enzymes* (Sigman, D. S., Ed.) pp 187-233, Academic Press Inc., New York.

48. Tao, B. Y., Reilly, P. J., and Robyt, J. F. (1989) *Biochim. Biophys. Acta 995*, 214-220.

49. Legler, G., Roeser, K. R., and Illig, H. K. (1979) *Eur. J. Biochem. 101*, 85-92.

50. Bause, E., and Legler, G. (1974) *Hoppe-Seyler's Z. Physiol. Chem. 355*, 438-442.

51. Roeser, K. R., and Legler, G. (1981) *Biochim. Biophys. Acta. 657*, 321-333.

52. Weber, J. P., and Fink, A. L. (1980) *J. Biol. Chem. 255*, 9030-9032.

53. Herrchen, M., and Legler, G. (1984) *Eur. J. Biochem. 138*, 527-531.

54. Gebler, J. C., Aebersold, R., and Withers, S. G. (1992) *J. Biol. Chem. 267*, 11126-11130.

55. Street, I. P., Kempton, J. B., and Withers, S. G. (1992) *Biochemistry 31*, 9970-9978.

56. Withers, S. G., Warren, R. A. J., Street, I. P., Rupitz, K., Kempton, J. B., and Aebersold, R. (1990) *J. Am. Chem. Soc. 112*, 5887-5889.

57. Miao, S., Ziser, L., Aebersold, R., and Withers, S. G. (1994) *Biochemistry 33*, 7027-7032.

58. MacKenzie, L. F., Brooke, G. S., Cutfield, J. F., Suillivan, P. A., and Withers, S. G. (1997) *J. Biol. Chem. 272*, 3161-3167.

59. Tull, D., Withers, S. G., Gilkes, N. G., Kilburn, D. G., Warren, R. A. J., and Aebersold, R. (1991) *J. Biol. Chem. 266*, 15621-15625.

60. Wang, Q., Tull, D., Meinke, A., Gilkes, N. R., Warren, R. A., Aebersold, R., and Withers, S. G. (1993) *J. Biol. Chem. 268*, 14096-14102.

61. MacKenzie, L. F., Davies, G. J., Schulein, M., and Withers, S. G. (1997) *Biochemistry 36*, 5893-5901.

62. Miao, S., McCarter, J. D., Grace, M. E., Grabowski, G. A., Aebersold, R., and Withers, S. G. (1994) *J. Biol. Chem. 269*, 10975-10978.

63. McCarter, J. D., Burgonye, D. L., Miao, S., Zhang, S., Callahan, J. W., and Withers, S. G. (1997) *J. Biol. Chem. 272*, 396-400.

64. He, S., and Withers, S. G. (1997) *J. Biol. Chem. 272*, 24864-24867.

65. Vocadlo, D., Mackenzie, L., He, S., Zeikus, G. J., and Withers, S. G. (1998) *Biochem. J. accepted.*

66. Withers, S. G., and Street, I. P. (1988) *J. Am. Chem. Soc. 110*, 8551-8553.

67. White, A., Tull, D., Johns, K., Withers, S. G., and Rose, D. R. (1996) *Nat. Struct. Biol. 3*, 149-154.

68. Braun, C. (1995) *PhD Thesis, University of British Columbia.*

69. Kajimoto, T., Liu, K. K., Pederson, R. L., Zhong, Z., Ichikawa, Y., Porco, J. A., and Wong, C. H. (1991) *J. Am. Chem. Soc. 113*, 6187-6196.

70. Winkler, D. A., and Holan, G. (1989) *J. Med. Chem. 32*, 2084-2089.

71. McCarter, J. D., and Withers, S. G. (1996) *J. Am. Chem. Soc. 118*, 241-242.

72. Howard, S., He, S., and Withers, S. G. (1998) *J. Biol. Chem. 273*, 2067-2072.

73. McCarter, J. D. (1995) *PhD Thesis, University of British Columbia.*

74. Braun, C., Brayer, G. D., and Withers, S. G. (1995) *J. Biol. Chem. 270*, 26778-26781.

75. Braun, C., Lindhorst, T., Madsen, N. B., and Withers, S. G. (1996) *Biochemistry 35*, 5458-5463.

76. Saenger, W. (1980) *Angew. Chem. Int. Ed. Engl. 19*, 344-362.

77. Bender, H. (1986) *Adv. Biotech. Proc. 6*, 31-71.

78. Lawson, C. L., van Montfort, R., Strokopytov, B., Rozeboom, H. J., Kalk, K. H., de Vries, G. E., Penninga, D., Dijkhuizen, L., and Dijkstra, B. W. (1994) *J. Mol. Biol. 236*, 590-600.

79. Strokopytov, B., Penninga, D., Rozeboom, H. J., Kalk, K. H., Dijkhuizen, L., and Dijkstra, B. W. (1995) *Biochemistry 34*, 2234-2240.

80. Qian, M., Haser, R., Buisson, G., Duee, E., and Payan, F. (1994) *Biochemistry 33*, 6284-6294.

81. Nakamura, A., Haga, K., and Yamane, K. (1993) *Biochemistry 32*, 6624-6631.

82. Knegtel, R. M., Strokopytov, B., Penninga, D., Faber, O. G., Rozeboom, H. J., Kalk, K. H., Dijkhuizen, L., and Dijkstra, B. W. (1995) *J. Biol. Chem. 270*, 29256-29264.

83. Strokopytov, B., Knegtel, R. M., Penninga, D., Rozeboom, H. J., Kalk, K. H., Dijkhuizen, L., and Dijkstra, B. W. (1996) *Biochemistry 35*, 4241-4249.

84. Buisson, G., Duee, E., Haser, R., and Payan, F. (1987) *EMBO J 6*, 3909-3916.

85. Larson, S. B., Greenwood, A., Cascio, D., Day, J., and McPherson, A. (1994) *J. Mol. Biol. 235*, 1560-1584.

86. Qian, M., Haser, R., and Payan, F. (1993) *J. Mol. Biol. 231*, 785-799.

87. Brayer, G. D., Luo, Y., and Withers, S. G. (1995) *Protein Sci. 4*, 1730-1742.

88. Cottaz, S., Apparu, C., and Driguez, H. (1991) *J. Chem. Soc. Perkin. Trans. I*, 2235-2241.

89. MacLeod, A., Tull, D., Rupitz, K., Warren, R. A. J., and Withers, S. G. (1996) *Biochemistry 35*, 13165-13172.

90. Penninga, D., Strokopytov, B., Rozeboom, H. J., Lawson, C. L., Dijkstra, B. W., Bergsma, J., and Dijkhuizen, L. (1995) *Biochemistry 34*, 3368-3376.

91. Penninga, D., van der Veen, B. A., Knegtel, R. M., van Hijum, S. A., Rozeboom, H. J., Kalk, K., Dijkstra, B., and Dijkhuizen, L. (1996) *J. Biol. Chem. 271*, 32777-32784.

92. Junnemann, J., Thiem, J., and Pedersen, C. (1993) *Carbohydr. Res. 249*, 91-94.

93. Lindhorst, T. K., Braun, C., and Withers, S. G. (1995) *Carbohydr. Res. 268*, 93-106.

94. Withers, S. G., Percival, M. D., and Street, I. P. (1989) *Carbohydr. Res. 187*, 43-66.

95. Lawson, S. L., Wakarchuk, W. W., and Withers, S. G. (1997) *Biochemistry 36*, 2257-2265.

96. Klein, C., Hollender, J., Bender, H., and Schulz, G. E. (1992) *Biochemistry 31*, 8740-8746.

97. Davies, G. J. (1997) *Biochem. J. 321*, 557-559.

98. White, A., and Rose, D. R. (1997) *Curr. Opin. Struct. Biol. 7*, 645-651.

99. Deslongchamps, P. (1983) *Stereoelectronic Effects in Organic Chemistry*, Pergamon Press, Oxford.

100. Sinnott, M. L. (1990) *Chem. Rev. 90*, 1171-1202.

101. Tews, I., Perrakis, A., Oppenheim, A., Dauter, Z., Wilson, K. S., and Vorgias, C. E. (1996) *Nat. Struct. Biol. 3*, 638-648.

102. Sulzenbacher, G., Driguez, H., Henrissat, B., Schulein, M., and Davies, G. J. (1996) *Biochemistry 35*, 15280-15287.

103. Braun, C., Meinke, A., Ziser, L., and Withers, S. G. (1993) *Anal. Biochem. 212*, 259-262.

104. Borhan, B., Jones, A. D., Pinot, F., Grant, D., Kurth, M. J., and Hammock, B. D. (1995) *J. Biol. Chem. 270*, 26923-26930.

105. Verschueren, K. H., Seljee, F., Rozeboom, H. J., Kalk, K., and Dijkstra, B. W. (1993) *Nature 363*, 693-698.

106. Yang, G., Liang, P., and Dunaway-Mariano, D. (1994) *Biochemistry 33*, 8527-8531.

107. Schanstra, J., Ridder, I. S., Heimeriks, G. J., Rink, R., Poelarends, G. J., Kalk, K., Dijkstra, B. W., and Janssen, D. (1996) *Biochemistry 35*, 13186-13195.

108. Taylor, K., Liu, R., Liang, P., Price, J., Dunaway-Mariano, D., Tonge, P., Clarkson, J., and Carey, P. (1995) *Biochemistry 34*, 13881-13888.

109. Crooks, G., Xu, L., Barkley, R., and Copley, S. (1995) *J. Am. Chem. Soc. 117*, 10791-10798.

110. Liu, R., Liang, P., Scholten, J., and Dunaway-Mariano, D. (1995) *J. Am. Chem. Soc. 117*, 5003-5004.

111. Benning, M. M., Taylor, K. L., Liu, R. Q., Yang, G., Xiang, H., Wesenberg, G., Dunaway-Mariano, D., and Holden, H. M. (1996) *Biochemistry 35*, 8103-8109.

112. Franken, S. M., Rozeboom, H. J., Kalk, K. H., and Dijkstra, B. W. (1991) *EMBO J. 10*, 1297-1302.

113. Nakamura, A., Haga, K., Ogawa, S., Kuwano, K., Kimura, K., and Yamane, K. (1992) *FEBS 296*, 37-40.

114. Takase, K., Matsumoto, T., Mizuno, H., and Yamane, K. (1992) *Biochim. Biophys. Acta 1120*, 281-288.

115. Huber, R., and Chivers, P. (1993) *Carbohydr. Res. 250*, 9-18.

116. Mosi, R., He, S., Uitdehaag, J., Dijkstra, B., and Withers, S. G. (1997) *Biochemistry 36*, 9927-9934.

117. Mader, M. M., and Bartlett, P. A. (1997) *Chem. Rev. 97*, 1281-1301.

118. Bartlett, P. A., and Marlowe, C. K. (1983) *Biochemistry 22*, 4618-4624.

119. Hanson, J. E., Kaplan, A. P., and Bartlett, P. A. (1989) *Biochemistry 28*, 6294-6305.

120. Namchuk, M. (1993) *Ph. D. Thesis, University of British Columbia.*

121. Phillips, M. A., Kaplan, A. P., Rutter, W. J., and Bartlett, P. A. (1992) *Biochemistry 31*, 959-963.

122. Berland, C. R., Sigurskjold, B. W., Stoffer, B., Frandsen, T. P., and Svensson, B. (1995) *Biochemistry 34*, 10153-10164.

123. Wilcox, E. R., and Whitaker, R. J. (1984) *Biochemistry 23*, 1783-1791.

124. Svensson, B., and Sierks, M. R. (1992) *Carbohydr. Res. 227*, 29-44.

125. Baliga, B. S., and Fonseca, V. A. (1997) *American Family Physician 55*, 817-824.

126. Scheen, A. J. (1997) *Drugs 54*, 355-368.

127. Yee, H. S., and Fong, N. T. (1996) *Pharmacotherapy 16*, 792-805.

128. Aleshin, A. E., Firsov, L. M., and Honzatko, R. B. (1994) *J. Biol. Chem. 269*, 15631-15639.

129. Brzozowski, A. M., and Davies, G. J. (1997) *Biochemistry 36*, 10837-10845.

130. Wind, R. D., Uitdehaag, J. C., Buitelaar, R., Dijkstra, B. W., and Dijkhuizen, L. (1998) *J. Biol. Chem. 273*, 5771-5779.

131. Tanaka, Y., Tao, W., Blanchard, J. S., and Hehre, E. J. (1994) *J. Biol. Chem. 269*, 32306-32312.

132. Cori, C. F., and Cori, G. T. (1936) *Proc. Soc. Exp. Biol. Med. 34*, 702-705.

133. Nakano, K., Kikumoto, Y., and Fukui, T. (1984) in *Chemical and Biological Aspects of Vitamin B_6 Catalysis: Part A* (Evangelopopoulous, A. E. Ed.) pp 171-180, Alan R. Liss, Inc., New York.

134. Fukui, T., Shinomura, S., and Nakano, K. (1982) *Mol. Cell. Biochem. 42*, 129-144.

135. Acharya, K. R., Stuart, D. I., Varvill, K. M., and Johnson, L. N. (1991) *Glycogen Phosphorylase b: Description of the Protein Structure*, World Scientific Publishing, Singapore.

136. Sprang, S., Acharya, K. R., Goldsmith, E. J., Stuart, D. I., Varvill, K. M., Fletterick, R. J., Madsen, N. B., and Johnson, L. N. (1988) *Nature 336*, 215-221.

137. Barford, D., and Johnson, L. N. (1989) *Nature 340*, 609-616.

138. Sprang, S., Withers, S. G., Goldsmith, E. J., Fletterick, R. J., and Madsen, N. B. (1991) *Science 254*, 1367-1371.

139. Barford, D., Hu, S. H., and Johnson, L. N. (1991) *J. Mol. Biol. 218*, 233-260.

140. Johnson, L. N. (1992) *FASEB J. 6*, 2274-2282.

141. Oikonomakos, N. G., Acharya, K. R., and Johnson, L. N. (1991) in *Post Translational Modification of Proteins* (Crabbe, J. and Harding, J. Eds.) pp 82-151, CRC Press, Boca Raton, Florida.

142. Johnson, L. N., Barford, D., Acharya, R., Oikonomakos, N. G., and Martin, J. L. (1992) *Chapter 2: Allosteric Regulation of Glycogen Phosphorylase* pp 17-35, Robert A. Welch Foundation, Houston, Texas.

143. Hecht, H. J., Jahnke, K., and Buhner, M. (1984) *Collected Abstracts of the 13th International Congress of Crystallography, Aug. 9-18, Hamburg Abstract 01.3-2.*

144. McLaughlin, P. J., Stuart, D. I., Klein, H. W., Oikonomakos, N. G., and Johnson, L. N. (1984) *Biochemistry 23*, 5862-5873.

145. Withers, S. G., and Rupitz, K. (1990) *Biochemistry 29*, 6405-6409.

146. Klein, H. W., Im, M. J., and Palm, D. (1986) *Eur. J. Biochem. 157*, 107-114.

147. Tu, J.-I., Jacobson, G. R., and Graves, D. J. (1971) *Biochemistry 10*, 1229-1236.

148. Firsov, L. M., Bogacheva, T. I., and Bresler, S. E. (1974) *Eur. J. Biochem 42*, 605-609.

149. Gold, A. M., Legrand, E., and Sanchez, G. R. (1971) *J. Biol. Chem. 246*, 5700-5706.

150. Mitchell, E. P., Withers, S. G., Ermert, P., Vasella, A. T., Garman, E. F., Oikonomakos, N. G., and Johnson, L. N. (1996) *Biochemistry 35*, 7341-7355.

151. Illingworth, B., Jansz, H. S., Brown, D. H., and Cori, C. F. (1958) *Proc. Natl. Acad. Sci. USA 44*, 1180-1191.

152. Madsen, N. B., and Withers, S. G. (1986) in *Vitamin B6 Pyridoxal Phosphate: Chemical, Biochemical, and Medical Aspects, Part B* (Dolphin, D., Poulson, R., Avramovic, O., Eds.) pp 335-389, John Wiley & Sons, New York.

153. Helmreich, E. J. M. (1992) *BioFactors 3*, 159-172.

154. Palm, D., Klein, H. W., Schinzel, R., Buehner, M., and Helmreich, E. J. M. (1990) *Biochemistry 29*, 1099-1107.

155. Klein, H. W., Palm, D., and Helmreich, E. J. M. (1982) *Biochemistry 21*, 6675-6684.

156. Klein, H. W., Im, M. J., Palm, D., and Helmreich, E. J. M. (1984) *Biochemistry 23*, 5853-5861.

157. Parrish, R. F., Uhing, R. J., and Graves, D. J. (1977) *Biochemistry 16*, 4824-4831.

158. Withers, S. G., Shechosky, S., and Madsen, N. B. (1982) *Biochem. Biophys. Res. Comm. 108*, 322-328.

159. Oikonomakos, N. G., Zographos, S. E., Tsitsanou, K. E., Johnson, L. N., and Acharya, K. R. (1996) *Protein Sci. 5*, 2416-2428.

160. Stirtan, W. G., and Withers, S. G. (1996) *Biochemistry 35*, 15057-15064.

161. Oikonomakos, N. G., Johnson, L. N., Acharya, K. R., Stuart, D. I., Barford, D., Hadju, J., Varvill, K. M., Melpidou, A. E., Papageorgiou, T., Graves, D. J., and Palm, D. (1987) *Biochemistry 26*, 8381-8389.

162. Madsen, N. B., and Withers, S. G. (1984) in *Chemical and Biological Aspects of Vitamin B_6 Catalysis, Part A* (Evangelopopoulous, A. E. Ed.) pp. 117-126, Alan R. Liss, New York.

163. Chang, Y. C., McCalmont, T., and Graves, D. J. (1983) *Biochemistry 22*, 4987-4993.

164. Engers, H. D., Bridger, W. A., and Madsen, N. B. (1969) *J. Biol. Chem. 244*, 5936-5942.

165. Engers, H. D., Bridger, W. A., and Madsen, N. B. (1970) *Can. J. Biochem. 48*, 755-758.

166. Engers, H. D., Shechosky, S., and Madsen, N. B. (1970) *Can. J. Biochem. 48*, 746-754.

167. Kokesh, F. C., and Kakuda, Y. (1977) *Biochemistry 16*, 2467-2473.

168. Withers, S. G. (1990) *Carbohydr. Res. 196*, 61-73.

169. Smith, E. E. (1971) *Arch. Biochem. Biophys. 146*, 380-390.

170. Kasvinsky, P. J., Madsen, N. B., Fletterick, R. J., and Sygusch, J. (1978) *J. Biol. Chem. 253*, 1290-1296.

171. Takrama, J., and Madsen, N. B. (1988) *Biochemistry 27*, 3308-3314.

172. Tabata, S., and Dohi, Y. (1992) *Carbohydr. Res. 230*, 179-183.

173. Haldane, J. B. S. (1930) *Enzymes,* Longmans, Green & Co., London, U.K.

174. Jencks, W. P. (1987) *Catalysis in Chemistry and Enzymology*, Dover Publications Inc., Mineola, New York.

175. O'Reilly, M., Watson, K., Schinzel, R., Palm, D., and Johnson, L. N. (1997) *Nat. Struct. Biol. 4*, 405-412.

176. Raushel, F. M., and Villafranca, J. J. (1988) *Crit. Rev. Biochem. 23*, 1-26.

177. Morgan, P. M., Sala, R. F., and Tanner, M. E. (1997) *J. Am. Chem. Soc. 119*, 10269-10277.

178. Singh, A. N., Hester, L. S., and Raushel, F. M. (1987) *J. Biol. Chem. 262*, 2554-2557.

179. Midelfort, C. F., and Rose, I. A. (1976) *J. Biol. Chem. 251*, 5881-5587.

180. Hester, L. S., and Raushel, F. M. (1987) *Biochemistry 26*, 6465-6471.

181. Cohn, M., and Hu, A. (1978) *Proc. Natl. Acad. Sci. USA 75*, 200-203.

182. Kokesh, F. C., and Kakuda, Y. (1977) *Can. J. Biochem. 55*, 548-554.

183. Sabesan, S., and Neira, S. (1992) *Carbohydr. Res. 223*, 169-185.

184. Street, I. P. (1988) *Ph.D. Thesis, University of British Columbia.*

185. Staerk, J., and Schlenk, H. (1967) *Biochim. Biophys. Acta. 146*, 120-128.

186. Avramovic-Zikic, O., Breindenbach, W. C., and Madsen, N. B. (1974) *Can. J. Biochem. 52*, 146-148.

187. Battell, M. L., Zarkadas, C. G., Smillie, L. B., and Madsen, N. B. (1968) *J. Biol. Chem. 243*, 6202-6209.

188. Takagi, S., Kobayashi, M., and Matsuda, K. (1989) *J. Biochem. 105*, 933-938.

189. Dreyfus, M., Vandenbunder, B., and Buc, H. (1980) *Biochemistry 19*, 3634-3642.

190. Ariki, M., and Fukui, T. (1975) *J. Biochem. 78*, 1191-1199.

191. Palm, D., Blumenauer, G., Klein, H. W., and Blanc-Muesser, M. (1983) *Biochem. Biophys. Res. Comm. 111*, 530-536.

192. Knapp, S., Purandare, A., Rupitz, K., and Withers, S. G. (1994) *J. Am. Chem. Soc. 116*, 7461-7462.

193. Hu, H. Y., and Gold, A. M. (1975) *Biochemistry 14*, 2224-2230.

194. Wolfrom, M. L. and Thompson, A. (1963) in *Methods in Carbohydrate Chemistry, Vol. II* (Whistler, R. L., and Wolfrom, M. L., Eds.) pp 211-215, Academic Press, New York.

195. Leatherbarrow, R. J. (1994) *Gra-Fit, Version 3.0, Erithacus Software Ltd.*, London, U.K.

196. Ashwell, G. (1957) *Methods Enzymol. 3*, 73-105.

197. Fischer, E. H., and Krebs, E. G. (1962) *Methods Enzymol. 5*, 369-373.

198. Kamogawa, A., Fukui, T., and Nikuni, Z. (1968) *J. Biochem. 63*, 361-369.

199. Takrama, J., and Madsen, N. B. (1988) *Biochemistry 27*, 3308-3314.

200. Liu, W., Madsen, N. B., Braun, C., and Withers, S. G. (1991) *Biochemistry 30*, 1419-1424.

201. Braun, C., and Withers, S. G. (1995) *Carbohydr. Res. 271*, 113-118.

202. Suganuma, T., Kitazono, J. I., Yoshinaga, K., Fujimoto, S., and Nagahama, T. (1991) *Carbohydr. Res. 217*, 213-220.

203. Konermann, L., Collings, B. A., and Douglas, D. J. (1997) *Biochemistry 36*, 5554-5559.

204. Zechel, D. L., Konermann, L., Withers, S. G., and Douglas, D. J. (1998) *Biochemistry 37*, 7664-7669.

205. Motawia, M. S., Olsen, C. E., Enevoldsen, K., Marcussen, J., and Moller, B. L. (1995) *Carbohydr. Res. 277*, 109-123.

206. Bock, K. (1987) *Pure & Applied Chemistry 59*, 1447-1456.

APPENDIX A

ENZYME KINETICS

A-1 FUNDAMENTAL EQUATIONS OF ENZYME KINETICS

In 1913, Michaelis and Menten proposed a simple model to account for the relationship between the rate of catalysis and the concentration of substrate. Later, Briggs and Haldane (1925) expanded on this by introducing the concept of the steady state. The general scheme for an enzyme catalyzed reaction is shown below. Free enzyme, E, combines with free substrate, S, to form an enzyme-substrate complex, ES, which is then turned over to yield product, P.

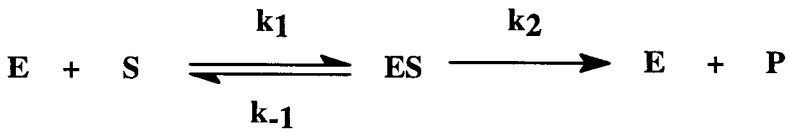

Under steady state conditions,

$$\frac{d[ES]}{dt} = k_1[E][S] - k_{-1}[ES] - k_2[ES] = 0 \qquad (1)$$

The total concentration of enzyme $[E]_o$, is equal to the concentration of free enzyme [E], plus the concentration of the enzyme bound in the ES complex, [ES].

$$[E]_o = [E] + [ES] \qquad (2)$$

Solving for ES using equations 1 and 2,

$$[ES] = \frac{[E]_o[S]}{[S] + (k_{-1} + k_2) / k_1} \qquad (3)$$

Assuming that the formation of products is the rate limiting step (k_2), the initial velocity of the reaction, v, is equal to the rate of formation of product,

$$v = \frac{dP}{dt} = k_2[ES] \qquad (4)$$

By substituting the expression for [ES] from equation 3 into equation 4, one obtains

$$v = \frac{k_2[E]_o[S]}{\left(\frac{k_{-1} + k_2}{k_1}\right) + [S]} \qquad (5)$$

The ratio of rate constants $(k_{-1}+k_2)/k_1$ is defined as K_m, the Michaelis constant.

The rate constant, k_2 is defined as the catalytic constant or k_{cat} (the turnover number).

Therefore equation 5 can be expressed in a more general format, also known as the Michaelis Menten equation,

$$v = \frac{k_{cat}[E]_o[S]}{K_m + [S]} \qquad (6)$$

Therefore when the initial rate of the reaction is equal to one-half the maximal velocity ($v=V_{max}/2$), the substrate concentration is equal to K_m. In its simplest form, the Michaelis constant is a measure of the binding affinity of an enzyme for a particular substrate. An enzyme with a high binding affinity for a substrate has a low value of K_m.

A graphical representation of the Michaelis Menten equation is given below (Figure A-1). It can also be plotted as a reciprocal plot (1/v vs 1/[S]), also known as the Lineweaver-Burke plot (Figure A-2).

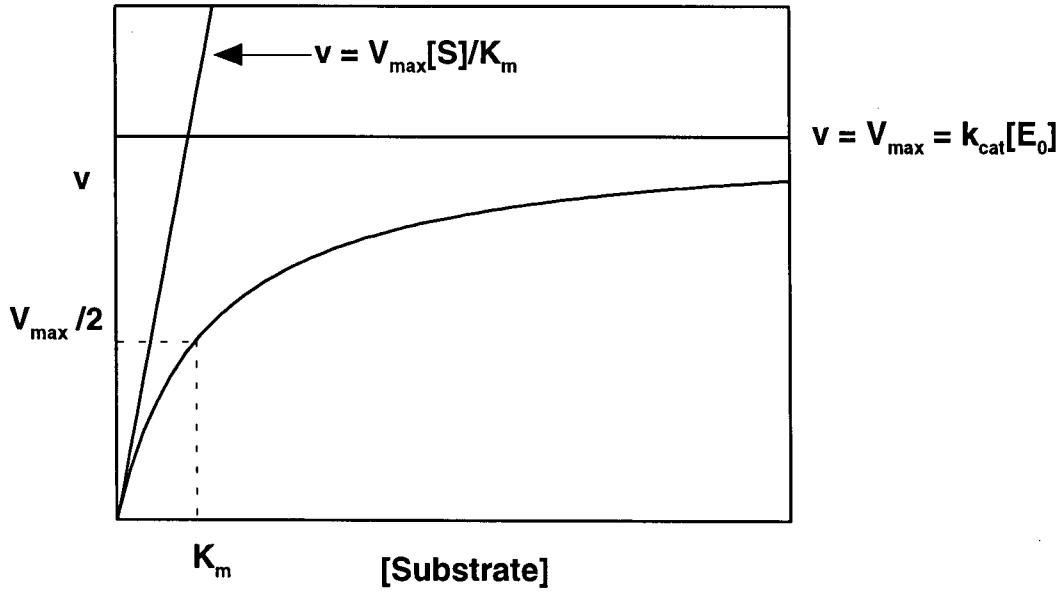

Figure A-1 A typical Michaelis-Menten plot for the determination of K_m and V_{max}

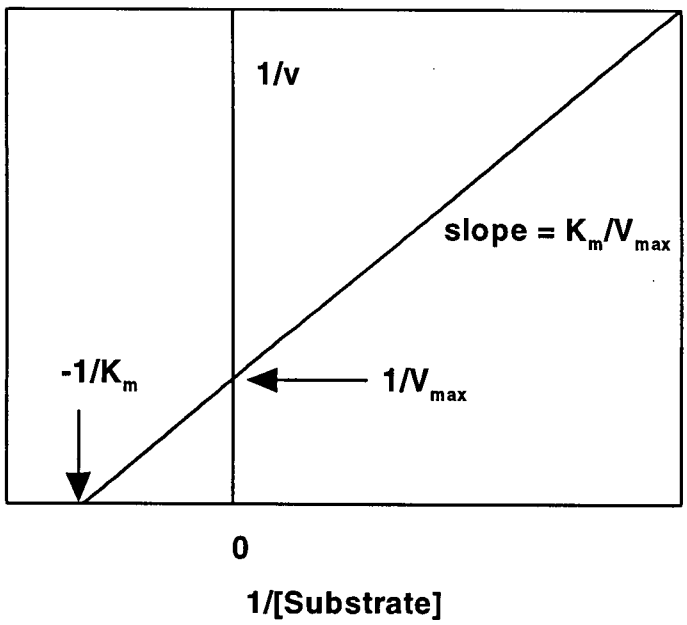

Figure A-2 A typical Lineweaver-Burke plot for the determination of K_m and V_{max}

At high substrate concentrations ([S] >> K_m), v approaches its maximal value, V_{max}, and the rate becomes independent of substrate concentration. Thus, the Michaelis Menten equation can be rewritten in the form,

$$V_{max} = k_{cat}[E]_o \qquad (7)$$

At low concentrations of substrate ([S]<< K_m), the initial rate of the reaction is proportional to the substrate concentration,

$$v = \frac{k_{cat}[E]_o[S]}{Km} \qquad (8)$$

The Michaelis Menten approach can be expanded to more complex enzyme systems in which two or more distinct reaction steps occur. Such is the case for the double displacement mechanism followed by retaining α-glycosyl transferases (see Section 1.3). The reaction scheme for this mechanism is as follows. Free enzyme, E, combines with free substrate, S, to form an enzyme-substrate complex, ES, with a rate constant, k_1 (association step). The conversion of ES to EP is termed the glycosylation step (k_2) and the turnover of EP to P is the deglycosylation step (k_3).

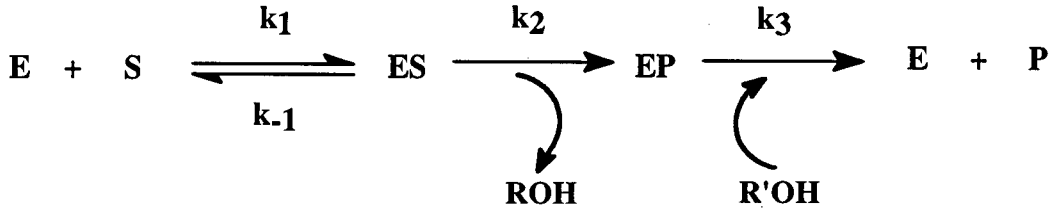

Assuming that a steady state concentration of both EP and ES is reached,

$$k_2[ES] = k_3[EP] \tag{9}$$

$$\frac{d[ES]}{dt} = k_1[E][S]-k_{-1}[ES]-k_2[ES] = 0 \tag{10}$$

The total concentration of enzyme $[E]_o$ is equal to free enzyme plus all of the enzyme bound species,

$$[E]_o = [E] + [ES] + [EP] \tag{11}$$

By substituting for [EP] using equation 9, one obtains,

$$[E]_o = [E] + [ES] + \frac{k_2}{k_3}[ES] \tag{12}$$

By solving equation 12 for [E] and substituting for [E] into equation 10, followed by a rearrangement,

$$[ES] = \frac{k_1[E]_o[S]}{k_{-1} + k_2 + \frac{k_1(k_2 + k_3)}{k_3}[S]} \tag{13}$$

At steady state, the rate of product formation is equal to

$$\frac{dP}{dt} = k_3[EP] = k_2[ES] \tag{14}$$

Substituting equation 13 into equation 14, yields an expression in the form of the Michaelis Menten equation.

$$v = \frac{\frac{k_2k_3}{k_2 + k_3}[E]_o[S]}{\frac{k_3}{k_2 + k_3}\frac{k_{-1} + k_2}{k_1} + [S]} \qquad (15)$$

From the form of the Michaelis Menten equation,

$$k_{cat} = \frac{k_2k_3}{k_2 + k_3} \qquad (16)$$

$$K_m = \left(\frac{k_3}{k_2 + k_3}\right)\left(\frac{k_{-1} + k_2}{k_1}\right) \qquad (17)$$

Therefore, it becomes evident that the values obtained experimentally for k_{cat} and K_m are composed of the values of the individual rate constants.

A-2 ENZYME KINETICS IN THE PRESENCE OF A REVERSIBLE INHIBITOR

There are three main types of reversible inhibition, competitive, noncompetitive and uncompetitive.

i. Competitive inhibition

A competitive inhibitor competes directly with the substrate for binding to the active site of the enzyme. The simple enzyme-catalyzed reaction must be expanded to include a second equilibrium,

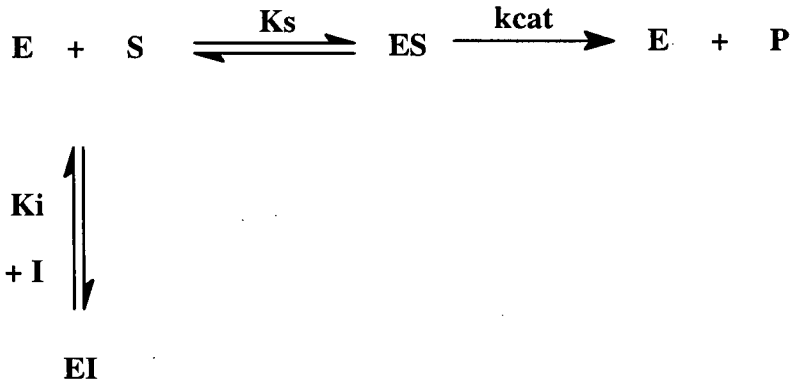

K_s is the dissociation constant of the enzyme-substrate complex (K_s = [E][S]/[ES]). K_i is the dissociation constant for the enzyme-inhibitor complex (K_i = [E][I]/[EI]).

The total concentration of enzyme is now equal to

$$[E]_o = [E] + [ES] + [EI] \qquad (18)$$

Using the steady state approach (d[ES]/dt = 0) and substituting into the Michaelis Menten equation 6,

$$v = \frac{V_{max}[S]}{K_m\left(1+\frac{[I]}{K_i}\right)+[S]} \qquad (19)$$

Therefore, a competitive inhibitor increases the apparent K_m by a factor of 1 + [I]/K_i. The value of V_{max} is unaffected as at high concentrations of substrate, the inhibitor is displaced from the enzyme.

b. Noncompetitive inhibition

Noncompetitive inhibition occurs when the inhibitor and substrate can bind simultaneously to the enzyme instead of competing for the same binding site.

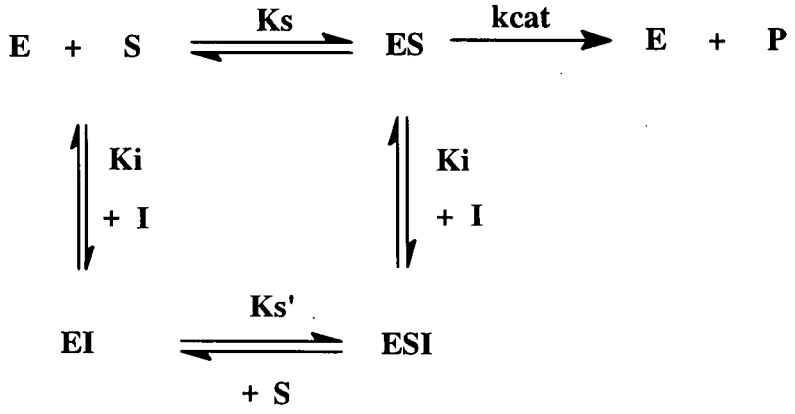

$$[E]_o = [E] + [ES] + [EI] + [ESI] \qquad (20)$$

When the dissociation constant of S from ESI is the same as that from ES ($K_s = K_s'$) and by incorporating this expression into the steady state assumption for the concentration of [ES] and the expression $v = k_2[ES]$, one obtains

$$v = \frac{\left(\dfrac{V_{max}}{1 + \dfrac{[I]}{K_i}}\right)[S]}{K_m + [S]} \qquad (21)$$

A noncompetitive inhibitor does not change the value of K_m. However, the value of V_{max} is decreased by a value of $(1 + [I]/K_i)$.

c. Uncompetitive inhibition

An uncompetitive inhibitor binds only to the enzyme-substrate complex.

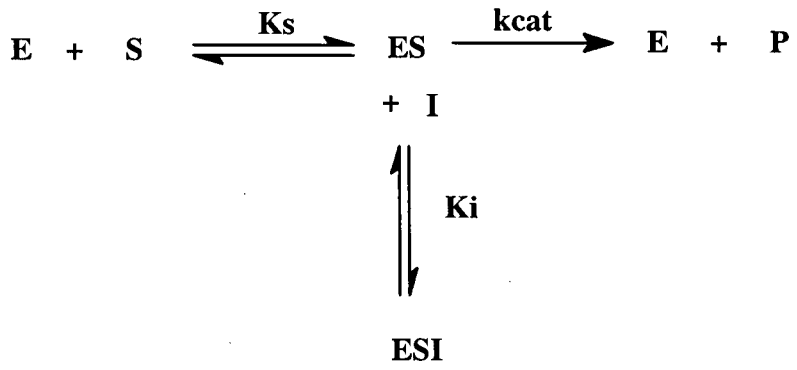

$$[E]_o = [E] + [ES] + [ESI] \qquad (22)$$

Again, using the steady state approximation of $d[ES]/dt = 0$ and $v = k_2[ES]$, one obtains

$$v = \frac{\left(\frac{V_{max}}{1+\frac{[I]}{K_i}}\right)[S]}{\left(\frac{Km}{1+\frac{[I]}{K_i}}\right)+[S]} \qquad (23)$$

An uncompetitive inhibitor decreases the value of both the apparent V_{max} and the apparent K_m by a factor of $(1 + [I]/K_i)$.

The three types of reversible inhibition can be distinguished graphically using a Lineweaver-Burke plot. These are shown in Figure A-3.

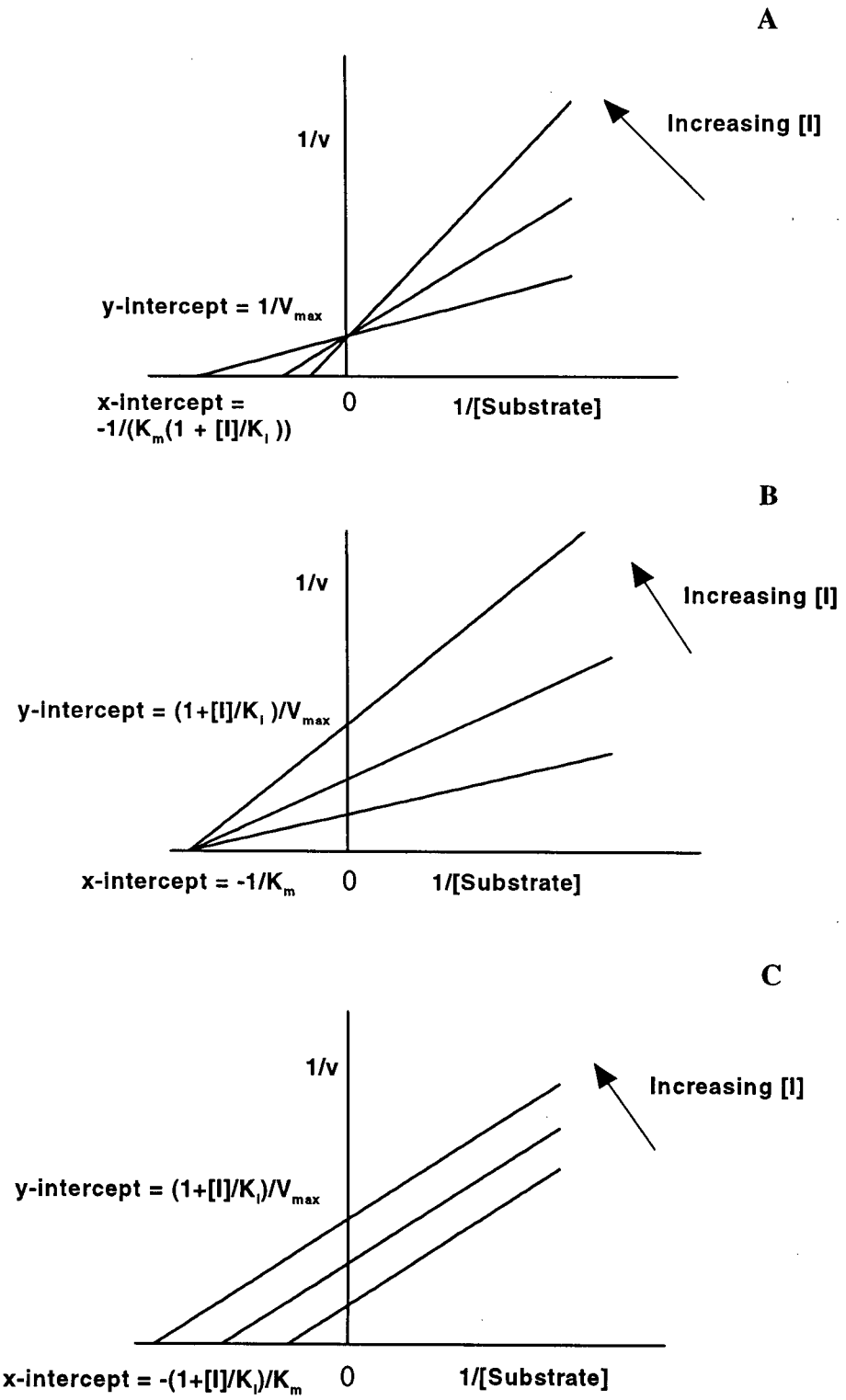

Figure A-3 Graphical representation for the determination of the modes of inhibition with a Lineweaver-Burke plot. (A) Competitive Inhibition, (B) Noncompetitive Inhibition, (C) Uncompetitive Inhibition.

APPENDIX B

GRAPHICAL REPRESENTATION OF KINETIC DATA

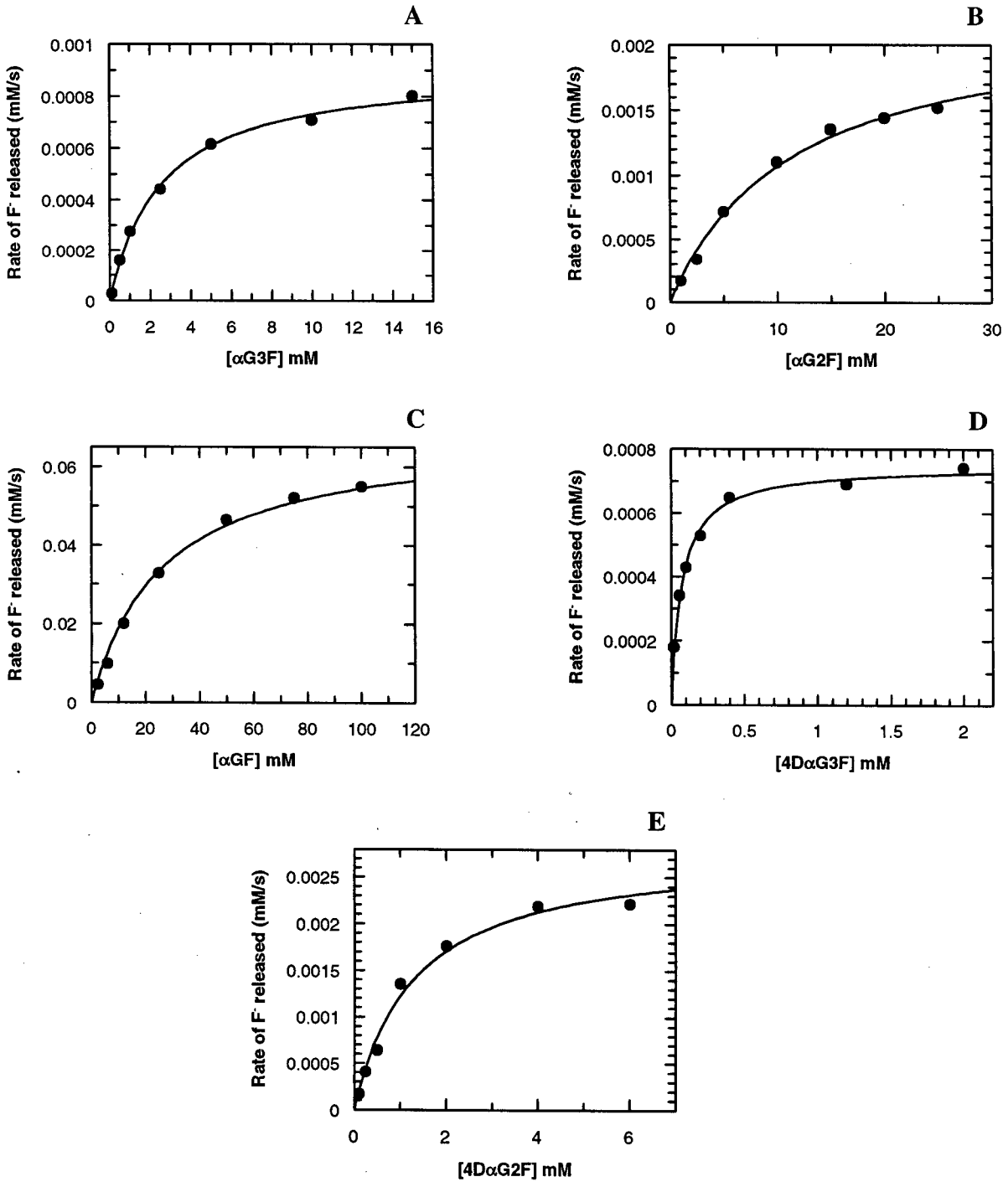

Figure B-1 The Michaelis Menten plots for the reaction of wt CGTase with glycosyl fluorides. **(A)** αG3F + CGTase (0.0033 μM), **(B)** αG2F + CGTase (0.0074 μM), **(C)** αGF + CGTase (0.223 μM), **(D)** 4DαG3F + CGTase (0.35 μM), **(E)** 4DαG2F + CGTase (0.32 μM).

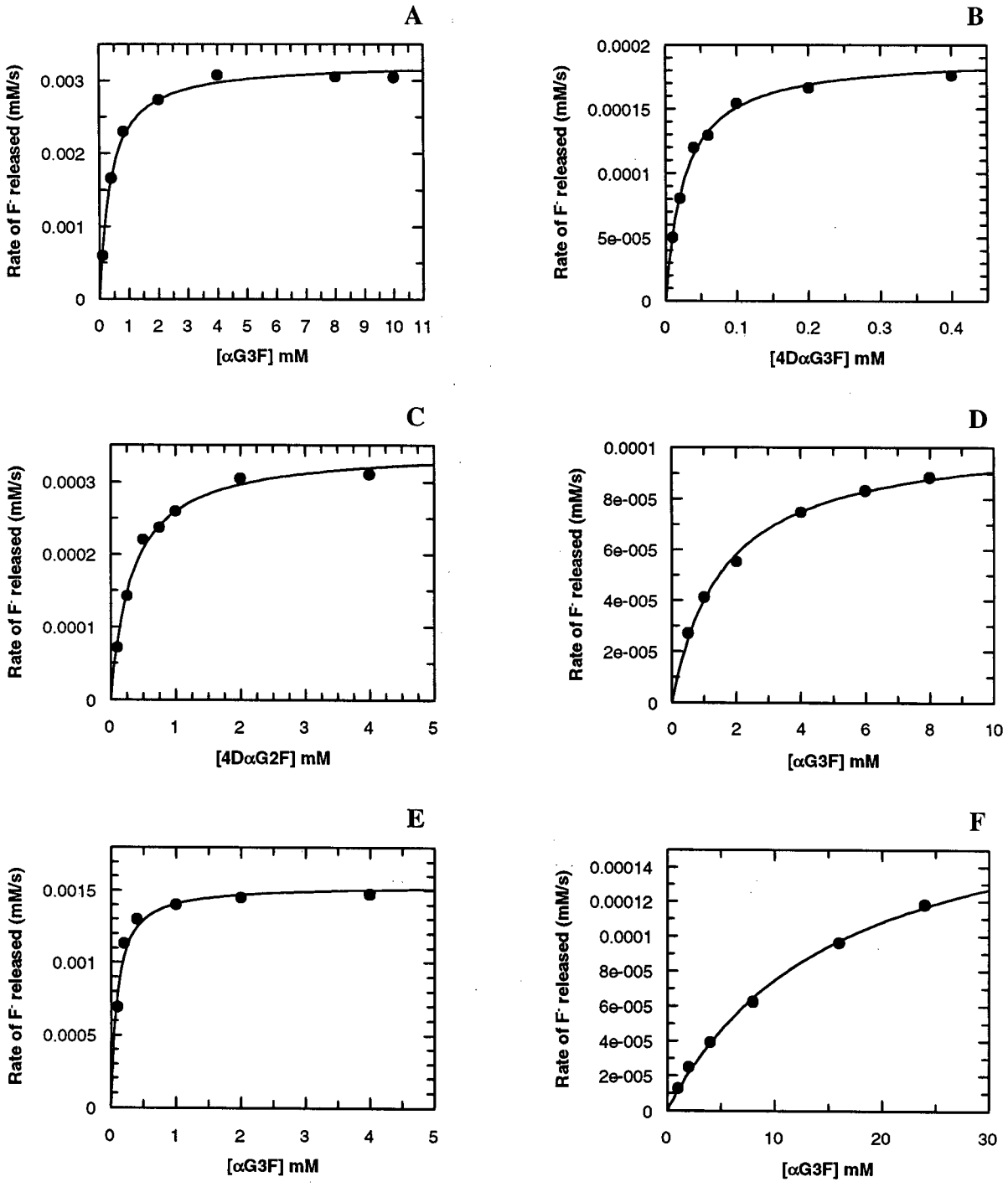

Figure B-2 The Michaelis Menten plots for the reaction of CGTase mutants with glycosyl fluorides. **(A)** αG3F + E257Q (3.13 μM), **(B)** 4DαG3F + E257Q (0.32 μM), **(C)** 4DαG2F + E257Q (0.32 μM), **(D)** αG3F + E257A (0.93 μM), **(E)** αG3F + D229N (0.66 μM), **(F)** αG3F + D229A (2.45 μM).

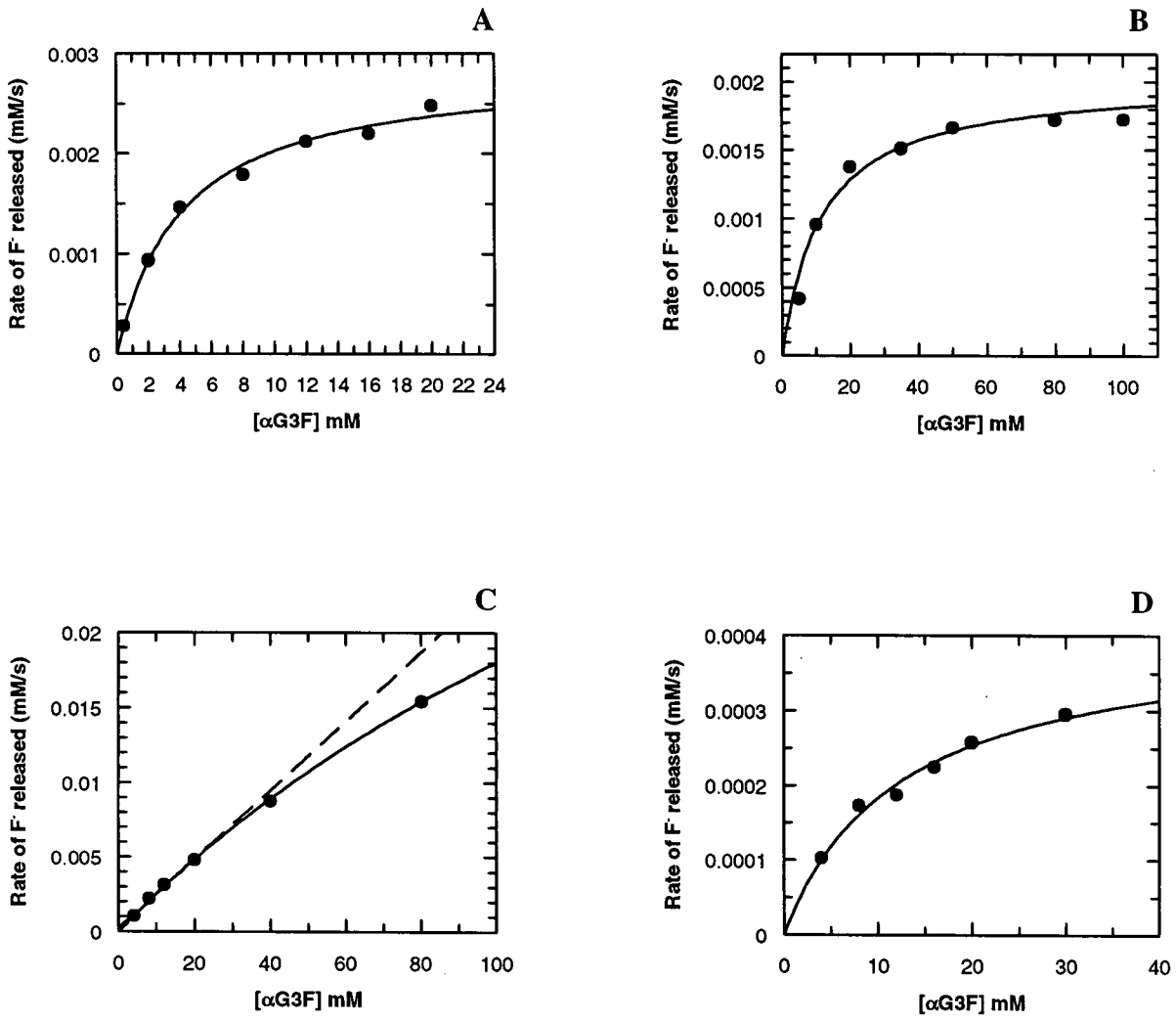

Figure B-3 The Michaelis Menten plots for the reaction of CGTase mutants with αG3F. **(A)** Y195F (0.0143 μM), **(B)** Y195L (0.0143 μM), **(C)** Y195G (0.043 μM), **(D)** N326Q (0.043 μM).

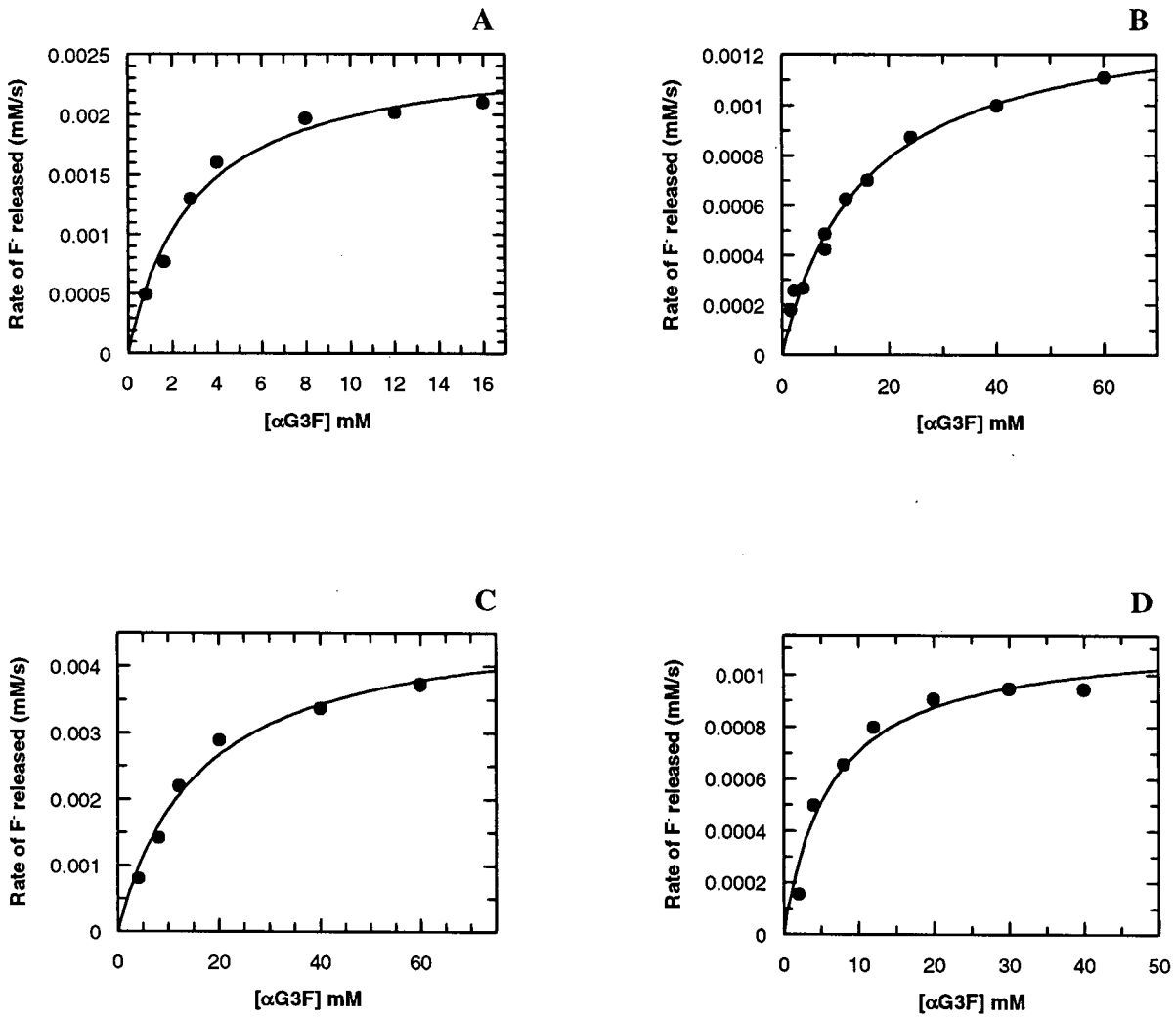

Figure B-4 The Michaelis Menten plots for the reaction of CGTase mutants and αG3F. **(A)** S145E (0.01467 μM), **(B)** S146P (0.178 μM), **(C)** D371N (0.0223 μM), **(D)** N193G (0.0199 μM).

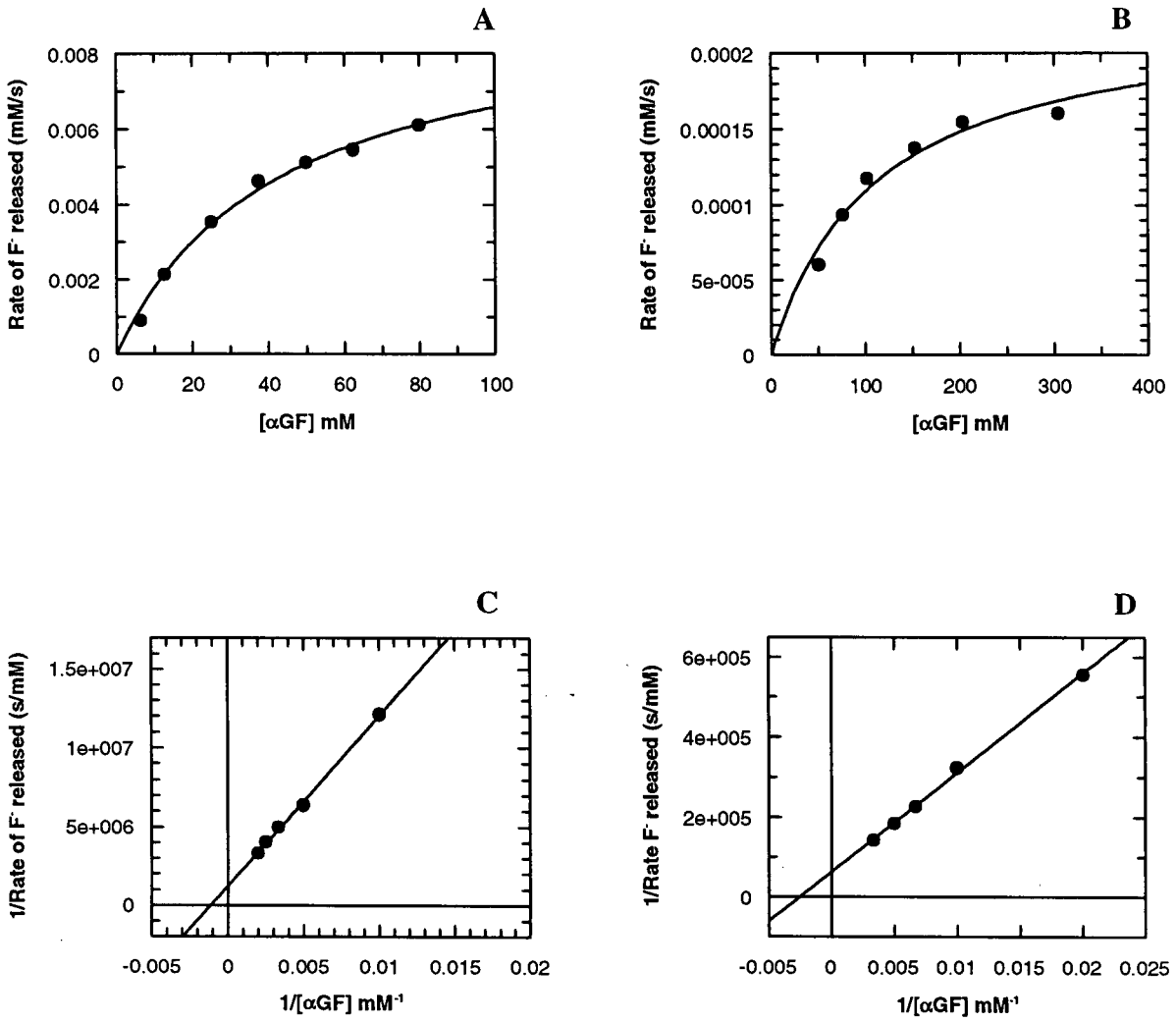

Figure B-5 The Michaelis Menten/Lineweaver Burke plots for the reaction of CGTase mutants with αGF. **(A)** Y195F (0.22 μM), **(B)** Y195L (0.375 μM), **(C)** Y195G (3.68 μM), **(D)** N326Q (3.39 μM). (Note: C & D are plotted in the form of Lineweaver Burke plots as saturation was not achieved).

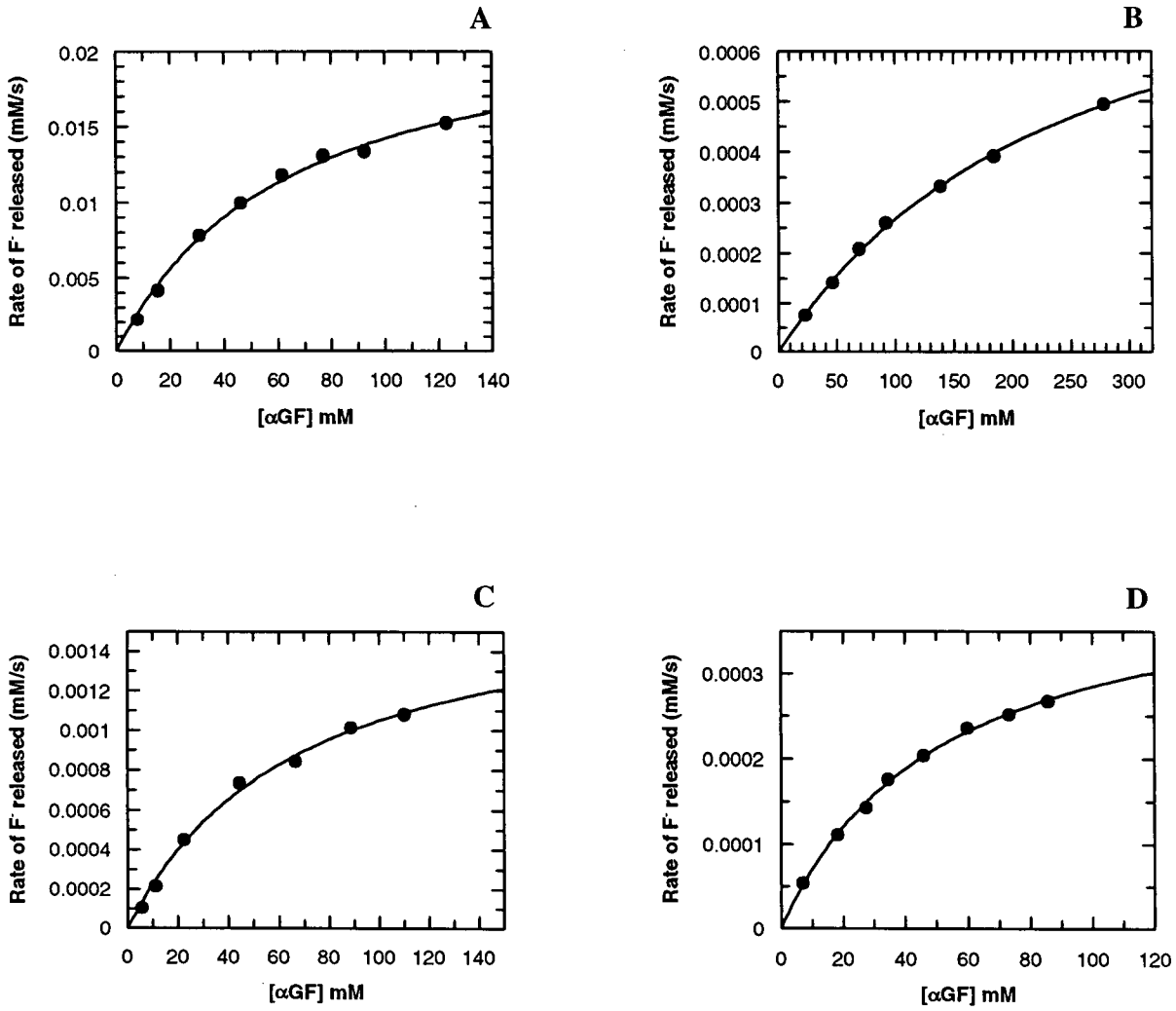

Figure B-6 The Michaelis Menten plots for the reaction of CGTase mutants with αGF. **(A)** S145E (0.257 μM), **(B)** S146P (5.55 μM), **(C)** D371N (1.30 μM), **(D)** N193G (0.867 μM).

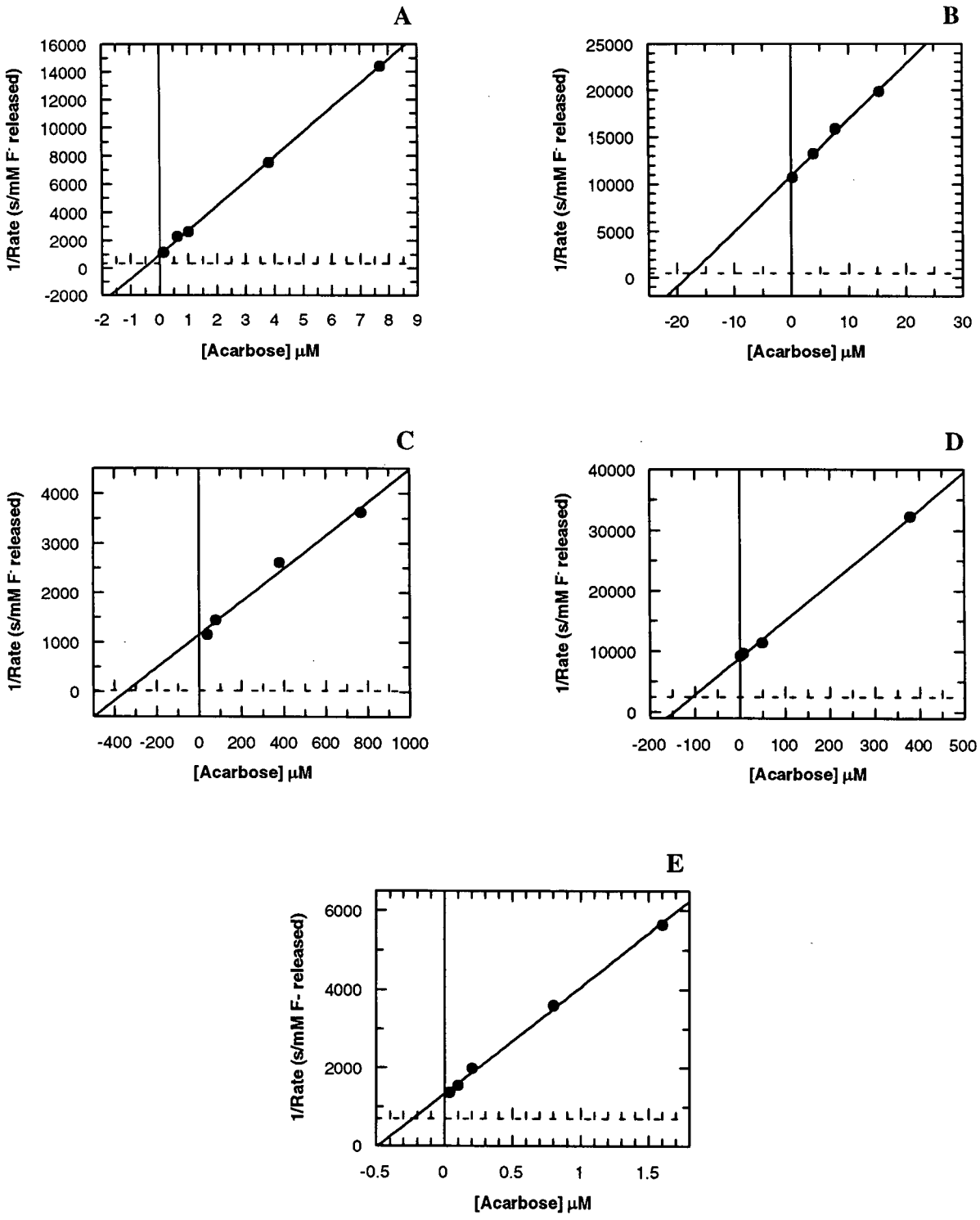

Figure B-7 Range finder K_i plots for CGTase mutants with acarbose as inhibitor (dotted lines are $1/V_{max}$ for αG3F). **(A)** Y195F (0.0143) µM, **(B)** Y195L (0.0143 µM), **(C)** Y195G (0.043 µM), **(D)** N326Q (0.043 µM), **(E)** wt (0.00327 µM).

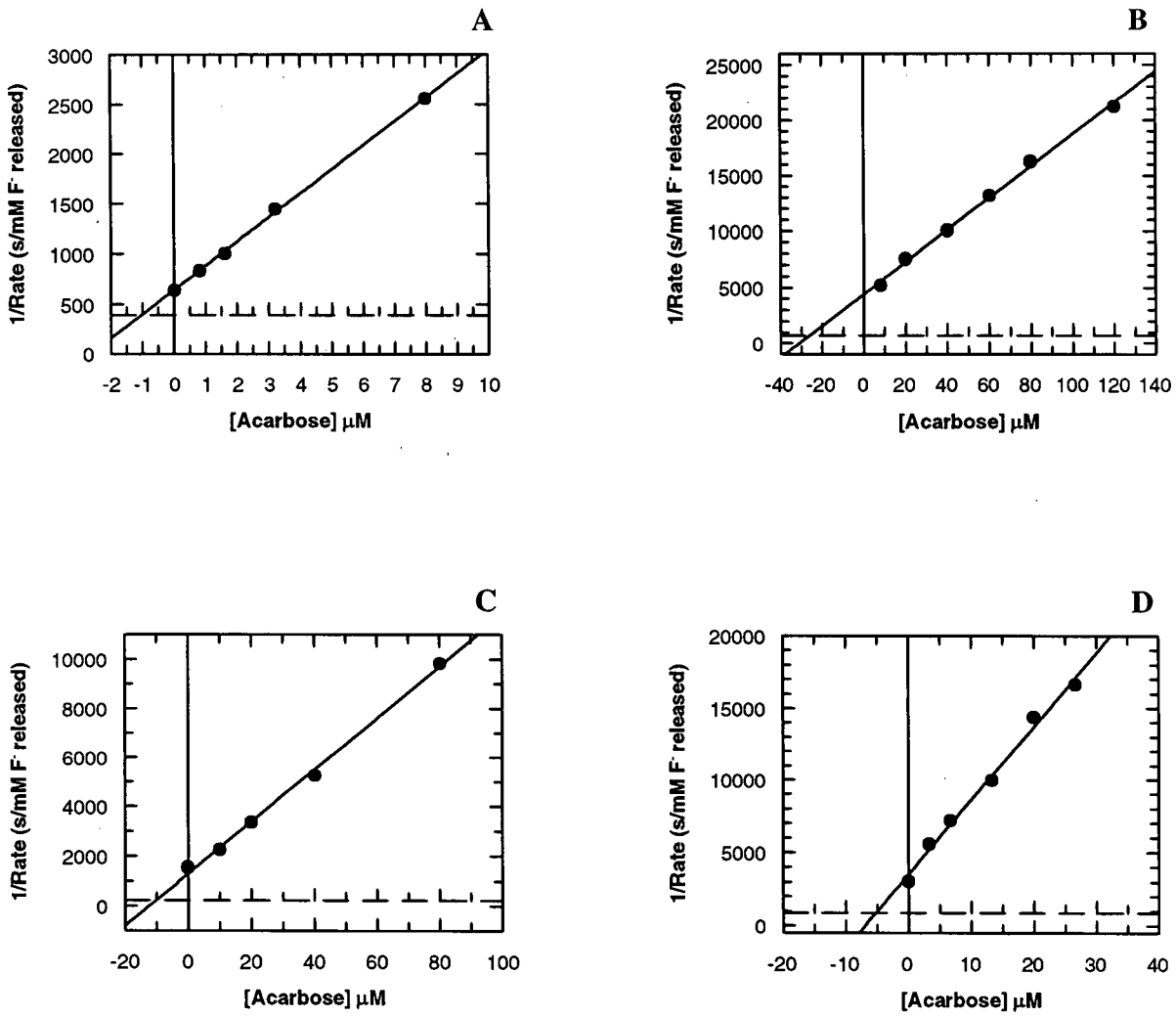

Figure B-8 Range finder K_i plots for CGTase mutants with acarbose as inhibitor (dotted lines are $1/V_{max}$ for αG3F). **(A)** S145E (0.01467 μM), **(B)** S146P (0.178 μM), **(C)** D371N (0.0223 μM), **(D)** N193G (0.0199 μM).

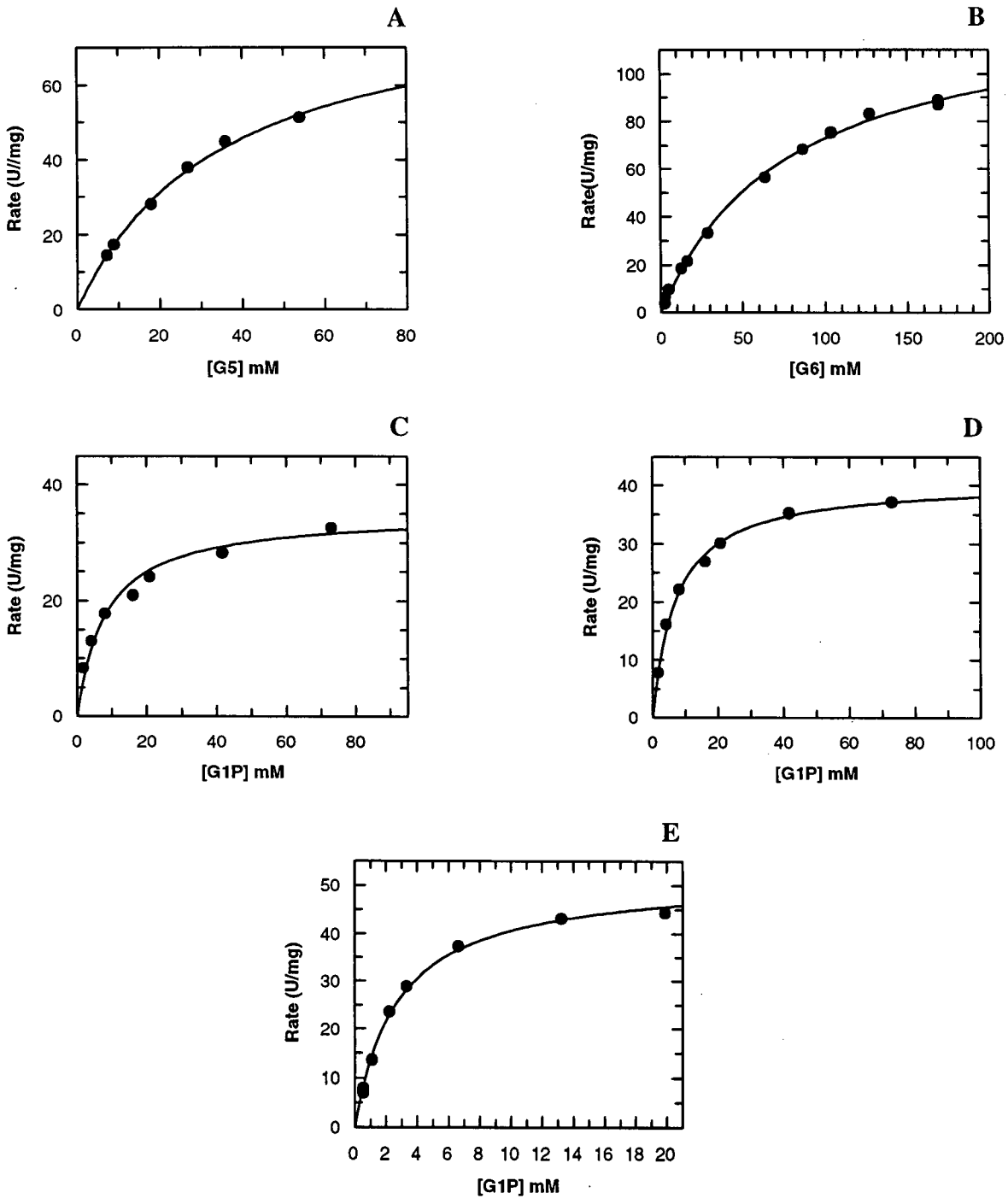

Figure B-9 Michaelis Menten plots for the determination of K_m and V_{max} in the synthesis direction for glycogen phosphorylase. **(A)** [G1P] = 75 mM, [phos b] = 0.051 μM; **(B)** [G1P] = 75 mM, [phos b] = 0.103 μM; **(C)** [G5] = 35 mM, [phos b] = 0.103 μM; **(D)** [G6] = 36 mM, [phos b] = 0.103 μM; **(E)** [Glycogen] = 1.0%, [phos b] = 0.053 μM.

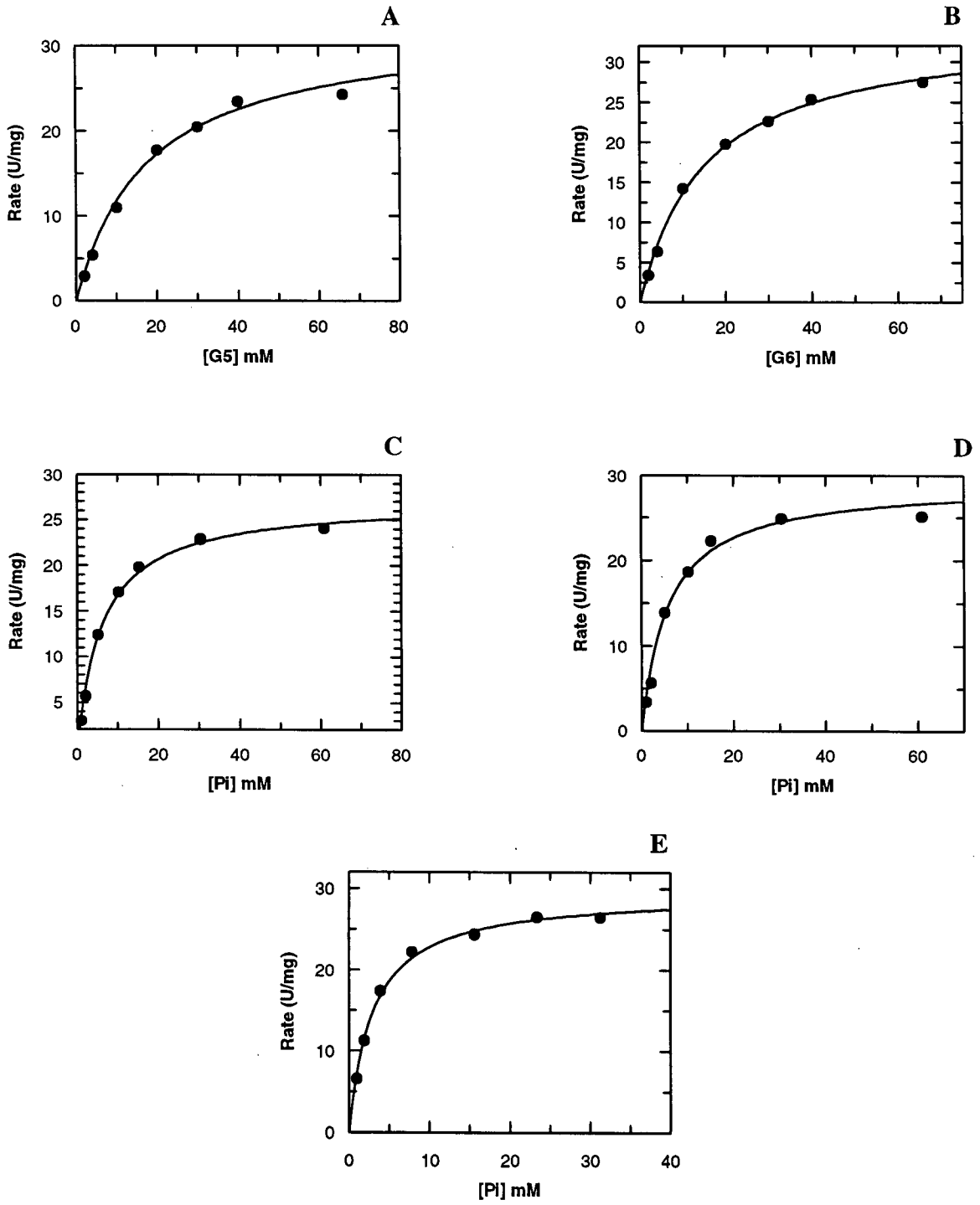

Figure B-10 Michaelis Menten plots for the determination of K_m and V_{max} in the degradation direction for glycogen phosphorylase. **(A)** [Pi] = 21.3 mM, [phos b] = 0.016 μM; **(B)** [Pi] = 21.3 mM, [phos b] = 0.016 μM; **(C)** [G5] = 40 mM, [phos b] = 0.016 μM; **(D)** [G6] = 40 mM, [phos b] = 0.016 μM; **(E)** [glycogen] = 1.0%, [phos b] = 0.015 μM.

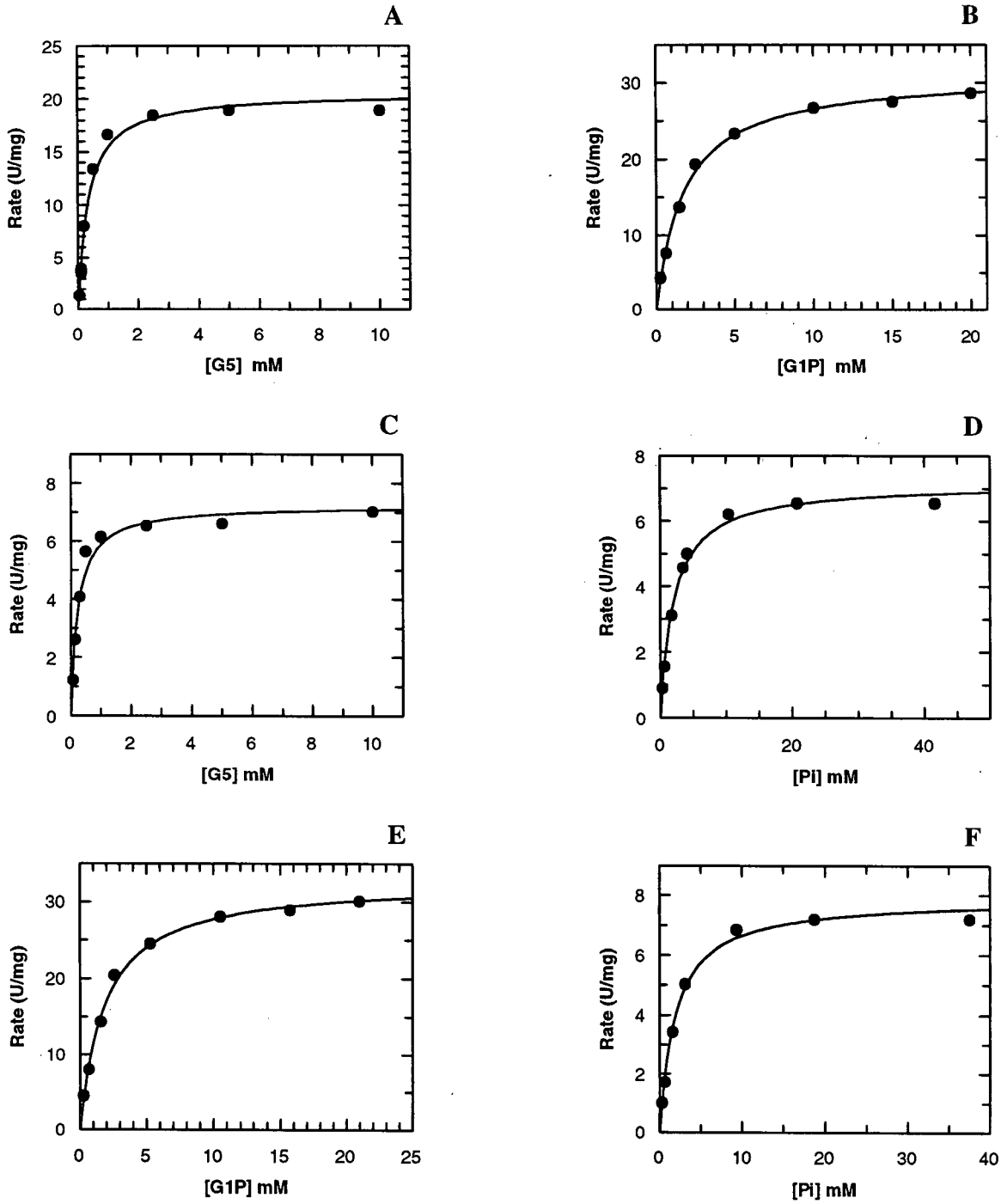

Figure B-11 Michaelis Menten plots for the determination of K_m/V_{max} for potato phosphorylase in the synthesis and degradation directions. **(A)** [G1P] = 10 mM, [pot phos] = 0.121 μM; **(B)** [G5] = 5 mM, [pot phos] = 0.121 μM; **(C)** [Pi] = 10.2 mM, [pot phos] = 0.019 μM; **(D)** [G5] = 4.9 mM, [pot phos] = 0.019 μM, **(E)** [starch] = 0.5%, [pot phos] = 0.121 μM; **(F)** [starch] = 0.5%, [pot phos] = 0.019 μM.

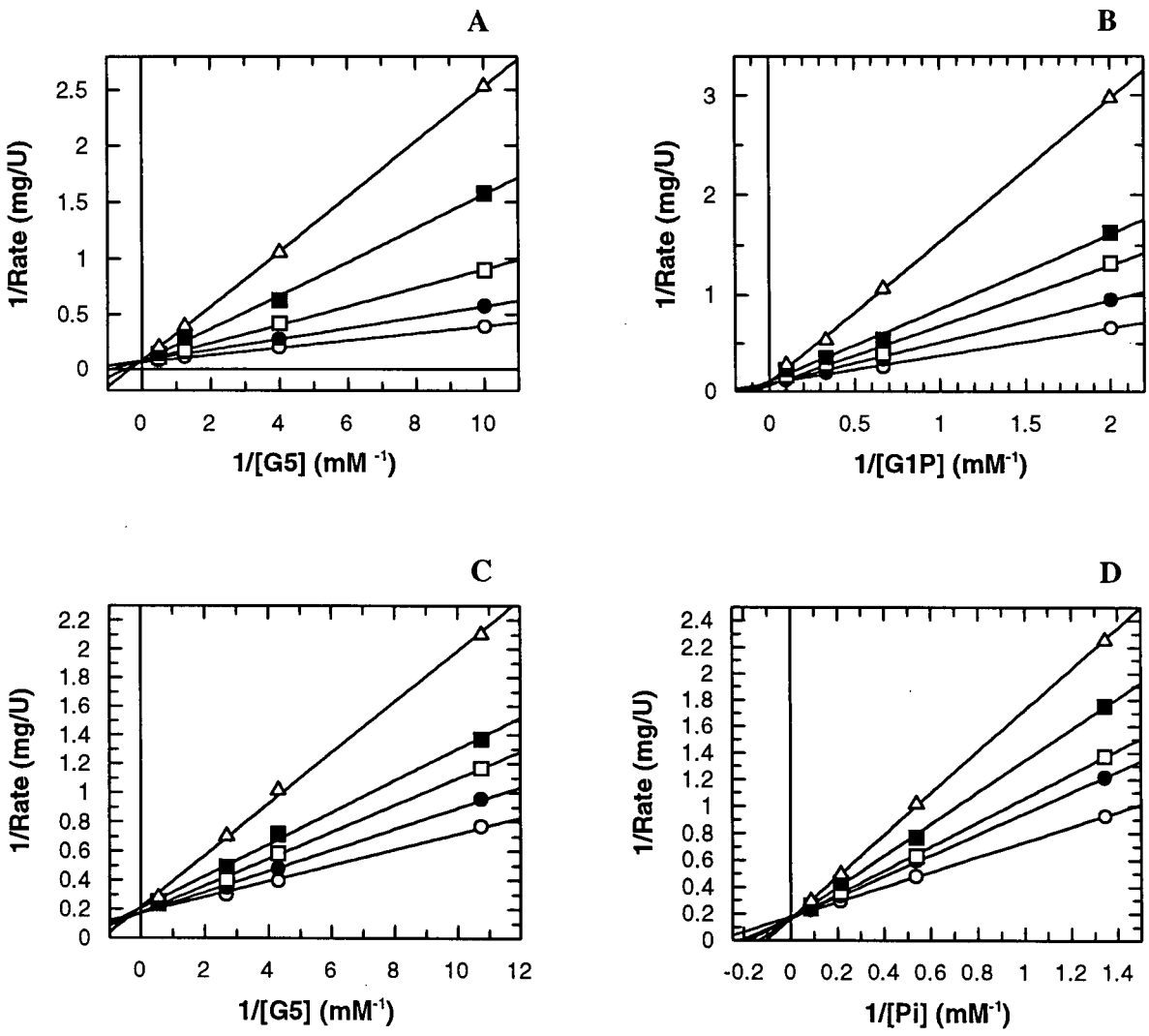

Figure B-12 Lineweaver Burke plots for the inhibition of potato phosphorylase by α-cyclodextrin (I). **(A)** [G1P] = 10.0 mM, [enz] = 0.18 μM, [I]: ❍= 0 mM; ● = 0.075 mM; □ = 0.15 mM; ■ = 0.375 mM; Δ = 0.75 mM, **(B)** [G5] = 0.9 mM, [enz] = 0.21 μM, [I]: ❍= 0 mM; ● = 0.075 mM; □ = 0.15 mM; ■ = 0.375 mM; Δ = 0.75 mM, **(C)** [Pi] = 11.6 mM, [enz] = 0.049 μM, [I]: ❍= 0 mM; ● = 0.070 mM; □ = 0.14 mM; ■ = 0.349 mM; Δ = 0.680 mM, **(D)** [G5] = 2.79 mM, [enz] = 0.049 μM, [I]: ❍= 0 mM; ● = 0.139 mM; □ = 0.279 mM; ■ = 0.680 mM; Δ = 1.35 mM.

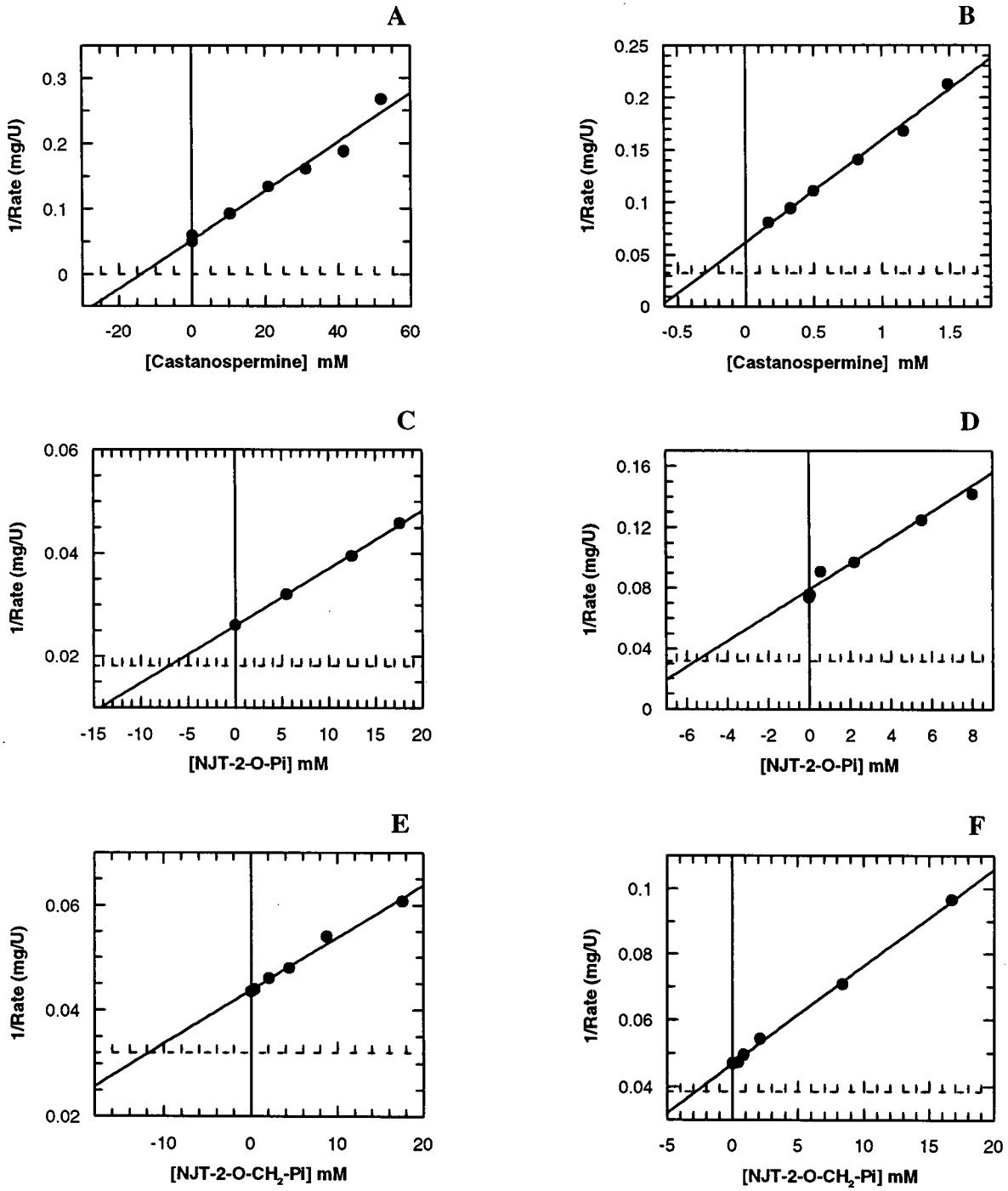

Figure B-13 Range finder K_i plots for muscle phosphorylase with various analogues as inhibitors (dotted lines are $1/V_{max}$ for the respective substrate, Pi or G1P). In all experiments [glycogen] = 1% and [AMP] = 1 mM **(A)** Castanospermine: [phos b] = 0.15 μM, [G1P] = 3.92 mM; **(B)** Castanospermine: [phos b] = 0.015 μM, [Pi] = 3.13 mM; **(C)** NJT-2-O-Pi: [phos b] = 0.014 μM, [G1P] = 2.3 mM; **(D)** NJT-2-O-Pi: [phos b] = 0.014 μM, [Pi] = 3.75 mM; **(E)** NJT-2-O-CH_2-Pi: [phos b] = 0.10 μM, [G1P] = 5.77 mM; **(F)** NJT-2-O-CH_2-Pi: [phos b] = 0.015 μM, [Pi] = 23.8 mM.

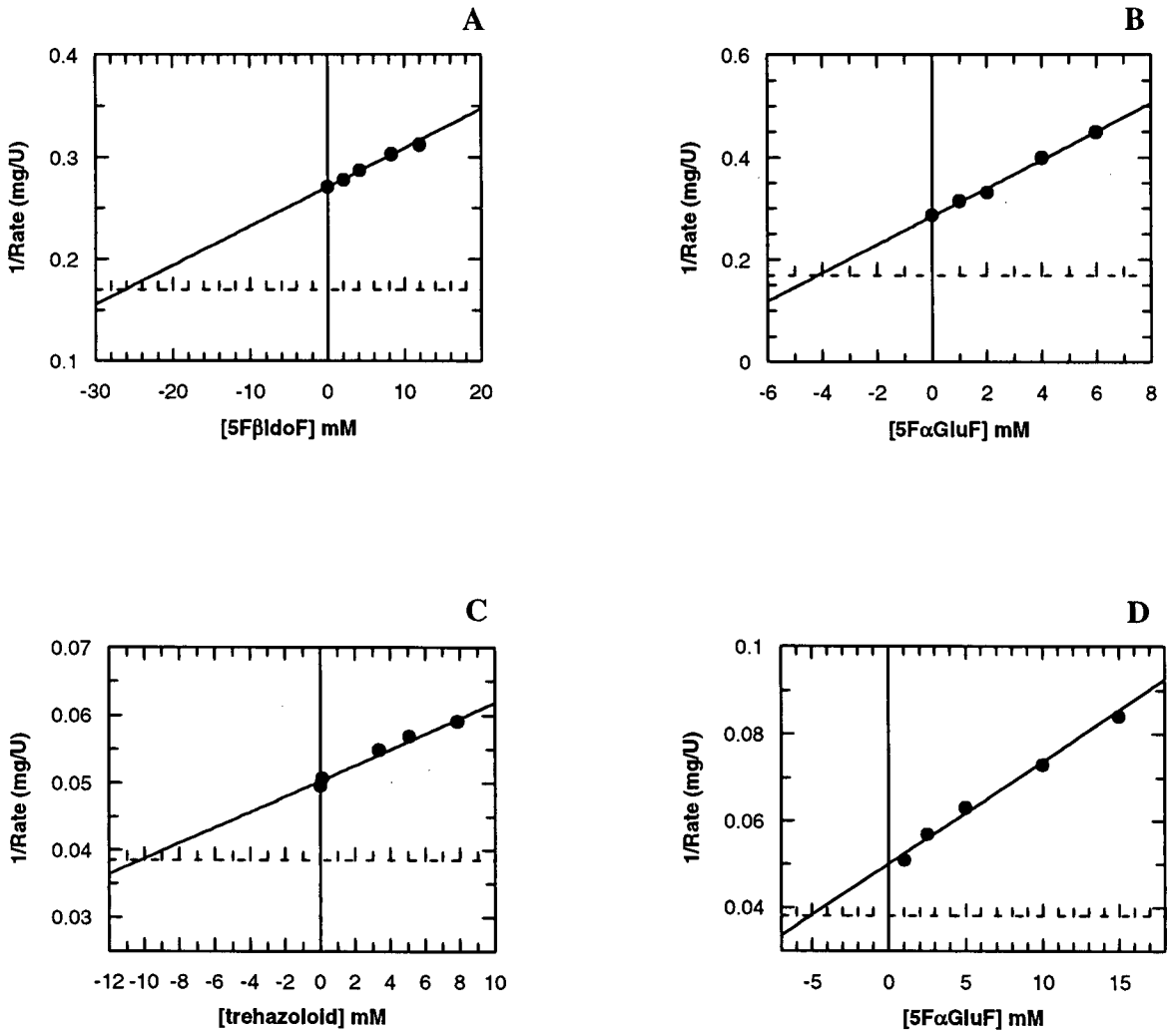

Figure B-14 Range finder K_i plots for phosphorylase (muscle and potato) with various analogues as inhibitors (dotted lines are $1/V_{max}$ for the respective substrate, Pi or G1P). **(A)** 5FβIdoF: [pot phos] = 0.058 μM, [G5] = 2.85 mM, [Pi] = 2 mM; **(B)** 5FαGluF: [pot phos] = 0.058 μM, [G5] = 2.85 mM, [Pi] = 2 mM; **(C)** Trehazoloid: [phos b] = 0.015 μM, [Pi] = 23.8 mM, [glycogen] = 0.5%, [AMP] = 1 mM; **(D)** 5FαGluF: [phos b] = 0.015 μM, [Pi] = 23.8 mM.